



COMILLAS
UNIVERSIDAD PONTIFICIA

ICAI

MÁSTER UNIVERSITARIO EN INGENIERÍA
INDUSTRIAL

TRABAJO FIN DE MÁSTER

INFLUENCE OF ACTIVE MUSCULATURE ON INJURY
RISK PREDICTION ON FRONTAL CRASHES

Autor: Pablo Lozano Gil

Director: Francisco José López Valdés

Madrid
Julio de 2021

|

Declaro, bajo mi responsabilidad, que el Proyecto presentado con el título
Influence of active musculature on injury risk prediction on frontal crashes
en la ETS de Ingeniería - ICAI de la Universidad Pontificia Comillas en el
curso académico 2020/21 es de mi autoría, original e inédito y
no ha sido presentado con anterioridad a otros efectos.

El Proyecto no es plagio de otro, ni total ni parcialmente y la información que ha sido
tomada de otros documentos está debidamente referenciada.



Fdo.: Pablo Lozano Gil

Fecha: 12 / 07 / 2021

Autorizada la entrega del proyecto

EL DIRECTOR DEL PROYECTO

LOPEZ VALDES

FRANCISCO JOSE

- 09437440B

Firmado digitalmente por
LOPEZ VALDES FRANCISCO

JOSE - 09437440B

Fecha: 2021.07.13 11:39:53
-04'00'

Fdo.: Francisco José López Valdés

Fecha: 13 / 07 / 2021

|



COMILLAS
UNIVERSIDAD PONTIFICIA

ICAI

MÁSTER UNIVERSITARIO EN INGENIERÍA
INDUSTRIAL

TRABAJO FIN DE MÁSTER

INFLUENCE OF ACTIVE MUSCULATURE ON INJURY
RISK PREDICTION ON FRONTAL CRASHES

Autor: Pablo Lozano Gil

Director: Francisco José López Valdés

Madrid
Julio de 2021

|

Acknowledgements

I would like to thank my supervisors Alexandros Leledakis and Emma Larsson for their exceptional support throughout the project as they were always available for my questions and always ready to help me. I want to thank them as well for the opportunity they gave me of working in this exciting project at Volvo Cars Safety Centre.

Thank you also to all the coworkers from Volvo Cars Safety Centre that helped me during the development of the project, teaching me how to solve several problems and giving me advice on the project, especially to Sarah El-Mobader for her great help and support to this project and for the fikas we had together.

Gothemburg, July 2021
Pablo Lozano Gil

|

INFLUENCIA DE LA MUSCULATURA ACTIVA EN LA PREDICCIÓN DEL RIESGO DE LESIÓN EN COLISIONES FRONTALES

Autor: Lozano Gil, Pablo.

Supervisor: López Valdés, Francisco José.

Entidad Colaboradora: Volvo Cars, ICAI – Universidad Pontificia Comillas & Chalmers University of Technology.

Resumen del proyecto Los modelos activos de cuerpo humano son una herramienta importante para estudiar la interacción de los ocupantes con los sistemas de seguridad de un vehículo en maniobras evasivas como el frenado y/o la dirección. Sin embargo, es necesario estudiar la influencia de la musculatura activa en la posible fase de choque que puede ocurrir después de una maniobra evasiva. En este estudio, se utiliza un modelo de cuerpo humano de elementos finitos con controladores musculares en la cabeza y la parte inferior del tronco para estudiar la influencia de la musculatura activa en la predicción del riesgo de lesiones en colisiones frontales. Se simularon nueve combinaciones diferentes de maniobras previas a la colisión y escenarios de colisión con y sin la musculatura activa para evaluar la influencia de dicha activación en la predicción del riesgo de lesiones del modelo. En primer lugar, se realizó una simulación de referencia completa con las fases de inicialización, pre-colisión y colisión con la musculatura activa. Después, se extrajo el estado de la simulación al final de la maniobra previa a la colisión y se utilizó el modelo pasivo para ejecutar la misma fase de colisión con diferentes entradas como la postura o la velocidad al final de la colisión previa. Se utilizaron las excursiones, las aceleraciones y las predicciones de riesgo de lesiones para hacer comparaciones entre los modelos. Además, se utilizó el software CORAplus para valorar la proximidad de los modelos pasivos al modelo de referencia activo. Los resultados muestran que la metodología utilizada para recrear la fase de colisión activa no es capaz de reproducir fielmente la fase de colisión de referencia, ya que la calificación máxima de CORA fue de 0,873. Sin embargo, la mejor combinación de entradas desde una perspectiva global para reproducir el modelo activo de referencia es incluir la postura, la velocidad inicial y las tensiones iniciales en el modelo pasivo del cuerpo humano. Como parece que el nivel de actividad muscular no influye en los resultados e incluso podría empeorar los valores obtenidos, se puede concluir que la musculatura activa puede no influir en la predicción del riesgo de lesión durante la fase de colisión.

Palabras clave Human Body Model, Active Musculature, Occupant Parameters, Frontal collision, Pre-crash maneuver, LS-DYNA, ANSA, Oasys Primer, Python.

I. INTRODUCCIÓN

El sector de la movilidad se dirige hacia la conducción autónoma a un ritmo muy alto. No es raro ver nuevos prototipos de vehículos que son capaces de maniobrar de forma autónoma o incluso de conducir por sí mismos en algunas carreteras.

Hoy en día los coches están llegando casi al nivel 3 de automatización, pero hay muchas empresas que están mostrando sus nuevos conceptos de conducción autónoma. Todo esto apunta a que veremos vehículos autónomos en las carreteras de los próximos años, lo que implica que los coches tradicionales convivirán con los vehículos autónomos en las calles. El

problema de esta coexistencia es que, debido a errores humanos o a diferentes situaciones posibles, los coches autónomos podrían necesitar hacer maniobras evasivas en algunas situaciones para evitar un posible choque.

Esta situación conlleva que los coches actúen en caso de emergencia realizando una maniobra evasiva que no ha sido planificada por el conductor ni por los pasajeros. Esta maniobra evasiva podría afectar a la postura de los ocupantes dentro del coche, pudiendo afectar también a las lesiones que puedan tener en el caso de que la maniobra evasiva no se evite y el coche acabe en una colisión. Este reto es el que motiva este estudio y uno de los principales objetivos será estudiar cómo el cambio de postura en la fase de colisión afecta a la predicción del riesgo de lesión. Este estudio se realizará utilizando el método de los elementos finitos y un Modelo del Cuerpo Humano (HBM) activo para simular diferentes escenarios con distintas maniobras previas a la colisión para ver la influencia de la musculatura activa sobre el riesgo de lesión del ocupante. Las simulaciones se realizarán con y sin musculatura activa. Por lo tanto, los principales objetivos de este proyecto son los siguientes

- Revisar la literatura disponible sobre los efectos de la musculatura en el riesgo de lesiones de los ocupantes, así como la validación realizada con modelos de cuerpo humano activo (A-HBM).
- Investigar un conjunto de maniobras previas a la colisión (dirección, frenado y una combinación de ambas) combinadas con impactos frontales y oblicuos. Las combinaciones de pre-colisión y colisión se asignarán de forma estadística.
- Simular la secuencia completa (pre-colisión y colisión) con y sin activación muscular y comparar las excursiones de los ocupantes y las predicciones de riesgo de lesión utilizando los criterios de lesión ya existentes.

Estudiar diferentes aspectos del movimiento del ocupante antes de la colisión e identificar qué afecta más al riesgo de lesión.

II. METODOLOGÍA

Para el desarrollo de este estudio se utilizó el método de los elementos finitos con el fin de simular diferentes escenarios antes y después del choque. Se utilizó LS-DYNA MPP R9.3.1 (LSTC, Livermore, CA, US) como solver explícito para las simulaciones. Como preprocesadores se utilizaron ANSA 21.1.0 (BETA CAE Systems International AG, Root, Suiza) y Primer 17.1 (Oasys Ltd. LS-DYNA Environment). El postprocesado se realizó con META 21.1.0 (BETA CAE Systems International AG, Root, Suiza) y LS-PrePost (Ansys Livermore Software Technology). Por último, la gestión y el análisis de los datos se realizaron utilizando Spyder 3-ver 1.4 y Python 3.10 como lenguaje de programación principal.

El HBM utilizado en todas las simulaciones fue el SAFER HBM v10 de cuerpo entero. Este modelo representa a un hombre de tamaño medio. Las versiones anteriores se basaban originalmente en el modelo de cuerpo entero para la seguridad AM50 versión 3.0 (THUMS, Toyota Corporation, 2008) [1]. La antropometría del modelo se basa en el percentil 50 de los varones, según [2], tiene una estatura de 175 cm y pesa 77 kg. El modelo consta de 219 000 elementos sólidos, 190 000 elementos de cáscara y 2400 elementos unidimensionales. La mayoría de los elementos utilizados en el modelo eran hexaédricos/cuadrilaterales y

deformables, las únicas excepciones fueron las vértebras torácicas, el sacro y las placas terminales vertebrales, que son rígidas.

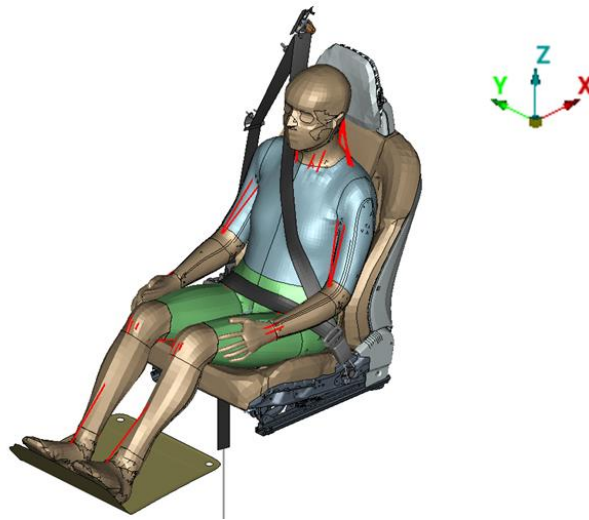


Figura 1: HBM colocado en el modelo de asiento en la posición de referencia para las simulaciones

La musculatura del modelo está formada por elementos de tipo Hill 1D que fueron controlados por varios controladores PID de lazo cerrado. En el caso de este estudio, se utilizaron dos controladores: uno para el cuello y otro para la musculatura lumbar. Sin embargo, el modelo tiene también la posibilidad de utilizar un controlador para la musculatura de las piernas y la de los brazos. Este último controlador está diseñado para ser utilizado si el HBM se coloca en la simulación como el conductor y tiene un volante para poner los brazos, de modo que el modelo puede replicar la fuerza que un conductor real hará con sus manos en caso de colisión.

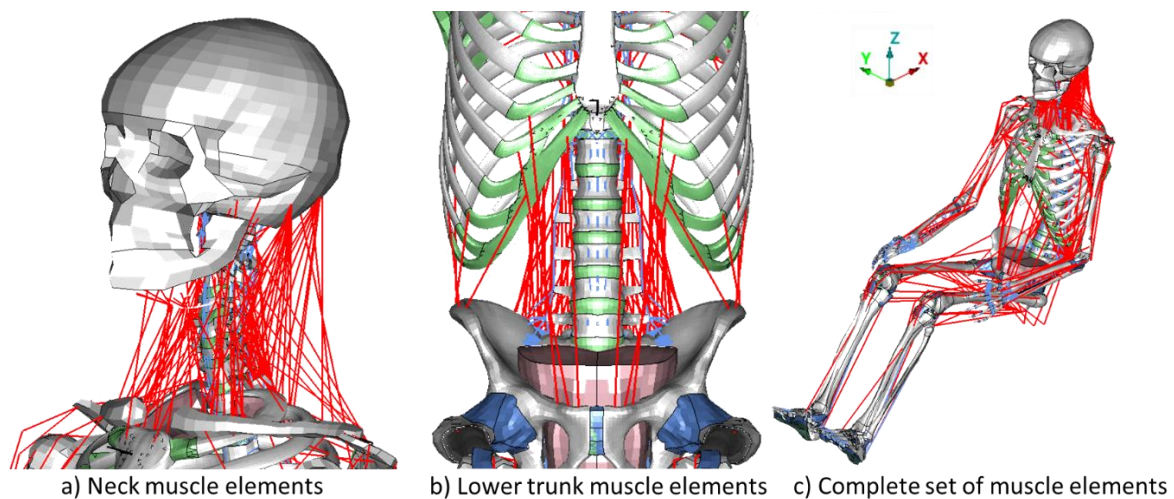


Figura 2: Elementos musculares del HBM. Los elementos musculares se muestran en color rojo y se muestran sin tejido blando para una mejor visibilidad. Sin embargo, en las simulaciones se utiliza carne y tejido blando.

El modelo tiene también dos tipos de bucles de retroalimentación para los controladores PID de los músculos: MIMO (Multiple Input Multiple Output) y SIMO (Simple Input Multiple Output controllers). El controlador MIMO se llama MLF (Muscle Length Feedback) y tiene la capacidad de controlar independientemente la longitud de cada músculo y tener como entrada la longitud de cada músculo también. El controlador SIMO se llama APF (Angular Position Feedback) y controla la longitud de cada músculo, pero teniendo como entrada las traslaciones

y rotaciones de la cabeza. El bucle de retroalimentación MFL emula el reflejo de estiramiento de los músculos y el APF emula la retroalimentación vestibular del sistema nervioso central, que trata de estabilizar la cabeza en el espacio [1].

Para este estudio, se eligió el bucle de retroalimentación APF con dos controladores PID, uno para la cabeza y otro para la parte inferior del tronco. Se puede encontrar más información sobre el controlador en el documento principal.

En cuanto al entorno en el que se utiliza el HBM, todas las simulaciones se realizaron utilizando como condición de contorno un modelo de trineo representativo de un SUV de tamaño medio. Este trineo estaba equipado con un airbag frontal para el pasajero, un asiento y un cinturón de seguridad con el fin de sujetar adecuadamente el HBM y recrear un entorno real. Todas las piezas de este modelo de EF fueron proporcionadas por Volvo Cars. Todos los impulsos utilizados para las diferentes simulaciones se aplicaron sobre el modelo de trineo rígido. Todos los impulsos consistían en series temporales de 6DOF (grados de libertad) que definían las traslaciones x, y, z y las rotaciones x, y, z del trineo durante la simulación.

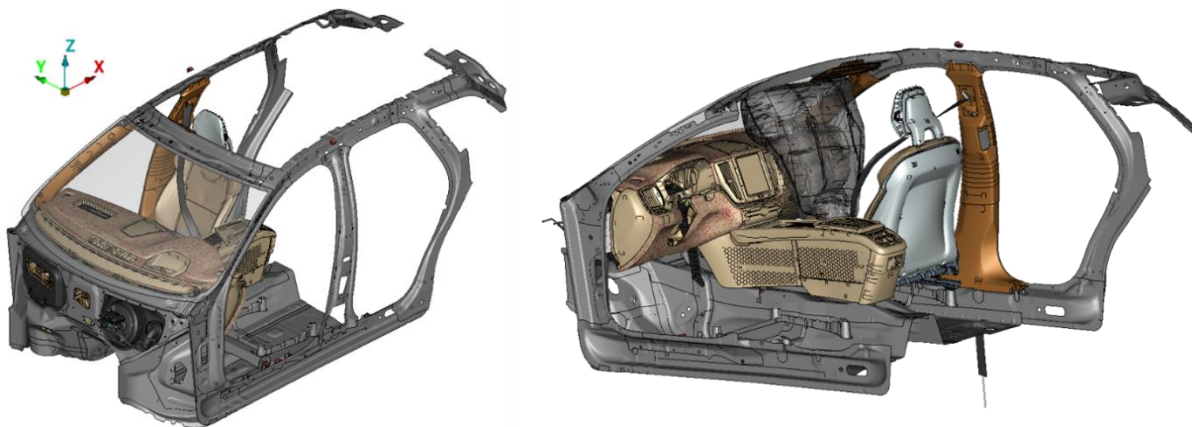


Figura 3: Modelo de sled

Configuración de la simulación

El modelo se coloca en el espacio de forma que la parte delantera del coche se dirija hacia la parte negativa del eje x. El sistema de coordenadas se define como un sistema de coordenadas a la derecha con x hacia atrás, y hacia el lado derecho y z hacia arriba (figura 3).

Para el desarrollo del estudio, se utilizaron dos tipos de simulaciones: simulaciones de línea de base (secuencia completa) y simulaciones pasivas (en colisión).

Todas las simulaciones de referencia tenían los controladores de la musculatura activa activados para el HBM y todas ellas constan de tres fases: inicialización, pre-colisión y colisión. Estas simulaciones se utilizaron como línea de base para estudiar la influencia de la musculatura activa en la predicción del riesgo de lesiones. El proceso de inicialización se utilizó para alcanzar un estado de equilibrio entre el HBM y el entorno y para estabilizar las señales en los controladores musculares del HBM. En esta fase se activó la gravedad para que la postura del HBM fuera lo más natural posible. Se aplastó la espuma del asiento y se eliminaron las vibraciones generadas por las señales de control a lo largo de los 300 ms que duró esta fase.

La fase de pre-colisión se utilizó para reproducir una maniobra de evasión. Se utilizó un impulso real previo a la colisión proporcionado por el estudio de Emma Larsson [1] para

simular el movimiento de un coche real y recrear la posición de un humano real tras la maniobra evasiva utilizando el modelo HBM. En esta fase se modificó la postura del ocupante y la musculatura activa entró en acción tratando de estabilizar el HBM simulando la musculatura lumbar y cervical humana real.

Por último, la fase de choque recrea una colisión en la que se despliega el airbag en función del tipo de choque y del retractor del cinturón de seguridad. Los impulsos utilizados para esta fase fueron proporcionados por Volvo Cars. La gran mayoría de ellos seguían choques estandarizados del Euro NCAP [3] y del IIHS (Insurance Institute for Highway Safety) [4]. Todos los impulsos utilizados para este estudio son choques frontales. Todo el análisis se centró en la fase de colisión.

Una vez realizada la simulación de referencia, se crearon varias simulaciones pasivas basadas en la simulación inicial. Estas simulaciones pasivas tenían parámetros diferentes a los de la simulación de referencia, como la postura del ocupante al final en la pre-colisión, sus velocidades, las tensiones de los elementos, o la última señal del controlador para cada músculo del modelo; y sólo simulaban la fase de colisión.

Este procedimiento se realizó para reducir el tiempo de cálculo necesario para cada simulación. Por término medio, la maniobra previa a la colisión duró entre 500 ms y 850 ms, y la fase de colisión duró entre 120 ms y 300 ms. Ejecutar una simulación de referencia con las tres fases (inicialización [300ms] + pre-crash[500-850ms] + in-crash [120-300]) suponía ejecutar unos 1300 ms de simulación. El número de CPUs (Unidades Centrales de Procesamiento) utilizadas por simulación fue de unas 120. Con este número de CPUs, ejecutando 1300 ms de media, el tiempo de simulación fue de unos 7 días completos de simulación. Como se describe más adelante, para este proyecto era necesario simular al menos 72 simulaciones. Si todas las simulaciones tuvieran las tres fases, se habrían necesitado 72 semanas sólo para simular, suponiendo que todas las simulaciones se ejecutaran correctamente y no tuvieran errores numéricos. Incluso si pudiéramos ejecutar algunas en paralelo, la cantidad de tiempo necesaria para este proyecto no habría sido razonable.

Sin embargo, la simulación de la fase de colisión sólo lleva un día de media, por lo que establecer sólo una simulación de colisión con el HBM colocado de acuerdo con la posición final y las velocidades del final de la fase de pre-colisión de la simulación de referencia hace que el uso del tiempo de simulación sea mucho más eficiente, teniendo sólo que simular 9 simulaciones de referencia (9 semanas) y 64 ejecuciones pasivas (64 días).

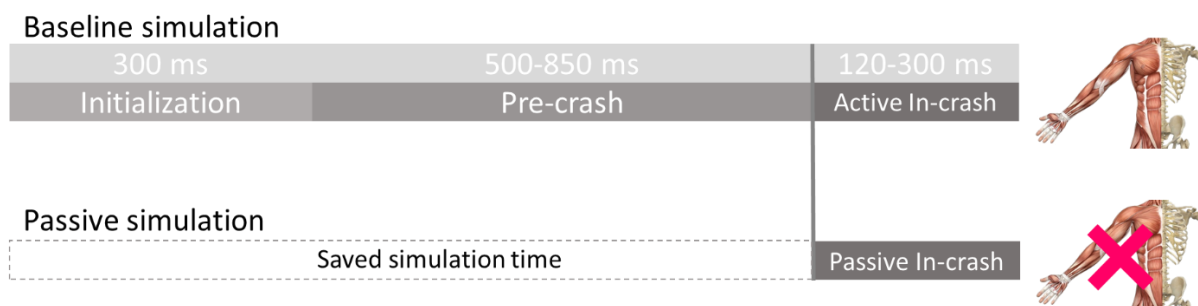


Figura 4: Diagrama de configuración de las simulaciones básicas y pasivas. En las simulaciones pasivas, la musculatura seguía ahí, sólo que los controladores que gestionan la longitud y la fuerza de los músculos estaban desactivados.

Combinaciones de pre-colisión y colisión

Para este estudio, se asumió que la maniobra evasiva fallaba y el coche acababa entrando en una fase de colisión. Por lo tanto, las simulaciones de referencia combinaron una maniobra previa a la colisión con una fase de colisión.

Para seleccionar los tipos de choque más probables para los diferentes escenarios, se utilizó como referencia [5] [6] [7], ya que esos tres artículos estudian las diferentes posibilidades de choque en los escenarios comentados anteriormente. A continuación, todos los tipos de colisión se cotejaron con un pulso de colisión estandarizado del Euro NCAP o del IIHS.

Combinando las maniobras previas a la colisión con los diferentes ensayos de colisión se obtiene la siguiente matriz de precolisión/colisión.

Tabla 1: Matriz de combinaciones de pre-colisión y colisión

		Maniobras de pre-colisión				
		Frenar	Girar a la izquierda	Girar a la derecha	Girar a la izquierda y frenar	Girar a la derecha y frenar
Colisiones frontales	Full-Width Rigid Barrier					
	Moderate Overlap Frontal Test					
	Mobile Progressive Deformable Barrier					
	Passenger-side Small Overlap					

Sin embargo, no todas las combinaciones tienen la misma probabilidad de ocurrir en un escenario real. Las casillas marcadas en azul muestran las combinaciones que se dan con mayor frecuencia en los escenarios descritos anteriormente, por lo que fueron las combinaciones que se utilizaron para este estudio. Se puede encontrar más información sobre estas combinaciones en el documento principal. Además, con las combinaciones seleccionadas es posible comparar la misma fase de choque con diferentes maniobras de pre-colisión para estudiar la importancia de la maniobra, y es posible estudiar cómo difieren los diferentes escenarios de choque cuando comparten la misma maniobra de pre-colisión.

Como se mencionó anteriormente, a partir de estas simulaciones de referencia, se crearán algunas ejecuciones pasivas adicionales utilizando diferentes entradas de la simulación de evento completo, como la postura del HBM o la velocidad que tenía al final de la fase de pre-colisión. Las combinaciones que se simularon son las siguientes:

Tabla 2: Combinación de inputs para las diferentes simulaciones pasivas

Passive simulation	HBM Inputs			
	Posición	Velocidad	Stress	PID muscular
0				
1				
2				
3				
4				
5				
6				

Los inputs empleados son los siguientes:

- Posición: la postura del HBM al final del pre-colisión. Se refiere a la posición de cada nodo del HBM al final de la pre-colisión. Esta información se extrajo del último estado de la simulación de referencia antes de entrar en la fase in-crash y luego se introdujo en el nuevo modelo utilizando Python para gestionar las coordenadas de cada nodo.
- Velocidad: se refiere a la velocidad final de cada nodo del HBM al final de la pre-colisión. En el caso de las simulaciones pasivas, se trata de una velocidad inicial que se establece como condición de contorno para la simulación de la colisión. Esta información se extrajo del último estado de la simulación de referencia antes de entrar en la fase de colisión y luego se introdujo en el nuevo modelo utilizando Python para gestionar la velocidad de cada nodo. Las velocidades iniciales se definieron utilizando la tarjeta *INITIAL_VELOCITY_NODE de LS-DYNA.
- Stress: representa las tensiones de todos los sólidos, shells y vigas del modelo al final de la pre-colisión. Estas tensiones se obtuvieron del último estado de la simulación de referencia antes de entrar en la fase de colisión y luego se introdujeron en el nuevo modelo utilizando Python. Las tarjetas utilizadas para introducir esta información en el modelo fueron *INITIAL_STRESS_SOLID, *INITIAL_STRESS_SHELL, y *INITIAL_STRESS_BEAM, respectivamente.
- PID muscular: representa el nivel de actividad muscular en el último estado de la simulación de referencia. Es el último valor de la señal de los controladores PID que gestionan la longitud y la fuerza de cada músculo. Con la configuración propuesta para las simulaciones, se estudiaron tres casos diferentes basados en los controladores musculares:
 - Modelo pasivo completo: el HBM no tiene actividad muscular, los músculos del rayo no funcionan. Este escenario representa a un humano que no hace ninguna fuerza con sus músculos durante el choque, no hay fuerza en los músculos, el cuerpo sólo se mueve debido a su inercia y al movimiento del coche. Toda simulación pasiva sin MPID (PID muscular o muscle PID).
 - Modelo pasivo con MPID: el HBM retiene la última señal del controlador PID, y la longitud y la fuerza de cada músculo no varía con el tiempo. En este caso se supone que la rigidez del cuerpo humano no cambia durante el in-crash y se mantiene constante con el último valor de la fase pre-crash, ya que la fase in-

crash no dura más de 300 ms. Todas las simulaciones que tienen MPID como input.

- Modelo activo: el HBM en este escenario tiene la capacidad de cambiar la longitud y la fuerza de cada músculo durante la fase de in-crash, pero siempre con 20ms de retraso, lo que representa el retraso en un cerebro humano real entre que se procesa una entrada y se realiza la acción muscular consecuente. En este escenario, se asume que un humano puede variar la fuerza que hace con los músculos durante la in-crash. Todas las simulaciones de referencia.

El objetivo de esta configuración es estudiar la influencia de cada parámetro de entrada por separado y ver cómo cada parámetro de entrada adicional mejora la respuesta del HBM en comparación con la simulación de referencia.

Análisis de datos

Para estudiar la influencia de la musculatura activa en la predicción del riesgo de lesión y en el resultado de la simulación, se comparó la cinemática del HBM y la predicción del riesgo de lesión de los modelos utilizando tres métodos diferentes.

Comparación de excursiones

Se realizó una inspección visual de las diferentes simulaciones para evaluar cómo las diferentes entradas y la musculatura activa influyen en las excursiones de la cabeza, el tórax y la pelvis. Dichas excursiones se trazaron en los planos x-y y x-z para estudiar los desplazamientos laterales y frontales de la cabeza, el tórax y la pelvis durante la fase de choque.

Comparación cinemática

También se compararon las aceleraciones x, y y z de la cabeza, el tórax y la pelvis utilizando la correlación cruzada del software CORAplus 4.0.4 (CORrelation and Analysis) [8] para estudiar lo cerca que pueden estar las simulaciones pasivas de la simulación de referencia activa en función de las entradas utilizadas. Este software calcula el nivel de correlación entre dos señales/historias temporales dando un resultado entre 0 y 1 dependiendo de la calidad de la coincidencia. La calificación 1 representa una coincidencia perfecta con las tolerancias predefinidas, y 0 significa una mala coincidencia. El programa ofrece dos métricas para estudiar la igualdad de dos curvas: el análisis de correlación cruzada y el método del corredor. El método de correlación cruzada analiza tres características de las señales: el desplazamiento de fase, el tamaño (amplitud) y la forma de ambas curvas para evaluar lo cerca que está la señal de la curva de referencia. Estos tres parámetros también se ponderan, por lo que el usuario puede dar más importancia a un parámetro concreto.

El método del corredor evalúa la desviación entre dos señales mediante el ajuste del corredor. Se definen cuatro curvas alrededor de la señal de referencia para crear un corredor interior y otro exterior. Si la curva estudiada se ajusta dentro del corredor interior, se asigna una calificación de 1. Si la curva está fuera del corredor exterior, se asigna una calificación de 0. La estructura general de clasificación del programa se muestra en la siguiente figura.

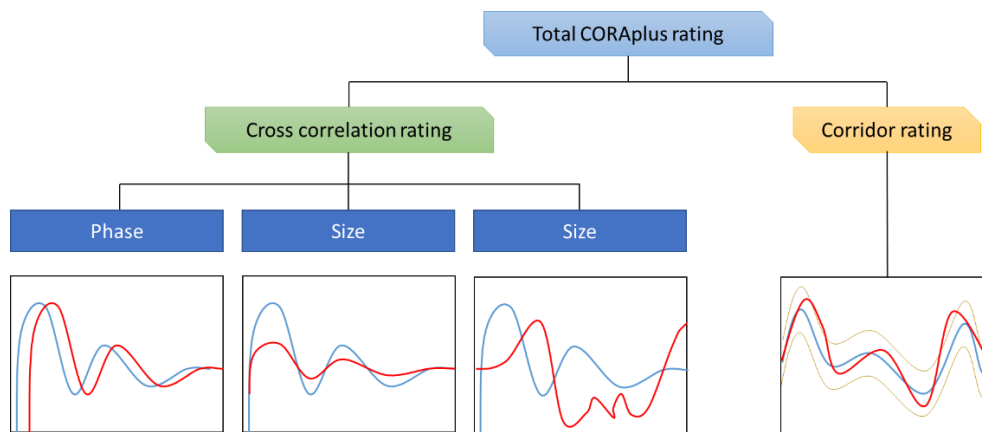


Figura 5: Estructura de la puntuación de CORA

Para este estudio, sólo se utilizó la calificación de correlación cruzada para evaluar las señales, ya que la calificación del corredor está diseñada para comparar un promedio de curvas de prueba reales con los resultados de la simulación. Los resultados de las pruebas tienen una desviación estándar que puede utilizarse para establecer el corredor. En el caso de este estudio, sólo se compararon las curvas de simulación, por lo que sólo se realizó el análisis de correlación cruzada. Las valoraciones de cada parámetro se muestran en la Tabla 3 y muestran la configuración recomendada según el manual de usuario de CORAplus [8].

Tabla 3: Ponderación de CORA

Cross correlation rating	Weight
Phase	0.25
Size	0.25
Shape	0.5

Para facilitar la interpretación de las calificaciones del CORA, los resultados se clasificaron como excelentes, buenos, regulares y deficientes siguiendo el manual del software [8].

Tabla 4: Categorías de CORA

Category	CORA rating interval
Excellent	$0.94 < \text{Rating} \leq 1$
Good	$0.8 < \text{Rating} \leq 0.94$
Fair	$0.58 < \text{Rating} \leq 0.8$
Poor	$0 \leq \text{Rating} \leq 0.58$

Las señales utilizadas para este análisis se filtraron utilizando un CFC 60 (Channel Frequency Class 60 Hz), un filtro de paso bajo comúnmente utilizado para reducir la cantidad de ruido en las señales de las pruebas de choque. El filtrado se realizó para obtener señales claras y desarrollar un análisis de correlación basado en la parte significativa de la señal y no en el ruido que puede generarse en la fase de choque.

Las aceleraciones en X, Y y Z se estudiaron por separado ya que los escenarios de in-crash estudiados son todos frontales y las aceleraciones en el eje X tienen una amplitud mucho mayor que las aceleraciones en Y y Z, que representan principalmente vibraciones o desplazamientos muy pequeños que pueden ser menos representativos que el movimiento de avance. Para

obtener una calificación final, se hizo una media ponderada entre los tres ejes, dando un peso de 0,5 a las aceleraciones en X, 0,25 a las aceleraciones en Y y 0,25 a las aceleraciones en Z.

Predicciones de riesgo de lesión

Por último, se compararon los indicadores de riesgo de lesión entre simulaciones que compartían las mismas fases de pre-colisión y colisión. Mediante un script de posprocesado, se obtuvieron varios valores de riesgo de lesión como HIC15, NIC o Nij en función de la cinemática del modelo. Además, el modelo HBM dispone de varios modelos de deformación que generan valores relevantes para su estudio. Yendo de la cabeza del modelo a la parte inferior, se estudiaron las siguientes predicciones de riesgo de lesión.

En cuanto a la cabeza del HBM, se utilizó el modelo de deformación cerebral [9], el HIC y el BrIC para evaluar la lesión. Según S. Kleive [9], el modelo de deformación cerebral es adecuado para movimientos de la cabeza con cinemática traslacional y rotacional, y es más preciso que el HIC por sí solo. La combinación del modelo de deformación, el HIC y el BrIC se utilizó para evaluar la diferencia de riesgo de lesión entre el modelo de musculatura activa y los pasivos.

En cuanto al cuello, se utilizaron las fuerzas en las secciones transversales del cuello combinadas con el Nij y el NIC. El Nij se utiliza con frecuencia para evaluar las lesiones en el cuello en impactos de alta velocidad. El NIC se utiliza para evaluar las lesiones en el cuello causadas por los gradientes de presión, sin embargo, es más preciso en los impactos traseros, por lo que se analizará en combinación con los predictores de riesgo de lesión mencionados anteriormente.

En tercer lugar, con respecto al tórax, se utilizó el modelo de fractura de costillas [10] para evaluar la integridad de la caja torácica. El riesgo de fractura de diferentes cantidades de costillas en función de la tensión de las mismas se utilizó para comparar las simulaciones de referencia con las pasivas.

En cuanto a la zona lumbar, se estudiaron las fuerzas lumbares.

III. RESULTADOS

Frenar + Full-Width rigid Barrier

En cuanto a las excursiones de la cabeza, el tórax y la pelvis, hay dos grupos diferenciados en cuanto a las simulaciones pasivas: la simulación pasiva sin entradas y las simulaciones pasivas que tienen como entrada la postura del HBM al final de la pre-colisión.

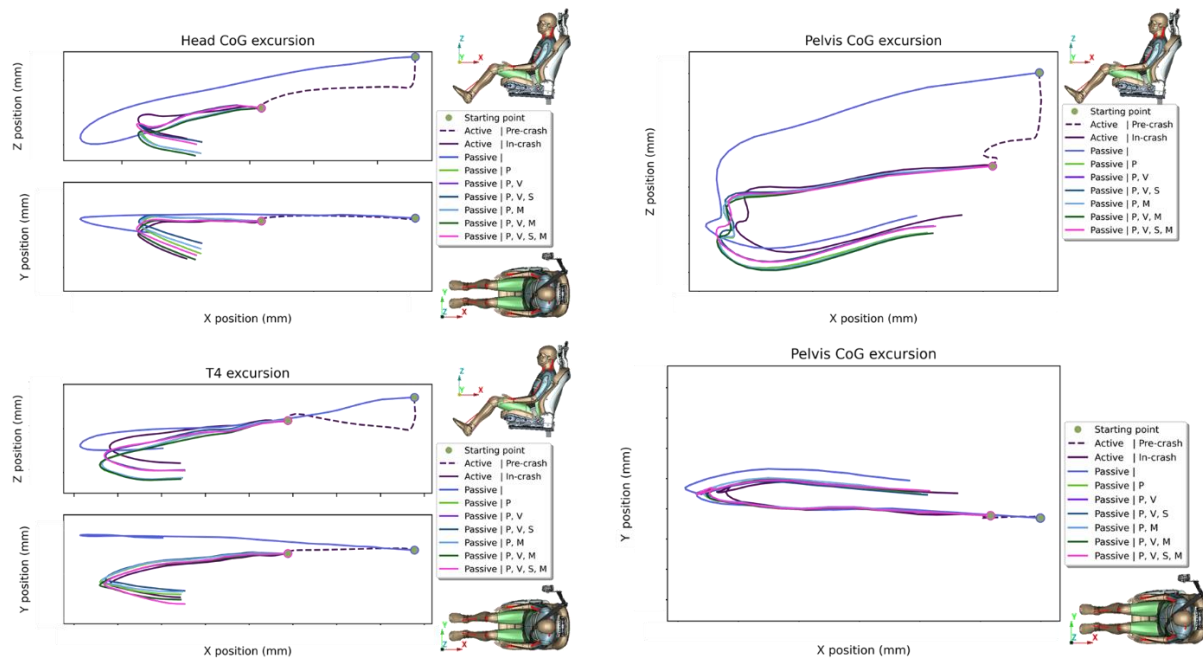


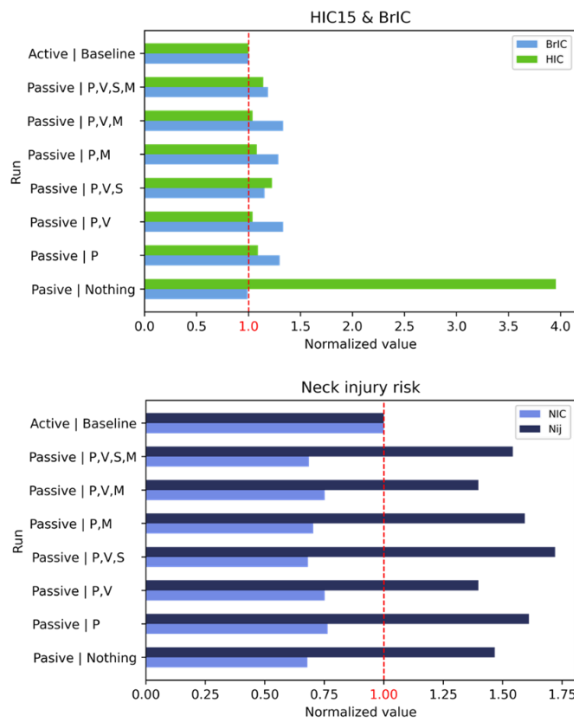
Figura 6: Excursiones del HBM. Frenar y Full-Width Rigid Barrier

Se puede observar que las excursiones de la cabeza, el tórax y la pelvis en la simulación pasiva sin entradas son muy diferentes en comparación con el resto de las simulaciones pasivas. En cuanto al resto de las simulaciones pasivas, hay dos grupos diferenciados de excursiones: las simulaciones pasivas con tensiones y las simulaciones pasivas sin tensiones. Las excursiones de las simulaciones que tienen tensiones parecen estar más cerca de las excursiones de la simulación de referencia.

En cuanto a los criterios de lesión, todos los resultados se han normalizado tomando como referencia el valor de la simulación de referencia. En consecuencia, todas las predicciones de riesgo de lesión de la línea de base tienen valor 1 y los valores de la simulación pasiva oscilan en torno al valor 1. Así, se pueden observar las variaciones de las simulaciones pasivas con

respecto

a



la

activa.

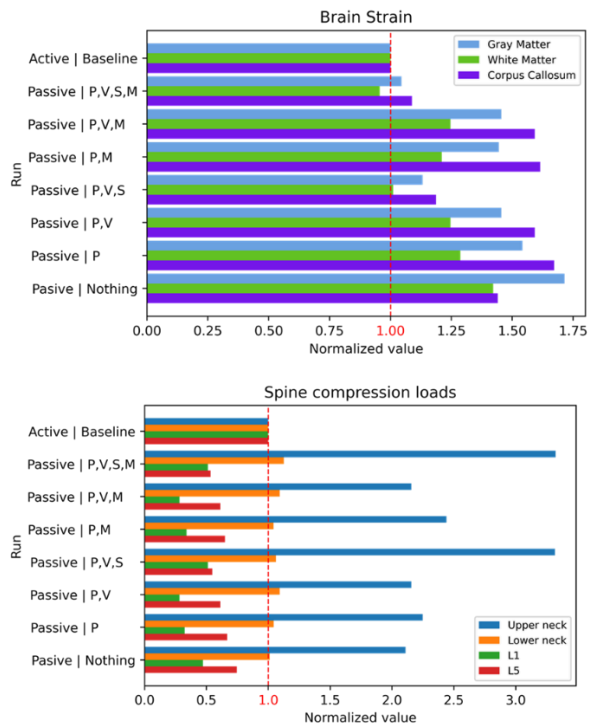


Figura 7: Predicciones de riesgo de lesión. Frenar y Full Width Rigid Barrier

En lo que respecta a la cabeza, el HIC 15 ms se sobrepasa en gran medida en comparación con el modelo de referencia en la simulación sin entradas, y las tensiones en el cerebro son las mayores de todas las simulaciones pasivas. Se puede apreciar que la adición de entradas adicionales mejora la predicción de la tensión cerebral, obteniendo los valores más cercanos cuando se añaden a la simulación la postura, la velocidad y las tensiones. Sin embargo, el nivel de actividad muscular (MPID) no parece afectar a los resultados.

En lo que respecta al cuello y la columna vertebral, las cargas de compresión en la parte superior del cuello se sobreestiman en comparación con el modelo de referencia en todos los casos y las cargas de compresión lumbar se subestiman. Estas predicciones obtienen los valores más cercanos cuando sólo se incluyen la postura y las velocidades iniciales del HBM. El NIC y el Nij son predichos erróneamente en comparación con el modelo de referencia por las simulaciones pasivas en comparación con la línea de base. Los valores más cercanos se obtienen para la simulación de la postura y la velocidad inicial.

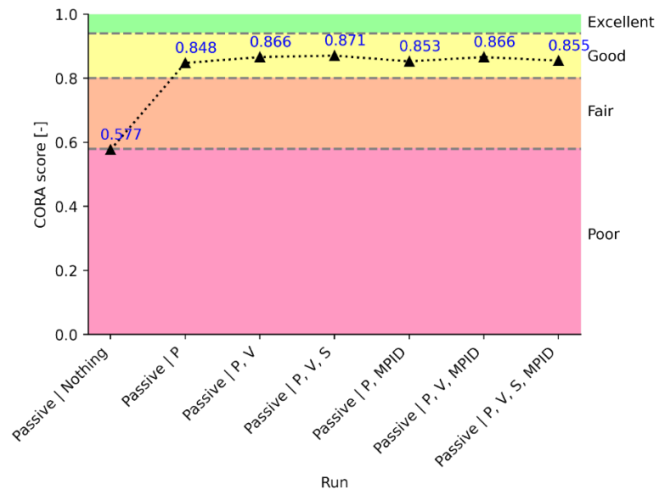


Figure 8: CORAplus acceleration ratings. Braking and Full Width Rigid Barrier

Por último, en lo que respecta a las calificaciones de CORAplus, hay una gran mejora si se añade la postura del ocupante como entrada en la simulación pasiva, cambiando la calificación global de "Pobre" a "Buena". Si se añade la velocidad o la velocidad y la tensión, la calificación mejora un poco más, pero el modelo pasivo no es capaz de reproducir las aceleraciones del modelo activo con una calificación "Excelente". La actividad a nivel muscular no mejora los resultados. Además, en algunas ocasiones añadir el MPID empeora la calificación.

También se obtuvieron resultados para todas las combinaciones de simulación propuestas para el análisis. Debido a la limitada extensión del documento, estos resultados no se mostrarán, pero pueden consultarse en el documento principal.

IV. CONCLUSIONES

El estudio comparó las excursiones, aceleraciones y predicciones de riesgo de lesión entre un HBM activo y un HBM pasivo para estudiar la influencia de la musculatura activa sobre las predicciones de riesgo de lesión. El estudio concluyó que la musculatura activa puede no influir en las predicciones de riesgo de lesión, las excursiones y las aceleraciones, ya que no hay una diferencia significativa en los resultados entre la simulación pasiva más cercana y esa misma simulación con nivel de actividad muscular. Además, las predicciones de los modelos pasivos relacionadas con la columna vertebral fueron muy diferentes de las del modelo activo y es justo en el cuello y la columna lumbar donde actúa la musculatura activa. Sin embargo, el estudio también demostró que la metodología utilizada para recrear la fase de colisión activa no es capaz de reproducir fielmente la fase de colisión de la línea de base, ya que el índice CORA máximo fue de 0,873 y las excursiones de los modelos pasivos difirieron considerablemente de las de la línea de base activa.

En segundo lugar, el estudio demostró que, en caso de que no sea posible utilizar la musculatura activa en el HBM, la adición de la postura mejora significativamente los resultados, haciendo que los resultados de la simulación se acerquen más a los que se habrían obtenido. Además, si se dispone de la velocidad y las tensiones del HBM, podrían añadirse también para obtener resultados aún más cercanos, aunque parecen no ser tan esenciales como la postura del ocupante. Sin embargo, el nivel de actividad muscular (MPID) no influye en los resultados e incluso podría empeorar los valores obtenidos.

Si se utilizan simulaciones pasivas para el estudio, las lesiones craneales y cerebrales parecen predecirse bien en comparación con el modelo de referencia si se incluyen algunas entradas. Sin embargo, las predicciones del riesgo de lesiones en el cuello y la columna vertebral no deben utilizarse si el modelo es pasivo; en su lugar, debe considerarse la musculatura activa, ya que los músculos del HBM actúan directamente sobre el cuello y la parte inferior del tronco del modelo.

V. REFERENCIAS

- [1] E. Larsson, J. Iraeus, J. Fice, B. Pipkorn, L. Jakobsson, E. Brynskog, K. Brodin y J. Davidsson, «Active Human Body Model Predictions Compared to Volunteer Response in Experiments with Braking,» 2019.
- [2] D. Robbins, *Anthropometric specifications for mid-sized male dummy*, Washington, DC: US Department of Transportation DTNH22-80-C-07502, 1983.
- [3] Euro NCAP, «Adult occupant protection,» Euro NCAP, 2021. [En línea]. Available: <https://www.euroncap.com/en/vehicle-safety/the-ratings-explained/adult-occupant-protection/>. [Último acceso: 21 06 2021].
- [4] IIHS HLDI, «About our tests,» 2021. [En línea]. Available: <https://www.iihs.org/ratings/about-our-tests>. [Último acceso: 21 06 2021].
- [5] Luke E. Riexinger, Hampton C. Gabler, «A Preliminary Characterisation of Driver Manoeuvres in Road Departure Crashes,» *IRCOBI*, vol. 79, n° 18, pp. 484-492, 2018.
- [6] Luke E. Riexinger, Rini Sherony, Hampton C. Gabler, «A Preliminary Characterisation of Driver Evasive Manoeuvres in Cross-Centreline Vehicle-to-Vehicle Collisions,» *IRCOBI*, vol. 15, n° 19, pp. 58-69, 2019.
- [7] Scanlon, John & Kusano, Kristofer & Gabler, Hampton., «Analysis of Driver Evasive Maneuvering Prior to Intersection Crashes Using Event Data Recorders,» *Traffic injury prevention*, pp. 182-189, 2015.
- [8] C. Thunert, «CORApplus Release 4.0.4 User's Manual,» 2017.
- [9] S. Kleiven, «Evaluation of head injury criteria using a finite element model validated against experiments on localized brain motion, intracerebral acceleration, and intracranial pressure,» *International Journal of Crashworthiness*, vol. 1, n° 11, pp. 65-79, 2006.
- [10] Johan Iraeus, Linus Lundin, Simon Storm, Amanda Agnew, Yun-Seok Kang, Andrew Kemper, Devon Albert, Sven Holcombe & Bengt Pipkorn, «Detailed subject-specific FE rib modeling for fracture prediction,» *Traffic Injury Prevention*, vol. 20, n° sup2, pp. S88-S95, 2019.

INFLUENCE OF ACTIVE MUSCULATURE ON INJURY RISK PREDICTION ON FRONTAL CRASHES

Author: Lozano Gil, Pablo.

Supervisor: López Valdés, Francisco José.

Collaborating Entities: Volvo Cars, ICAI – Universidad Pontificia Comillas & Chalmers University of Technology.

Abstract Active human body models are an important tool to study occupant interaction with safety systems of a vehicle in evasive maneuvers such as braking and/or steering. However, it is necessary to study the influence of the active musculature in the possible in-crash phase that may occur after an evasive maneuver. In this study, a finite element human body model with muscle controllers on the head and lower trunk is used to study the influence of active musculature on injury risk prediction on frontal crashes. Nine different combinations of pre-crash maneuvers and in-crash scenarios were simulated with and without the active musculature to assess the influence of that activation on the injury risk prediction of the model. First, a complete baseline simulation with initialization, pre-crash and in-crash phases was run with the active musculature. Afterward, the state of the simulation at the end of the pre-crash maneuver was extracted and the passive model was used to run the same in-crash phase with different inputs like the posture or the velocity at the end of the pre-crash. Excursions, accelerations, and injury risk predictions were used to do comparisons between models. Also, CORAplus software was used to rate how close the passive models were to the active baseline model. The results show that the methodology used to recreate the active in-crash phase is not able to reproduce closely the baseline in-crash phase, as the maximum CORA rating was 0.873. However, the best combination of inputs from an overall perspective to reproduce the baseline active model is to include posture, initial velocity, and initial stresses in the passive human body model. As it seems that muscle activity level does not influence the results and it might even worsen the values obtained, it can be concluded that active musculature may not influence the injury risk prediction during the in-crash phase.

Keywords Human Body Model, Active Musculature, Occupant Parameters, Frontal collision, Pre-crash maneuver, LS-DYNA, ANSA, Oasys Primer, Python.

I. INTRODUCTION

The mobility sector is heading towards autonomous driving at a very high pace. It is not uncommon to see new prototypes of vehicles that are able to maneuver autonomously or even drive on their own on some highways.

Nowadays cars are almost reaching level 3 of automation, but there are a lot of companies that are showing their new concepts in autonomous driving. All this points to seeing autonomous vehicles on the roads of the coming years, which implies that traditional cars will coexist with autonomous vehicles on the streets. The problem with this coexistence is that due to human errors or different possible situations, autonomous cars might need to do evasive maneuvers in some situations in order to avoid a possible crash.

This situation entails that cars will act in an emergency making an evasive maneuver that has not been planned by the driver nor the passengers. This evasive maneuver could affect the occupant's posture inside the car, potentially also affecting the injury they may have in the case that the evasive maneuver fails to avoid and the car ends in a collision. This challenge is what motivates this study and one of the main objectives will be to study how the change of posture in the in-crash phase affects the injury risk prediction. This study will be performed using the finite element method and an active Human Body Model (HBM) to simulate different scenarios with different pre-crash maneuvers to see the influence of active musculature over the injury risk of the occupant. Simulations will be run with and without active musculature. Therefore, the principal aims of this project are as follows:

- Review the available literature on muscle effects in occupant injury risk as well as validation performed to active human body models (A-HBM).
- Investigate a set of pre-crash maneuvers (steering, braking, and a combination of both) combined with frontal and oblique impacts. Pre-crash and in-crash combinations will be assigned statistically based.
- Simulate the full sequence (pre-crash and in-crash) with and without muscle activation and compare occupant excursions and injury risk predictions using already existing injury criteria.

Study different aspects of occupant's pre-crash movement and identify what affects the injury risk more.

II. METHODOLOGY

For the development of this study, the finite element method was used in order to simulate different pre-crash and in-crash scenarios. LS-DYNA MPP R9.3.1 (LSTC, Livermore, CA, US) was used as the explicit solver for the simulations. As pre-processors, ANSA 21.1.0 (BETA CAE Systems International AG, Root, Switzerland) and Primer 17.1 (Oasys Ltd. LS-DYNA Environment) were used. Post-processing was done using META 21.1.0 (BETA CAE Systems International AG, Root, Switzerland) and LS-PrePost (Ansys Livermore Software Technology). Lastly, data management and analysis were performed using Spyder 3-ver 1.4 and Python 3.10 as the main programming language.

The HBM used in all simulations was the SAFER HBM v10 whole body. This model represents an average-size male. Previous versions were originally based on the Total Human Model for Safety AM50 version 3.0 (THUMS, Toyota Corporation, 2008) [1]. The model anthropometry is based on the 50th percentile male reported by [2], it has a stature of 175 cm and it weighs 77kg. The model consists of 219 000 solid elements, 190 000 shell elements, and 2400 one-dimensional elements. The majority of the elements used in the model were hexahedral/quadrilateral and deformable, the only exceptions were the thoracic vertebrae, sacrum, and vertebral endplates, which are rigid.

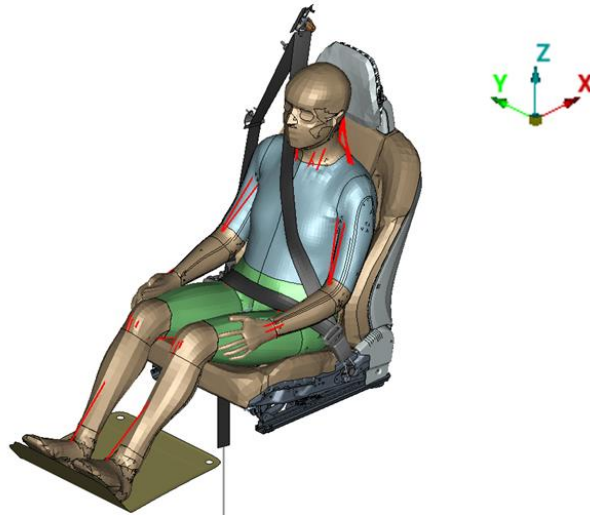


Figure 9: HBM model placed in the seat model in the reference position for the simulations

The musculature of the model consists of 1D Hill-type elements that were controlled by several closed loops PID controllers. In the case of this study, two controllers were used: one for the neck and one for the lumbar musculature. However, the model has also the possibility of using a controller for the leg's musculature and the arms musculature as well. This last controller is designed to be used if the HBM is placed in the simulation as the driver and has a steering wheel to put the arms on, so the model can replicate the force that an actual driver will do with his hands in case of a collision.

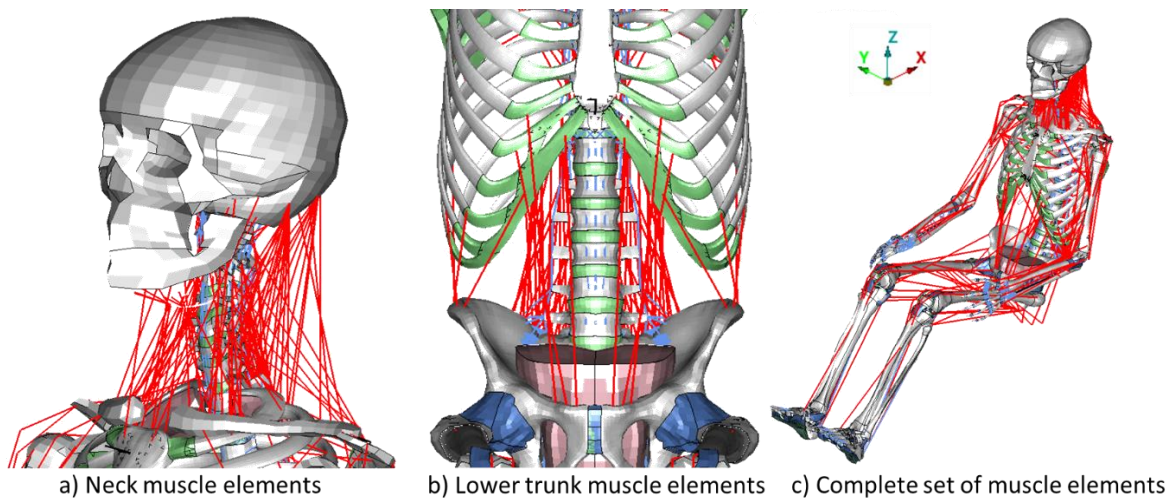


Figure 10: HBM muscle elements. Muscle elements are shown in red color and are shown without flesh for better visibility. However, flesh and soft tissue are used in the simulations.

The model has as well two types of feedback loops for the PID controllers for the muscles: MIMO (Multiple Input Multiple Output) and SIMO (Simple Input Multiple Output controllers). The MIMO controller is called MLF (Muscle Length Feedback) and it has the ability to control independently the length of each muscle and having as an input the length of each muscle as well. The SIMO controller is called APF (Angular Position Feedback) and it controls the length of each muscle but having just as an input the translations and rotations of the head. The MFL feedback loop emulates the stretch reflex in the muscles and the APF

emulates vestibular feedback from the central nervous system, which tries to stabilize the head in space [1].

For this study, the APF feedback loop was chosen with two PID controllers, one for the head and one for the lower trunk. More information about the controller can be found in the main document.

Regarding the environment in which the HBM is used, all the simulations were run using a model of a sled that is representative of an average size SUV as the boundary condition. This sled was equipped with a frontal passenger airbag, seat, and seatbelt in order to restraint properly the HBM and recreate a real environment. All the parts of this FE model were provided by Volvo Cars. All the pulses used for the different simulations were applied over the rigid sled model. All the pulses consisted of 6DOF (Degrees Of Freedom) time series that defined the x, y, z translations and x, y, z rotations of the sled during the simulation.

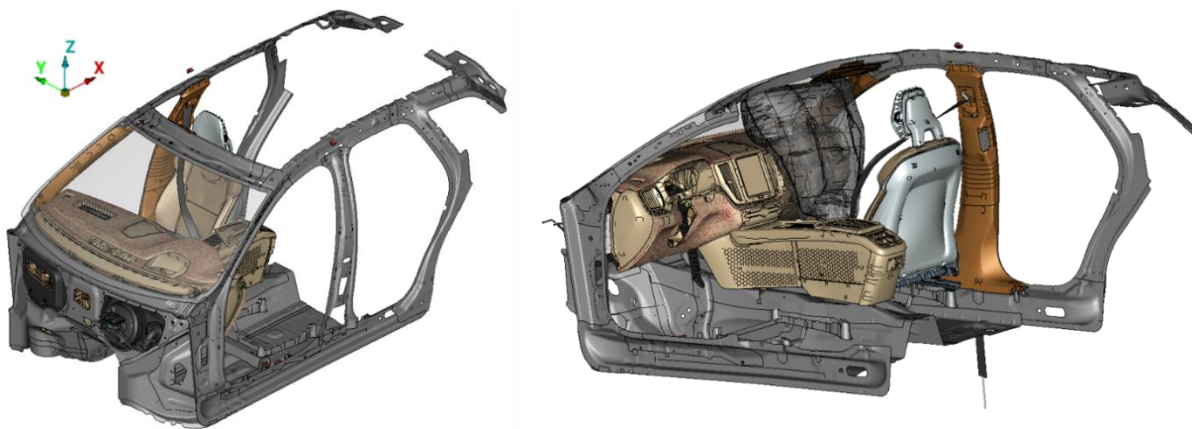


Figure 11: Sled model

Simulation Set-up

The model is placed in space in a way that the front of the car is heading towards the negative part of the x-axis. The coordinate system is defined as a right-handed coordinate system with x rearward, y to the right side, and z upward (Figure 3).

For the development of the study, two types of simulations were used: baseline (full-sequence) simulations and passive (in-crash) simulations.

All the baseline simulations had the active musculature controllers activated for the HBM and they all consist of three phases: initialization, pre-crash, and in-crash. These simulations were used as baseline simulations to study the influence of active musculature on injury risk prediction. The initialization process was used to reach an equilibrium state between the HBM and the surroundings and for stabilizing the signals in the HBM muscle controllers. Gravity was activated in this phase to have the most naturalistic posture for the HBM possible. The foam of the seat was squashed, and vibrations generated by the control signals were eliminated along the 300ms that this phase lasted.

The pre-crash phase was used to reproduce an evasive maneuver. A real pre-crash pulse provided from Emma Larsson's study [1] was used to simulate the motion of a real car and to recreate the position of a real human after the avoiding maneuver using the HBM model. In

this phase, the posture of the occupant was modified, and the active musculature was in action trying to stabilize the HBM simulating real lumbar and neck human musculature.

Lastly, the in-crash phase recreates a collision in which the airbag is deployed according to the type of crash and the retractor of the seatbelt. The pulses used for this phase were provided by Volvo Cars. The great majority of them followed standardized crashes from the Euro NCAP [3] and the IIHS (Insurance Institute for Highway Safety) [4]. All the pulses used for this study are frontal crashes. All the analysis was focused on the in-crash phase.

Once the baseline simulation was run, several passive simulations were created based on the initial simulation. These passive simulations had different parameters from the baseline one like the posture of the occupant at the end on the pre-crash, its velocities, the elements stresses, or the last signal of the controller for each muscle of the model; and they just simulated the in-crash phase.

This procedure was done to reduce the amount of computing time needed for each simulation. On average, the pre-crash maneuver lasted between 500 ms and 850 ms, and the in-crash lasted between 120 ms and 300 ms. Running a baseline simulation with all the three phases (initialization [300ms] + pre-crash[500-850ms] + in-crash [120-300]) meant running around 1300 ms of simulation. The number of CPUs (Central Processing Units) used per simulation was about 120. With this number of CPUs, running 1300 ms on average, the simulation time was about 7 full days of simulation. As described below, for this project at least 72 simulations needed to be simulated. If all the simulations had the three phases, it would have taken 72 weeks just to simulate, assuming that all the simulations run correctly and had no numerical errors. Even if we were able to run some in parallel, the amount of time needed for this project would not have been reasonable.

Simulating just the in-crash phase however just takes around one day on average, so setting just an in-crash simulation with the HBM placed according to the final position and velocities of the end of the pre-crash phase from the baseline simulation makes the use of simulation time much more efficient, having just to simulate 9 baseline simulations (9 weeks) and 64 passive runs (64 days).

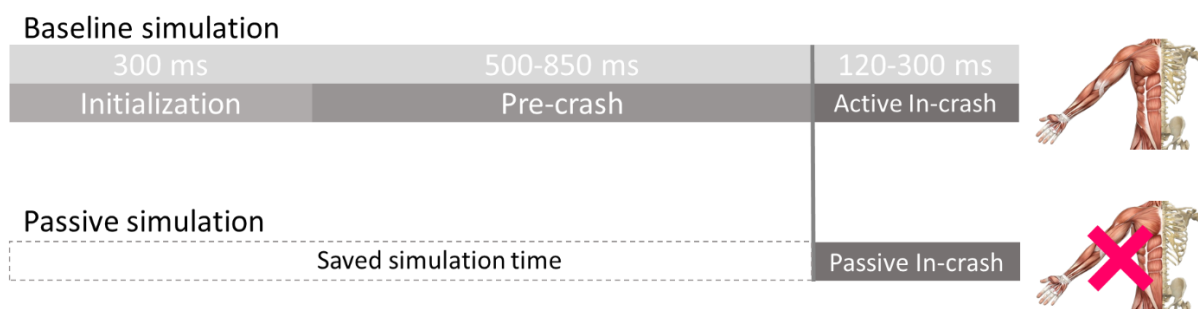


Figure 12: Baseline and passive simulations set-up diagram. In the passive simulations, the musculature was still there, just the controllers that manage the muscles length and force were deactivated.

Pre-crash and In-crash combinations

For this study, it was assumed that the evasive maneuver failed, and the car eventually entered an in-crash phase. Therefore, baseline simulations combined a pre-crash maneuver with an in-crash phase.

To select the most probable types of crashes for the different scenarios, [5] [6] [7] were used as a reference, as those three articles study the different crash possibilities in the scenarios

commented before. All the crash types were then matched with a standardized crash pulse from the Euro NCAP or the IIHS.

Combining the pre-crash maneuvers with the different collision tests results in the following pre-crash/crash matrix.

Table 5: Pre-crash and crash combination matrix

		Pre-crash maneuvers				
		Braking	Turn left	Turn right	Turn left & Braking	Turn right & Braking
Frontal In-crash	Full-Width Rigid Barrier					
	Moderate Overlap Frontal Test					
	Mobile Progressive Deformable Barrier					
	Passenger-side Small Overlap					

However, not all the combinations are equally likely to happen in a real-life scenario. The cells marked in blue show the combinations that happen more frequently in the previously described scenarios, so they were the combinations that were used for this study. More information about these combinations can be found in the main document. Also, with the selected combinations it is possible to compare the same in-crash phase with different pre-crash maneuvers to study the importance of the maneuver, and it is possible to study how different crash scenarios differ between them when they share the same pre-crash maneuver.

As mentioned before, from these baseline simulations, some extra passive runs will be created using different inputs from the full-event simulation such as the posture of the HBM or the velocity it had at the end of the pre-crash phase. The combinations that were simulated are the following ones:

Table 6: Combination of inputs for the different passive simulations

Passive simulation	HBM Inputs			
	Posture	Velocity	Stress	Muscle PID
0				
1				
2				
3				
4				
5				
6				

The inputs used for the HBM are the following:

- Posture: the posture of the HBM at the end of the pre-crash. It refers to the position of each node of the HBM at the end of the pre-crash. This information was extracted from the last state of the baseline simulation before entering the in-crash phase and then introduced to the new model using Python to manage the coordinates of each node.
- Velocity: it refers to the final velocity of each node of the HBM at the end of the pre-crash. For the passive simulations, it is an initial velocity that is set as a boundary condition for the in-crash simulation. This information was extracted from the last state of the baseline simulation before entering the in-crash phase and then introduced to the new model using Python to manage the velocity of each node. The initial velocities were defined using the *INITIAL_VELOCITY_NODE card from LS-DYNA.
- Stress: it stands for the stresses of all the solids, shells, and beams of the model at the end of the pre-crash. These stresses were obtained from the last state of the baseline simulation before entering the in-crash phase and then introduced to the new model using Python. The cards used to introduce this information in the model were *INITIAL_STRESS_SOLID, *INITIAL_STRESS_SHELL, and *INITIAL_STRESS_BEAM, respectively.
- Muscle PID: it stands for the muscle activity level on the last state of the baseline simulation. It is the last value of the signal of the PID controllers that manage the length and strength of each muscle. With the proposed setup for the simulations, three different cases were studied based on the muscle controllers:
 - Complete passive model: the HBM has no muscle activity, beam muscles do not work. This scenario represents a human that does not make any force with his muscles during the in-crash, there is no strength in the muscles, the body just moves due to its inertia and the movement of the car. Every passive simulation with no MPID (Muscle PID).
 - Passive model with MPID: the HBM retains the last signal from the PID controller, and the length and force of each muscle does not vary over time. It is assumed in this case that the stiffness of a human body does not change during the in-crash and stays constant with the last value of the pre-crash phase, as the in-crash phase lasts no more than 300 ms. All the simulations that have MPID as an input.
 - Active model: the HBM in this scenario has the ability to change the length and force of each muscle during the in-crash phase, but always with 20ms of delay, which represents the delay in a real human brain between an input is processed and the consequent muscle action is delivered. In this scenario, it is assumed that a human can vary the strength he is doing with the muscles during the in-crash. All the baseline simulations.

The objective of this configuration is to study the influence of each input parameter separately and see how each extra input parameter improves the response of the HBM compared to the baseline simulation.

Data analysis

To study the influence of active musculature on injury risk prediction and on the simulation output, the kinematics of the HBM and the injury risk prediction of the models were compared using three different methods.

Excursion comparison

A visual inspection of the different simulations was made in order to evaluate how the different inputs and the active musculature influence the head, chest, and pelvis excursions. Those excursions were plotted on the x-y and x-z planes to study the lateral and frontal displacements of the head, chest, and pelvis during the in-crash phase.

Kinematic comparison

The x, y, and z accelerations of the head, chest, and pelvis were also compared using cross-correlation from the software CORAplus 4.0.4 (CORrelation and Analysis) [8] to study how close passive simulations can get to the active baseline simulation based on the inputs used. This software calculates the level of correlation between two signals/time histories giving a result between 0 and 1 depending on the quality of the match. Rating 1 represents a perfect match with the predefined tolerances, and 0 means a poor match. The program offers two metrics to study how equal two curves are: the cross-correlation analysis and the corridor method.

The cross-correlation method analyses three characteristics of the signals: phase shift, size (amplitude), and shape of both curves to evaluate how close the signal is from the reference curve. These three parameters are also weighted, so the user can give more importance to one specific parameter.

The corridor method evaluates the deviation between two signals by means of corridor fitting. Four curves are defined around the reference signal to create an inner and an outer corridor. If the studied curve fits inside the inner corridor, a rating of 1 is assigned. If the curve is outside the outer corridor, a 0 rating is assigned.

The overall rating structure of the program is shown in the following figure.

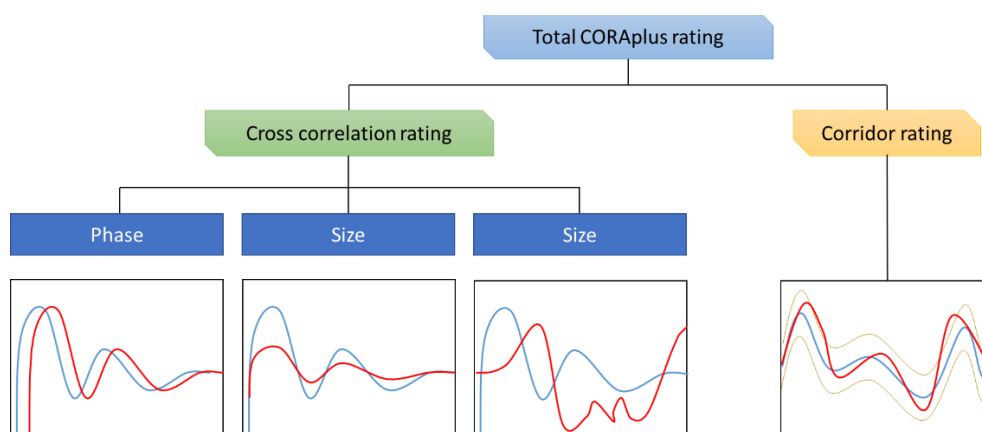


Figure 13: CORA rating structure

For this study, just the cross-correlation rating was used to evaluate the signals, as the corridor rating is designed to compare an average of real test curves with simulation results. The tests results have a standard deviation that can be used for setting up the corridor. In the case of this study, just single simulation curves were compared, so just the cross-correlation analysis was

made. The ratings of each parameter are shown in Table 3 and show the recommended configuration according to the CORAplus user's manual [8].

Table 7: CORA settings

Cross correlation rating	Weight
Phase	0.25
Size	0.25
Shape	0.5

To facilitate the interpretation of the CORA ratings, results were categorized as excellent, good, fair, and poor following the software manual [8].

Table 8: CORA rating categorization

Category	CORA rating interval
Excellent	$0.94 < \text{Rating} \leq 1$
Good	$0.8 < \text{Rating} \leq 0.94$
Fair	$0.58 < \text{Rating} \leq 0.8$
Poor	$0 \leq \text{Rating} \leq 0.58$

The signals used for this analysis were filtered using a CFC 60 (Channel Frequency Class 60 Hz), a commonly used low pass filter to reduce the amount of noise in crash test signals. The filtering was made to obtain clear signals and develop a correlation analysis based on the significant part of the signal and not on the noise that may be generated in the in-crash phase. X, Y, and Z accelerations were studied separately as the in-crash scenarios studied are all frontal and accelerations in the X-axis have a much higher amplitude than accelerations in Y and Z, which represent mainly vibrations or very little displacements that can be less representative than forwarding motion. To obtain a final rating, a weighted average was made between the three axes, giving a wight of 0.5 to X accelerations, 0.25 for Y accelerations, and 0.25 for Z accelerations.

Injury risk predictions

Lastly, injury risk indicators were compared between simulations that shared the same pre-crash and in-crash phases. Using a post-processing script, several injury risk values like HIC15, NIC, or Nij were obtained based on the kinematics of the model. Also, the HBM model has several strain models that generate relevant values to study. Going from the head of the model to the bottom, the following injury risk predictions were studied.

Regarding the head of the HBM, the brain strain model [9], HIC, and BrIC were used to evaluate the injury. According to S. Kleive [9] n, the brain strain model is suitable for head motions with translational and rotational kinematics, and it is more precise than HIC alone. The combination of the strain model, HIC, and BrIC was used to assess the injury risk difference between the active musculature model and the passive ones.

Regarding the neck, forces in the cross-sections of the neck were used combined with the Nij and the NIC. Nij is frequently used to assess neck injury in high-velocity impacts. NIC is used to assess neck injuries caused by pressure gradients, however, it is more precise in rear-end

impacts, so it will be analyzed in combination with the previously mentioned injury risk predictors.

Thirdly, regarding the thorax, the rib fracture model [10] was used to assess the integrity of the rib cage. The risk of fracture of different amounts of ribs based on the strain of the ribs was used to compare the baseline simulations with the passive ones.

Concerning the lumbar area, lumbar forces were studied.

III. RESULTS

Braking + Full-Width rigid Barrier

Regarding excursions of the head, chest, and pelvis; there are two differentiated groups regarding passive simulations: the passive simulation with no inputs and the passive simulations that have the posture of the HBM at the end of the pre-crash as input.

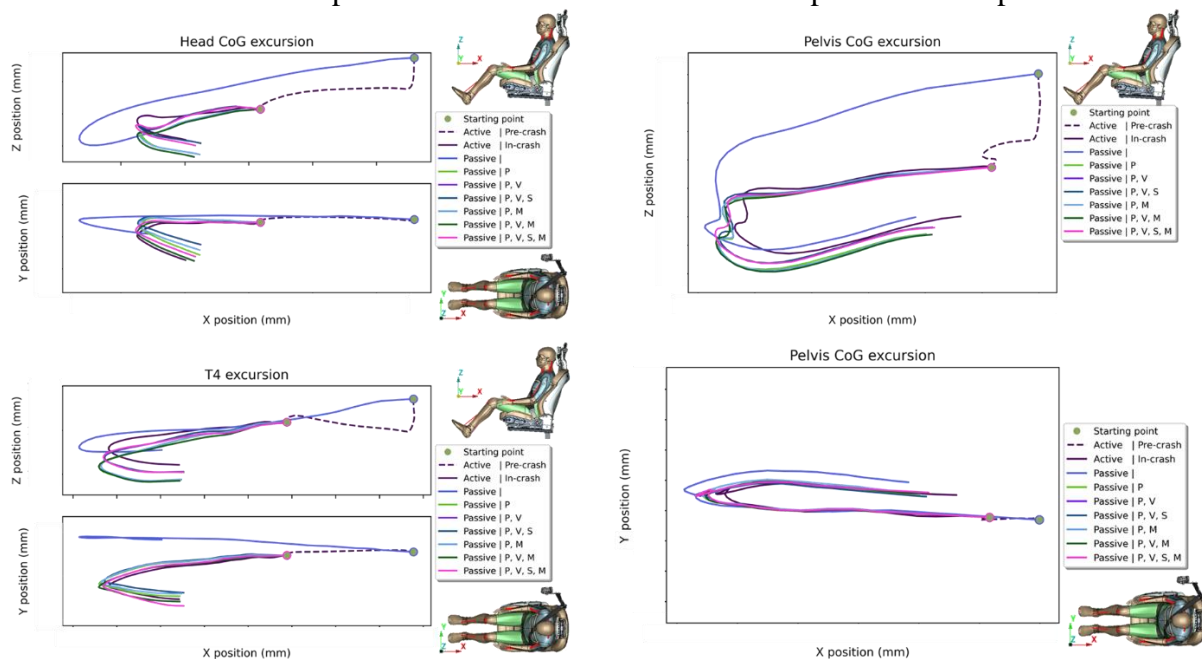


Figure 14: Excursions of the HBM. Braking and Full-Width Rigid Barrier

It can be observed that the excursions of the head, chest, and pelvis in the passive simulation with no inputs are very different compared to the rest of the passive simulations.

Regarding the rest of the passive simulations, there are two differentiated groups of excursions: passive simulations with stresses and passive simulations with no stresses. The excursions of the simulations that have stresses seem to be closer to the excursions of the baseline simulation.

Concerning injury criteria, all the results have been normalized using the baseline simulation value as a reference. Consequently, all the baseline injury risk predictions have value 1 and the passive simulation values oscillate around the value 1. Thus, the variations of the passive simulations with respect to the active one can be observed.

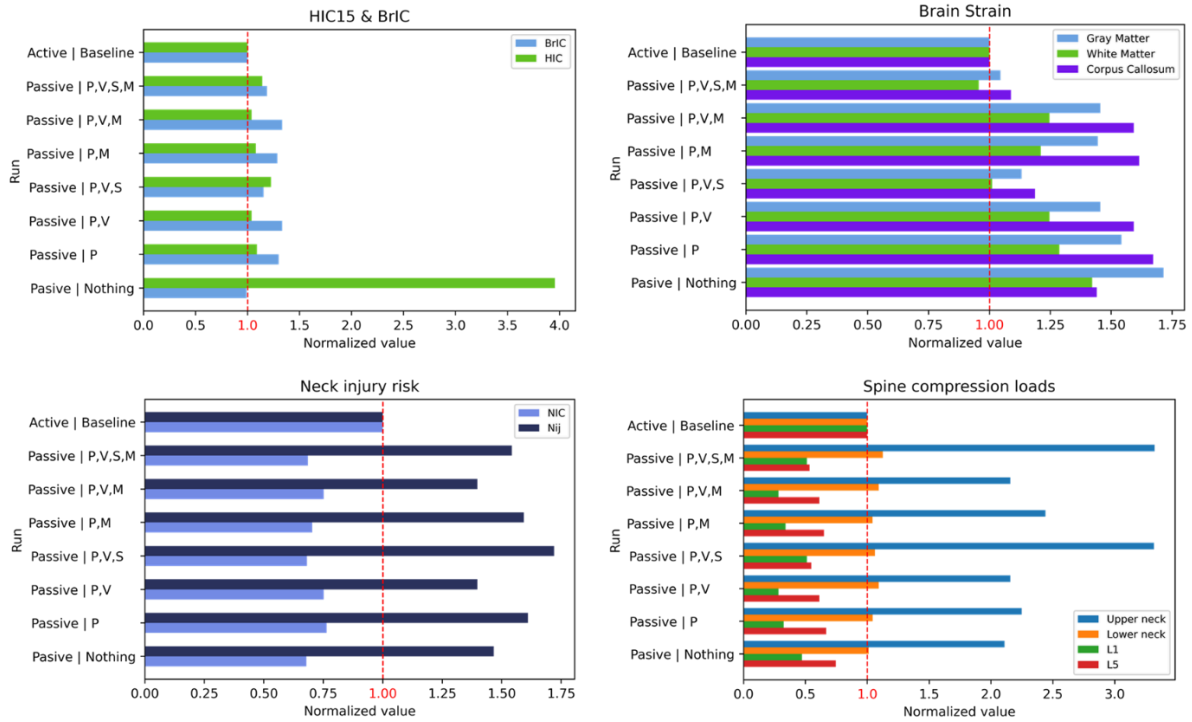


Figure 15: Injury risk predictions. Braking and Full Width Rigid Barrier

Regarding the head, HIC 15 ms is greatly overpredicted compared to the baseline model in the simulation with no inputs, and the strains in the brain are the largest of all the passive simulations. It can be appreciated that adding extra inputs improves the brain strain prediction, obtaining the closest values when posture, velocity, and stresses are added to the simulation. Muscle activity level (MPID) however seems to not affect the results.

Regarding the neck and the spine, compression loads in the upper neck are overpredicted compared to the baseline model in all cases and lumbar compression loads are underestimated. These predictions get the closest values when only posture and initial velocities of the HBM are included. The NIC and Nij are wrongly predicted compared to the baseline model by the passive simulations compared to the baseline. The closest values are obtained for posture and velocity input simulation.

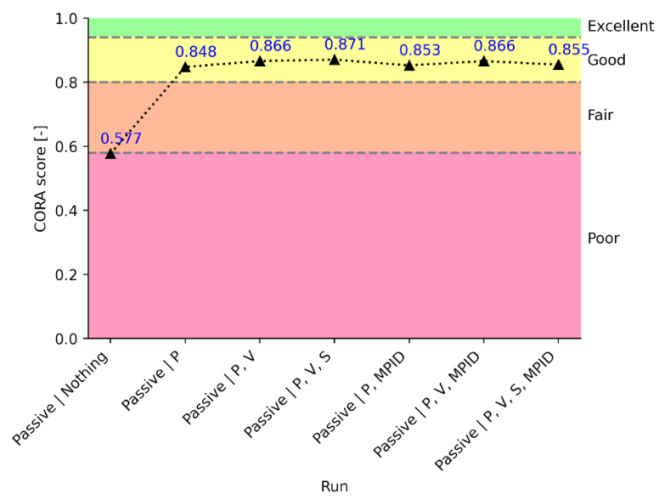


Figure 16: CORAplus acceleration ratings. Braking and Full Width Rigid Barrier

Lastly, regarding the CORAplus ratings, there is a big improvement if the posture of the occupant is added as an input in the passive simulation, changing the overall rating from “Poor” to “Good”. Adding velocity or velocity and stress improves the rating a bit more, but the passive model is not able to reproduce the accelerations of the active model with an “Excellent” rating. Muscle level activity does not improve results. Moreover, on some occasions adding the MPID worsens the rating.

Results were obtained as well for all the simulation combinations proposed for the analysis. Due to the limited length of the document, these results will not be shown but can be consulted in the main document.

IV. CONCLUSIONS

The study compared excursions, accelerations, and injury risk predictions between an active HBM and passive HBMs to study the influence of active musculature over injury risk predictions. The study concluded that active musculature may not influence the injury risk predictions, excursions, and accelerations; as there is not a significant difference in results between the closest passive simulation and that same simulation with muscle activity level. Moreover, predictions of the passive models related to the spine were very different from those of the active model and it is right on the neck and the lumbar spine where the active musculature act. However, the study also showed that the methodology used to recreate the active in-crash phase is not able to reproduce closely the baseline in-crash phase, as the maximum CORA rating was 0.873 and the excursions of the passive models differed considerably from the ones of the active baseline.

Secondly, the study showed that in case using active musculature in the HBM is not possible, adding posture improves significantly the results, making the results of the simulation closer to the ones that would have been obtained. Furthermore, if velocity and stresses of the HBM are available, they might be added as well to get even closer results even though they seem to be not as essential as the posture of the occupant. Muscle activity level (MPID) however does not influence the results and it might even worsen the values obtained.

If passive simulations are used for the study, head and brain injury seem to be well predicted compared to the baseline model if some inputs are included. However, neck and spine injury risk predictions should not be used if the model is passive; instead, active musculature should be considered, as the muscles of the HBM act directly on the neck and the lower trunk of the model.

V. REFERENCES

- [1] E. Larsson, J. Iraeus, J. Fice, B. Pipkorn, L. Jakobsson, E. Brynskog, K. Brodin y J. Davidsson, «Active Human Body Model Predictions Compared to Volunteer Response in Experiments with Braking,» 2019.
- [2] D. Robbins, *Anthropometric specifications for mid-sized male dummy*, Washington, DC: US Department of Transportation DTNH22-80-C-07502, 1983.

- [3] Euro NCAP, «Adult occupant protection,» Euro NCAP, 2021. [En línea]. Available: <https://www.euroncap.com/en/vehicle-safety/the-ratings-explained/adult-occupant-protection/>. [Último acceso: 21 06 2021].
- [4] IIHS HLDI, «About our tests,» 2021. [En línea]. Available: <https://www.iihs.org/ratings/about-our-tests>. [Último acceso: 21 06 2021].
- [5] Luke E. Riexinger, Hampton C. Gabler, «A Preliminary Characterisation of Driver Manoeuvres in Road Departure Crashes,» *IRCOBI*, vol. 79, n° 18, pp. 484-492, 2018.
- [6] Luke E. Riexinger, Rini Sherony, Hampton C. Gabler, «A Preliminary Characterisation of Driver Evasive Manoeuvres in Cross-Centreline Vehicle-to-Vehicle Collisions,» *IRCOBI*, vol. 15, n° 19, pp. 58-69, 2019.
- [7] Scanlon, John & Kusano, Kristofer & Gabler, Hampton., «Analysis of Driver Evasive Maneuvering Prior to Intersection Crashes Using Event Data Recorders,» *Traffic injury prevention*, pp. 182-189, 2015.
- [8] C. Thunert, «CORApplus Release 4.0.4 User's Manual,» 2017.
- [9] S. Kleiven, «Evaluation of head injury criteria using a finite element model validated against experiments on localized brain motion, intracerebral acceleration, and intracranial pressure,» *International Journal of Crashworthiness*, vol. 1, n° 11, pp. 65-79, 2006.
- [10] Johan Iraeus, Linus Lundin, Simon Storm, Amanda Agnew, Yun-Seok Kang, Andrew Kemper, Devon Albert, Sven Holcombe & Bengt Pipkorn, «Detailed subject-specific FE rib modeling for fracture prediction,» *Traffic Injury Prevention*, vol. 20, n° sup2, pp. S88-S95, 2019.



COMILLAS
UNIVERSIDAD PONTIFICIA

ICAI

MÁSTER UNIVERSITARIO EN INGENIERÍA
INDUSTRIAL

TRABAJO FIN DE MÁSTER

INFLUENCE OF ACTIVE MUSCULATURE ON INJURY
RISK PREDICTION ON FRONTAL CRASHES

Autor: Pablo Lozano Gil

Director: Francisco José López Valdés

Madrid
Julio de 2021

Contents

List of figures.....	5
List of tables.....	9
1.- Introduction	11
1.1.- Review of the state of the art, motivation, and objectives.....	12
State of art	13
Motivation	18
Project Aims	18
2.- Methodology	19
2.1.- Simulation set-up	22
2.2.- Pre-crash and In-crash combinations.....	23
2.3.- Active baseline simulation set-up	26
2.4.- Passive simulation set-up	29
HBM	29
Seat	29
Seatbelt.....	29
2.5.- Data analysis	31
Excursion comparison.....	31
Kinematic comparison	31
Injury risk predictions	32
3.- Results	35
3.1.- Braking + Full-Width rigid Barrier.....	35
3.2.- Braking + Moderate Overlap Frontal Test	40
3.3.- Braking + Mobile Progressive Deformable Barrier	46
3.4.- Turn right and braking + Passenger-side Small Overlap.....	52
3.5.- Turn left + Moderate Overlap Frontal Test	58
3.6.- Turn left and braking + Moderate Overlap Frontal Test	64
3.7.- Turn left + Mobile Progressive Deformable Barrier	70
3.8.- Turn left and Braking+ Mobile Progressive Deformable Barrier	76
4.- Discussion	83
4.1.- Influence of the pre-crash maneuver.....	83
4.2.- Influence of the in-crash phase.....	84
4.2.- Limitations	87
5.- Conclusions	89
References	91
Appendix A: HBM controller parameters.....	95
Appendix B: Pre-crash and in-crash combinations	97
Highway	97
Secondary road	99

Intersection.....	100
Appendix C: Sustainable Development Goals	103

List of figures

Figure 1: Levels of automation for on-road motor vehicles [12]	11
Figure 2: Principal causes of death in the world in 2019 (Obtained from https://vizhub.healthdata.org/gbd-compare/)	12
Figure 3: Evolution of fatalities in traffic accidents. Spain, 1960-2019 [16]	13
Figure 4: Trajectories and final position of 3-point belted passenger without classical "submarining" (a) vs a "submarining" 3-point belted passenger (b) [33]	14
Figure 5: Trajectories and final position of 3-point belted passenger without classical "submarining" (a) vs a "submarining" 3-point belted passenger (b) [33]	14
Figure 6: Harmonized Hybrid III 50th percentile Dummy	16
Figure 7: Toyota THUMS simulated in a frontal crash [22]	17
Figure 8: SAFER A-HBM [23]	17
Figure 9: HBM model placed in the seat model in the reference position for the simulations	19
Figure 10: HBM muscle elements. Muscle elements are shown in red color and are shown without flesh for better visibility. However, flesh and soft tissue are used in the simulations.	20
Figure 11: Sled model.....	21
Figure 12: Interior of the sled with all the restraint systems	21
Figure 13: Baseline and passive simulations set-up diagram. In the passive simulations, the musculature was still there, just the controllers that manage the muscles length and force were deactivated.	23
Figure 14: Passenger seat.....	26
Figure 15: HBM nominal position	27
Figure 16: Seat foam before and after the squashing deformation	27
Figure 17: HBM nominal position with seatbelt.....	28
Figure 18: Comparison between the baseline simulation model at the end of the pre-crash (a) and the new model extracted from the previous baseline simulation (b)	30
Figure 19: CORA rating structure	31
Figure 20: Head CoG excursion. Braking and Full Width Rigid Barrier	35
Figure 21: Chest excursion. Braking and Full Width Rigid Barrier	35
Figure 22: Pelvis CoG excursion. XZ plane. Braking and Full Width Rigid Barrier	36
Figure 23: Pelvis CoG excursion. XY plane. Braking and Full Width Rigid Barrier	36
Figure 24: HIC 15ms and BrIC. Braking and Full Width Rigid Barrier	37
Figure 25: Brain strain. Braking and Full Width Rigid Barrier	37
Figure 26: Neck injury risk. Braking and Full Width Rigid Barrier.....	38
Figure 27: Spine compression loads. Braking and Full Width Rigid Barrier	38
Figure 36: CORAplus acceleration ratings. Braking and Full Width Rigid Barrier	39
Figure 37: Head CoG excursion. XZ plane. Braking and Moderate Overlap Frontal Test	40
Figure 38: Head CoG excursion. XY plane. Braking and Moderate Overlap Frontal Test	40
Figure 39: Chest excursion. XZ plane. Braking and Moderate Overlap Frontal Test.....	41
Figure 40: Chest excursion. XY plane. Braking and Moderate Overlap Frontal Test.....	41
Figure 41: Pelvis CoG excursion. XZ plane. Braking and Moderate Overlap Frontal Test	42

Figure 42: Pelvis CoG excursion. XY plane. Braking and Moderate Overlap Frontal Test	42
Figure 43: HIC 15ms and BrIC. Braking and Moderate Overlap Frontal Test	43
Figure 44: Brain strain. Braking and Moderate Overlap Frontal Test	43
Figure 45: Neck injury risk. Braking and Moderate Overlap Frontal Test	44
Figure 46: Spine compression loads. Braking and Moderate Overlap Frontal Test	44
Figure 47: CORAplus acceleration ratings. Braking and Moderate Overlap Frontal Test	45
Figure 48: Head CoG excursion. XZ plane. Braking and Mobile Progressive Deformable Barrier	46
Figure 49: Head CoG excursion. XY plane. Braking and Mobile Progressive Deformable Barrier	46
Figure 50: Chest excursion. XZ plane. Braking and Mobile Progressive Deformable Barrier ..	47
Figure 51: Chest excursion. XY plane. Braking and Mobile Progressive Deformable Barrier ..	47
Figure 52: Pelvis CoG excursion. XZ plane. Braking and Mobile Progressive Deformable Barrier	48
Figure 53: Pelvis CoG excursion. XY plane. Braking and Mobile Progressive Deformable Barrier	48
Figure 54: HIC 15ms and BrIC. Braking and Mobile Progressive Deformable Barrier	49
Figure 55: Brain strain. Braking and Mobile Progressive Deformable Barrier	49
Figure 56: Neck injury risk. Braking and Mobile Progressive Deformable Barrier	50
Figure 57: Spine compression loads. Braking and Mobile Progressive Deformable Barrier ..	50
Figure 58: CORAplus acceleration ratings. Braking and Mobile Progressive Deformable Barrier	51
Figure 59: Head CoG excursion. XZ plane. Turn right and braking + Passenger-side Small Overlap	52
Figure 60: Head CoG excursion. XY plane. Turn right and braking + Passenger-side Small Overlap	52
Figure 61: Chest excursion. XZ plane. Turn right and braking + Passenger-side Small Overlap	53
Figure 62: Chest excursion. XY plane. Turn right and braking + Passenger-side Small Overlap	53
Figure 63: Pelvis CoG excursion. XZ plane. Turn right and braking + Passenger-side Small Overlap	54
Figure 64: Pelvis CoG excursion. XY plane. Turn right and braking + Passenger-side Small Overlap	54
Figure 65: HIC 15ms and BrIC. Turn right and braking + Passenger-side Small Overlap	55
Figure 66: Brain strain. Turn right and braking + Passenger-side Small Overlap	55
Figure 67: Neck injury risk. Turn right and braking + Passenger-side Small Overlap	56
Figure 68: Spine compression loads. Turn right and braking + Passenger-side Small Overlap	56
Figure 69: CORAplus acceleration ratings. Turn right and braking + Passenger-side Small Overlap	57
Figure 70: Head CoG excursion. XZ plane. Turn left + Moderate Overlap Frontal Test	58
Figure 71: Head CoG excursion. XY plane. Turn left + Moderate Overlap Frontal Test	58
Figure 72: Chest excursion. XZ plane. Turn left + Moderate Overlap Frontal Test	59

Figure 73: Chest excursion. XY plane. Turn left + Moderate Overlap Frontal Test	59
Figure 74: Pelvis CoG excursion. XZ plane. Turn left + Moderate Overlap Frontal Test.....	60
Figure 75: Pelvis CoG excursion. XY plane. Turn left + Moderate Overlap Frontal Test	60
Figure 76: HIC 15ms and BrIC. Turn left + Moderate Overlap Frontal Test	61
Figure 77: Brain strain. Turn left + Moderate Overlap Frontal Test	61
Figure 78: Neck injury risk. Turn left + Moderate Overlap Frontal Test	62
Figure 79: Spine compression loads. Turn left + Moderate Overlap Frontal Test	62
Figure 80: CORAplus acceleration ratings. Turn left + Moderate Overlap Frontal Test	63
Figure 81: Head CoG excursion. XZ plane. Turn left and Braking + Moderate Overlap Frontal Test.....	64
Figure 82: Head CoG excursion. XY plane. Turn left and Braking + Moderate Overlap Frontal Test.....	64
Figure 83: Chest excursion. XZ plane. Turn left and Braking + Moderate Overlap Frontal Test	65
Figure 84: Chest excursion. XY plane. Turn left and Braking + Moderate Overlap Frontal Test	65
Figure 85: Pelvis CoG excursion. XZ plane. Turn left and Braking + Moderate Overlap Frontal Test.....	66
Figure 86: Pelvis CoG excursion. XY plane. Turn left and Braking + Moderate Overlap Frontal Test.....	66
Figure 87: HIC 15ms and BrIC. Turn left and Braking + Moderate Overlap Frontal Test.....	67
Figure 88: Brain strain. Turn left and Braking + Moderate Overlap Frontal Test.....	67
Figure 89: Neck injury risk. Turn left and Braking + Moderate Overlap Frontal Test.....	68
Figure 90: Spine compression loads. Turn left and Braking + Moderate Overlap Frontal Test	68
Figure 91: CORAplus acceleration ratings. Turn left and Braking + Moderate Overlap Frontal Test.....	69
Figure 92: Head CoG excursion. XZ plane. Turn left + Mobile Progressive Deformable Barrier	70
Figure 93: Head CoG excursion. XY plane. Turn left + Mobile Progressive Deformable Barrier	70
Figure 94: Chest excursion. XZ plane. Turn left + Mobile Progressive Deformable Barrier ...	71
Figure 95: Chest excursion. XY plane. Turn left + Mobile Progressive Deformable Barrier ...	71
Figure 96: Pelvis CoG excursion. XZ plane. Turn left + Mobile Progressive Deformable Barrier	72
Figure 97: Pelvis CoG excursion. XY plane. Turn left + Mobile Progressive Deformable Barrier	72
Figure 98: HIC 15ms and BrIC. Turn left + Mobile Progressive Deformable Barrier	73
Figure 99: Brain strain. Turn left + Mobile Progressive Deformable Barrier	73
Figure 100: Neck injury risk. Turn left + Mobile Progressive Deformable Barrier	74
Figure 101: Spine compression loads. Turn left + Mobile Progressive Deformable Barrier ...	74
Figure 102: CORAplus acceleration ratings. Turn left + Mobile Progressive Deformable Barrier	75

Figure 103: Head CoG excursion. XZ plane. Turn left and Braking + Mobile Progressive Deformable Barrier	76
Figure 104: Head CoG excursion. XY plane. Turn left and Braking + Mobile Progressive Deformable Barrier	76
Figure 105: Chest excursion. XZ plane. Turn left and Braking + Mobile Progressive Deformable Barrier.....	77
Figure 106: Chest excursion. XY plane. Turn left and Braking + Mobile Progressive Deformable Barrier.....	77
Figure 107: Pelvis CoG excursion. XZ plane. Turn left and Braking + Mobile Progressive Deformable Barrier	78
Figure 108: Pelvis CoG excursion. XY plane. Turn left and Braking + Mobile Progressive Deformable Barrier	78
Figure 109: HIC 15ms and BrIC. Turn left and Braking + Mobile Progressive Deformable Barrier	79
Figure 110: Brain strain. Turn left and Braking + Mobile Progressive Deformable Barrier	79
Figure 111: Neck injury risk. Turn left and Braking + Mobile Progressive Deformable Barrier	80
Figure 112: Spine compression loads. Turn left and Braking + Mobile Progressive Deformable Barrier.....	80
Figure 113: CORAplus acceleration ratings. Turn left and Braking + Mobile Progressive Deformable Barrier	81
Figure 114: Influence of the pre-crash maneuver with Moderate Overlap Frontal Test in-crash	83
Figure 115: Influence of the pre-crash maneuver with Mobile Progressive Deformable Barrier in-crash.....	84
Figure 116: Influence of the crash pulse having Braking as pre-crash maneuver.....	85
Figure 117: Influence of the crash pulse having Turning left and Braking as pre-crash maneuver	85
Figure 118: Influence of the crash pulse having Turning left as pre-crash maneuver	86
Figure 119: PID controller diagram [32].....	95
Figure 120: Highway crash scenario	97
Figure 121: Option 1. Braking into Full-Width Rigid Barrier	98
Figure 122: Option 2. Turning right into Passenger-side Small Overlap.....	98
Figure 123: Option 3. Turning left and Moderate Overlap Frontal Crash.....	99
Figure 124: Secondary road crash scenario	99
Figure 125: Option 4. Turning left into Mobile Progressive Deformable Barrier	100
Figure 126: Option 5. Turning right and Passenger-side Small Overlap	100
Figure 127: Straight Crossing Path (SCP) and possible crash	101
Figure 128: Left Turn Path / Opposite Direction (LTAP/OD) and possible crash	102
Figure 129: Left Turn Across Path / Lateral Direction (LTAP/LD) and possible crash.....	102

List of tables

Table 1: Pre-crash and crash combination matrix	24
Table 2: Combination of inputs for the different passive simulations	24
Table 3: CORA settings	32
Table 4: CORA rating categorization	32
Table 9: HBM controller parameters values [1]	95

1.- Introduction

The mobility sector is heading towards autonomous driving at a very high pace. It is not uncommon to see new prototypes of vehicles that are able to maneuver autonomously or even drive on their own on some highways. According to SAE International [1], there are 5 different levels of automation for on-road motor vehicles.



SAE J3016™ LEVELS OF DRIVING AUTOMATION

	SAE LEVEL 0	SAE LEVEL 1	SAE LEVEL 2	SAE LEVEL 3	SAE LEVEL 4	SAE LEVEL 5
What does the human in the driver's seat have to do?	You are driving whenever these driver support features are engaged – even if your feet are off the pedals and you are not steering			You are not driving when these automated driving features are engaged – even if you are seated in "the driver's seat"		
	You must constantly supervise these support features; you must steer, brake or accelerate as needed to maintain safety			When the feature requests, you must drive	These automated driving features will not require you to take over driving	
What do these features do?	These are driver support features			These are automated driving features		
	These features are limited to providing warnings and momentary assistance	These features provide steering OR brake/acceleration support to the driver	These features provide steering AND brake/acceleration support to the driver	These features can drive the vehicle under limited conditions and will not operate unless all required conditions are met	This feature can drive the vehicle under all conditions	
Example Features	<ul style="list-style-type: none"> • automatic emergency braking • blind spot warning • lane departure warning 	<ul style="list-style-type: none"> • lane centering OR • adaptive cruise control 	<ul style="list-style-type: none"> • lane centering AND • adaptive cruise control at the same time 	<ul style="list-style-type: none"> • traffic jam chauffeur 	<ul style="list-style-type: none"> • local driverless taxi • pedals/steering wheel may or may not be installed 	<ul style="list-style-type: none"> • same as level 4, but feature can drive everywhere in all conditions

Figure 17: Levels of automation for on-road motor vehicles [2]

Level 0 stands for the lower level of automation. At this level, the car does not have control over any of the actuators and can just assist the driver with information. One example of a system that could be used in this level would be the LDW (Lane Departure Warning), a system that informs the driver when he is leaving the lane but does not act over the vehicle. In further levels, the car starts having some ways to act over the actuators, but it is the driver the one in charge of driving safely through the road. Until level 5 of automation, a level in which a car is considered to be completely autonomous and can drive safely in different environments in all conditions.

Nowadays cars are almost reaching level 3 of automation, but there are a lot of companies that are showing their new concepts in autonomous driving. All this, points to seeing autonomous vehicles on the roads of the coming years, which implies that traditional cars will coexist with autonomous vehicles on the streets. The problem with this coexistence is that due to human errors or different possible situations, autonomous cars might need to do evasive maneuvers in some situations in order to avoid a possible crash.

INTRODUCTION

This situation entails that cars will act in an emergency making an evasive maneuver that has not been planned by the driver nor the passengers. This evasive maneuver could affect the occupant's posture inside the car, potentially also affecting the injury they may have in the case that the evasive maneuver fails and the car ends in a collision. This challenge is what motivates this study and one of the main objectives will be to study how the change of posture in the in-crash phase affects the injury risk prediction. This study will be performed using the finite element method and an active Human Body Model (HBM) to simulate different scenarios with different pre-crash maneuvers to see the influence of active musculature over the injury risk of the occupant.

1.1.- Review of the state of the art, motivation, and objectives

The concern about human health has always been one of the most important issues humanity has faced. Historically, there have been several epidemics and pandemics that generated an enormous number of deaths. These global health issues are always treated as urgent issues, due to the high level of mortality they cause. However, there is a big cause of death, which has been affecting humanity for approximately 125 years, which is traffic accidents.

Traffic accidents represented the 7th cause of death in the world in 2019 [3]. This is a matter of concern, as road traffic has existed since the 19th century.

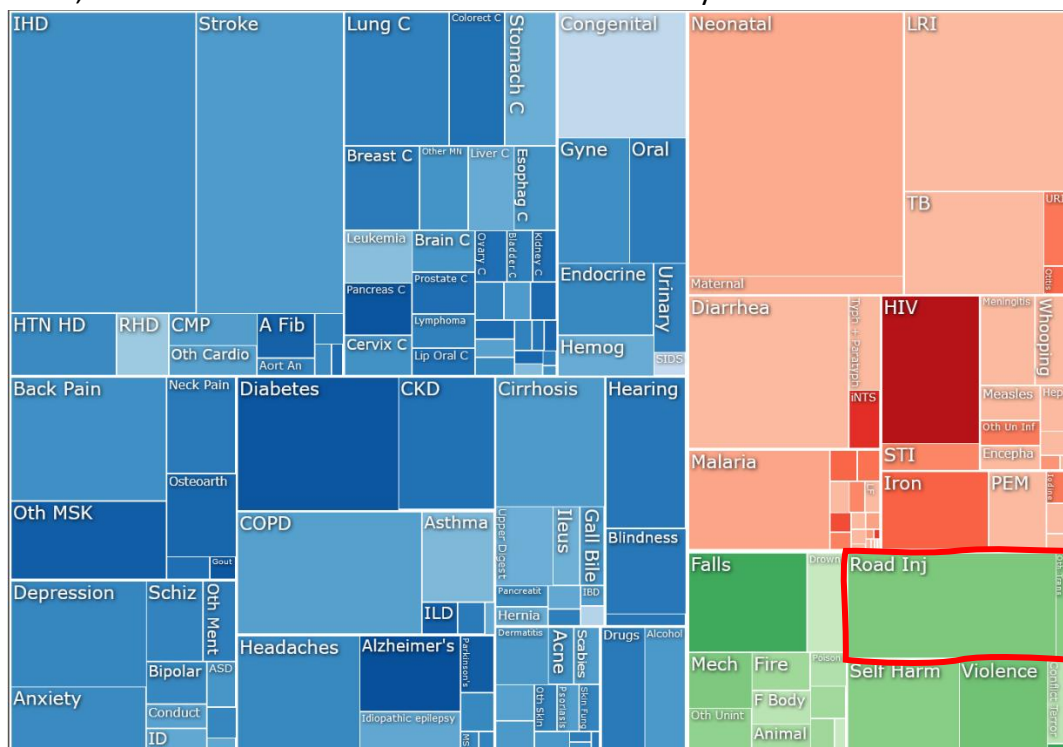


Figure 18: Principal causes of death in the world in 2019 (Obtained from <https://vizhub.healthdata.org/gbd-compare/>)

Bridget Driscoll is the first road traffic mortal victim [4]. Since her death, there have been numerous car accidents. The current estimation states that every year, there are 1.35 million

mortal victims due to traffic road injuries [5]. Considering the long development that road traffic and current vehicles have, this presents a huge problem.

For instance, only in Spain, the number of fatal accidents increased until the year 1989, reaching a record of 9344 people killed in road traffic accidents [6]. After that year, a big concern about road traffic deaths appeared, and several measures were applied to reduce the number of victims.

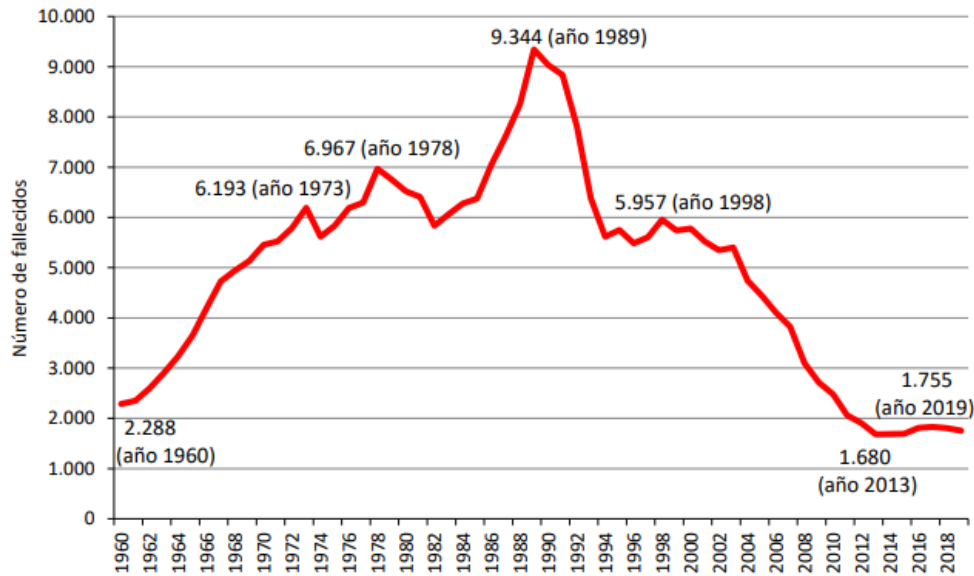


Figure 19: Evolution of fatalities in traffic accidents. Spain, 1960-2019 [6]

In 2019 in Spain the number of fatalities represents 1% of the total number of road traffic accidents, injured hospitalized people represent 6%, and injured non-hospitalized people represent 93% [6]. This evolution shows the improvement in safety measures, and it shows the current great concern about traffic injuries, which has brought up some global initiatives like SUM4all (Sustainable Mobility For All). They have the objective of reducing the number of traffic victims around the globe and they provide personalized recommendations in road traffic matters to make mobility safe, sustainable, and accessible for everyone.

As mentioned before, not only the mortal victims present a concerning issue. Non-fatal victims are also a big problem, due to the hard recovery that some injuries require, as well as the money invested in those recoveries.

With all these facts, it seems reasonable to study in detail how the forces and accelerations generated in a crash affect the human body.

State of art

Injury biomechanics is the science of forces acting on a biological structure and the mechanisms of resulting pathologies. Regarding automotive safety, there are three principal fields of study: in-crash safety, pre-crash safety, and integrated safety. In-crash safety is focused on mitigating injury in case of a collision, it acts once the crash has started. Pre-crash safety however focuses on avoiding the crash. Pre-crash safety systems actuate before the

INTRODUCTION

crash, operating over some controls of the car, helping the driver at the time of doing an emergency maneuver, or even avoiding the collision in a completely autonomous way. Lastly, integrated safety focuses on the integration between pre-crash and in-crash safety, studying the full sequence of a crash, starting from the pre-crash scenario, then the in-crash, and finally the post-crash.

The initial studies of biomechanics were focused on passive safety systems, developing the first seatbelt model back in 1940. The first official patent is attributed to the Swedish mechanical engineer from Volvo Cars, Nils Bohlin, who patented the three-point seatbelt that is used in cars nowadays [7]. The development of the concept of injury threshold started with John Stapp in the 1960s with his experiments in which he put himself on a sled and tested several decelerations over his own body to experiment how decelerations could affect the human body [8].

In 1970 the epidemiologist William Haddon published several articles in which he showed a completely different approach to the problem of road traffic injury. He was able to explain car collisions using the epidemiological triad in which the environment was the road full of cars in movement (with energy), the vectors were the cars and the host was the occupant of the vehicle. With this methodology, he concluded that injuries were caused by an uncontrolled energy transmission to the occupant. He also differentiated between accident and collision.

In 1975, Diemeter Adomeit and Alfred Heger wrote one of the most relevant articles for the development of restraint systems: *Motion Sequence Criteria and Design Proposals for Restraint Devices in Order to Avoid Unfavorable Biomechanic Conditions and Submarining*. The position of the occupant and the way in which he is restrained are extremely important to avoid injury in the case of a collision. They studied different variables that affect the motion and kinematics of the occupant in a crash and developed some recommendations to avoid unfavorable biomechanics conditions and submarining.

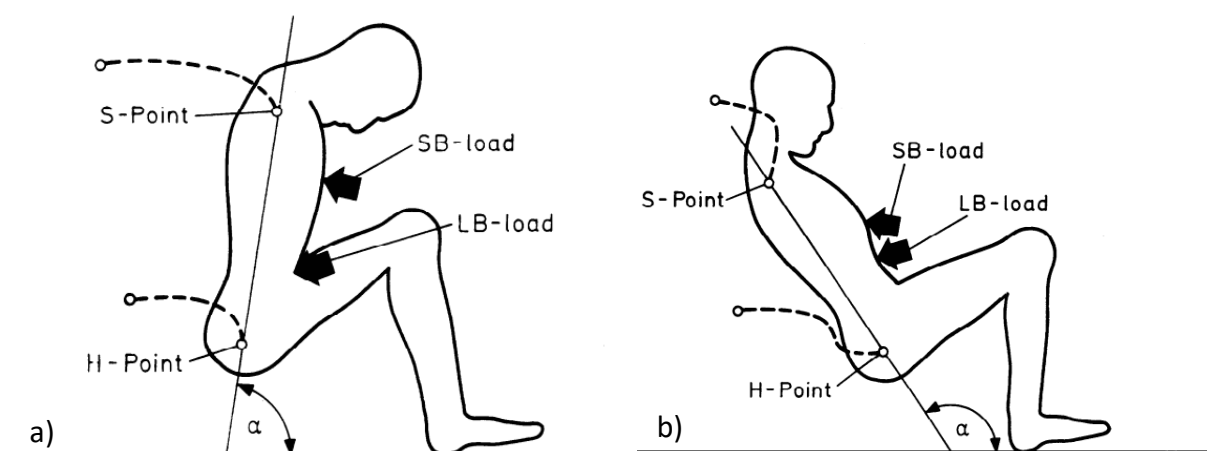


Figure 20: Trajectories and final position of 3-point belted passenger without classical "submarining" (a) vs a "submarining" 3-point belted passenger (b) [33]

With this information, several 3-point belts were developed with different levels of technology to approach the kinematic proposed by Adomeit. Firstly, the belt implemented in cars was a standard 3-point belt that limited the frontal excursion of the occupant inside the car blocking the belt in case of a collision.

Modern seatbelts include pretensioners and load limiters. Pretensioners have the objective to adjust occupants into a safer seating position in case of a collision before the deployment of the airbag raising as well the compliance of the restraint system [9] using a pyrotechnic device that retracts both the lap belt and the shoulder belt, forcing the hip and the rib cage to move towards the back of the seat, in order to couple the occupant's velocity with the vehicle's velocity. Load limiters have the mission to control the maximum force the body is receiving from the seatbelt in the case of a crash. In the event of a crash, they protect the occupant by limiting the force transmitted to the occupant to a predefined maximum. This can be made with a torsion bar, which releases webbing gradually, so the force keeps a constant value below the injury limit.

Another passive safety system is the airbag. It was developed after the seatbelt and it consists of a bag positioned on the interior frontal part of the car, that inflates in the event of a crash. Its principal objective is to distribute the restraining forces across the occupant [10] while reducing the forces generated by the seatbelt and reducing excessive head rotations. The airbag is therefore designed to actuate in combination with the seatbelt. Originally, airbags were only used for frontal crashes. However, there are currently many types of airbags situated in different parts of the car, in order to deploy them depending on the type of crash.

After the development of the airbag, the focus on automotive safety changed. Active safety systems or ADAS (Advanced Driver Assistant Systems) started to appear. They help the driver when maneuvering or braking. Some examples of these ADAS are the LKA (Lane Keeping Aid) or AEB (Autonomous Emergency Braking). As the last example, some of these ADAS may act in an autonomous way, helping the driver in case he/she cannot react in time. These kinds of systems can help to prevent several crashes developing some evasive maneuvers. However, even though their objective is to avoid a crash, they cannot ensure that the avoidance will be successful, and the car may end up colliding against another car or object. These maneuvers may affect the kinematics and posture of the occupant right before the crash, so it is important to study them in order to see if they influence the risk of injury to the occupant.

This is where the concept of integrated safety comes in. Every stage of a collision (pre-crash, in-crash, and post-crash) could be affected by the others, so it is essential to study their interactions. This is one of the main objectives of this study.

Historically, the study of collisions has been carried out by means of physical vehicle crash tests. To study how accelerations of a car collision might affect the passengers, anthropomorphic test devices (ATD) were developed.

INTRODUCTION

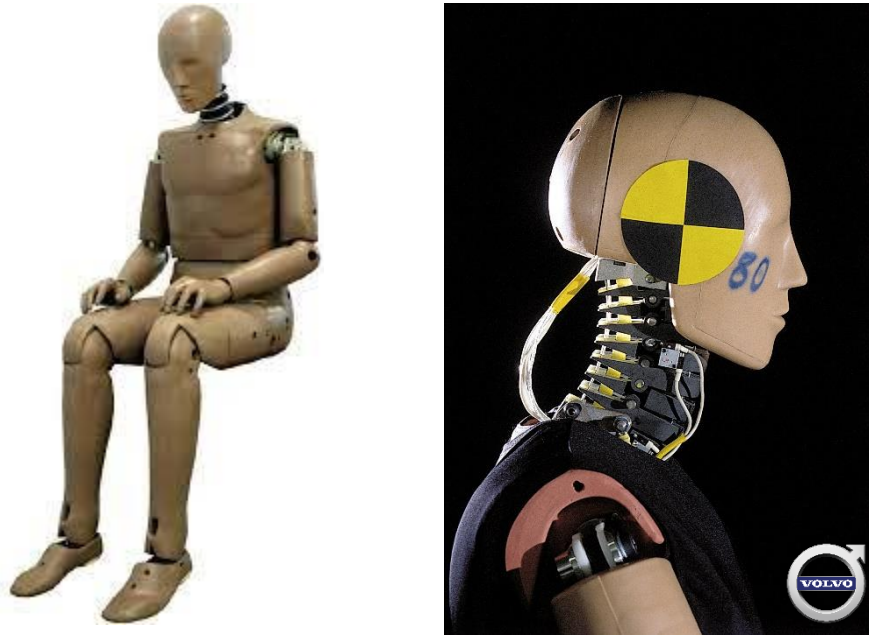


Figure 22: Harmonized Hybrid III 50th percentile Dummy

ATDs, also known as crash test dummies, are mechanical models created to surrogate the human body in replications of car crashes. They wear special instrumentation to monitor different parameters during the crash in order to predict possible injuries. Their principal problem is that they are not omnidirectional, ATDs are designed for a specific type of crash, and they do not have muscles, so they cannot recreate muscular activation

ATDs are widely used for a great number of tests, validations, and studies. The most remarkable ones are the regulatory crash tests, which consist of standardized tests to evaluate the vehicle's safety quality for the occupant in the event of a car crash.

However, in order to study the occupant and driver kinematics using models capable of reproducing human muscular activation, human body models (HBM) were created [11]. An HBM is a numerical model of a human body that is used for crash simulations. These simulations take place in different solvers, such as LS-DYNA, Madymo, etc.

HBM's are being developed by different companies. One of the most famous one is the Total Human Model for Safety (THUMS), developed by Toyota Motor Corporation. HBM's may potentially be very important in injury biomechanics research.

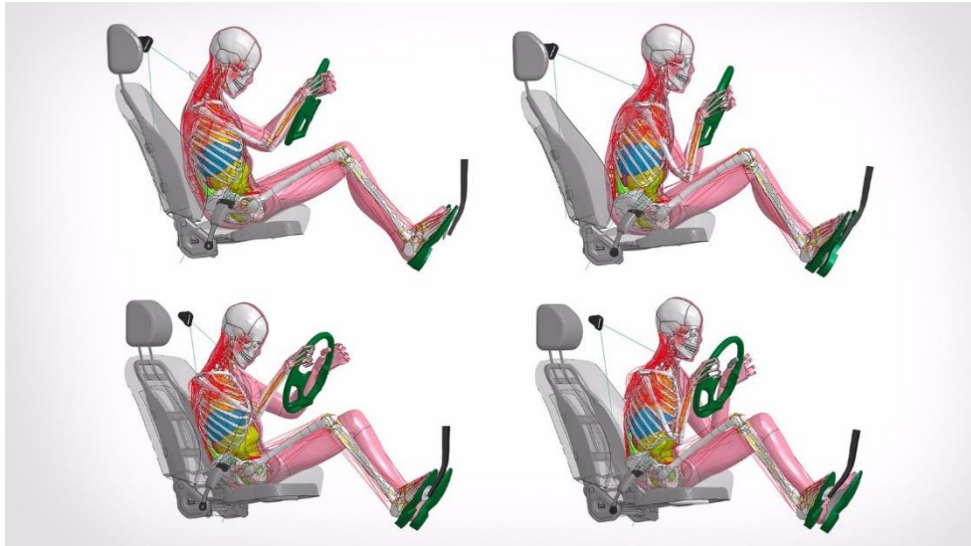


Figure 23: Toyota THUMS simulated in a frontal crash [12]

They are still in development, and several improvements have been made over the last few years. Some of these improvements include active musculature. Active musculature allows the model to react to certain accelerations and to try to maintain its original posture, generating an even more realistic scenario. The first active finite element HBM was developed by SAFER [11]. Under the name of SAFER-HBM, this model was developed in 2009 and it has been evolving since then. Its first aim was to replicate a frontal impact simulation, which was validated with real-life volunteer data. However, still work needs to be done in order to validate the SAFER-HBM v.10 as it is very new.

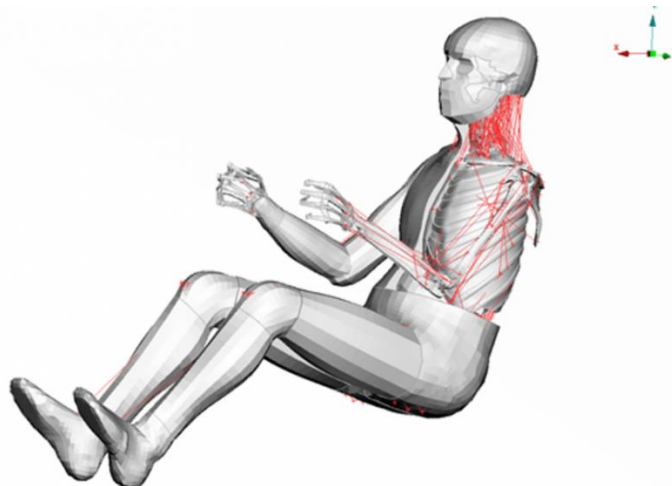


Figure 24: SAFER A-HBM [13]

Several studies state that occupants in a car are very sensitive to pre-crash maneuvers, for example [14]. As these maneuvers generate low-acceleration loads, it was found that musculature has a great influence over the kinematics of the volunteers. Therefore, it was found that A-HBM (Active Human Body Models) have a much bigger correlation with a real volunteer motion compared to passive models like ATD or standard HBMs.

INTRODUCTION

Nevertheless, still much work needs to be done in this sector, as pre-crash avoidance maneuvers might become increasingly common in real-life driving scenarios due to upcoming autonomous driving vehicles.

Motivation

A lot of work is recently being done in pre-crash maneuvers to develop and validate active HBMs in order to predict injury risk. As road traffic approaches to Autonomous Driving and pre-crash maneuvers are becoming more common, the need to design safety systems for occupant's response to these types of maneuvers is increasing. Hence, the motivation to develop this Project is based on the urgent need of utilizing Active HBMs to predict injury risk in order to design safer systems for the coming new pre-crash and in-crash phases.

Moreover, occupant safety is an interesting field that is becoming very important in the car industry, and it is encouraging to contribute to biomechanics and safety engineering research,

Project Aims

This project aims to study the influence of active musculature on injury risk prediction in frontal crash scenarios. Simulations using the SAFER-HBM will be run in order to compare the occupant's response with and without active musculature. Therefore, the principal aims of this project are as follows:

- Review the available literature on muscle effects in occupant injury risk as well as validation performed to active human body models (A-HBM).
- Investigate a set of pre-crash maneuvers (steering, braking, and a combination of both) combined with frontal and oblique impacts. Pre-crash and in-crash combinations will be assigned statistically based.
- Simulate the full sequence (pre-crash and in-crash) with and without muscle activation and compare occupant excursions and injury risk predictions using already existing injury criteria.
- Study different aspects of occupant's pre-crash movement and identify what affects the injury risk more.

2.- Methodology

For the development of this study, the finite element method was used in order to simulate different pre-crash and in-crash scenarios. LS-DYNA MPP R9.3.1 (LSTC, Livermore, CA, US) was used as the explicit solver for the simulations. As pre-processors, ANSA 21.1.0 (BETA CAE Systems International AG, Root, Switzerland) and Primer 17.1 (Oasys Ltd. LS-DYNA Environment) were used. Post-processing was done using META 21.1.0 (BETA CAE Systems International AG, Root, Switzerland) and LS-PrePost (Ansys Livermore Software Technology). Lastly, data management and analysis were performed using Spyder 3-ver 1.4 and Python 3.10 as the main programming language.

The HBM used in all simulations was the SAFER HBM v10 whole body. This model represents an average-size male. The SAFER HBM v10, is an evolution of the SAFER HBM v9, which was originally based on the Total HUMAN Model for Safety AM50 version 3.0 (THUMS, Toyota Corporation, 2008) [14]. The model anthropometry is based on the 50th percentile male reported by [15], it has a stature of 175 cm and it weighs 77kg. The model consists of 219 000 solid elements, 190 000 shell elements, and 2400 one-dimensional elements. The majority of the elements used in the model were hexahedral/quadrilateral and deformable, the only exceptions were the thoracic vertebrae, sacrum, and vertebral endplates, which are viscoelastic.

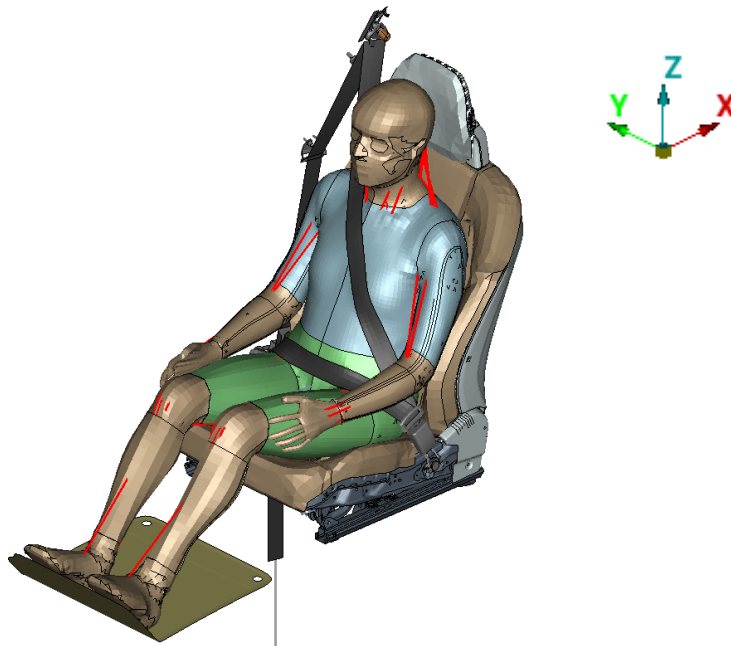


Figure 25: HBM model placed in the seat model in the reference position for the simulations

The musculature of the model consists of 1D Hill-type elements that were controlled by several closed loops PID controllers. In the case of this study, two controllers were used: one for the neck and one for the lumbar musculature. However, the model has also the possibility of using a controller for the leg's musculature and the arms musculature as well. This last controller is designed to be used if the HBM is placed in the simulation as the driver and has

METHODOLOGY

a steering wheel to put the arms on, so the model can replicate the force that an actual driver will do with his hands in case of a collision.

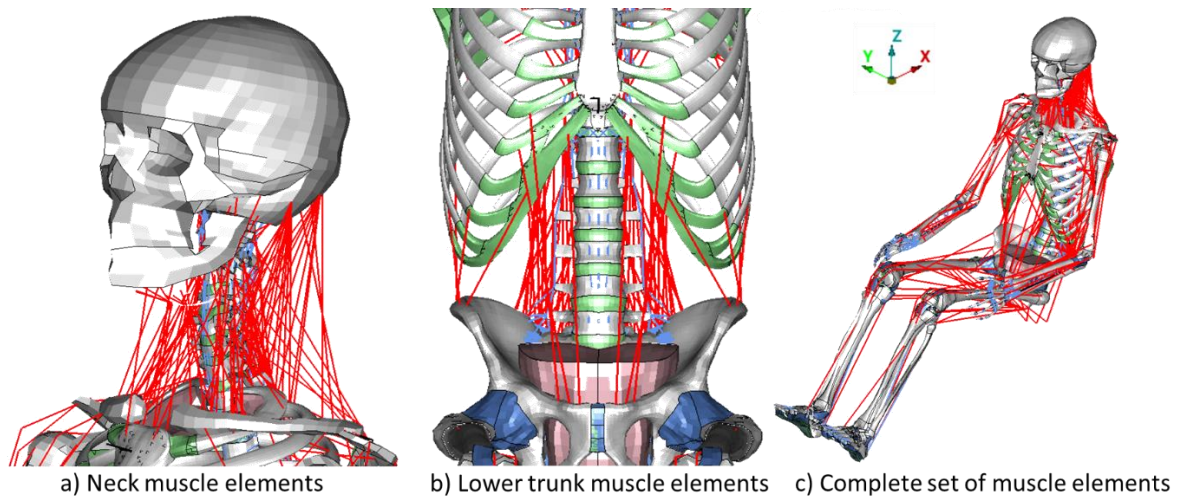


Figure 26: HBM muscle elements. Muscle elements are shown in red color and are shown without flesh for better visibility. However, flesh and soft tissue are used in the simulations.

The model has as well two types of feedback loops for the PID controllers for the muscles: MIMO (Multiple Input Multiple Output) and SIMO (Simple Input Multiple Output controllers). The MIMO controller is called MLF (Muscle Length Feedback) and it has the ability to control independently the length of each muscle and having as an input the length of each muscle as well. The SIMO controller is called APF (Angular Position Feedback) and it controls the length of each muscle but having just as an input the translations and rotations of the head. The MLF feedback loop emulates the stretch reflex in the muscles and the APF emulates vestibular feedback from the central nervous system, which tries to stabilize the head in space [14].

For this study, the APF feedback loop was chosen with two PID controllers, one for the head and one for the lower trunk. More information about the controller can be found in Appendix A.

Regarding the environment in which the HBM is used, all the simulations were run using a model of a sled that recreates an average size SUV as the boundary condition. This sled was equipped with a frontal passenger-side airbag, sun visor, seat, and seatbelt in order to restraint properly the HBM and recreate a real environment. All the parts of this FE model were provided by Volvo Cars. All the pulses used for the different simulations were applied over the rigid sled model. All the pulses consisted of 6DOF (Degrees Of Freedom) time series that defined the x, y, z translations and x, y, z rotations of the sled during the simulation.

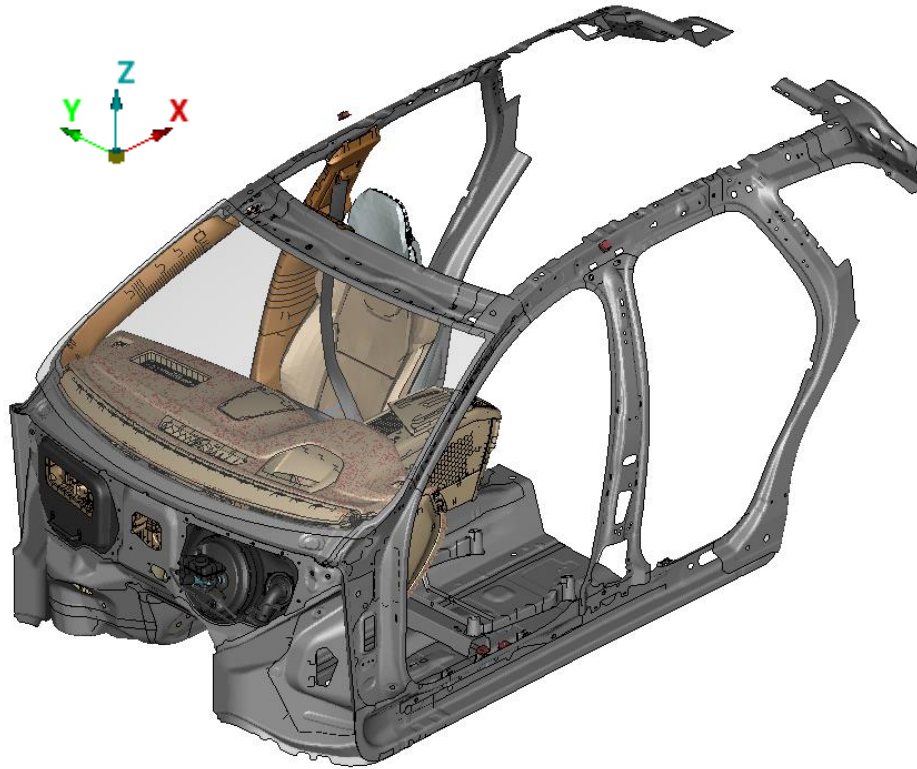


Figure 27: Sled model

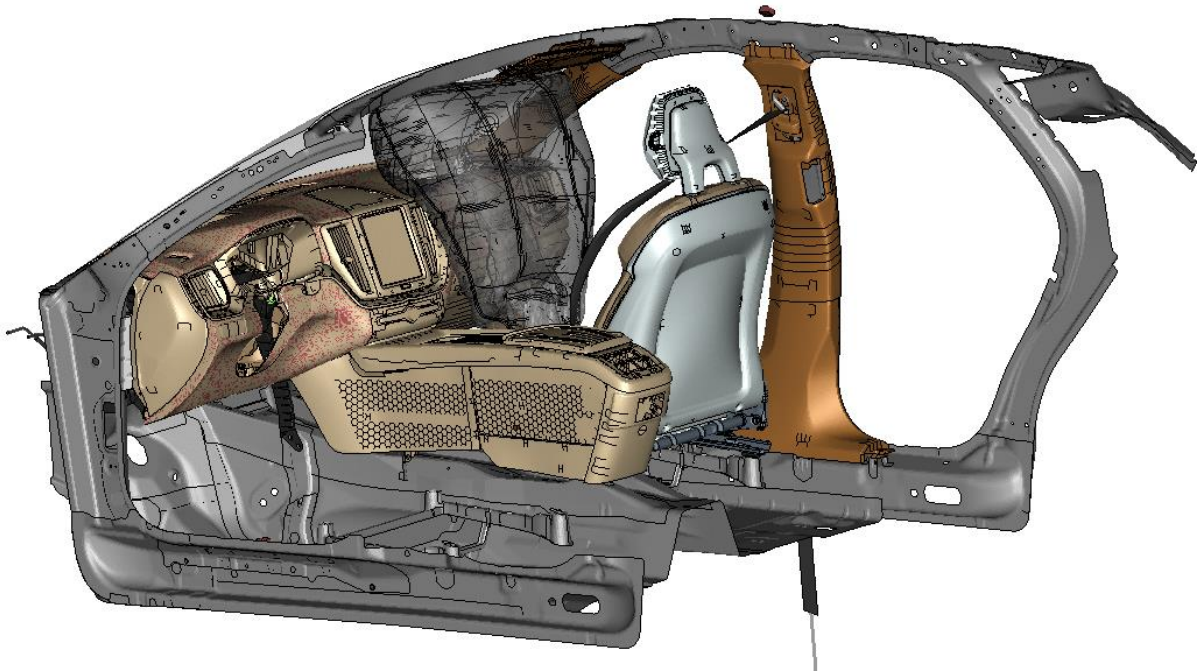


Figure 28: Interior of the sled with all the restraint systems

The model is placed in space in a way that the front of the car is heading towards the negative part of the x-axis. The coordinate system is defined as a right-handed coordinate system with x rearward, y to the right side, and z upward (Figure 11).

2.1.- Simulation set-up

For the development of the study, two types of simulations were used: baseline simulations and passive simulations.

All the baseline simulations had the active musculature controllers activated for the HBM and they all consist of three phases: initialization, pre-crash, and in-crash. These simulations were used as baseline simulations to study the influence of active musculature on injury risk prediction. The initialization process was used to reach an equilibrium state between the HBM and the surroundings and for stabilizing the signals in the HBM muscle controllers. Gravity was activated in all the phases with the objective of having the most naturalistic posture for the HBM possible. The foam of the seat was squashed, and vibrations generated by the control signals were eliminated along the 300ms that this phase lasted.

The pre-crash phase was used to reproduce an evasive maneuver. A pre-crash pulse provided from Emma Larsson's study [14] was used to simulate the motion of a real car and to recreate the position of a real human after the avoiding maneuver using the HBM model. In this phase, the posture of the occupant was modified, and the active musculature was in action trying to stabilize the HBM simulating real lumbar and neck human musculature.

Lastly, the in-crash phase recreates a collision in which the airbag is deployed according to the type of crash and the retractor of the seatbelt. The pulses used for the in-crash phase were provided by Volvo Cars. The great majority of them followed standardized crashes from the Euro NCAP [16] and the IIHS (Insurance Institute for Highway Safety) [17]. All the pulses used for this study are frontal crashes. All the analysis was focused on the in-crash phase.

Once the baseline simulation was run, several passive simulations were created based on the initial simulation. These passive simulations had different parameters from the baseline one like the posture of the occupant at the end on the pre-crash, its velocities, the elements stresses, or the last signal of the controller for each muscle of the model; and they just simulated the in-crash phase.

This procedure was done with the objective of reducing the amount of computing time needed for each simulation. On average, the pre-crash maneuver lasted between 500 ms and 850 ms, and the in-crash lasted between 120 ms and 300 ms. Running a baseline simulation with all the three phases (initialization [300ms] + pre-crash[500-850ms] + in-crash [120-300]) meant running around 1300 ms of simulation. The number of CPUs (Central Processing Units) used per simulation was about 120. With this number of CPUs, running 1300 ms on average, the simulation time was about 7 full days of simulation. As described below, for this project at least 72 simulations needed to be simulated. If all the simulations had the three phases, it would have taken 72 weeks just to simulate, assuming that all the simulations run correctly and had no numerical errors. Even if we were able to run some in parallel, the amount of time needed for this project would not have been reasonable.

Simulating just the in-crash phase however just takes around one day on average, so setting just an in-crash simulation with the HBM placed according to the final position and velocities of the end of the pre-crash phase from the baseline simulation makes the use of simulation time much more efficient, having just to simulate 9 baseline simulations (9 weeks) and 64 passive runs (64 days).

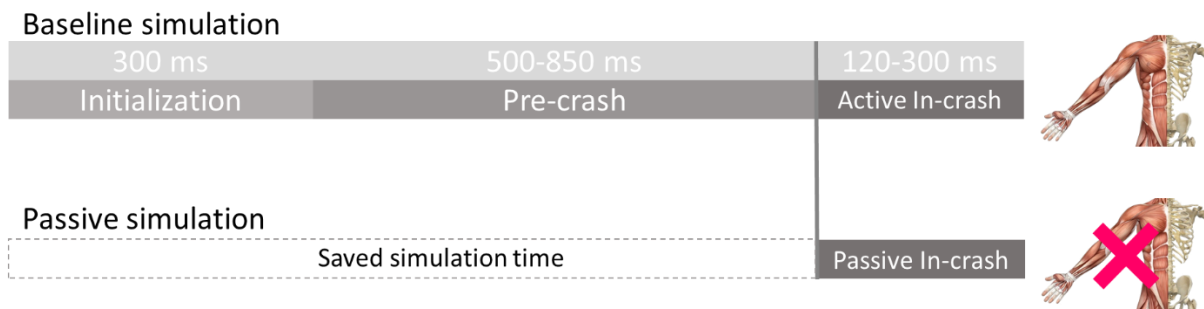


Figure 29: Baseline and passive simulations set-up diagram. In the passive simulations, the musculature was still there, just the controllers that manage the muscles length and force were deactivated.

The methodology of how these simulations were created and configured is described below in more detail.

2.2.- Pre-crash and In-crash combinations

For this study, it was assumed that the evasive maneuver was initiated without avoiding the conflict, and the car eventually entered an in-crash phase. Therefore, baseline simulations combined a pre-crash maneuver with an in-crash phase.

Nevertheless, there are different types of maneuvers and crashes, so there was a need to select the most realistic combinations. Regarding the environment, three main scenarios were chosen for the analysis: highways, secondary roads, and intersections. Scenarios are essential, as the maneuvers and type of crashes can vary depending on the scenario.

To select the most probable types of crash for the different scenarios, [18] [19] [20] were used as a reference, as those three articles study the different crash possibilities in the scenarios commented before. All the crash types were then matched with a standardized crash pulse from the Euro NCAP or the IIHS.

The most common evasive maneuvers in those scenarios were the following ones:

1. Braking
2. Turning left
3. Turning right
4. Turning left and braking
5. Turning right and braking

And finally, the most common frontal in-crash scenario for those environments were matched to:

1. Full-Width Rigid Barrier (FWRB)
2. Moderate Overlap Frontal Test (MOFT)
3. Mobile Progressive Deformable Barrier (MPDB)
4. Passenger-side Small Overlap

METHODOLOGY

Combining the pre-crash maneuvers with the different collision tests results in the following pre-crash/crash matrix.

Table 9: Pre-crash and crash combination matrix

		Pre-crash maneuvers				
		Braking	Turn left	Turn right	Turn left & Braking	Turn right & Braking
Frontal In-crash	Full-Width Rigid Barrier					
	Moderate Overlap Frontal Test					
	Mobile Progressive Deformable Barrier					
	Passenger-side Small Overlap					

However, not all the combinations are equally likely to happen in a real-life scenario. The cells marked in blue show the combinations that happen more frequently in the previously described scenarios, so they were the combinations that were used for this study. More information about these combinations can be found in Appendix B. Also, with the selected combinations it is possible to compare the same in-crash phase with different pre-crash maneuvers to study the importance of the maneuver, and it is possible to study how different crash scenarios differ between them when they share the same pre-crash maneuver.

As mentioned before, from these baseline simulations, some extra passive runs will be created using different inputs from the full-event simulation such as the posture of the HBM or the velocity it had at the end of the pre-crash phase. The combinations that were simulated are the following ones:

Table 10: Combination of inputs for the different passive simulations

Passive simulation	HBM Inputs			
	Posture	Velocity	Stress	Muscle PID
0				
1				
2				
3				
4				
5				
6				

The inputs used for the HBM are the following:

- Posture: the posture of the HBM at the end of the pre-crash. It refers to the position of each node of the HBM at the end of the pre-crash. This information was extracted

from the last state of the baseline simulation before entering the in-crash phase and then introduced to the new model using Python to manage the coordinates of each node.

- Velocity: it refers to the final velocity of each node of the HBM at the end of the pre-crash. For the passive simulations, it is an initial velocity that is set as a boundary condition for the in-crash simulation. This information was extracted from the last state of the baseline simulation before entering the in-crash phase and then introduced to the new model using Python to manage the velocity of each node. The initial velocities were defined using the *INITIAL_VELOCITY_NODE card from LS-DYNA.
- Stress: it stands for the stresses of all the solids, shells, and beams of the model at the end of the pre-crash. These stresses were obtained from the last state of the baseline simulation before entering the in-crash phase and then introduced to the new model using Python. The cards used to introduce this information in the model were *INITIAL_STRESS_SOLID, *INITIAL_STRESS_SHELL, and *INITIAL_STRESS_BEAM, respectively.
- Muscle PID: it stands for the muscle activity level on the last state of the baseline simulation. It is the last value of the signal of the PID controllers that manage the length and strength of each muscle. With the proposed setup for the simulations, three different cases were studied based on the muscle controllers:
 - Complete passive model: the HBM has no muscle activity, beam muscles do not work. This scenario represents a human that does not make any force with his muscles during the in-crash, there is no strength in the muscles, the body just moves due to its inertia and the movement of the car. Every passive simulation with no MPID (Muscle PID).
 - Passive model with MPID: the HBM retains the last signal from the PID controller, and the length and force of each muscle does not vary over time. It is assumed in this case that the stiffness of a human body does not change during the in-crash and stays constant with the last value of the pre-crash phase, as the in-crash phase lasts no more than 300 ms. All the simulations that have MPID as an input.
 - Active model: the HBM in this scenario has the ability to change the length and force of each muscle during the in-crash phase, but always with 20ms of delay, which represents the delay in a real human brain between an input is processed and the consequent muscle action is delivered. In this scenario, it is assumed that a human can vary the strength he is doing with the muscles during the in-crash. All the baseline simulations.

The objective of this configuration is to study the influence of each input parameter separately and see how each extra input parameter improves the response of the HBM compared to the baseline simulation.

2.3.- Active baseline simulation set-up

This subsection is intended to show how the baseline simulations were set up step by step.

The baseline simulation in the first simulation that needs to be set up, as the passive ones are created afterward using the model that has already run. The first thing to set in the simulation is the seat. The seat model was provided by Volvo Cars and is an adjustable model that models a real Volvo seat. As this study is a continuation of Lara's Wehrmeyer work [21] and the HBM used in that study had the same stature as the one used for this case study (Lara used the SAFER A-HBM v9 and the SAFER A-HBM v10 was used in this project), the seat used was the same and it was adjusted in the same way, medium height seat with low tilt and a 25° backrest.

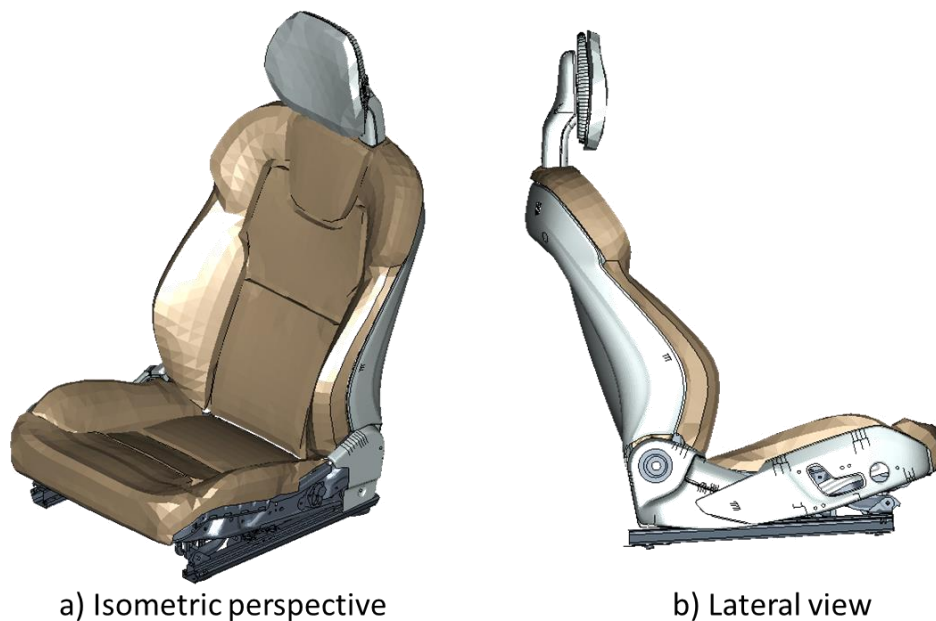


Figure 30: Passenger seat

Once the seat was adjusted to its final position, the HBM was placed on the seat. The process of positioning starts placing the HBM in a similar position to Lara's work [21]. Secondly, the torso and extremities of the HBM are adjusted in Primer using the three angles that can be modified for each joint. Some of the joints have certain angles restricted to recreate as close as possible a real human body. The adjustment of these angles was made following the protocols that Euro NCAP uses for their tests [22] adapting them for the HBM, as they are initially designed for the placement of ATDs in real car seats. Also, to have comparable results with Lara's work [21], the HBM was seated trying to have the pelvis, torso, and head in the same position as her previous model.

Primer, however, allows to modify the angles of the joints making parts of the HBM rigid, so it is necessary to pull the HBM to its final position running a positioning simulation. This simulation is set up dragging cables from the skeleton of the model to the places where those bones should be for the final posture. Running this simulation allows the HBM to deform to its final posture rather than making some tissues rigid with Primer. The resulting starting position is then extracted from the simulation.

The starting posture was used for every baseline simulation.

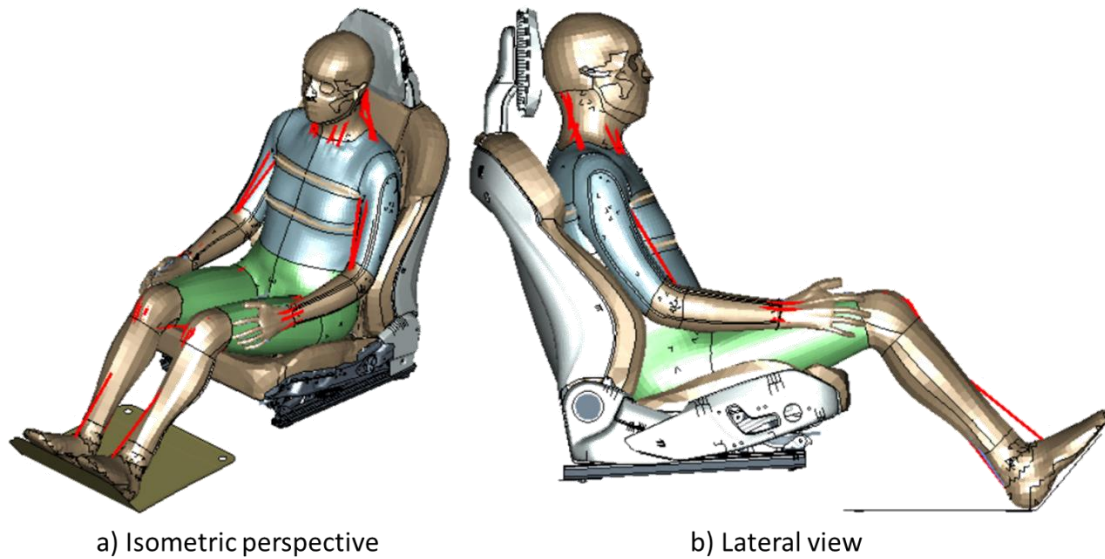


Figure 31: HBM nominal position

After the HBM positioning, the seat was squashed according to the penetrations of the HBM into the foam of the seat. As the HBM is in the final position, there are intersections between the HBM model and the seat model that need to be solved by squashing the foam of the seat. This process was done in ANSA using the seat depenetration tool. This tool deforms the foam of the seat using two sets of elements, the shells of the HBM that are in contact with the seat and the structural shells of the seat that will hold the foam. The foam is then adapted to both the HBM shape and the structure of the seat. The tool also generates an *INITIAL_REFERENCE_GEOMETRY card that LS-DYNA will use in the simulations to generate the stresses of the foam according to the deformation generated.

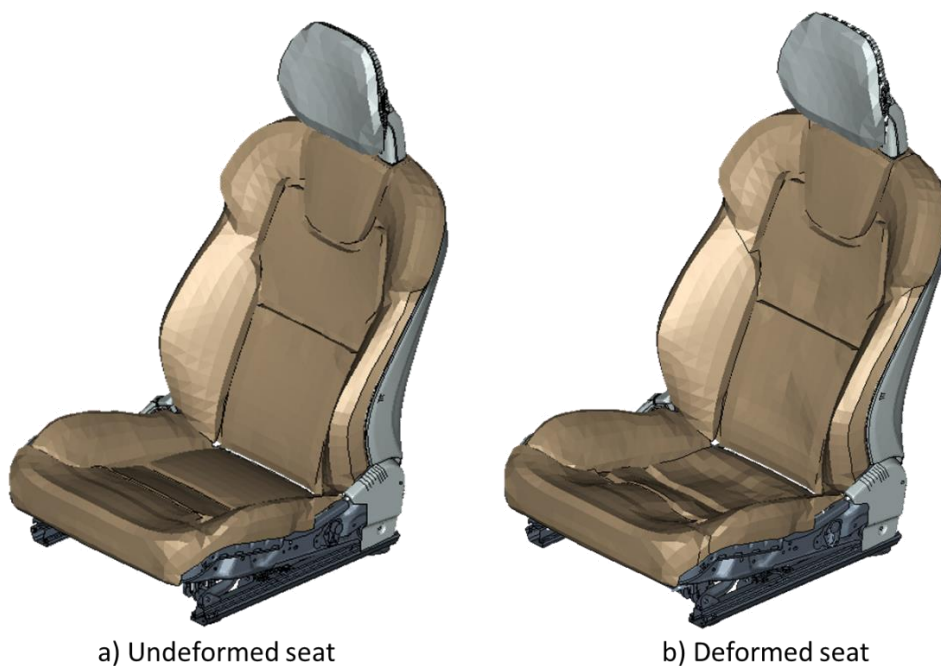


Figure 32: Seat foam before and after the squashing deformation

METHODOLOGY

Once both the seat and the HBM were ready for the simulation, the seatbelt was placed in order to restraint properly the HBM. The seatbelt model has mainly two parts: the belt webbing and all the pieces that link the webbing to the car such as the buckle, the anchor, or the slipping.

Secondly, once all the pieces are fixed, the webbing of the seatbelt is routed using Primer. The seatbelt is modeled as a two-dimensional shell that was routed picking several nodes of the model. Primer creates a route using the list of nodes picked from the model and it generates a loose webbing. After the webbing generation, there is a fitting process in which the belt adjusts to the body of the HBM, adopting the shape of its body and the elements that are in contact with the webbing.

After this procedure, the model obtained can be appreciated in the following figure.

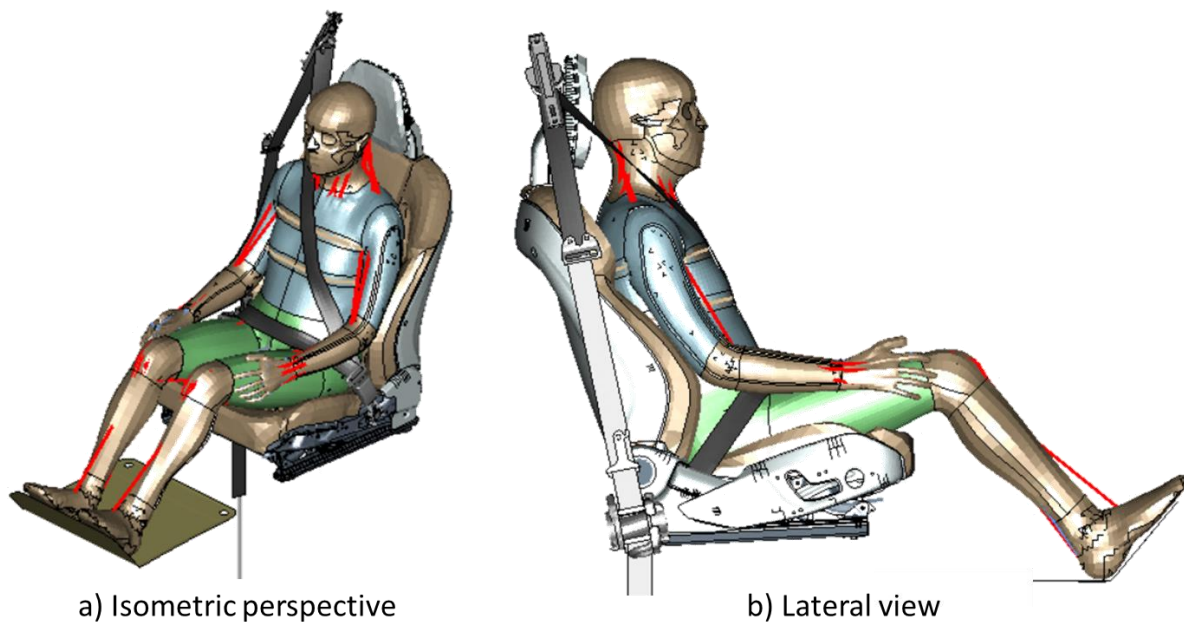


Figure 33: HBM nominal position with seatbelt

Lastly, the sled and the rest of the elements of the car were included so the HBM could interact with them. Contacts were created between the HBM and the environment so there was an interaction between them. Also, the airbag was included, and the firing strategy was determined according to the case study.

As the baseline simulations were used to extract information of the end of the pre-crash, two extra cards were added to extract all the information of the model from a certain state: `*CONTROL_STAGED_CONSTRUCTION` and `*DEFINE_CONSTRUCTION_STAGES`. These cards were used to define certain stages in the simulation (initialization, pre-crash, and in-crash) and they were used to control when an output of the state of the simulation was needed. The output generated from these cards has the coordinates of every node in the simulation, their velocity, the stresses of every element, etc. This information can be used to reproduce the state in a new simulation. However, this needed to be done using Python, as the output generated was so big that the ANSA pre-processor was not able to handle it.

2.4.- Passive simulation set-up

Once the baseline simulation had been run, passive simulations could be set up. The seat, belt, and HBM were extracted from the output file that was generated from the baseline. This file will be referenced as dynain from now on, and it has all the information that LS-DYNA needs to set up the following simulations. This file cannot be used as it is outputted from the previous simulation, as there is a huge amount of information that cannot be handled by a standard pre-processor.

For this reason, just the seat of the car, the anchor and the buckle of the belt, and the HBM were extracted using Python to look for the specific nodes of each model and update their position. The original models were used for the rest of the elements included in the simulation.

As the set-up of the passive simulation was complex, the whole operation was made using a Python code that read the baseline simulation and looked for the different *INCLUDEs it had and created the different passive simulation files, each one of those with different inputs depending on the passive simulation matrix. If the *INCLUDE was the HBM, the seat, or the seatbelt; a node update was made followed by extra information extraction depending on the model.

HBM

The HBM was updated following a four-step update. First, nodes, solid, shells, and beams of the model were loaded in Python as different variable arrays. Secondly, the program looked for those nodes in the dynain file to update their coordinates in the final model file. Thirdly, the velocity of those nodes was updated in order to be able to input them in the passive simulations that had velocity as an input. Lastly, element stresses were updated using *INITIAL_STRESS_BEAM, *INITIAL_STRESS_SHELL, *INITIAL_STRESS_SOLID cards. However, some of the shells used in the HBM model are defined with MAT_FABRIC, a type of material definition from LS-DYNA that cannot be reinitialized. As a result, those shells were not initialized with stresses even in the simulations that had stresses as an input.

Seat

The seat model was defined in two parts: the structural part and the foam. Both were updated in a similar way as the HBM. First, the nodes of the seat were stored as an array and secondly, the program looked for those nodes in the dynain file to update their coordinates. Lastly, the nodes were written in their corresponding include file.

Seatbelt

The seatbelt was a special model, as it had different parts and webbing. The initial objective was to update the whole model of the seatbelt, including the webbing and the retractor, nonetheless, it was not possible with the information of the dynain file to create a functional model of the seatbelt as the state of the retractor cannot be obtained as output. Furthermore, the initial and final nodes of the seatbelt webbing need to be in a specific spatial location and,

METHODOLOGY

as the webbing of the belt moved during the pre-crash, it was not possible to update their coordinates. As a result, just the anchor and buckle models of the belt were updated. The rest of the seatbelt model was included with the original pieces and the webbing was re-routed manually following as close as possible the coordinates of the nodes of the baseline simulation belt.

The last step was to introduce a transformation matrix for those elements that were updated using the Python script, as the pulses applied to the sled model made it move from the original position. This means that the HBM, seat, and seatbelt models were in the correct position with respect to the sled at the last state of the pre-crash in the baseline simulation, but all the sled and different elements had moved from their original state position due to the application of the pre-crash pulse. This issue was fixed using the *DEFINE_TRANSFORMATION card from LS-DYNA. It defined a transformation matrix that could be applied to several elements of the simulation model like the HBM or the seat. This transformation matrix can be a translation matrix, a rotation matrix, a mirror matrix, or a combination of them. For this model, a special matrix was used, the POS6N matrix. This matrix stands for positioning by 6 nodes, and it creates an affine transformation (translation and rotation, no scaling) given three start nodes and 3 final nodes. This matrix is then set up to make the original three nodes coincide with the three final nodes, applying all the translations or rotations needed for the model to fit.

Once all the previous steps were made, the model was ready to be simulated. A comparison between the last state of the pre-crash in a baseline simulation and the initial state of the consequent passive simulation is shown in the following figure.

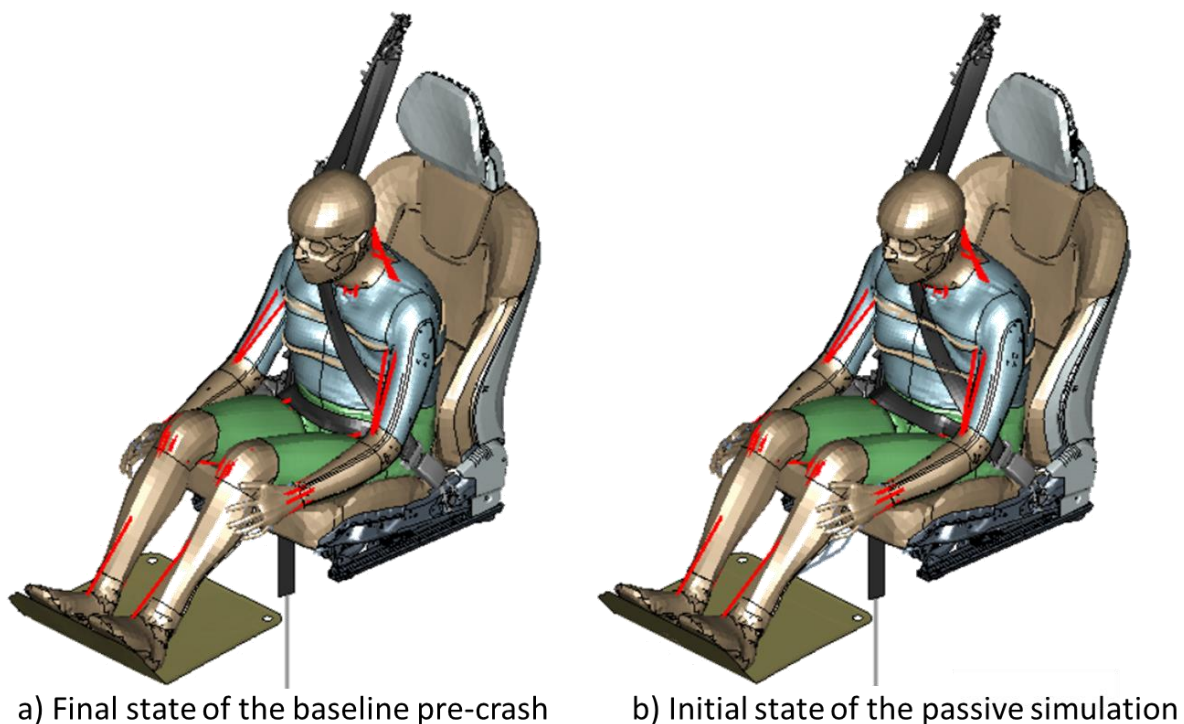


Figure 34: Comparison between the baseline simulation model at the end of the pre-crash (a) and the new model extracted from the previous baseline simulation (b)

2.5.- Data analysis

To study the influence of active musculature on injury risk prediction and on the simulation output, the kinematics of the HBM and the injury risk prediction of the models were compared using three different methods.

Excursion comparison

A visual inspection of the different simulations was made in order to evaluate how the different inputs and the active musculature influence the head, chest, and pelvis excursions. Those excursions were plotted on the x-y and x-z planes to study the lateral and frontal displacements of the head, chest, and pelvis during the in-crash phase.

Kinematic comparison

The x, y, and z accelerations of the head, chest, and pelvis were also compared using cross-correlation from the software CORAplus 4.0.4 (CORrelation and Analysis) [23] to study how close passive simulations can get to the active baseline simulation based on the inputs used. This software calculates the level of correlation between two signals/time histories giving a result between 0 and 1 depending on the quality of the match. Rating 1 represents a perfect match with the predefined tolerances, and 0 means a poor match. The program offers two metrics to study how equal two curves are: the cross-correlation analysis and the corridor method.

The cross-correlation method analyses three characteristics of the signals: phase shift, size (amplitude), and shape of both curves to evaluate how close the signal is from the reference curve. These three parameters are also weighted, so the user can give more importance to one specific parameter.

The corridor method evaluates the deviation between two signals by means of corridor fitting. Four curves are defined around the reference signal to create an inner and an outer corridor. If the studied curve fits inside the inner corridor, a rating of 1 is assigned. If the curve is outside the outer corridor, a 0 rating is assigned.

The overall rating structure of the program is shown in the following figure.

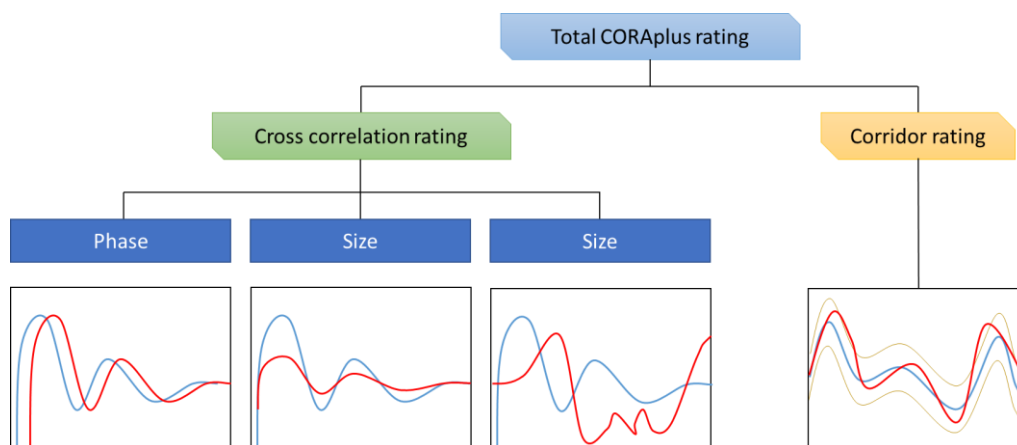


Figure 35: CORA rating structure

METHODOLOGY

For this study, just the cross-correlation rating was used to evaluate the signals, as the corridor rating is designed to compare an average of real test curves with simulation results. The tests results have a standard deviation that can be used for setting up the corridor. In the case of this study, just single simulation curves were compared, so just the cross-correlation analysis was made. The ratings of each parameter are shown in Table 3 and show the recommended configuration according to the CORAplus user's manual [23].

Table 11: CORA settings

Cross correlation rating	Weight
Phase	0.25
Size	0.25
Shape	0.5

To facilitate the interpretation of the CORA ratings, results were categorized as *excellent*, *good*, *fair*, and *poor* in accordance with the software manual [23].

Table 12: CORA rating categorization

Category	CORA rating interval
Excellent	$0.94 < \text{Rating} \leq 1$
Good	$0.8 < \text{Rating} \leq 0.94$
Fair	$0.58 < \text{Rating} \leq 0.8$
Poor	$0 \leq \text{Rating} \leq 0.58$

The signals used for this analysis were filtered using a CFC 60 (Channel Frequency Class 60 Hz), a commonly used low pass filter to reduce the amount of noise in crash test signals. The filtering was made to obtain clear signals and develop a correlation analysis based on the significant part of the signal and not on the noise that may be generated in the in-crash phase. X, Y, and Z accelerations were studied separately as the in-crash scenarios studied are all frontal and accelerations in the X-axis have a much higher amplitude than accelerations in Y and Z, which represent mainly vibrations or very little displacements that can be less representative than forwarding motion. To obtain a final rating, a weighted average was made between the three axes, giving a weight of 0.5 to X accelerations, 0.25 for Y accelerations, and 0.25 for Z accelerations.

Injury risk predictions

Lastly, injury risk indicators were compared between simulations that shared the same pre-crash and in-crash phases. Using a post-processing script, several injury risk values like HIC15, NIC, or Nij were obtained based on the kinematics and kinetics of the model. Also, the HBM model has several strain models that generate relevant values to study. Going from the head of the model to the bottom, the following injury risk predictions were studied.

Regarding the head of the HBM, the brain strain model, HIC, and BrIC were used to evaluate the injury. According to S. Kleiven [24], the brain strain model is suitable for head motions with translational and rotational kinematics, and it is more precise than HIC alone. The

combination of the strain model, HIC, and BrIC was used to assess the injury risk difference between the active musculature model and the passive ones.

Regarding the neck, forces in the cross-sections of the neck were used combined with the Nij and the NIC. Nij is frequently used to assess neck injury in high-velocity impacts. NIC is used to assess neck injuries caused by pressure gradients, however, it is more precise in rear-end impacts, so it will be analyzed in combination with the previously mentioned injury risk predictors.

Thirdly, regarding the thorax, the rib fracture model [25] was used to assess the integrity of the rib cage. The risk of fracture of different amounts of ribs based on the strain of the ribs was used to compare the baseline simulations with the passive ones.

Concerning the lumbar area, lumbar forces were studied.

METHODOLOGY

3.- Results

3.1.- Braking + Full-Width rigid Barrier

Regarding excursions of the head, chest, and pelvis; there are two differentiated groups regarding passive simulations: the passive simulation with no inputs and the passive simulations that have the posture of the HBM at the end of the pre-crash as input.

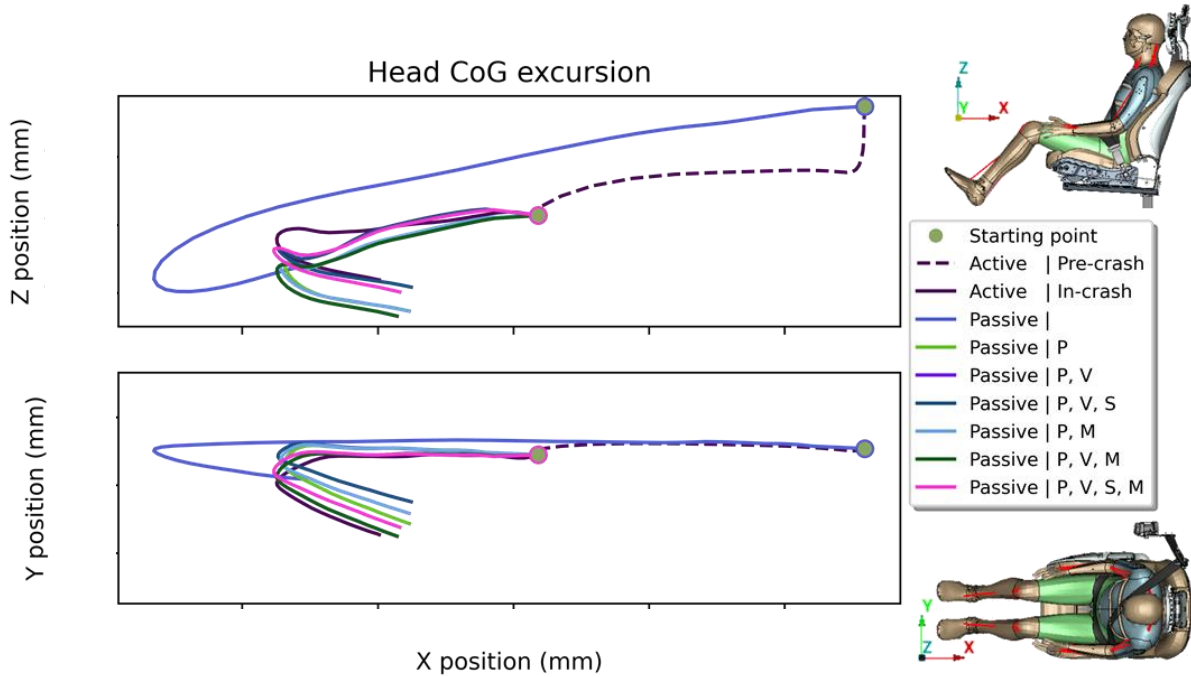


Figure 36: Head CoG excursion. Braking and Full Width Rigid Barrier

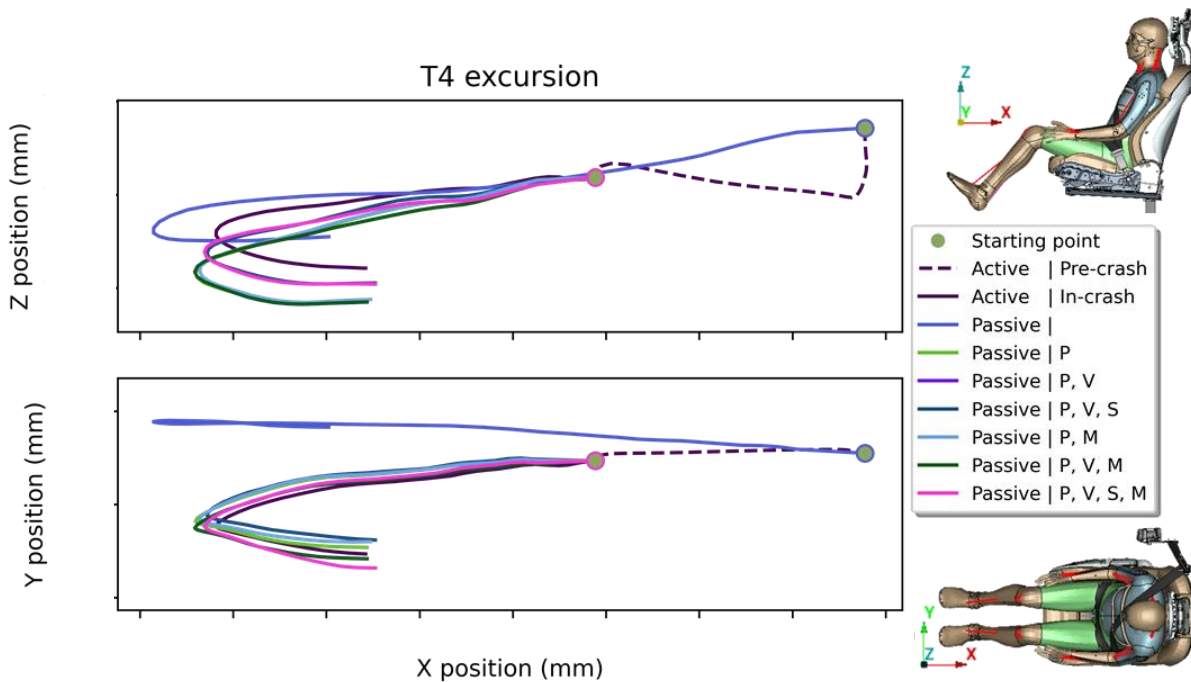


Figure 37: Chest excursion. Braking and Full Width Rigid Barrier

RESULTS

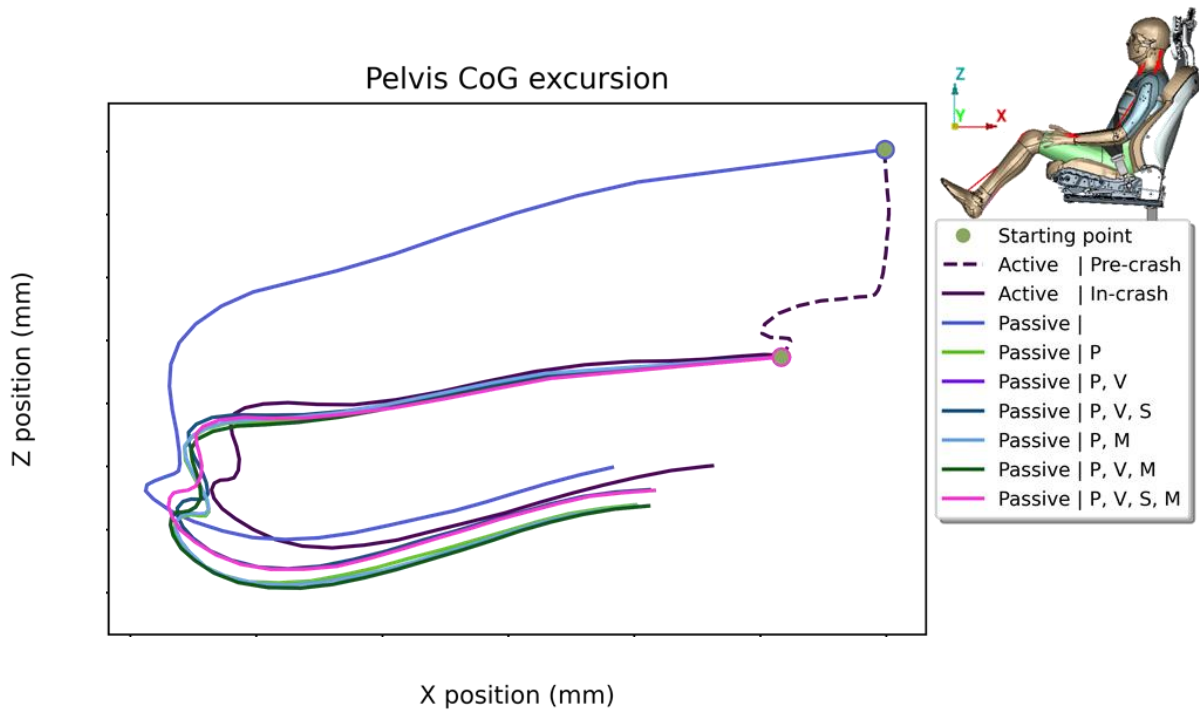


Figure 38: Pelvis CoG excursion. XZ plane. Braking and Full Width Rigid Barrier

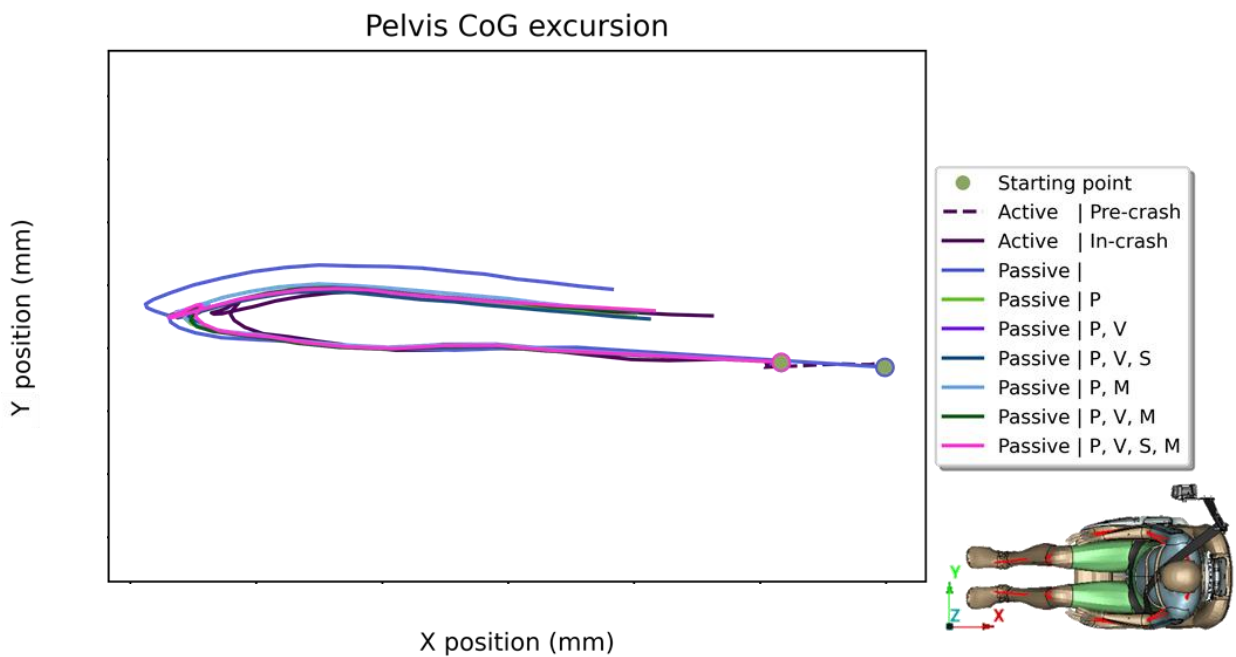


Figure 39: Pelvis CoG excursion. XY plane. Braking and Full Width Rigid Barrier

It can be observed that the excursions of the head, chest, and pelvis in the passive simulation with no inputs are very different compared to the rest of the passive simulations.

Regarding the rest of the passive simulations, there are two differentiated groups of excursions: passive simulations with stresses and passive simulations with no stresses. The excursions of the simulations that have stresses seem to be closer to the excursions of the baseline simulation.

Concerning injury criteria, all the results have been normalized using the baseline simulation value as a reference. Consequently, all the baseline injury risk predictions have value 1 and the passive simulation values oscillate around the value 1. Thus, the variations of the passive simulations with respect to the active one can be observed.

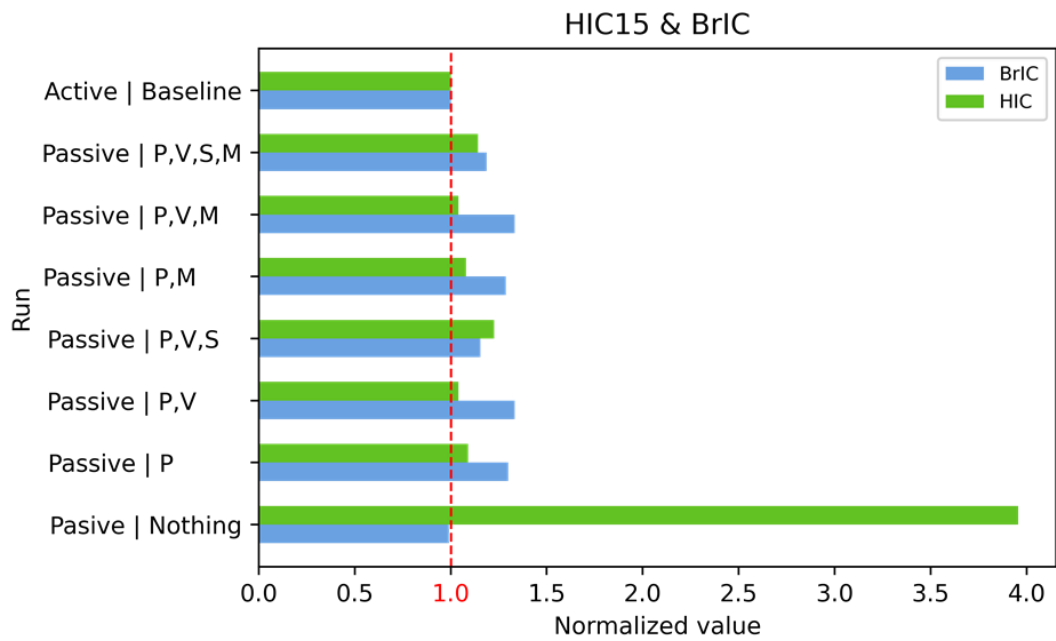


Figure 40: HIC 15ms and BrIC. Braking and Full Width Rigid Barrier

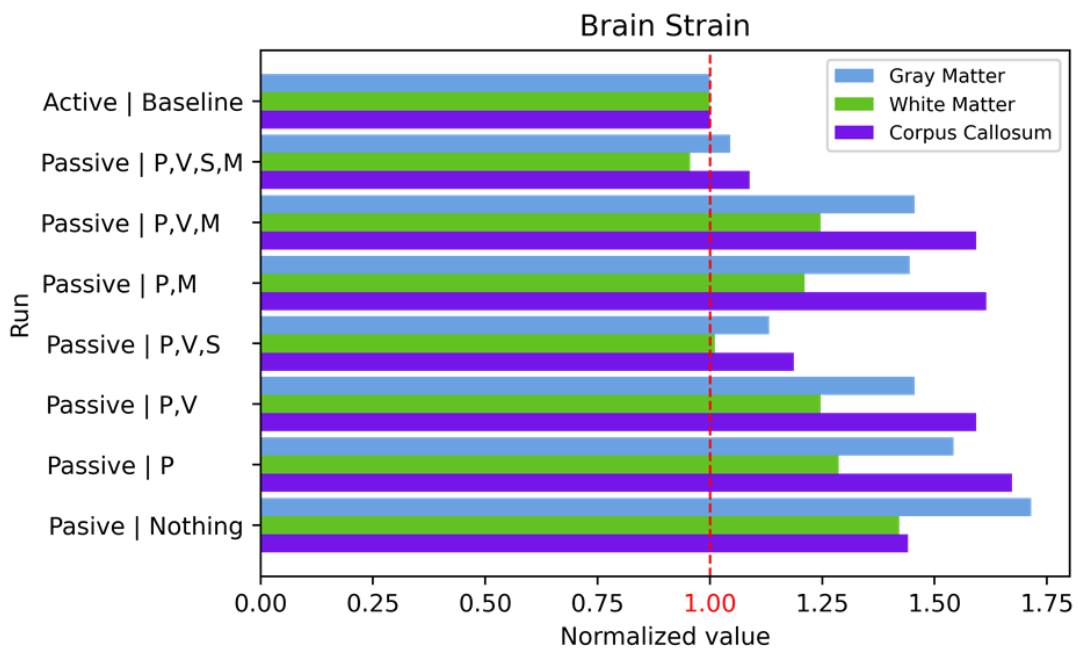


Figure 41: Brain strain. Braking and Full Width Rigid Barrier

RESULTS

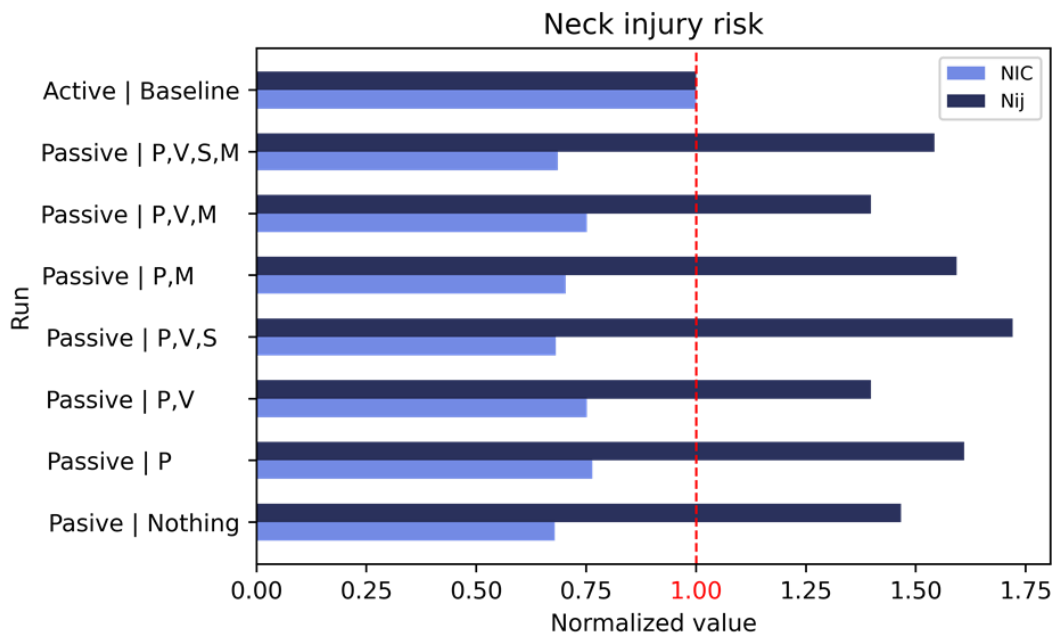


Figure 42: Neck injury risk. Braking and Full Width Rigid Barrier

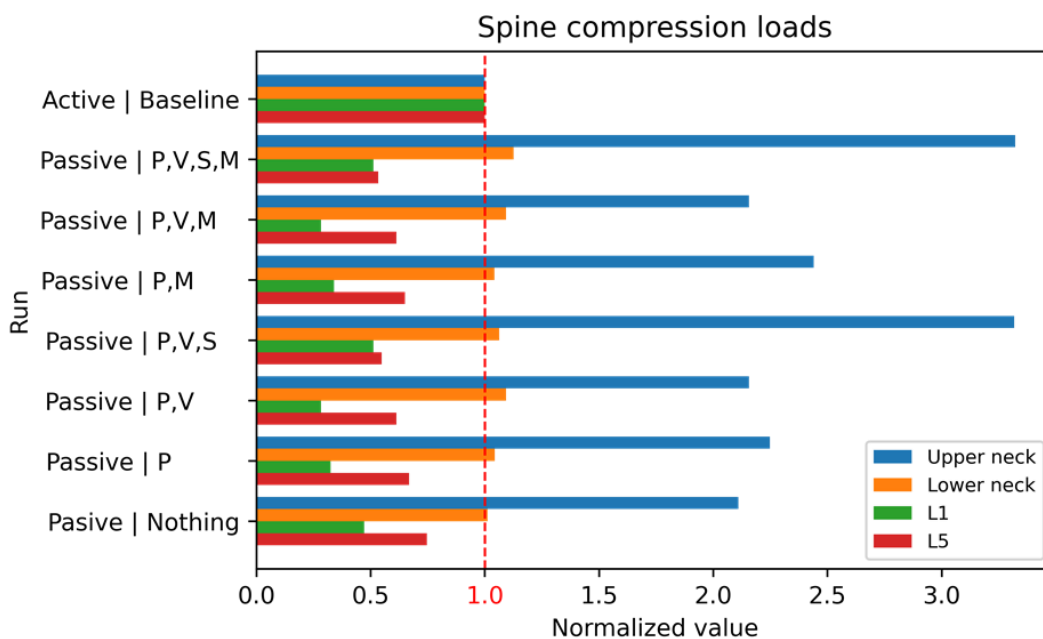


Figure 43: Spine compression loads. Braking and Full Width Rigid Barrier

Regarding the head, HIC 15 ms is greatly overpredicted compared to the baseline model in the simulation with no inputs, and the strains in the brain are the largest of all the passive simulations. It can be appreciated that adding extra inputs improves the brain strain prediction, obtaining the closest values when the posture, velocity, and stresses are added to the simulation. Muscle activity level (MPID) however seems to not affect the results.

Regarding the neck and the spine, compression loads in the upper neck are overpredicted compared to the baseline model in all cases and lumbar compression loads are underestimated. These predictions get the closest values when only posture and initial

velocities of the HBM are included. The NIC and Nij are wrongly predicted compared to the baseline model by the passive simulations compared to the baseline. The closest values are obtained for posture and velocity input simulation.

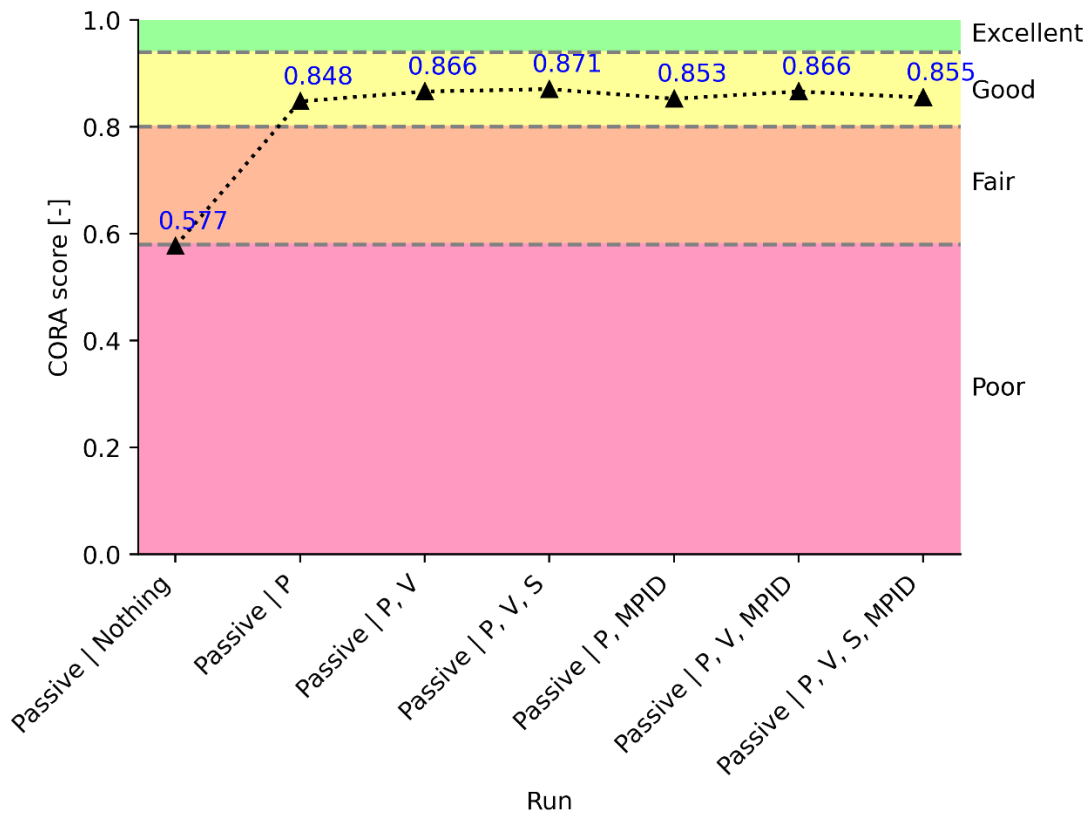


Figure 44: CORAplus acceleration ratings. Braking and Full Width Rigid Barrier

Lastly, regarding the CORAplus ratings, there is a big improvement if the posture of the occupant is added as an input in the passive simulation, changing the overall rating from “Poor” to “Good”. Adding velocity or velocity and stress improves the rating a bit more, but the passive model is not able to reproduce the accelerations of the active model with an “Excellent” rating. Muscle level activity does not improve results. Moreover, on some occasions adding the MPID worsens the rating.

RESULTS

3.2.- Braking + Moderate Overlap Frontal Test

Regarding excursions of the head, chest, and pelvis; there are two differentiated groups regarding passive simulations: the passive simulation with no inputs and the passive simulations that have the posture of the HBM at the end of the pre-crash as input.

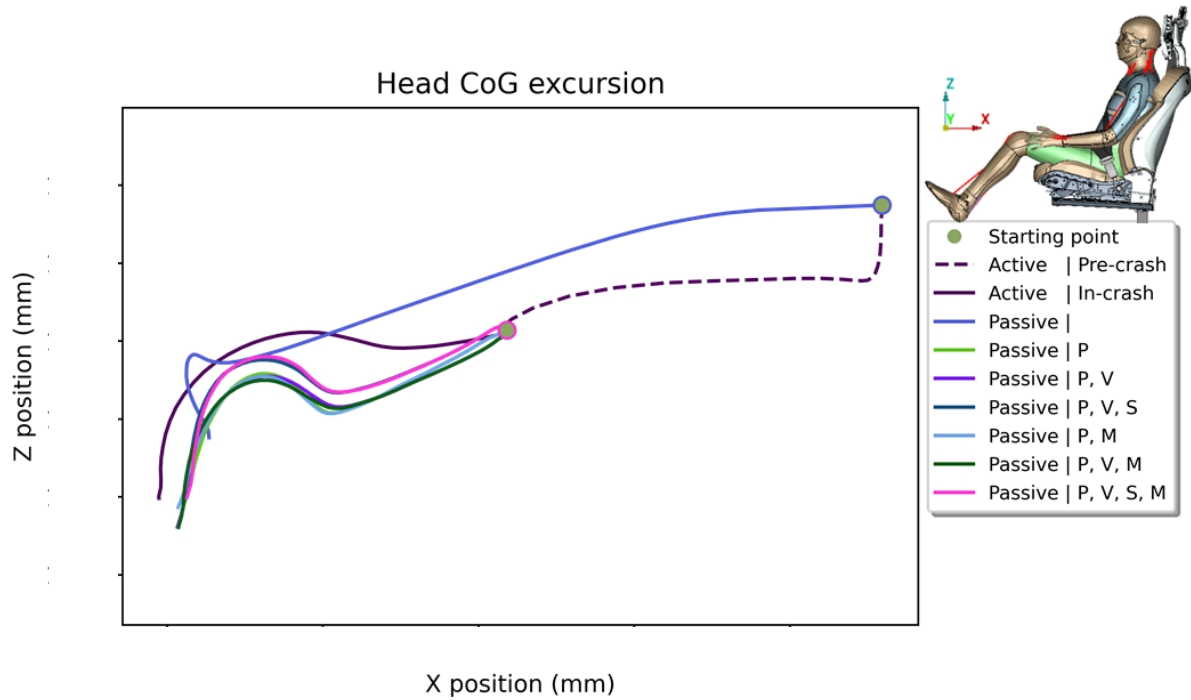


Figure 45: Head CoG excursion. XZ plane. Braking and Moderate Overlap Frontal Test

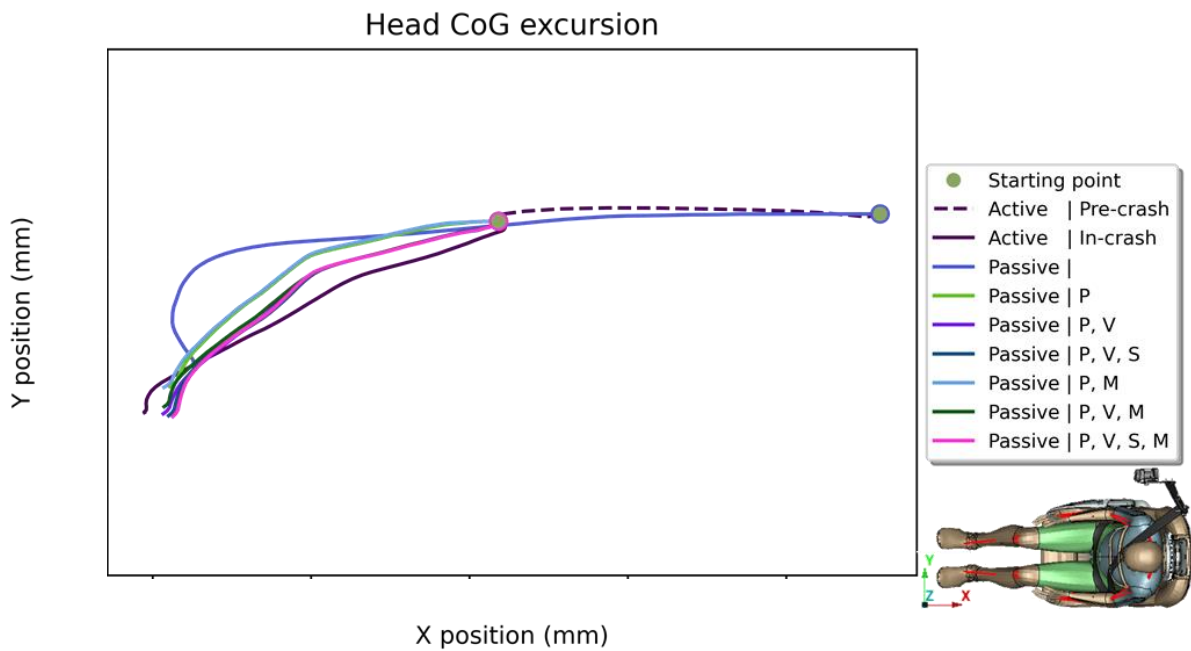


Figure 46: Head CoG excursion. XY plane. Braking and Moderate Overlap Frontal Test

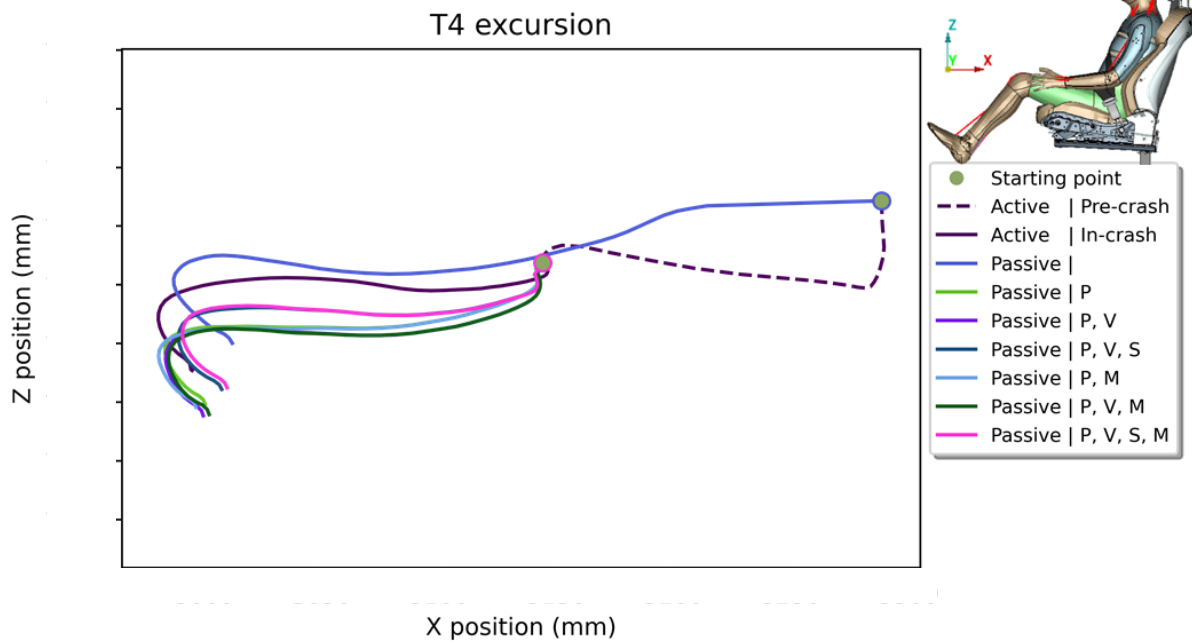


Figure 47: Chest excursion. XZ plane. Braking and Moderate Overlap Frontal Test

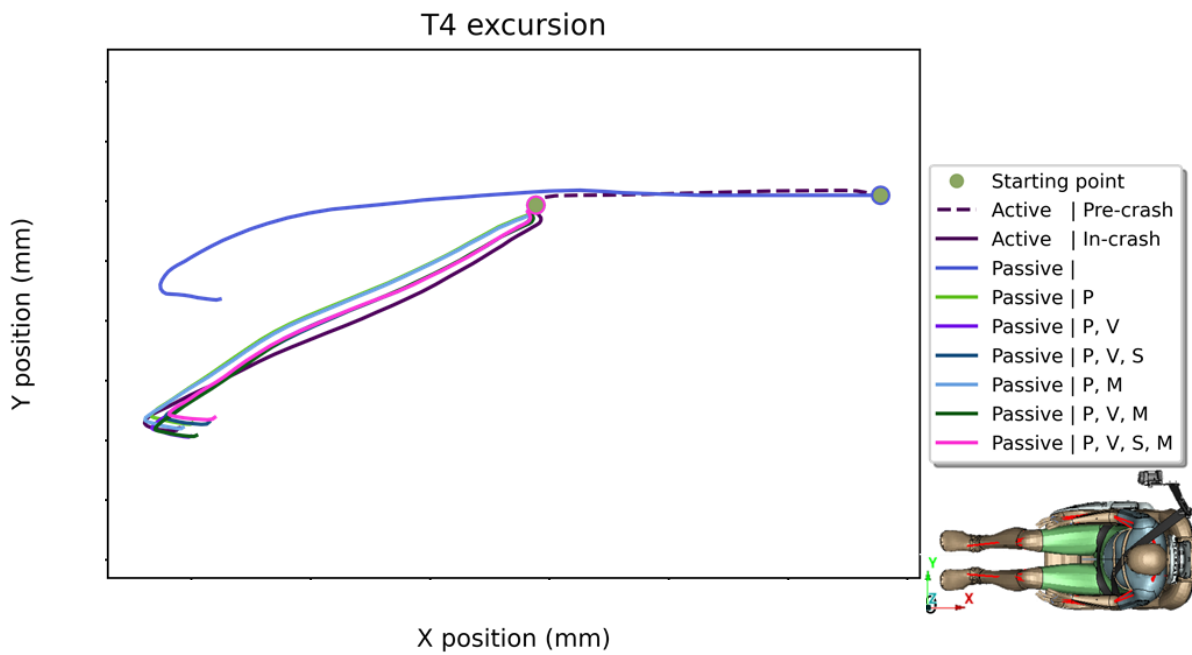


Figure 48: Chest excursion. XY plane. Braking and Moderate Overlap Frontal Test

RESULTS

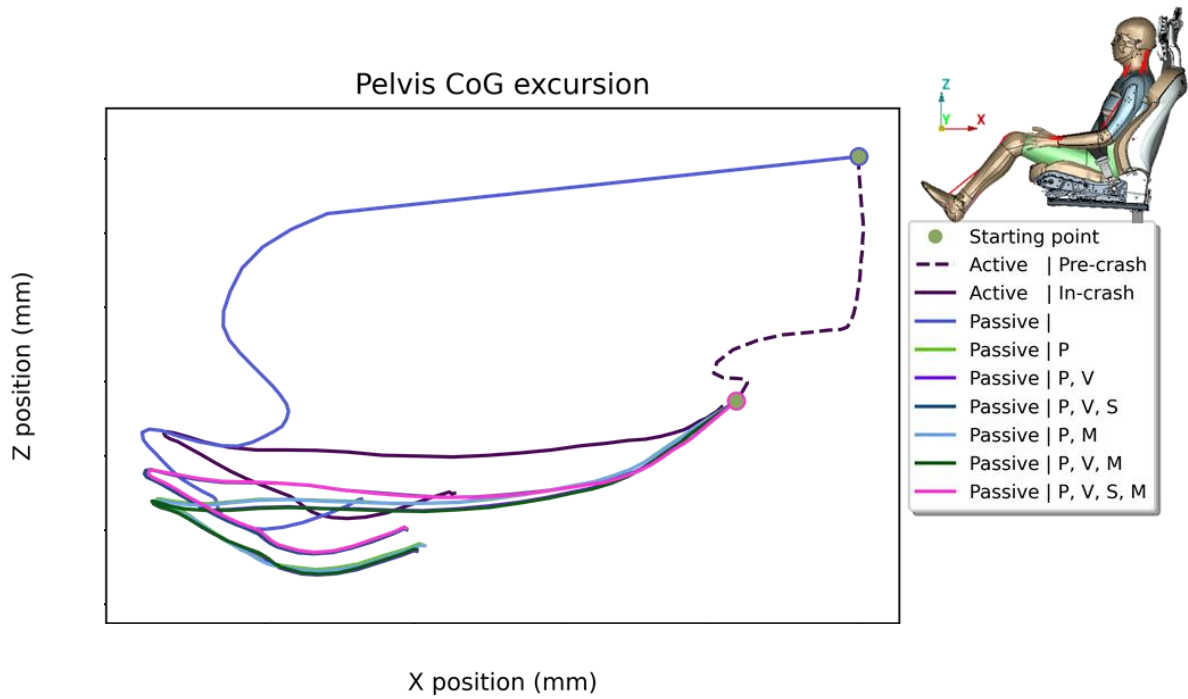


Figure 49: Pelvis CoG excursion. XZ plane. Braking and Moderate Overlap Frontal Test

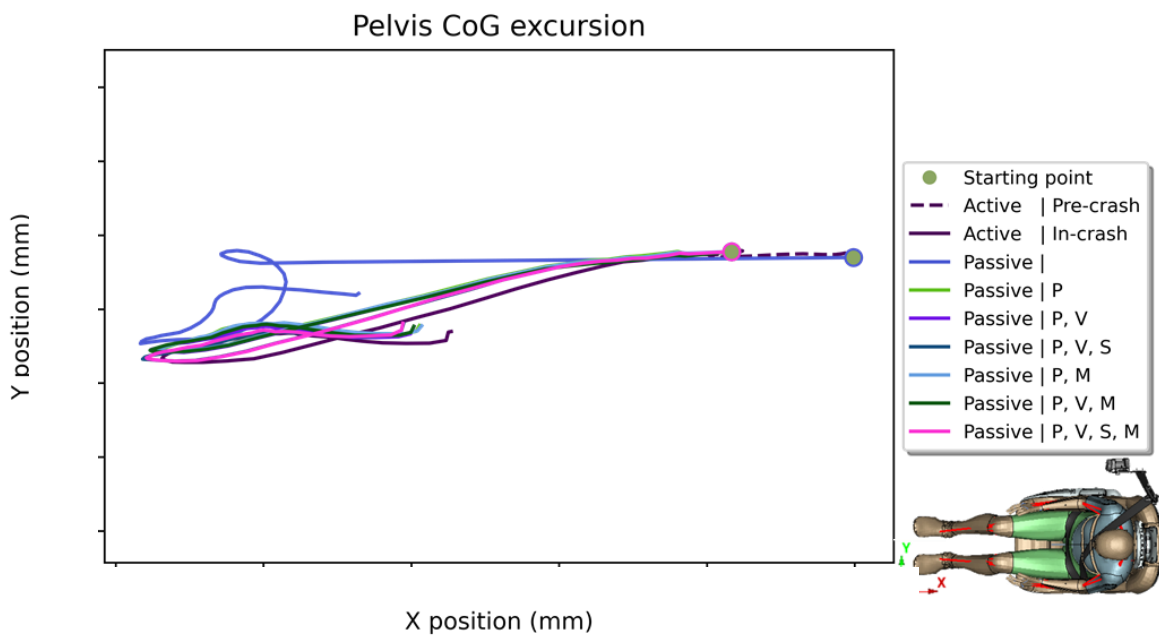


Figure 50: Pelvis CoG excursion. XY plane. Braking and Moderate Overlap Frontal Test

It can be observed that the excursions of the head, chest, and pelvis in the passive simulation with no inputs are very different compared to the rest of the passive simulations. Moreover, these excursions are very distant from the active simulation excursions.

Regarding the rest of the passive simulations, there are two differentiated groups of excursions: passive simulations with stresses and passive simulations with no stresses. The excursions of the simulations that have stresses seem to be closer to the excursions of the baseline simulation.

Concerning injury criteria, all the results have been normalized using the baseline simulation value as a reference. Consequently, all the baseline injury risk predictions have value 1 and the passive simulation values oscillate around the value 1. Thus, the variations of the passive simulations with respect to the active one can be observed.

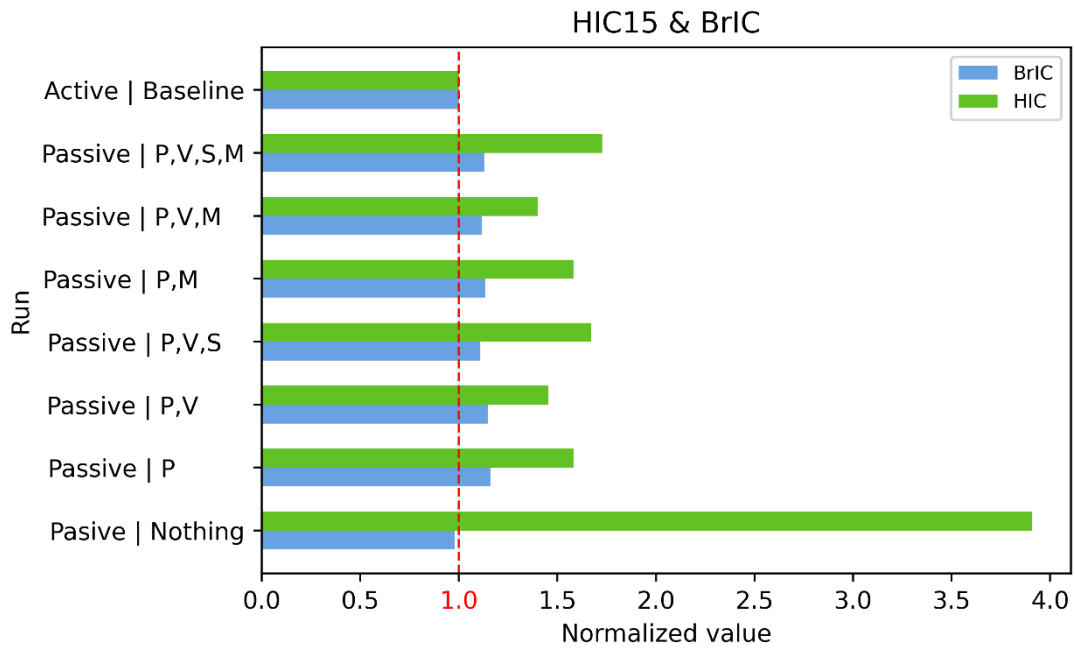


Figure 51: HIC 15ms and BrIC. Braking and Moderate Overlap Frontal Test

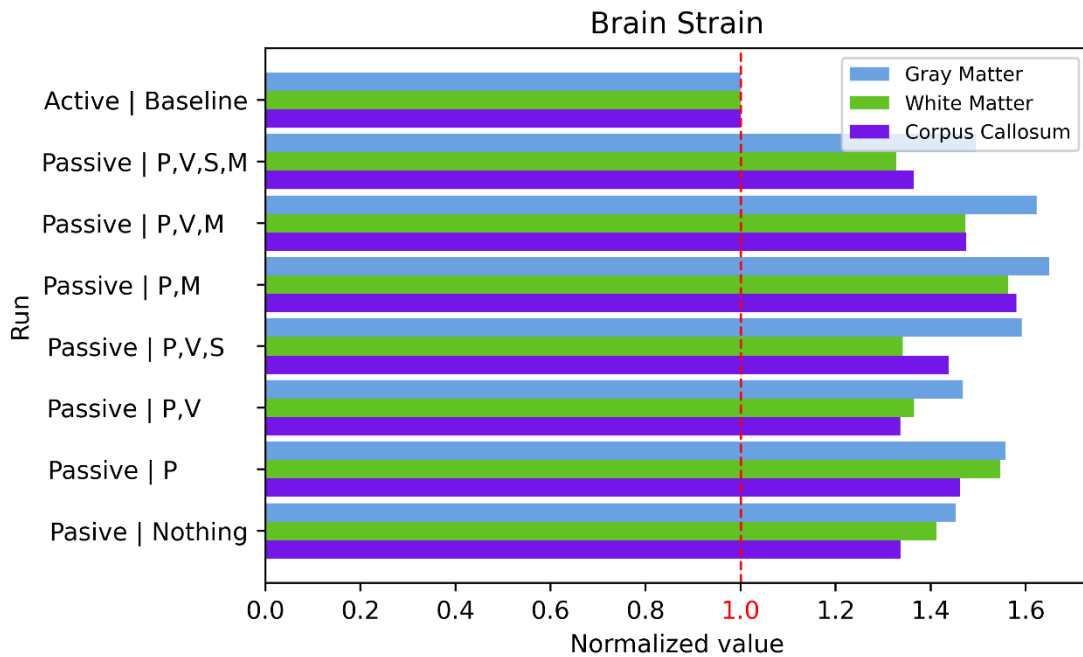


Figure 52: Brain strain. Braking and Moderate Overlap Frontal Test

RESULTS

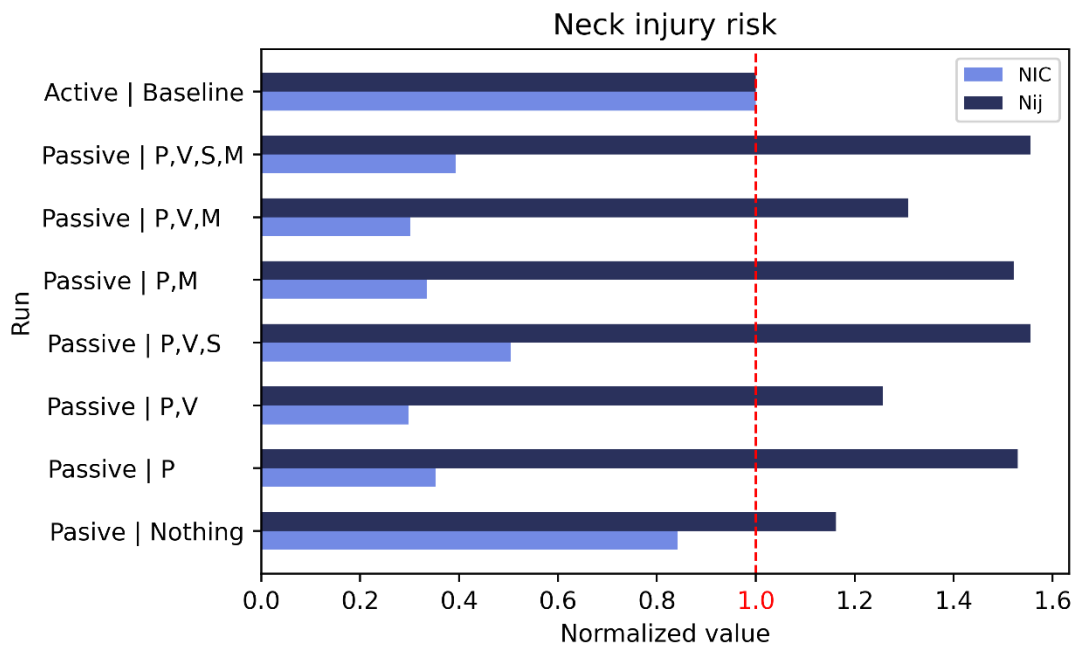


Figure 53: Neck injury risk. Braking and Moderate Overlap Frontal Test

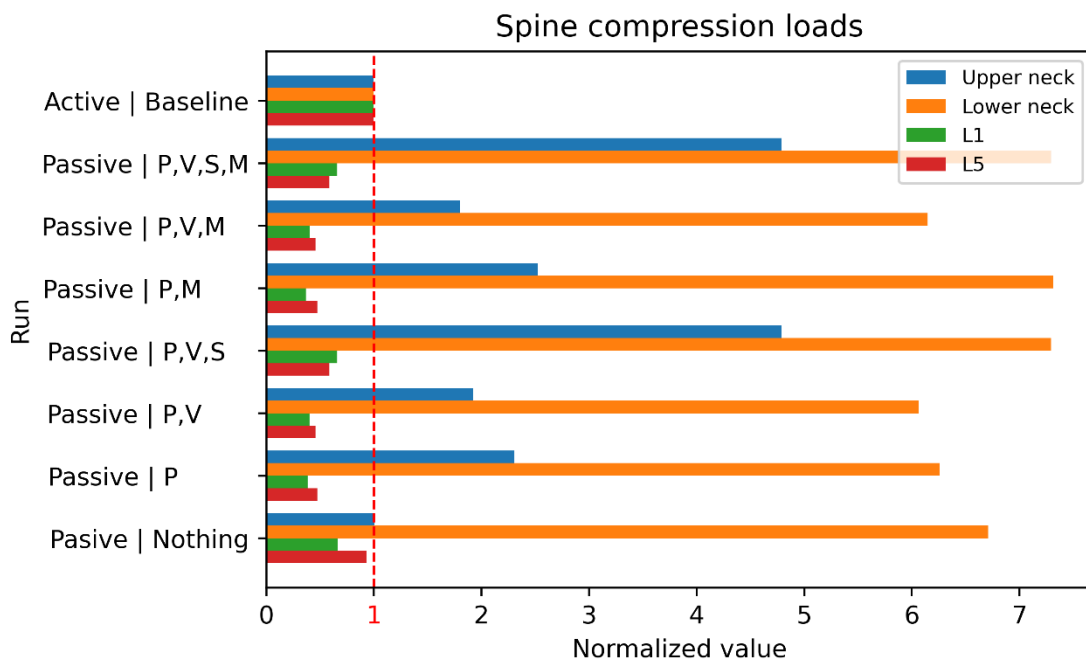


Figure 54: Spine compression loads. Braking and Moderate Overlap Frontal Test

Regarding the head, HIC 15 ms is greatly overpredicted compared to the baseline model in the simulation with no inputs. Brain strains however reach the maximum values in the simulation with posture and MPID as inputs. It can be appreciated that adding extra inputs improves the brain strain prediction, obtaining the closest values when posture and velocity are added to the simulation. Muscle activity level (MPID) however seems to not affect the results significantly.

Regarding the neck and the spine, compression loads in the upper neck are overpredicted in all cases and lumbar compression loads are underestimated. These predictions get the closest values when only posture and initial velocities of the HBM are included. The NIC and Nij are wrongly predicted compared to the baseline model by the passive simulations compared to the baseline. The closest values are obtained for no input simulation.

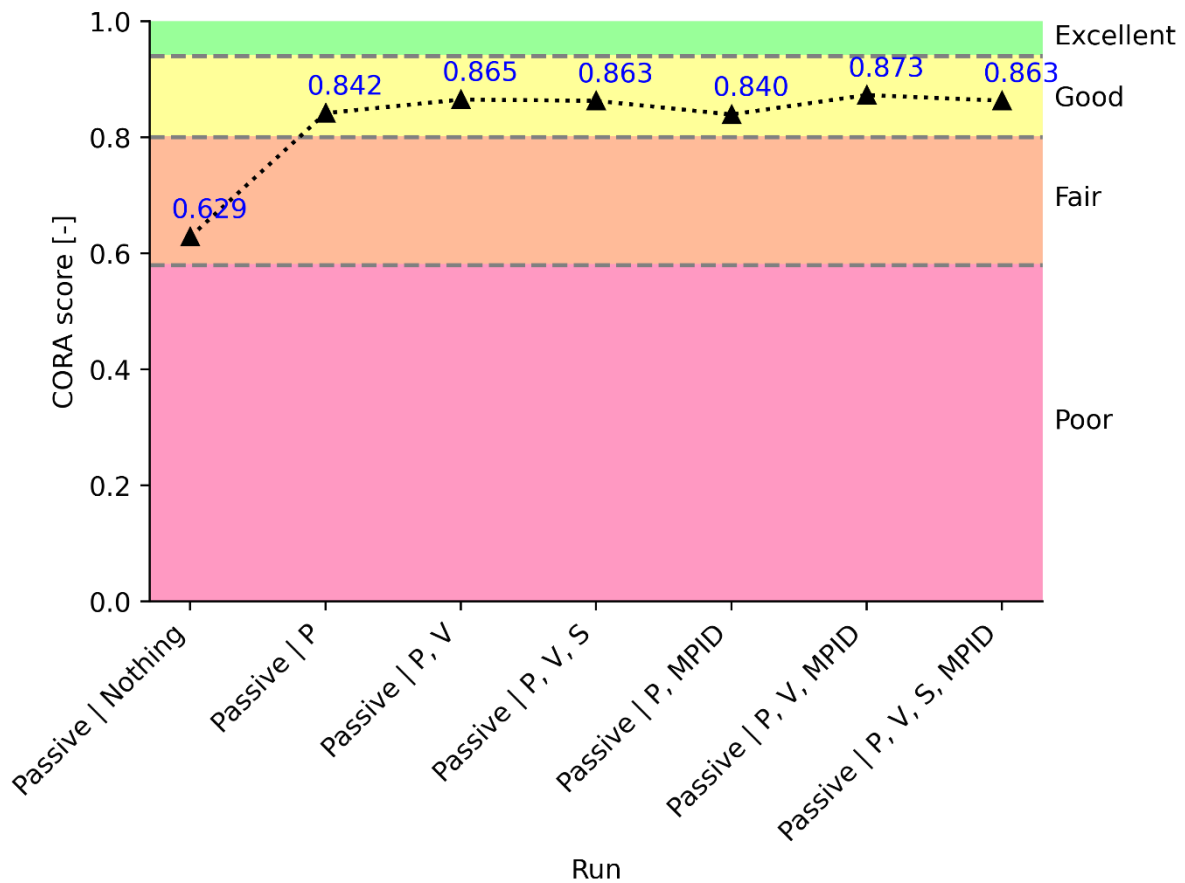


Figure 55: CORAplus acceleration ratings. Braking and Moderate Overlap Frontal Test

Lastly, regarding the CORAplus ratings, there is a big improvement if the posture of the occupant is added as an input in the passive simulation, changing the overall rating from “Fair” to “Good”. Adding velocity or velocity and stress improves the rating a bit more, but the passive model is not able to reproduce the accelerations of the active model with an “Excellent” rating. Muscle level activity does not improve results. Moreover, on some occasions adding the MPID worsens the rating.

RESULTS

3.3.- Braking + Mobile Progressive Deformable Barrier

Regarding excursions of the head, chest, and pelvis; there are two differentiated groups regarding passive simulations: the passive simulation with no inputs and the passive simulations that have the posture of the HBM at the end of the pre-crash as input.

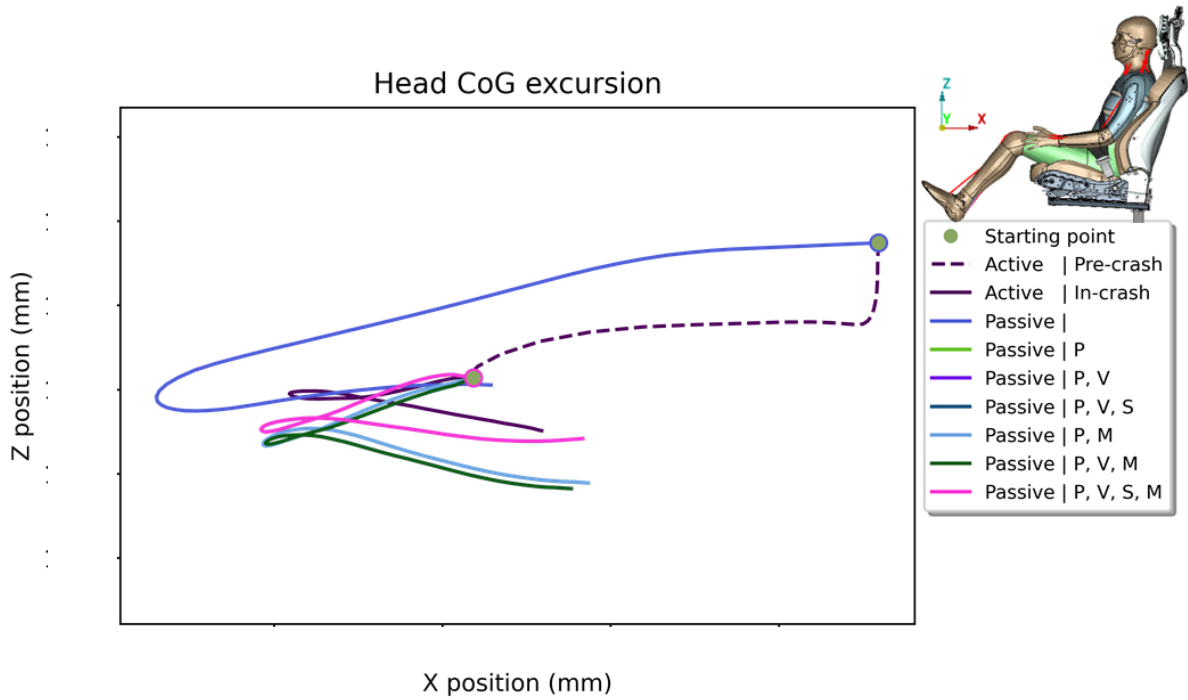


Figure 56: Head CoG excursion. XZ plane. Braking and Mobile Progressive Deformable Barrier

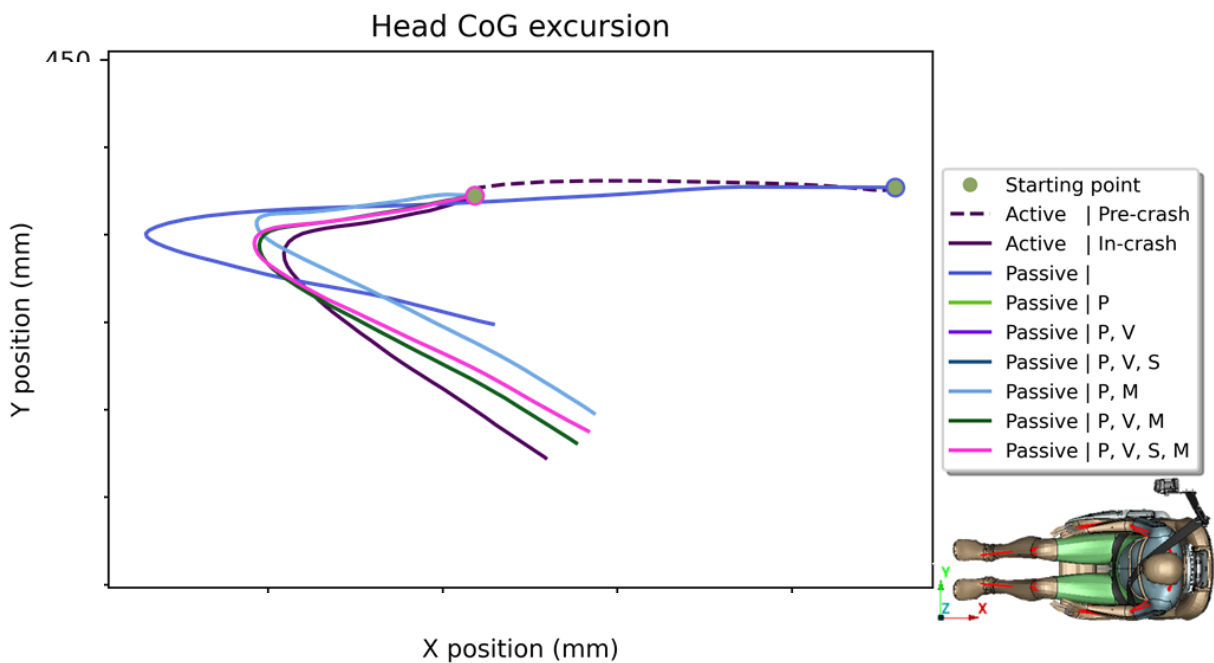


Figure 57: Head CoG excursion. XY plane. Braking and Mobile Progressive Deformable Barrier

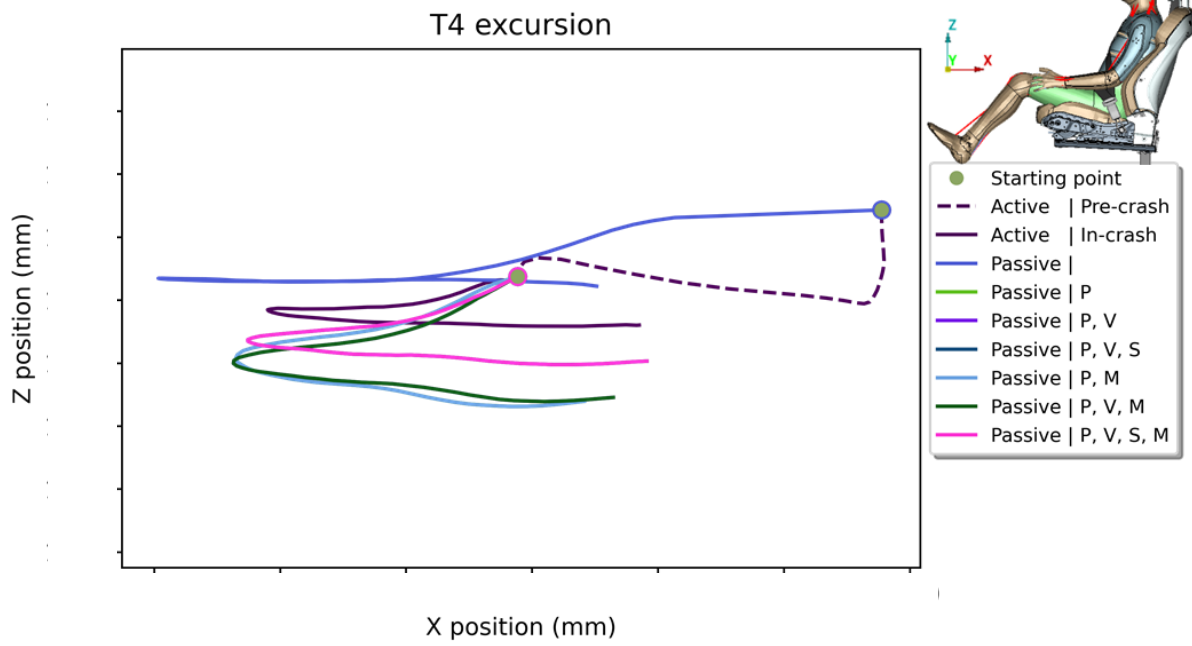


Figure 58: Chest excursion. XZ plane. Braking and Mobile Progressive Deformable Barrier

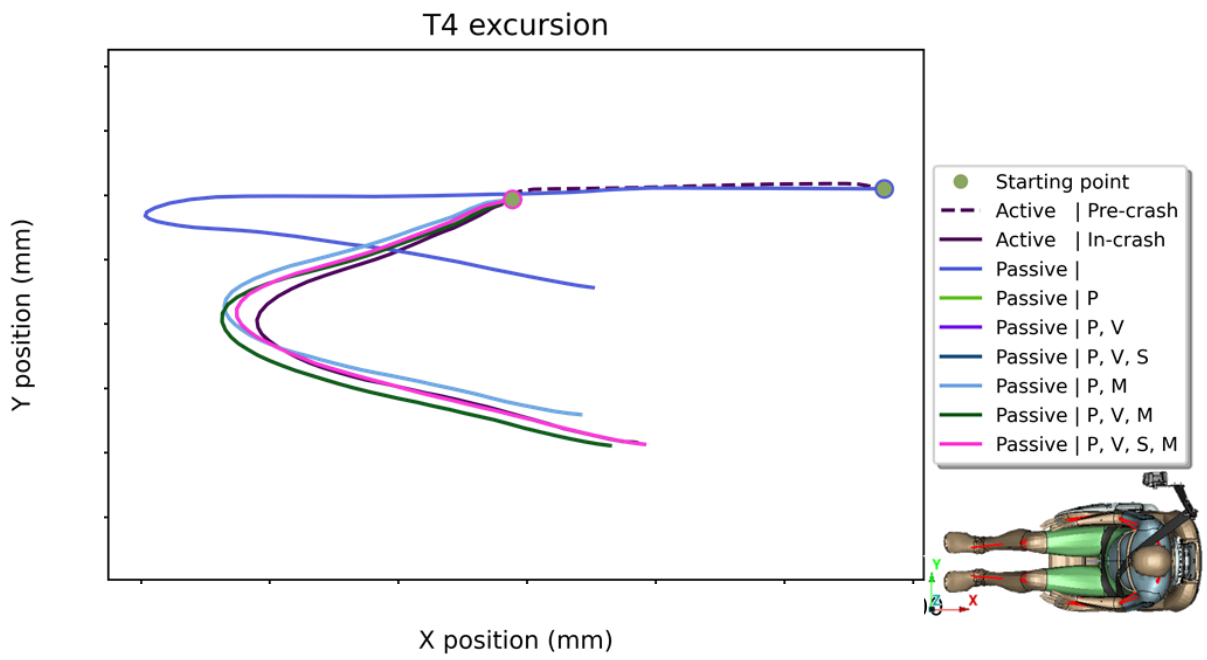


Figure 59: Chest excursion. XY plane. Braking and Mobile Progressive Deformable Barrier

RESULTS

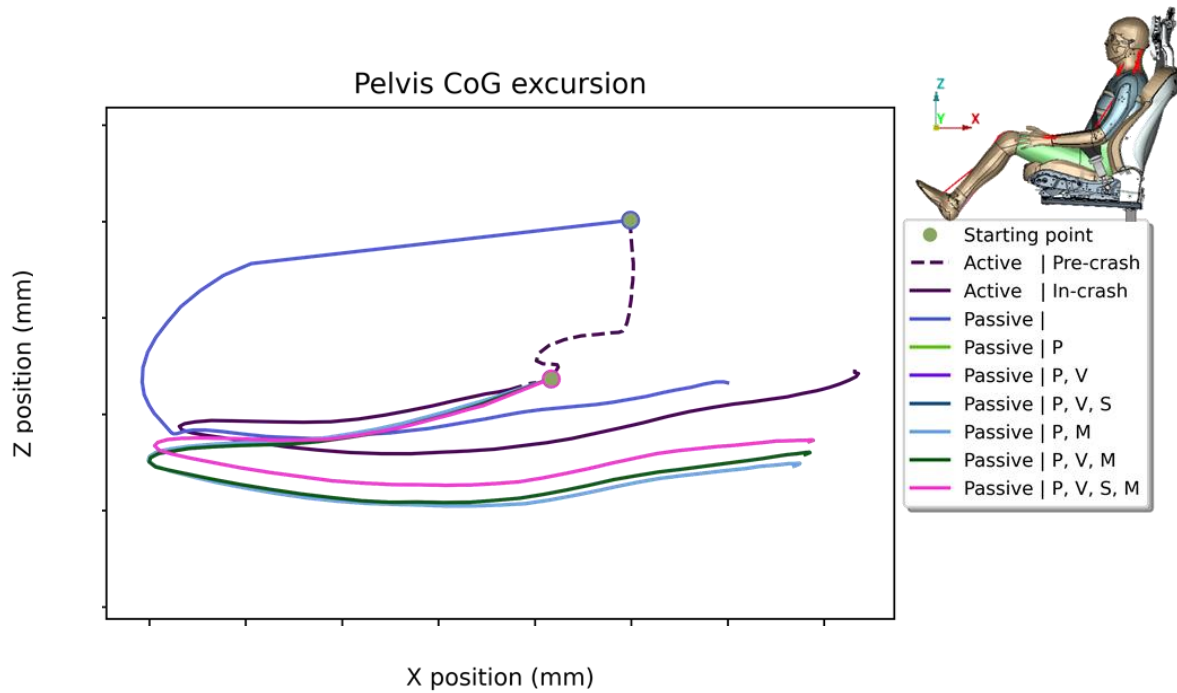


Figure 60: Pelvis CoG excursion. XZ plane. Braking and Mobile Progressive Deformable Barrier

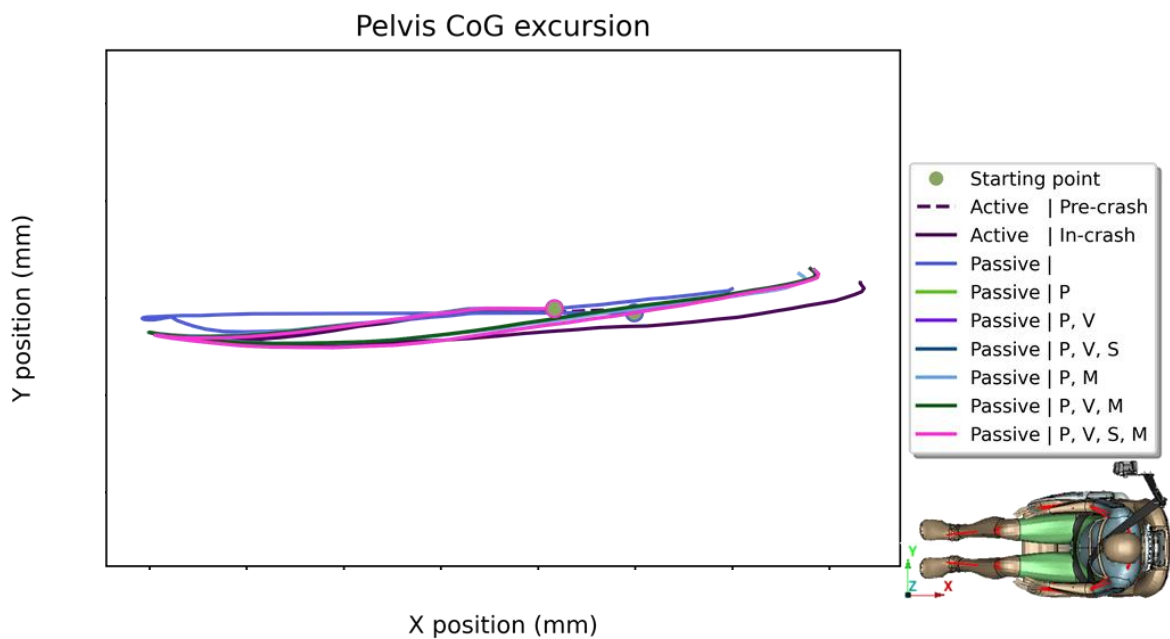


Figure 61: Pelvis CoG excursion. XY plane. Braking and Mobile Progressive Deformable Barrier

It can be observed that the excursions of the head, chest, and pelvis in the passive simulation with no inputs are very different compared to the rest of the passive simulations. Moreover, these excursions are very distant from the active simulation excursions.

Regarding the rest of the passive simulations, there are two differentiated groups of excursions: passive simulations with stresses and passive simulations with no stresses. The excursions of the simulations that have stresses seem to be closer to the excursions of the baseline simulation. However, there is still a slope difference between them that could be generated by the different belts used for each simulation.

Concerning injury criteria, all the results have been normalized using the baseline simulation value as a reference. Consequently, all the baseline injury risk predictions have value 1 and the passive simulation values oscillate around the value 1. Thus, the variations of the passive simulations with respect to the active one can be observed.

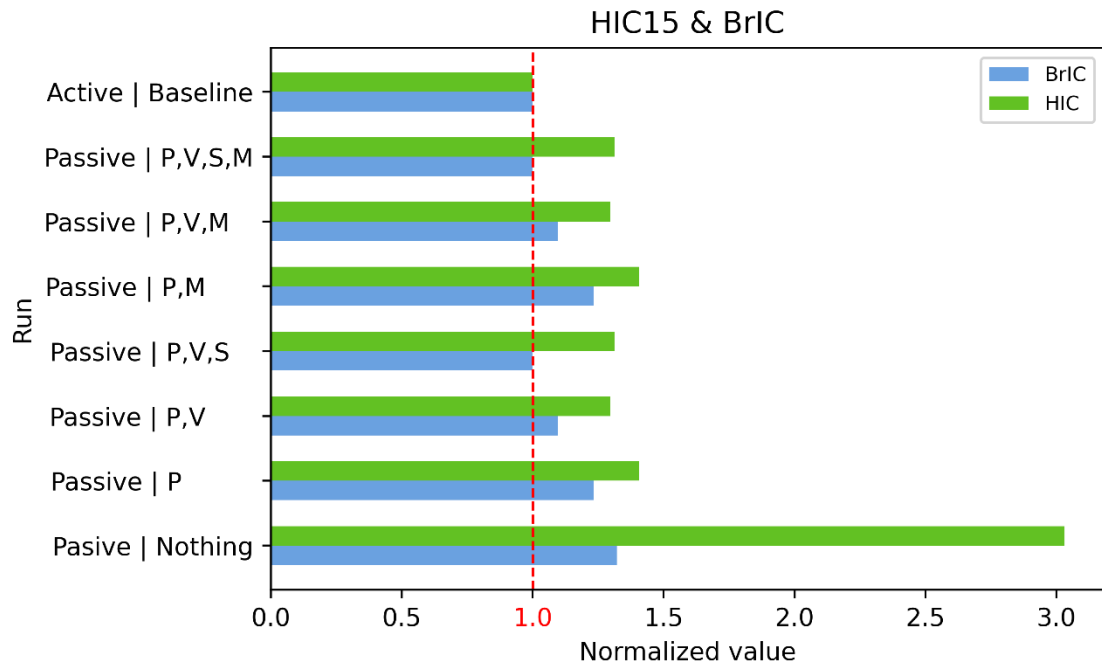


Figure 62: HIC 15ms and BrIC. Braking and Mobile Progressive Deformable Barrier

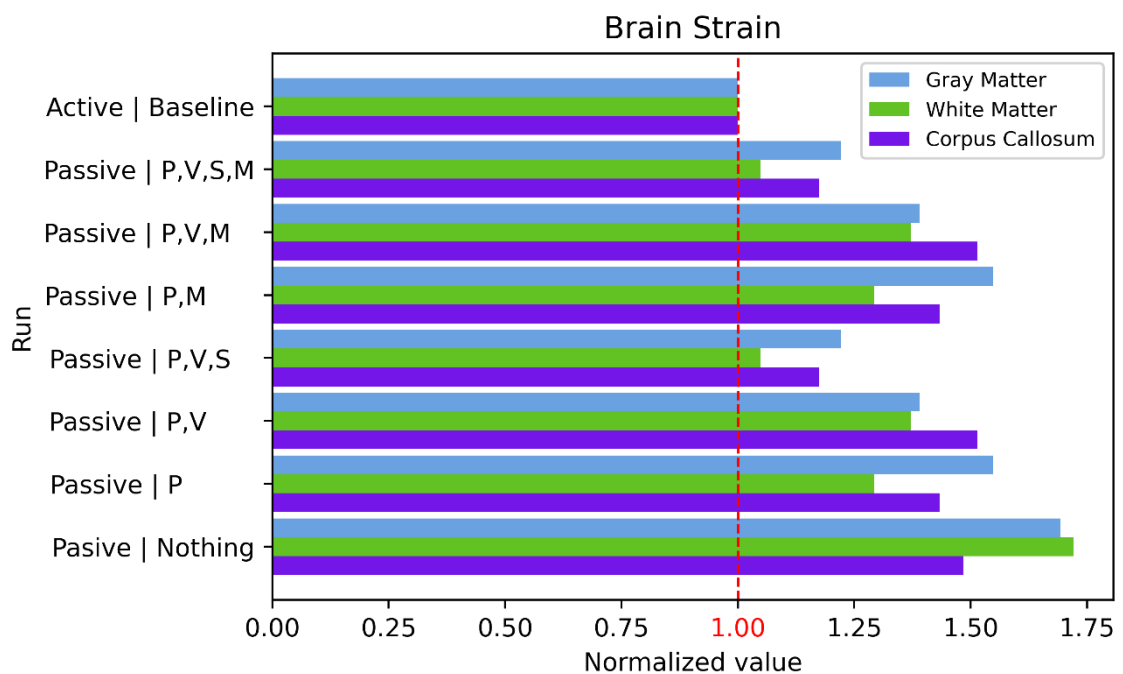


Figure 63: Brain strain. Braking and Mobile Progressive Deformable Barrier

RESULTS

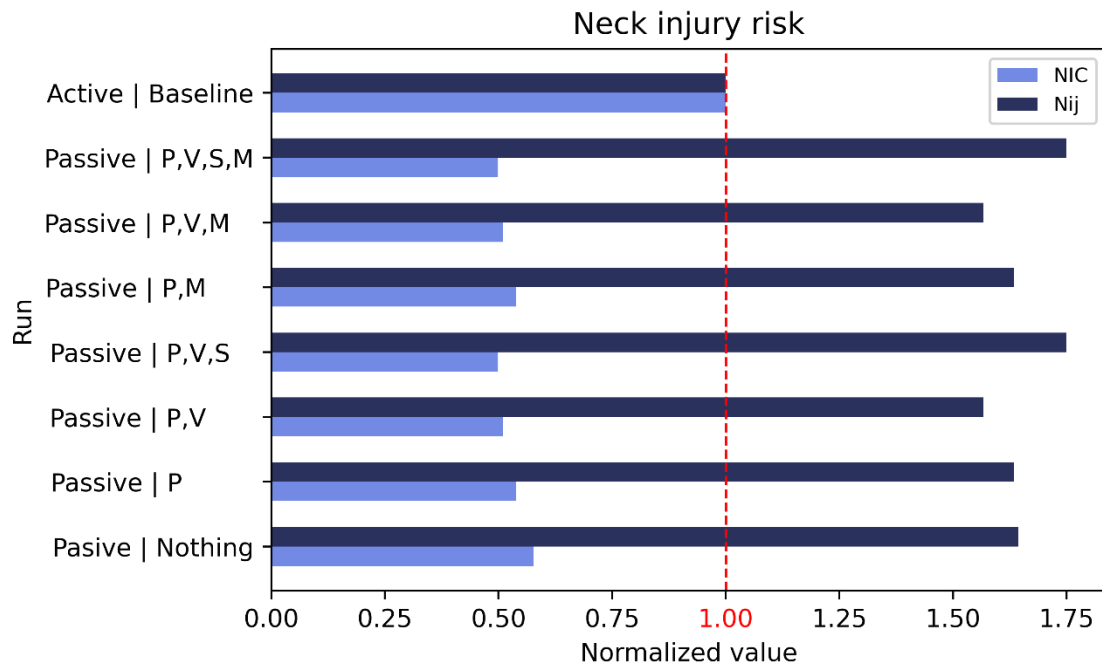


Figure 64: Neck injury risk. Braking and Mobile Progressive Deformable Barrier

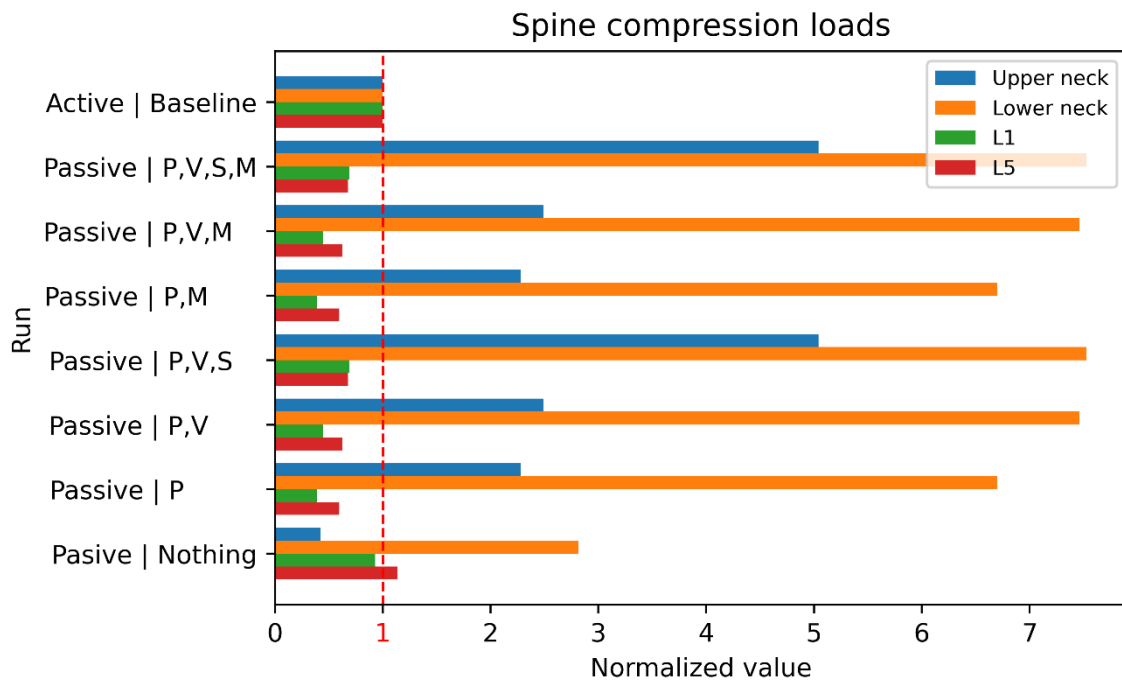


Figure 65: Spine compression loads. Braking and Mobile Progressive Deformable Barrier

Regarding the head, HIC 15 ms is greatly overpredicted compared to the baseline model in the simulation with no inputs, and the strains in the brain are the largest of all the passive simulations. It can be appreciated that adding extra inputs improves the brain strain prediction, obtaining the closest values when posture, velocity, and stresses are added to the simulation. Muscle activity level (MPID) however seems to not affect the results significantly.

Regarding the neck and the spine, compression loads in the upper neck are overpredicted compared to the baseline model in all cases and lumbar compression loads are underestimated. These predictions get the closest values only when the posture of the HBM is included. The NIC and Nij are wrongly predicted by the passive simulations compared to the baseline. The closest values are obtained for posture and velocity input simulation.

Regarding the rib cage strain model, risks of fracture are overpredicted compared to the baseline model in all the passive simulations for the three groups of ages.

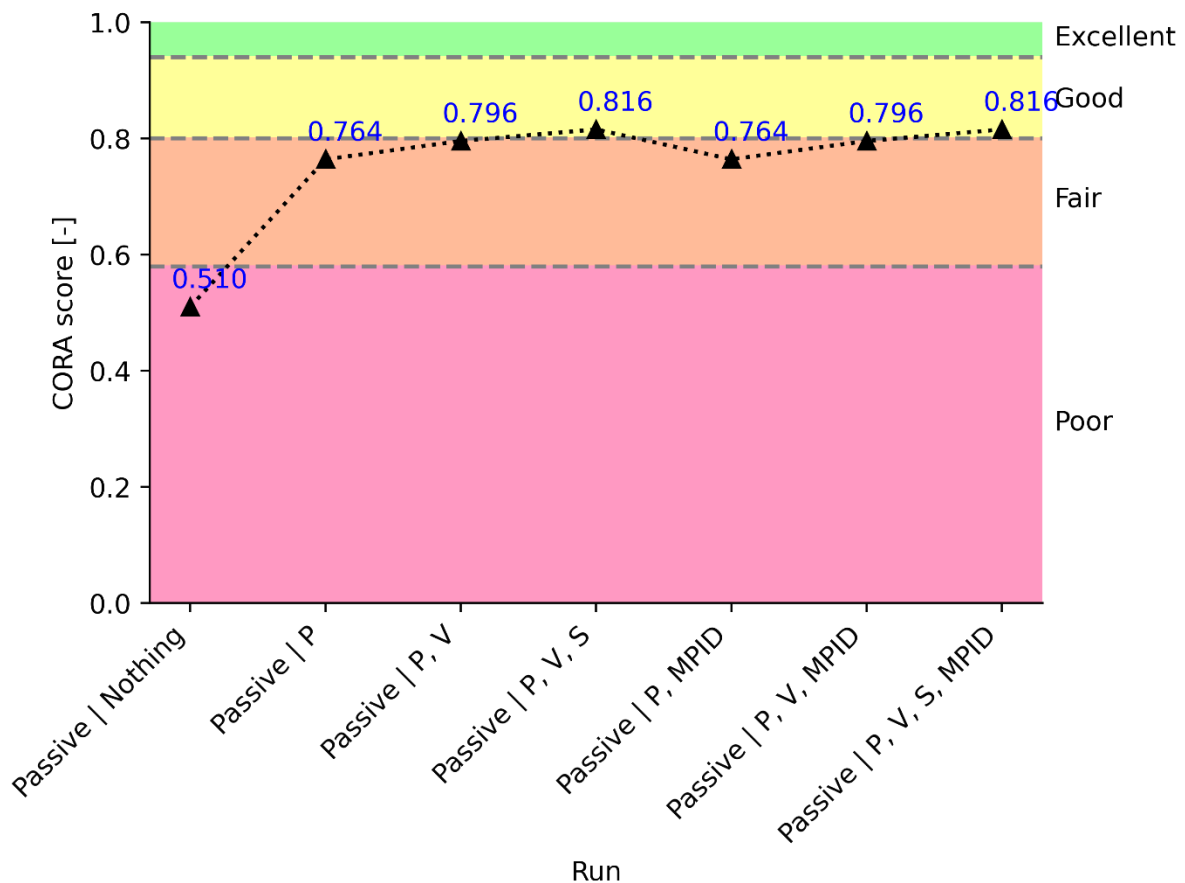


Figure 66: CORAplus acceleration ratings. Braking and Mobile Progressive Deformable Barrier

Lastly, regarding the CORAplus ratings, there is a big improvement if the posture of the occupant is added as an input in the passive simulation, changing the overall rating from “Poor” to “Fair”. Adding velocity improves the rating a bit more but adding velocity and stress make the CORA rating reach the “Good” category. However, the passive model is not able to reproduce the accelerations of the active model with an “Excellent” rating. Muscle level activity does not improve results.

RESULTS

3.4.- Turn right and braking + Passenger-side Small Overlap

Regarding excursions of the head, chest, and pelvis; there are two differentiated groups regarding passive simulations: the passive simulation with no inputs and the passive simulations that have the posture of the HBM at the end of the pre-crash as input.

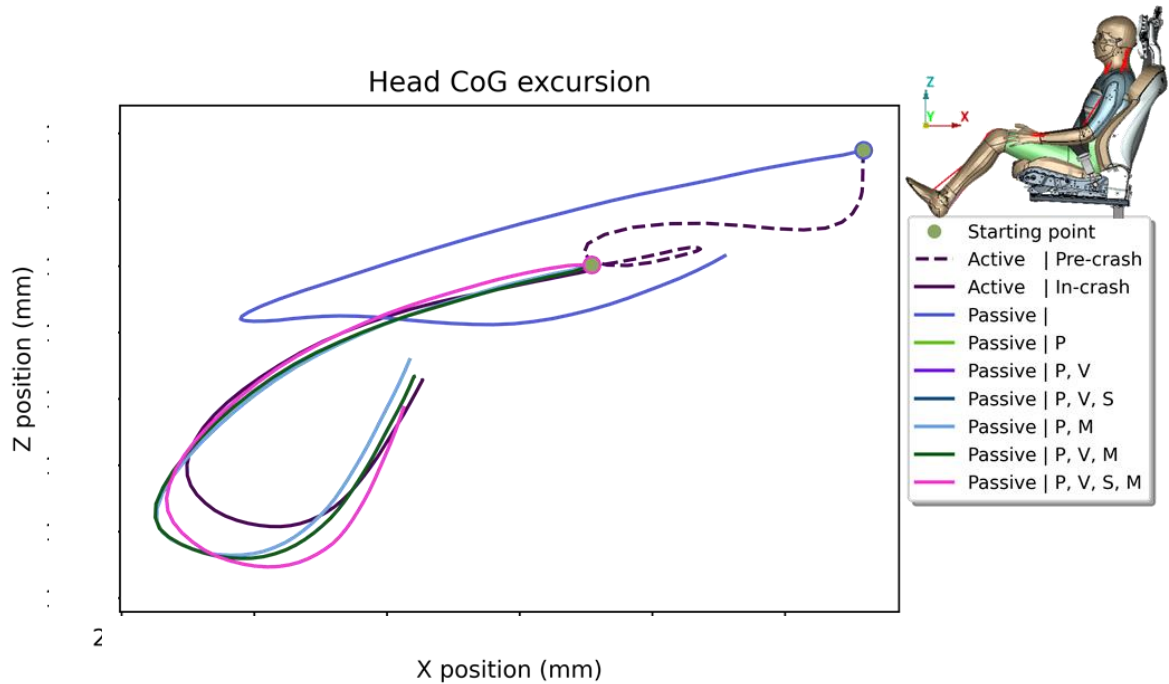


Figure 67: Head CoG excursion. XZ plane. Turn right and braking + Passenger-side Small Overlap

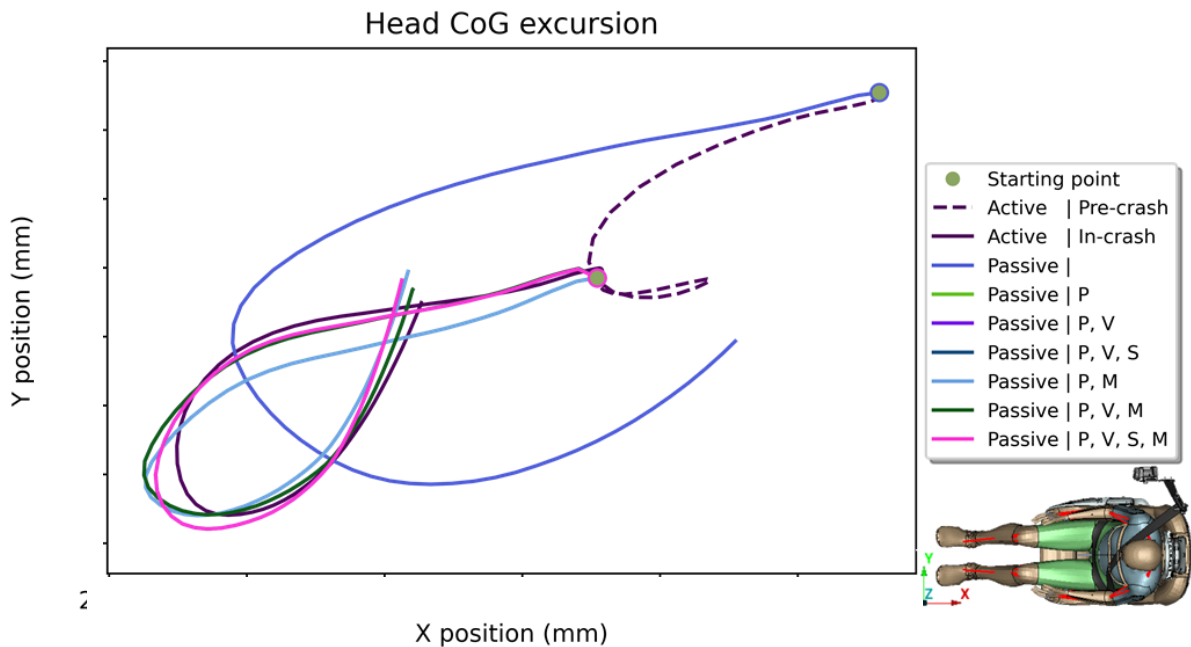


Figure 68: Head CoG excursion. XY plane. Turn right and braking + Passenger-side Small Overlap

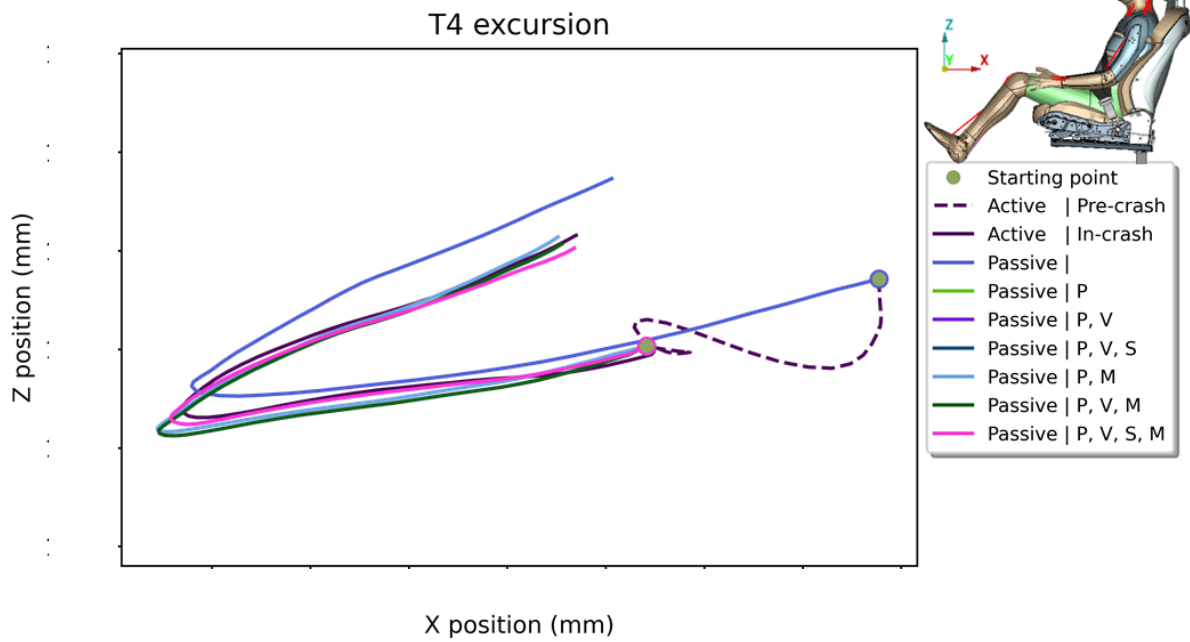


Figure 69: Chest excursion. XZ plane. Turn right and braking + Passenger-side Small Overlap

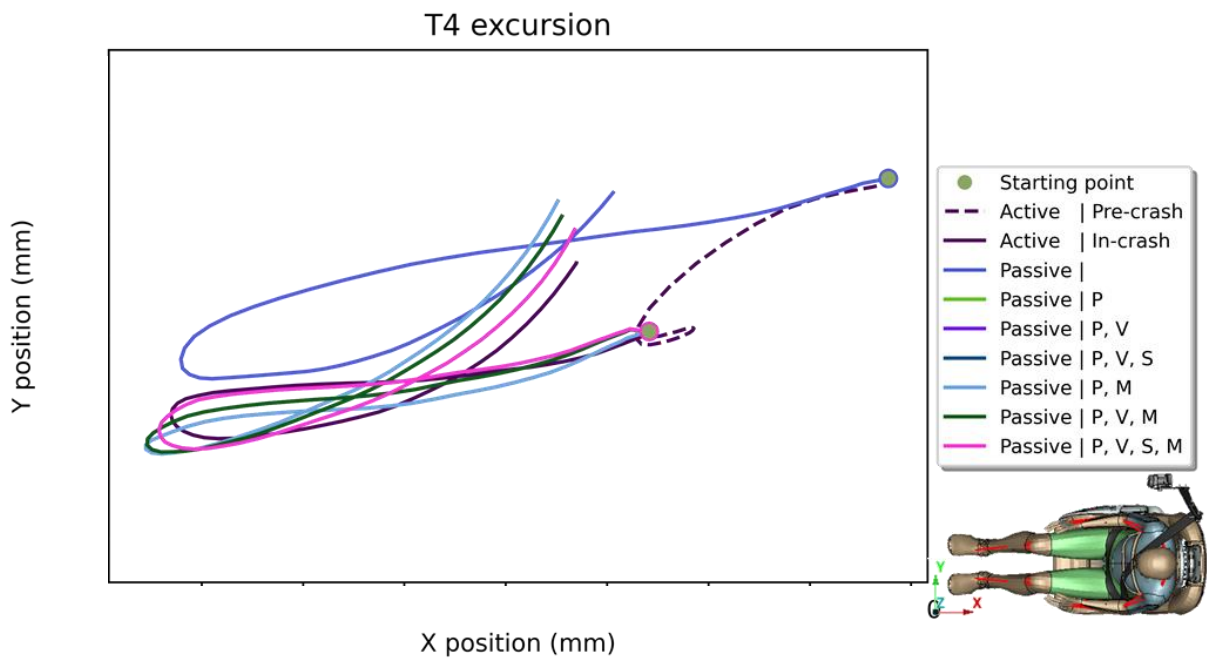


Figure 70: Chest excursion. XY plane. Turn right and braking + Passenger-side Small Overlap

RESULTS

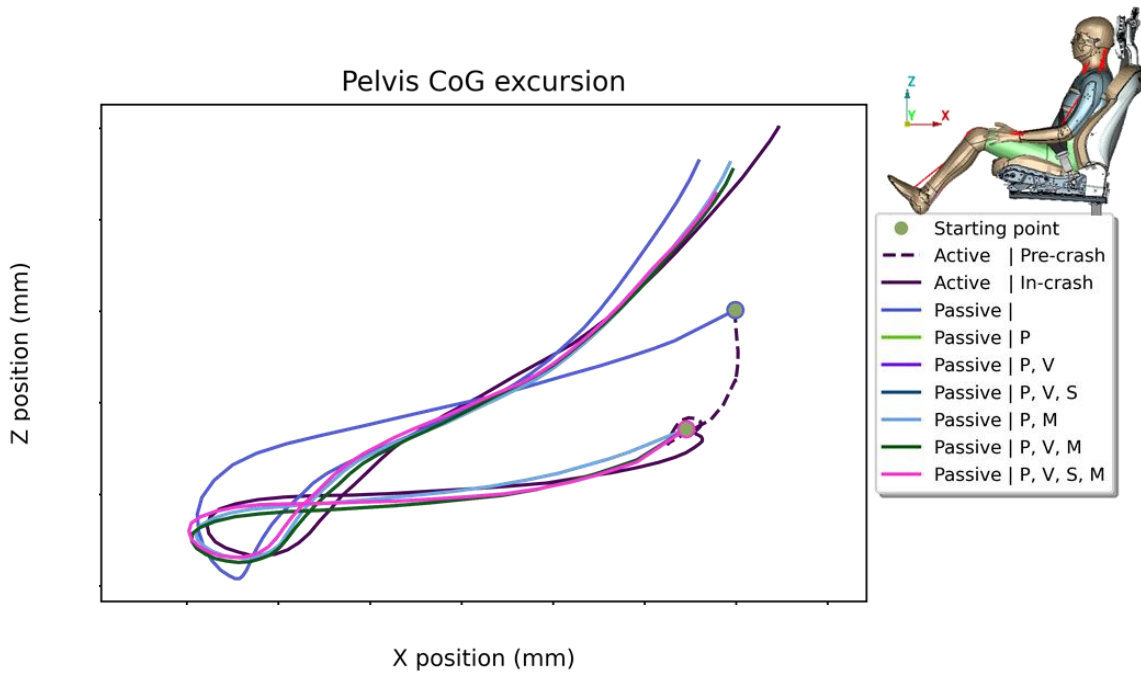


Figure 71: Pelvis CoG excursion. XZ plane. Turn right and braking + Passenger-side Small Overlap

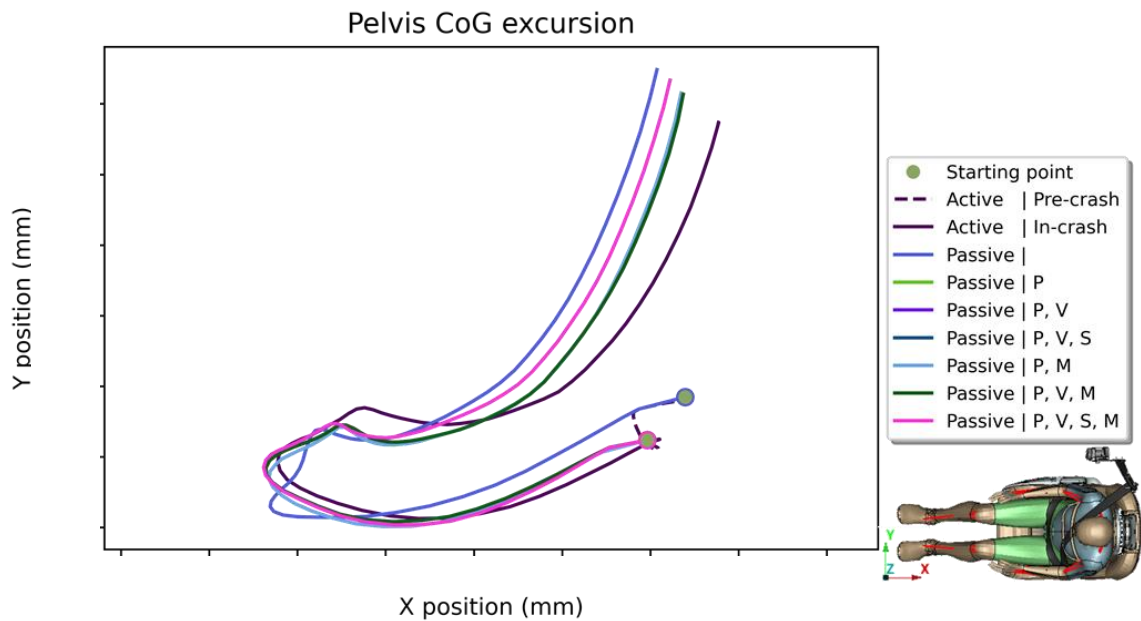


Figure 72: Pelvis CoG excursion. XY plane. Turn right and braking + Passenger-side Small Overlap

It can be observed that the excursions of the head, chest, and pelvis in the passive simulation with no inputs are very different compared to the rest of the passive simulations. Moreover, these excursions are very distant from the active simulation excursions.

Regarding the rest of the passive simulations, there are three differentiated groups of excursions: passive simulations with posture input, passive simulations with posture and velocity, and passive simulations with posture, velocity, and stresses. The excursions of the simulations that have stresses seem to be closer to the excursions of the baseline simulation. However, there are still significant differences between them that could be generated by the different belts used for each simulation.

Concerning injury criteria, all the results have been normalized using the baseline simulation value as a reference. Consequently, all the baseline injury risk predictions have value 1 and the passive simulation values oscillate around the value 1. Thus, the variations of the passive simulations with respect to the active one can be observed.

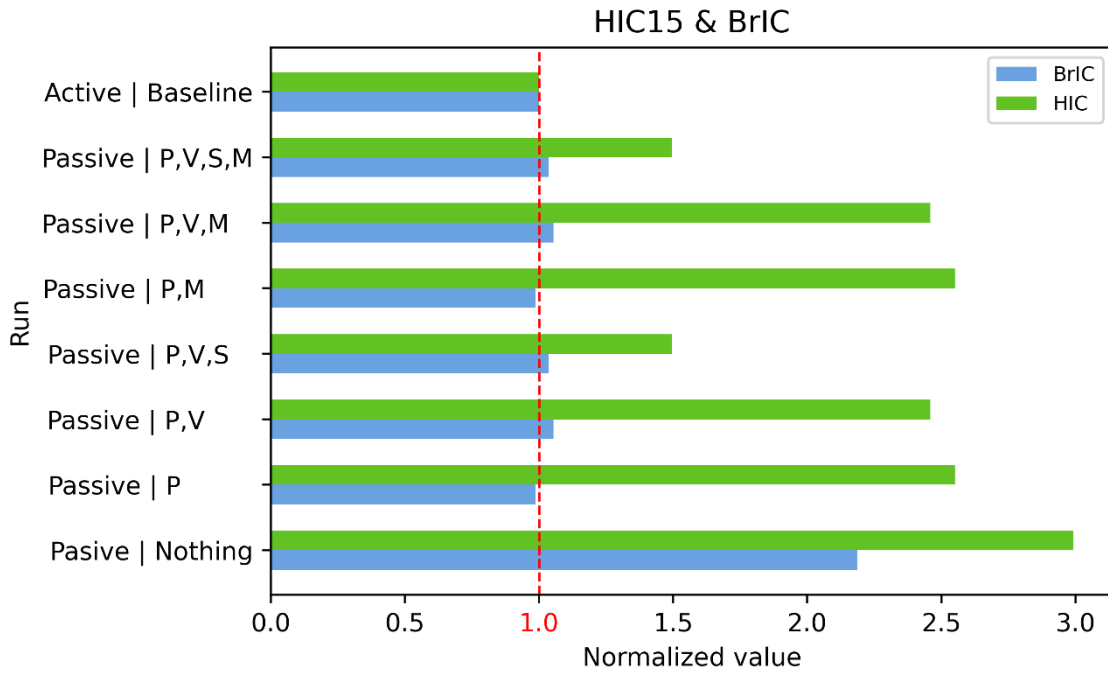


Figure 73: HIC 15ms and BrIC. Turn right and braking + Passenger-side Small Overlap

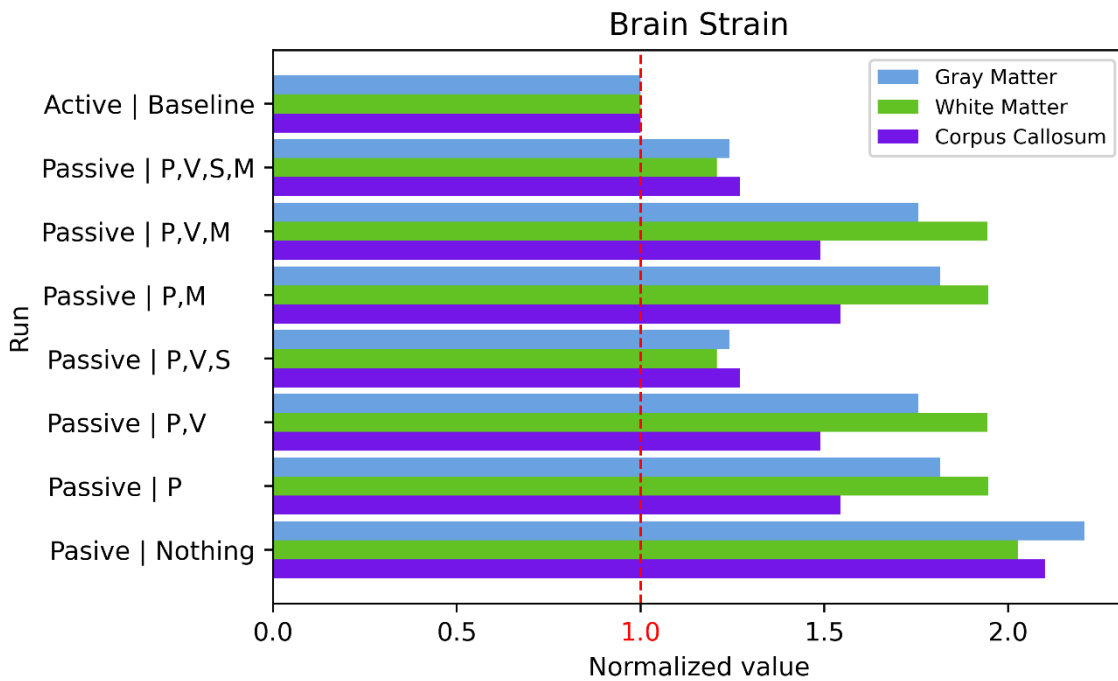


Figure 74: Brain strain. Turn right and braking + Passenger-side Small Overlap

RESULTS

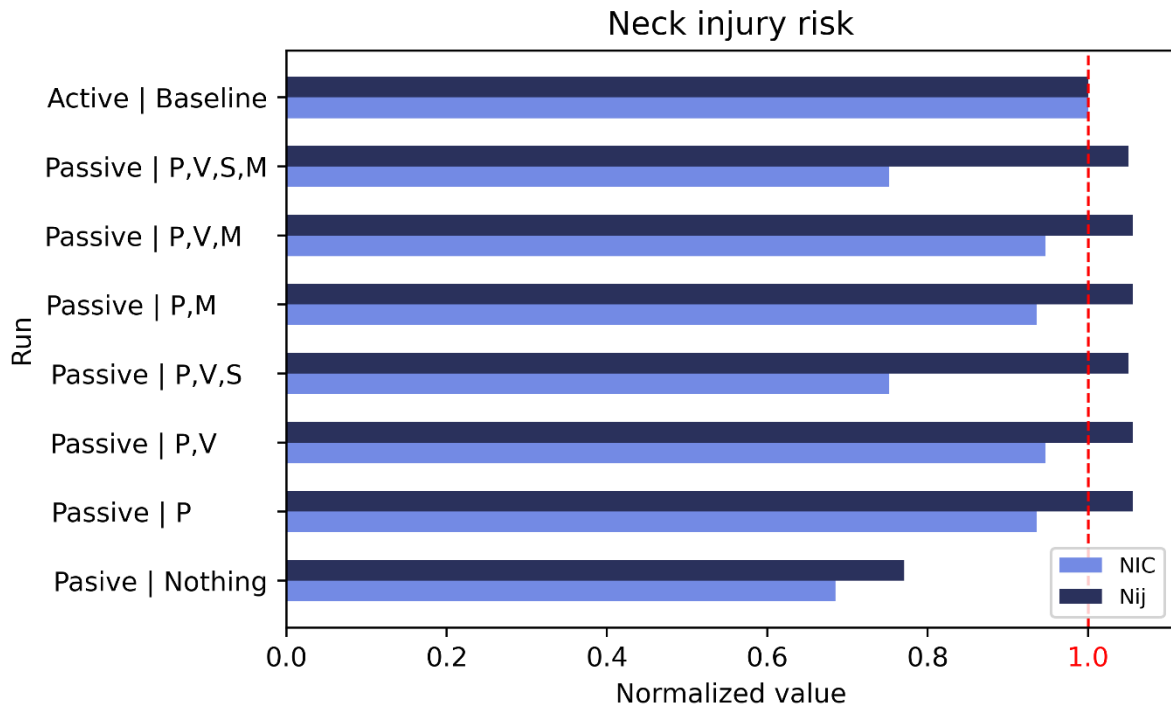


Figure 75: Neck injury risk. Turn right and braking + Passenger-side Small Overlap

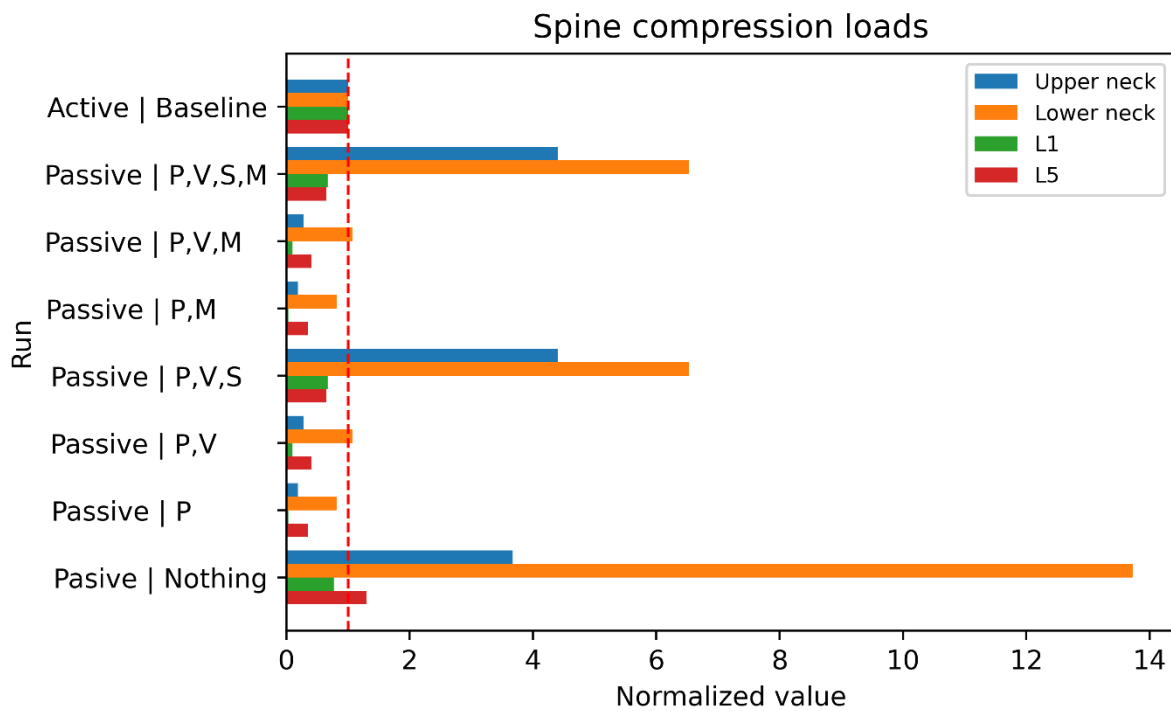


Figure 76: Spine compression loads. Turn right and braking + Passenger-side Small Overlap

Regarding the head, HIC 15 ms is overpredicted in the passive simulations, reaching the closest value in the simulation with posture, velocity, and stresses. BrIC however is precisely predicted by the passive simulations. The strains in the brain are also overpredicted compared to the baseline model but the minimum is reached as well in the simulation with posture,

velocity, and stress. Muscle activity level (MPID) however seems to not affect the results significantly.

Regarding the neck and the spine, compression loads in the upper neck are overpredicted compared to the baseline model in all cases and lumbar compression loads are underestimated compared to the baseline model. These predictions get the closest values when only the posture and velocity of the HBM are included. The NIC and Nij are predicted in a much closer way compared to the other crash simulations, but the passive simulation with no inputs is the one with the worst prediction. The closest values are obtained for posture and velocity input simulation.

Regarding the rib cage strain model, risks of fracture are a bit overpredicted compared to the baseline model in most of the passive simulations for the three groups of ages.

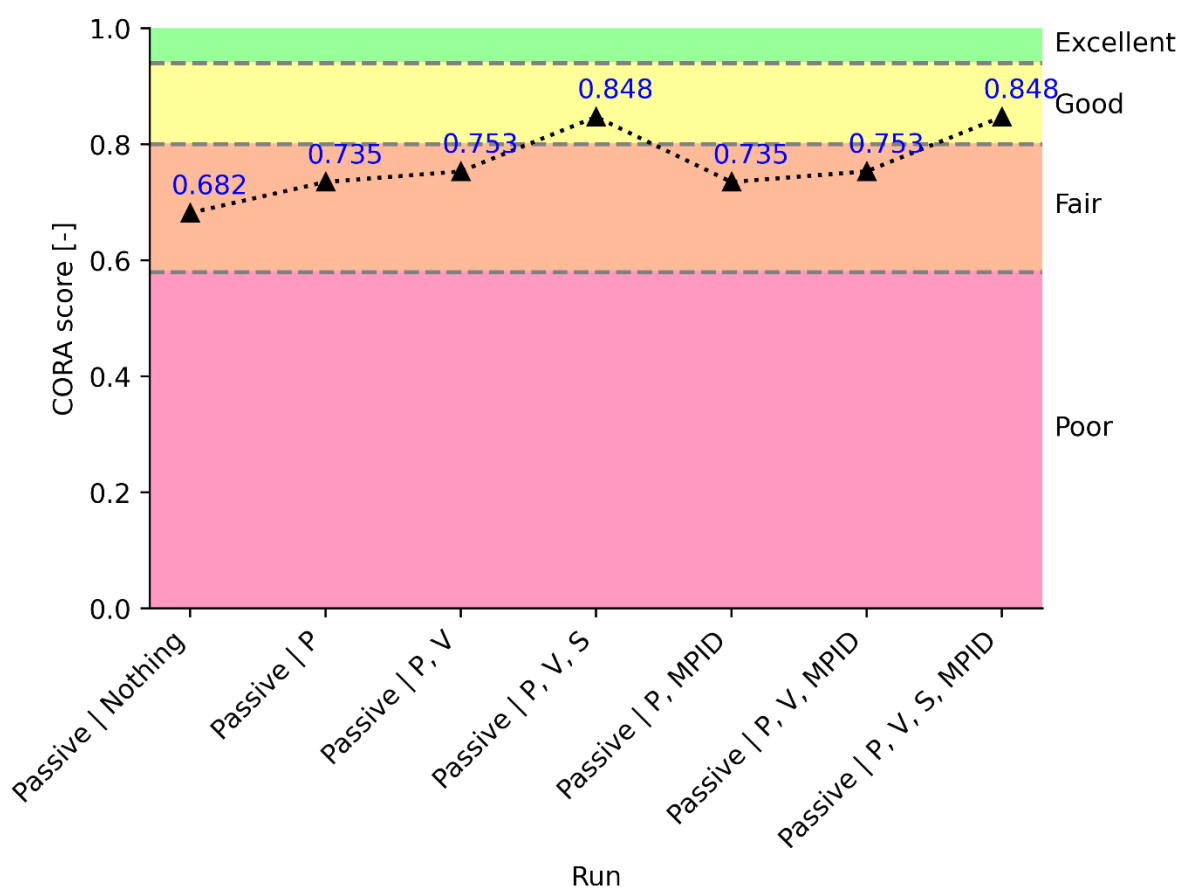


Figure 77: CORAplus acceleration ratings. Turn right and braking + Passenger-side Small Overlap

Lastly, regarding the CORAplus ratings, there is an improvement if the posture of the occupant is added as an input in the passive simulation. Adding velocity improves the rating a bit more but adding velocity and stress make the CORA rating reach the “Good” category. However, the passive model is not able to reproduce the accelerations of the active model with an “Excellent” rating. Muscle level activity does not improve results.

RESULTS

3.5.- Turn left + Moderate Overlap Frontal Test

Regarding excursions of the head, chest, and pelvis; there are two differentiated groups regarding passive simulations: the passive simulation with no inputs and the passive simulations that have the posture of the HBM at the end of the pre-crash as input.

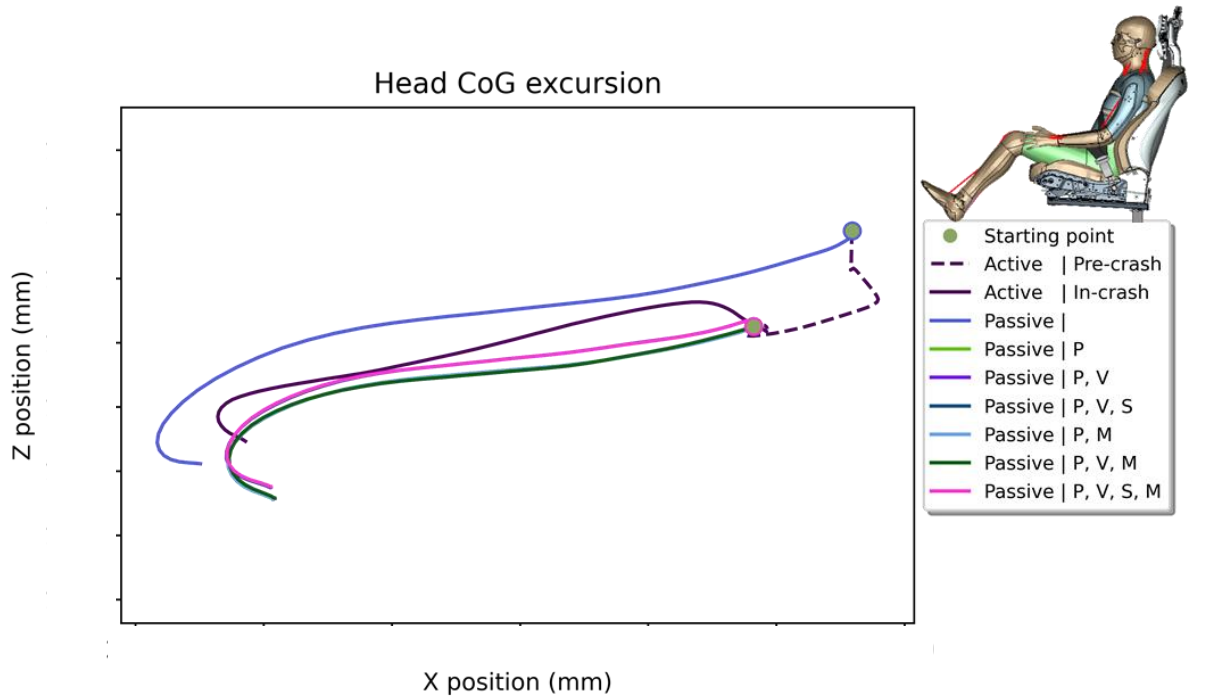


Figure 78: Head CoG excursion. XZ plane. Turn left + Moderate Overlap Frontal Test

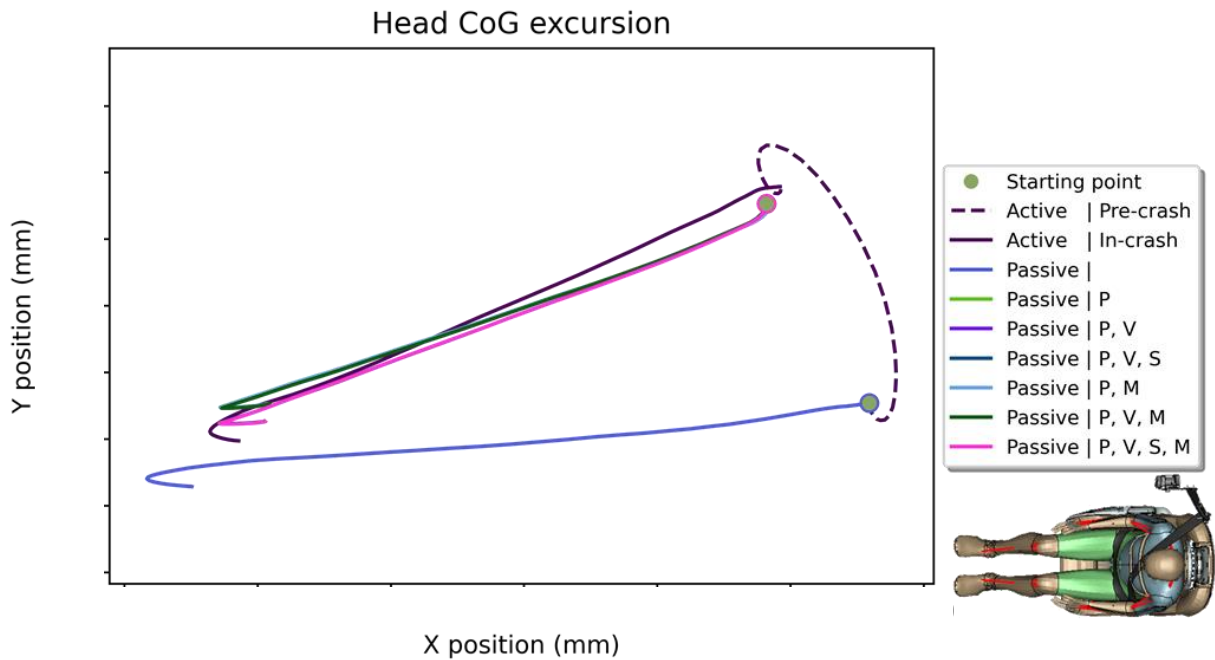


Figure 79: Head CoG excursion. XY plane. Turn left + Moderate Overlap Frontal Test

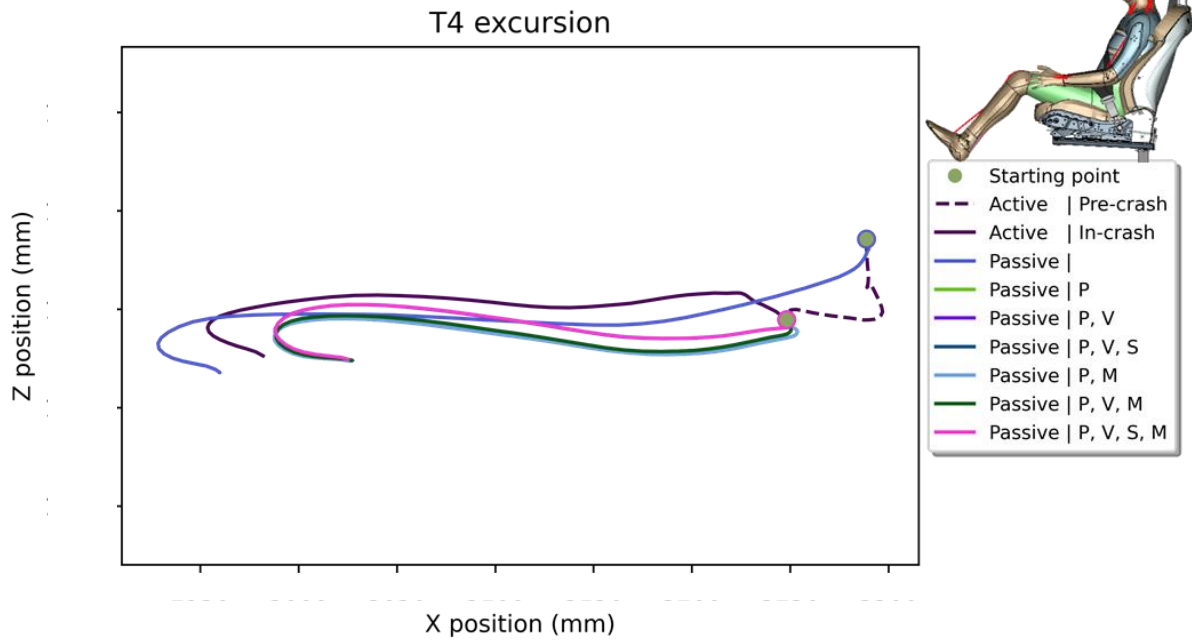


Figure 80: Chest excursion. XZ plane. Turn left + Moderate Overlap Frontal Test

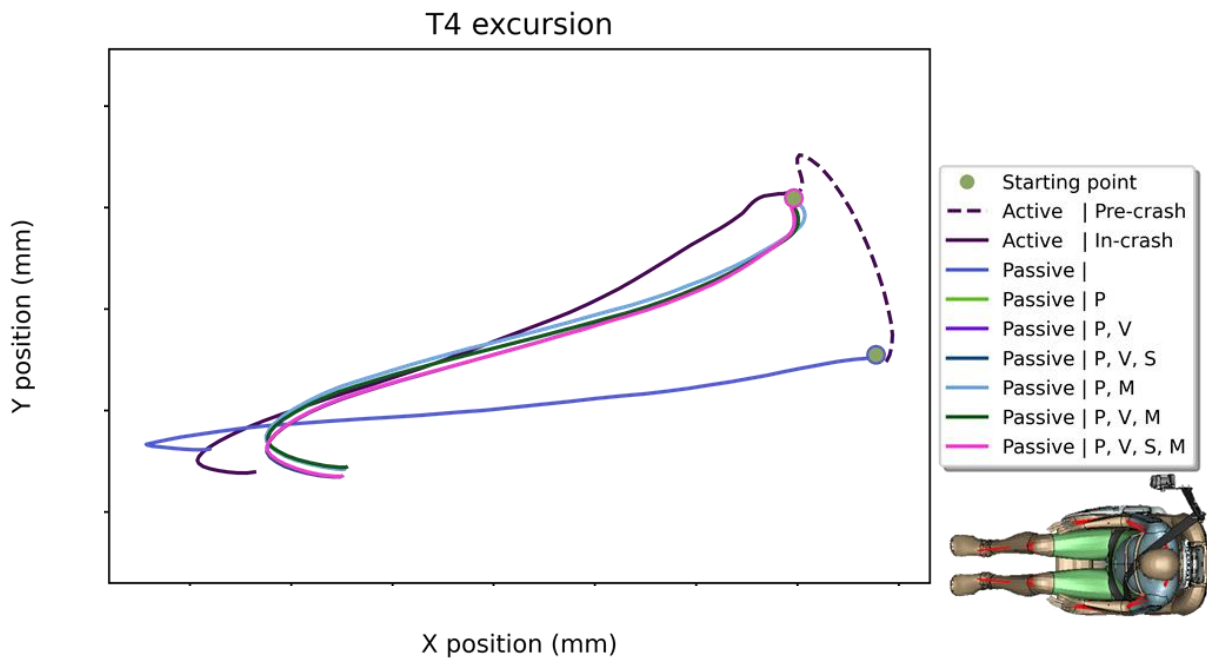


Figure 81: Chest excursion. XY plane. Turn left + Moderate Overlap Frontal Test

RESULTS

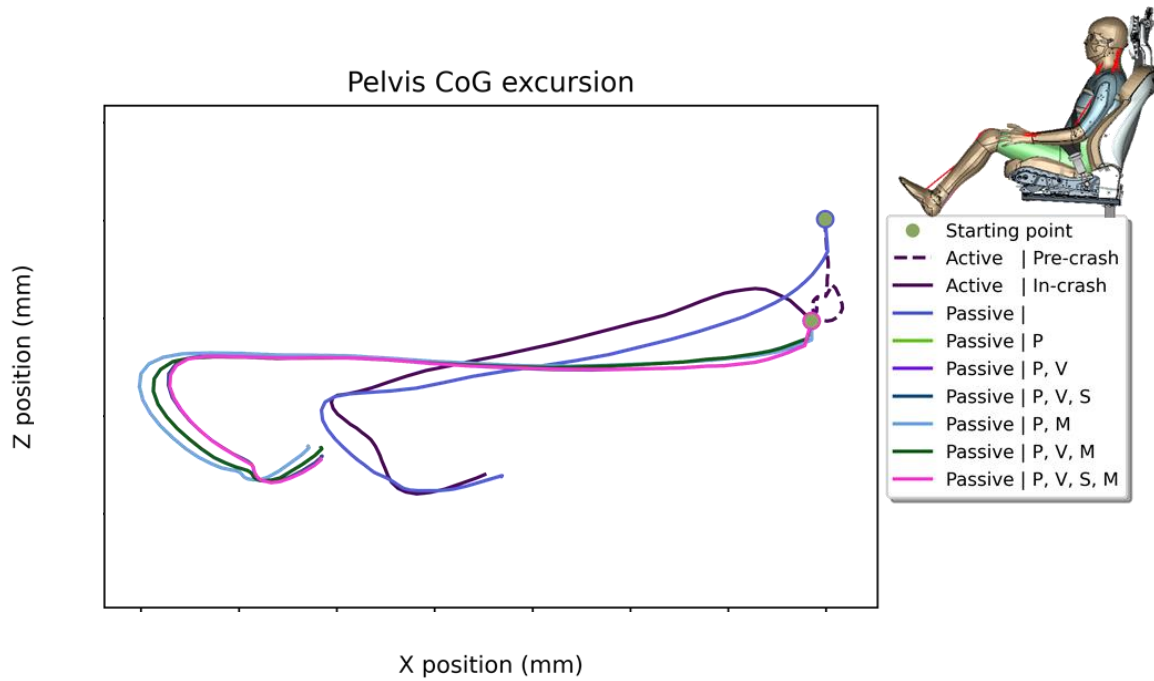


Figure 82: Pelvis CoG excursion. XZ plane. Turn left + Moderate Overlap Frontal Test

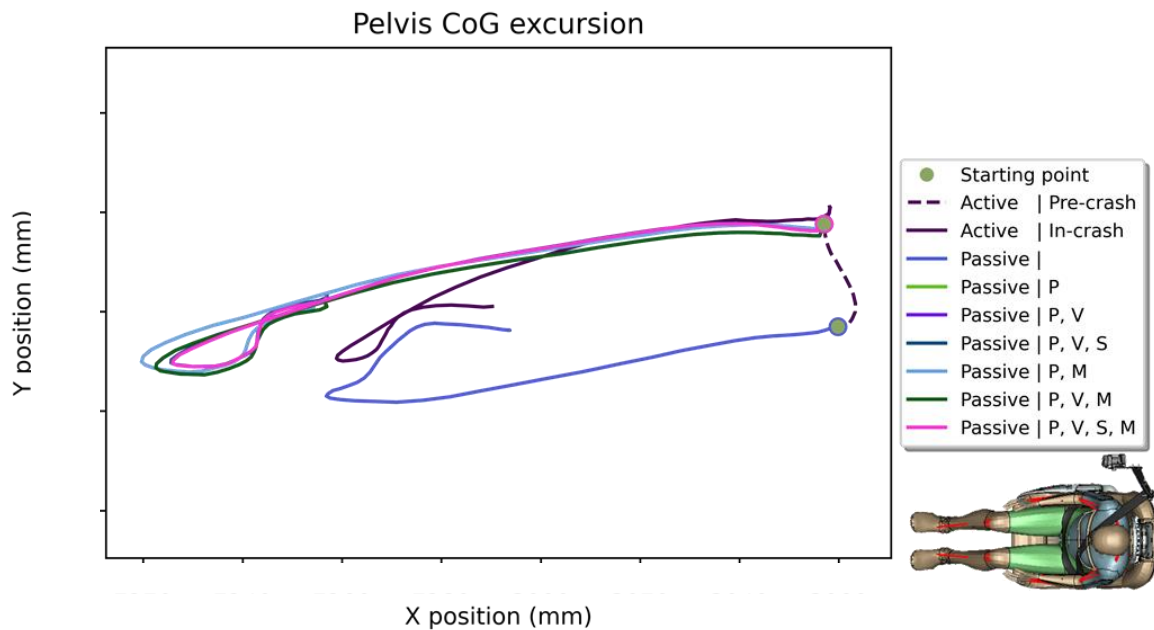


Figure 83: Pelvis CoG excursion. XY plane. Turn left + Moderate Overlap Frontal Test

It can be observed that the excursions of the head and chest in the passive simulation with no inputs are very different compared to the rest of the passive simulations. Moreover, these excursions are very distant from the active simulation excursions. However, there is an exception, the pelvis excursion of the simulation is more similar than the rest of the passive simulations with different inputs.

Regarding the rest of the passive simulations, all of them follow very similar excursions for the head, chest, and pelvis, and there are no big differences between them. These excursions seem to be closer to the excursions of the baseline simulation than the ones from the passive

simulation with no inputs regarding the head and the chest. However, there are still significant differences that could be generated by the different belts used for each simulation.

Concerning injury criteria, all the results have been normalized using the baseline simulation value as a reference. Consequently, all the baseline injury risk predictions have value 1 and the passive simulation values oscillate around the value 1. Thus, the variations of the passive simulations with respect to the active one can be observed.

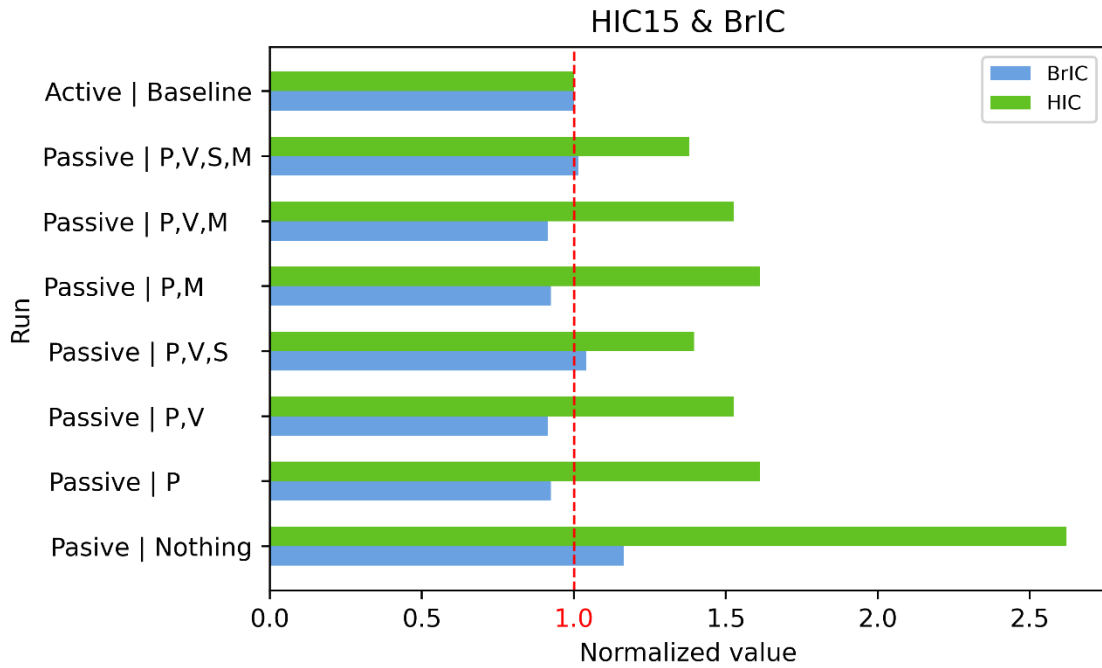


Figure 84: HIC 15ms and BrIC. Turn left + Moderate Overlap Frontal Test

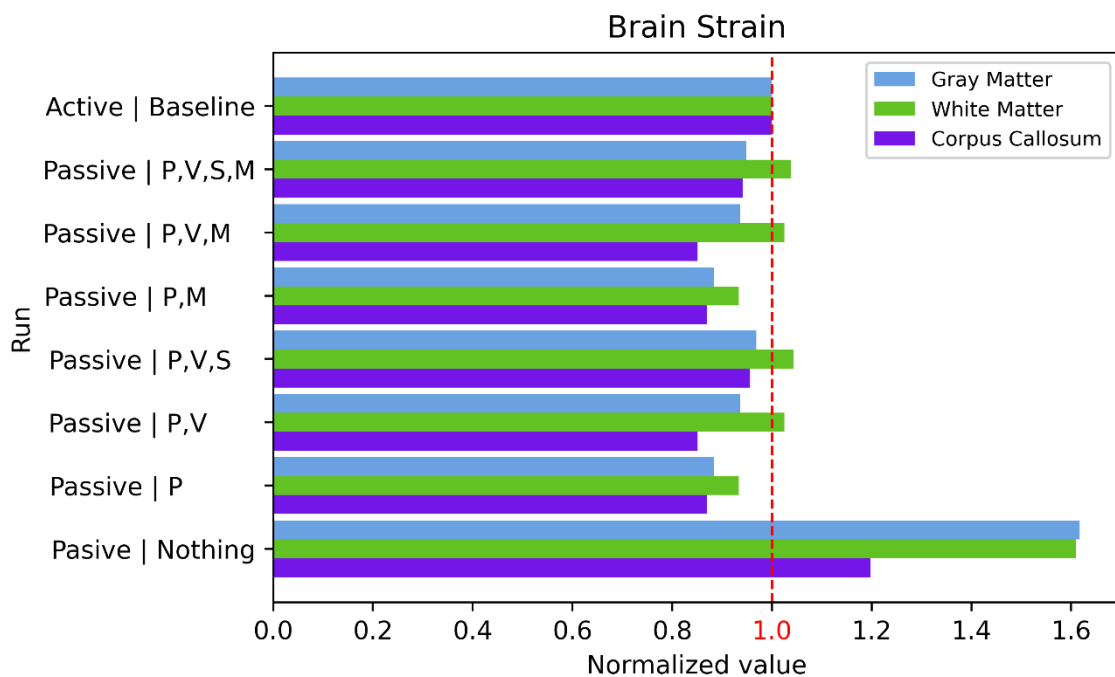


Figure 85: Brain strain. Turn left + Moderate Overlap Frontal Test

RESULTS

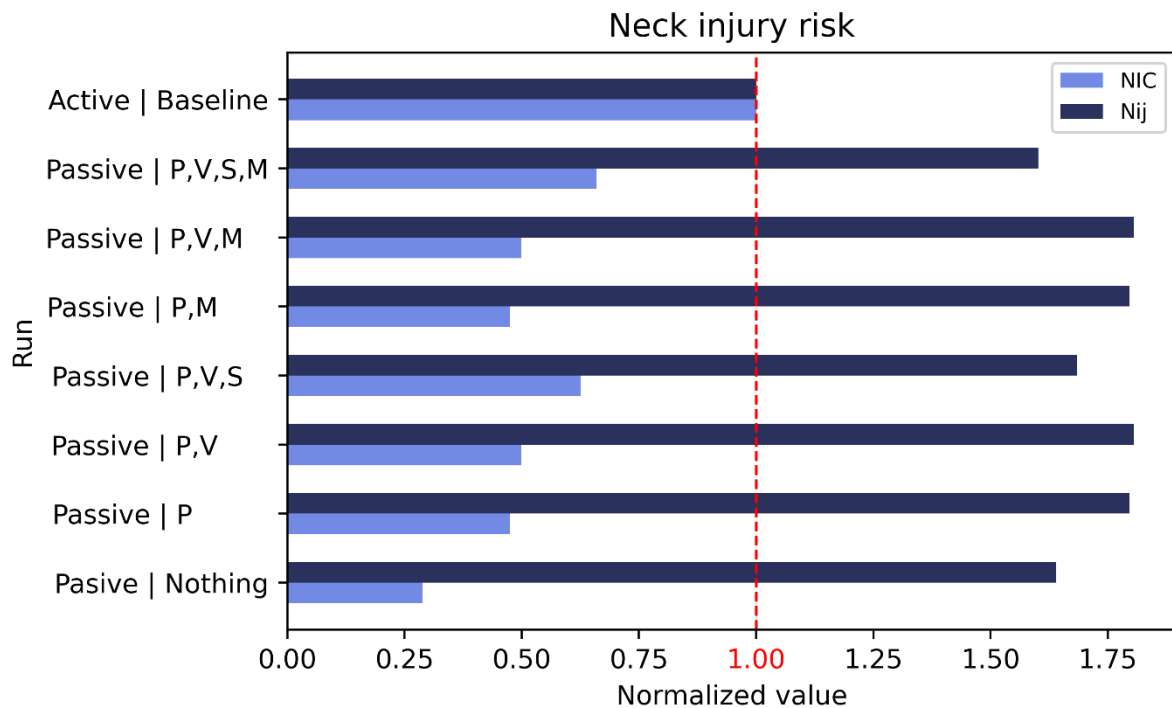


Figure 86: Neck injury risk. Turn left + Moderate Overlap Frontal Test

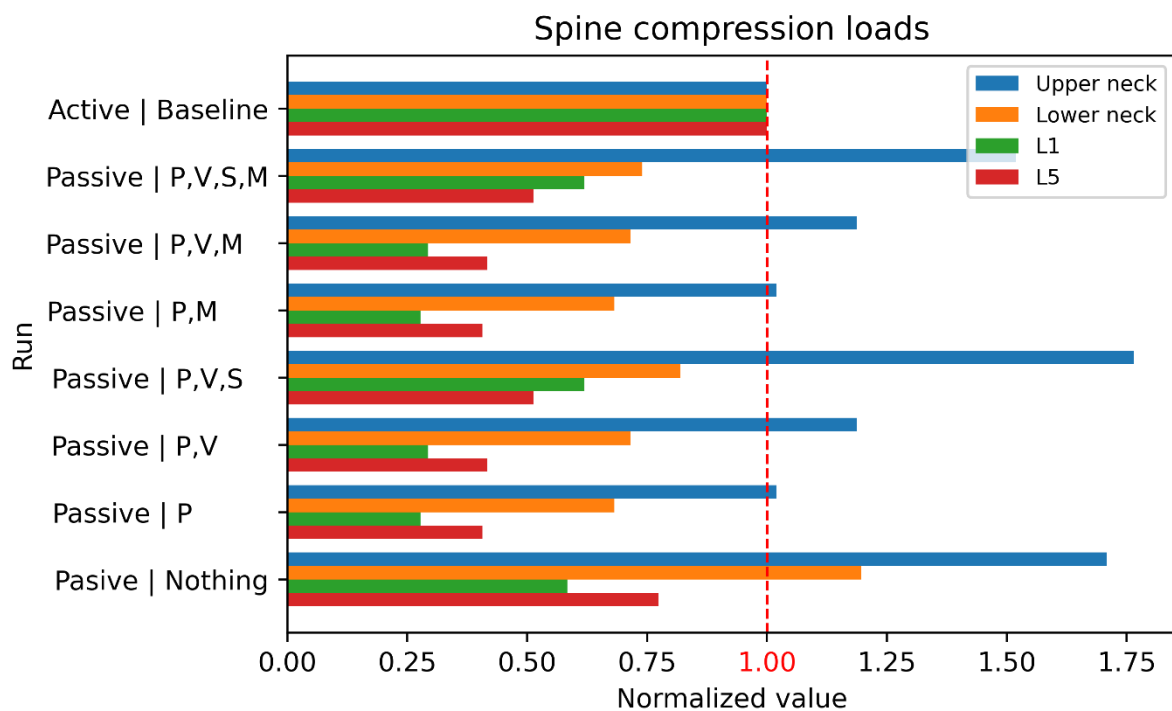


Figure 87: Spine compression loads. Turn left + Moderate Overlap Frontal Test

Regarding the head, HIC 15 ms is overpredicted in the passive simulations, reaching the closest value in the simulation with posture, velocity, and stresses. BrIC however is precisely predicted compared to the baseline model by the passive simulations. The strains in the brain are a bit underpredicted compared to the baseline model in general, predictions are very

precise compared to the baseline model, except in the case of the passive simulation with no input. Muscle activity level (MPID) seems to not affect the results significantly.

Regarding the neck and the spine, compression loads in the upper neck are overpredicted in all cases and lumbar compression loads are underestimated. These predictions get the closest values when only the posture and velocity of the HBM are included. The NIC and Nij are wrongly predicted by the passive simulations compared to the baseline. The closest values are obtained for posture, velocity, stress, and MPID input simulation.

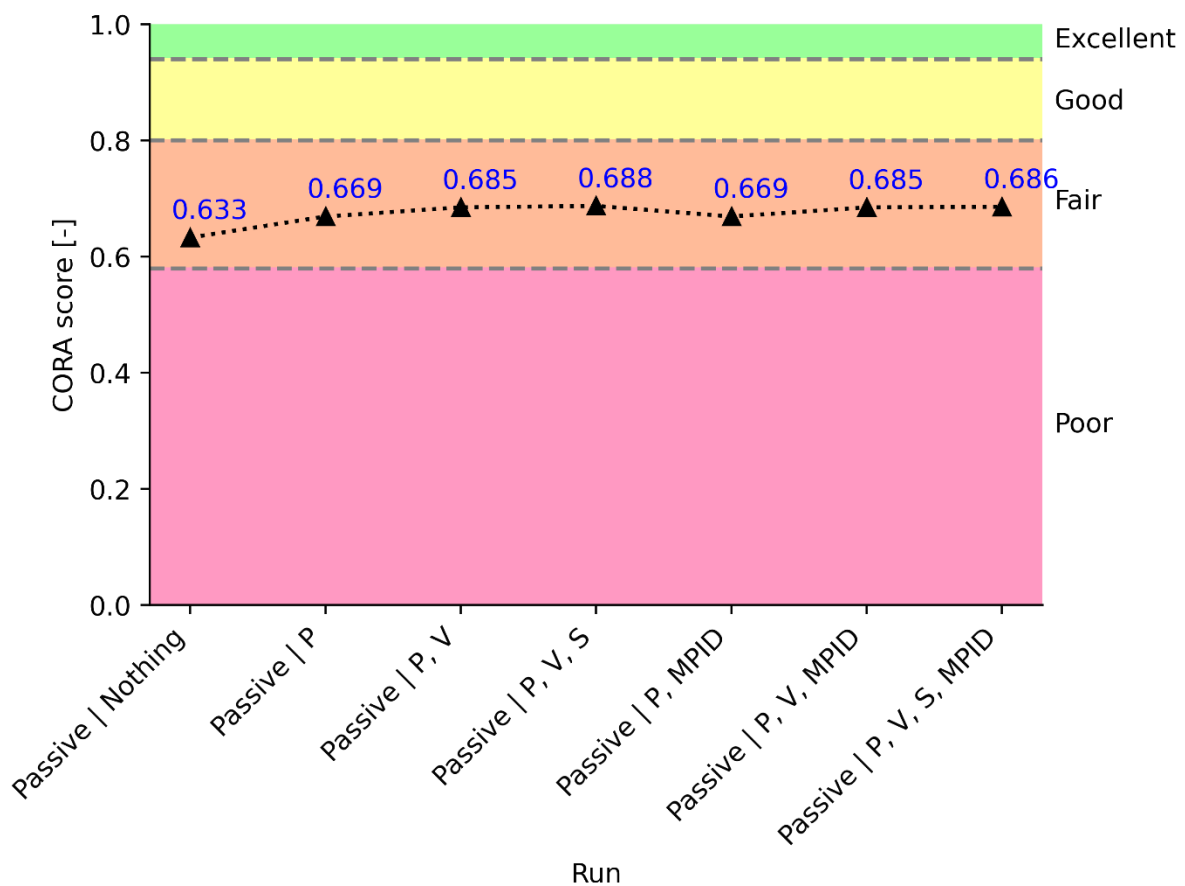


Figure 88: CORAplus acceleration ratings. Turn left + Moderate Overlap Frontal Test

Lastly, regarding the CORAplus ratings, there is an improvement if the posture of the occupant is added as an input in the passive simulation. Adding velocity and stress improves the rating a bit more but the CORA rating always stays in the “Fair” category. Muscle level activity does not improve results.

RESULTS

3.6.- Turn left and braking + Moderate Overlap Frontal Test

Regarding excursions of the head, chest, and pelvis; there are two differentiated groups regarding passive simulations: the passive simulation with no inputs and the passive simulations that have the posture of the HBM at the end of the pre-crash as input.

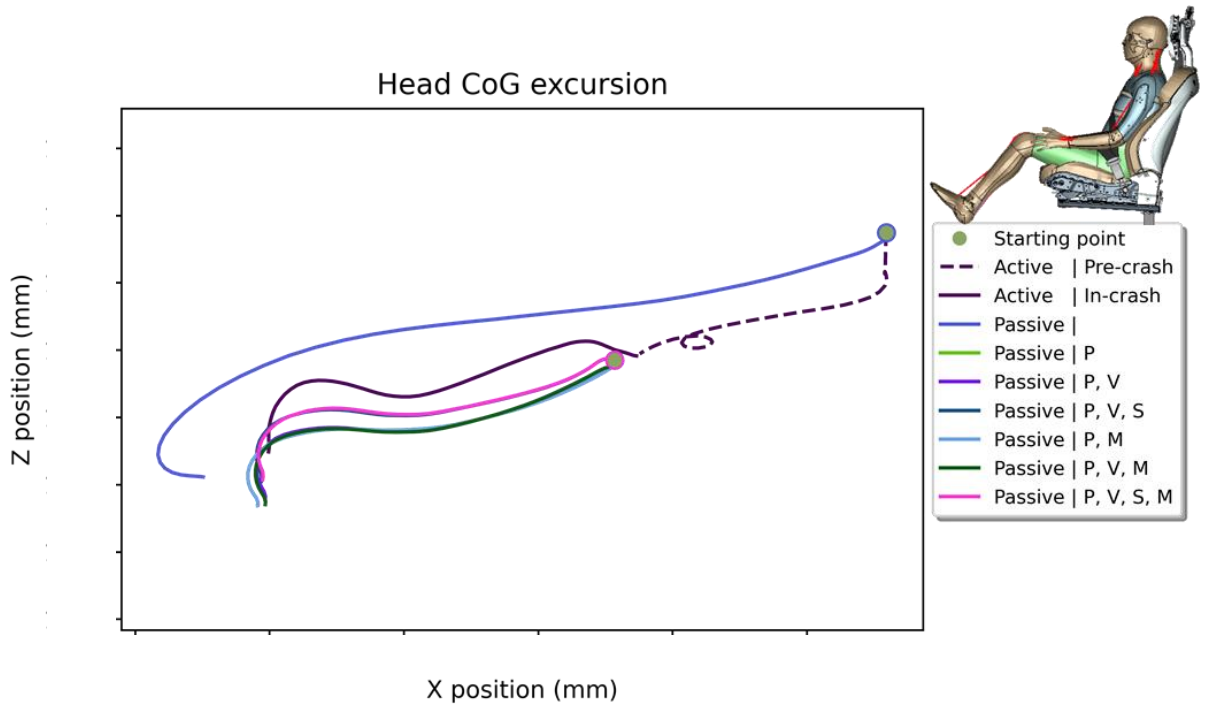


Figure 89: Head CoG excursion. XZ plane. Turn left and Braking + Moderate Overlap Frontal Test

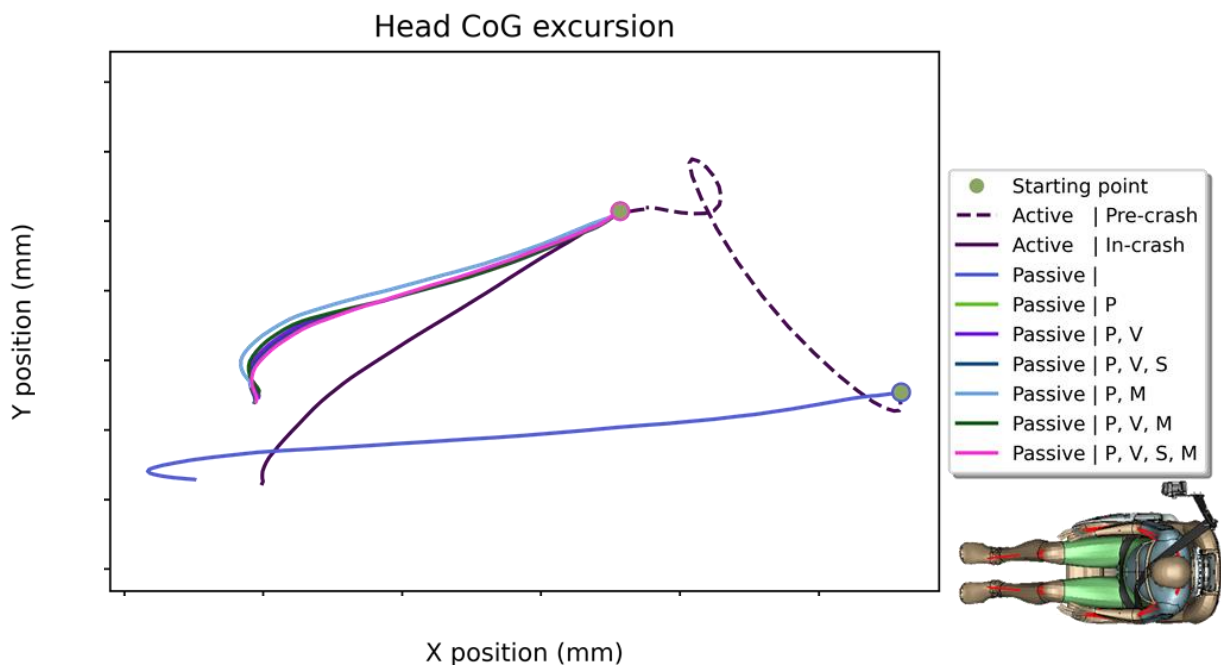


Figure 90: Head CoG excursion. XY plane. Turn left and Braking + Moderate Overlap Frontal Test

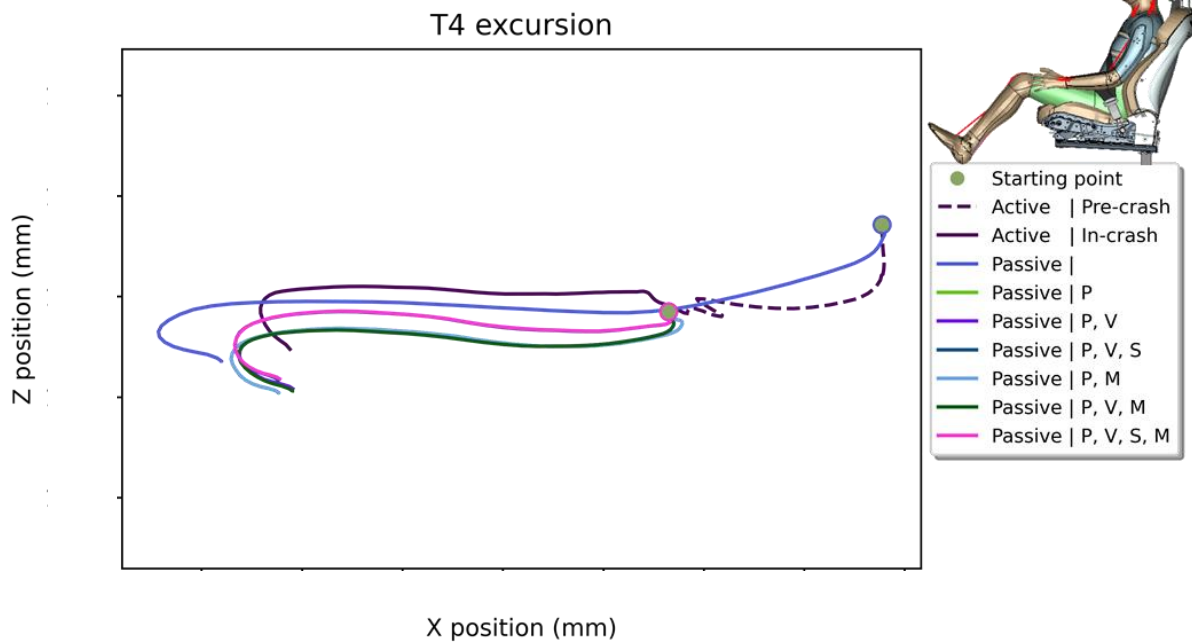


Figure 91: Chest excursion. XZ plane. Turn left and Braking + Moderate Overlap Frontal Test

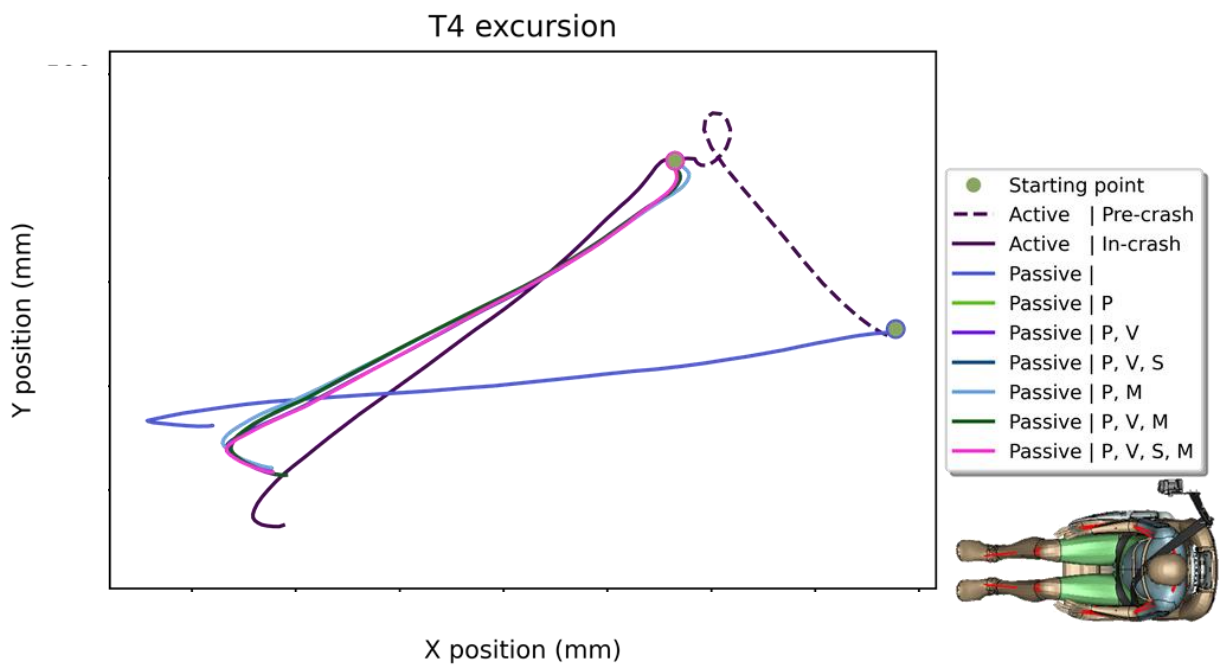


Figure 92: Chest excursion. XY plane. Turn left and Braking + Moderate Overlap Frontal Test

RESULTS

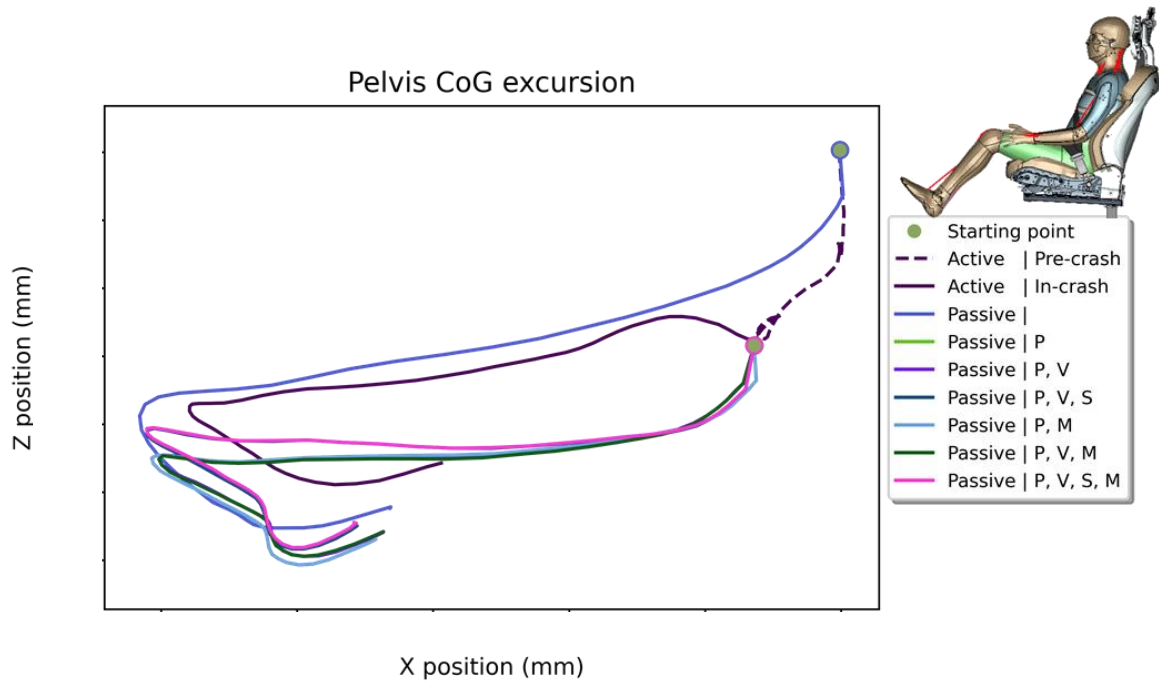


Figure 93: Pelvis CoG excursion. XZ plane. Turn left and Braking + Moderate Overlap Frontal Test

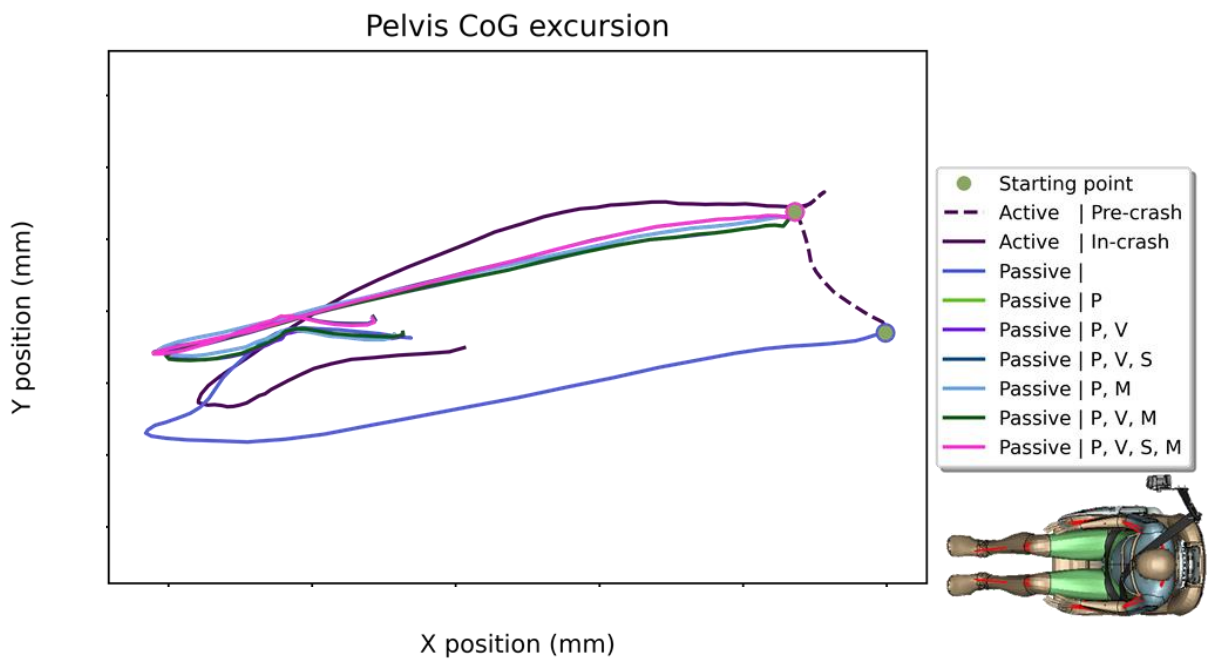


Figure 94: Pelvis CoG excursion. XY plane. Turn left and Braking + Moderate Overlap Frontal Test

It can be observed that the excursions of the head, chest, and pelvis in the passive simulation with no inputs are very different compared to the rest of the passive simulations. Moreover, these excursions are very distant from the active simulation excursions.

Regarding the rest of the passive simulations, there are two differentiated groups of excursions: passive simulations with stresses and passive simulations with no stresses. The excursions of the simulations that have stresses seem to be closer to the excursions of the

baseline simulation. However, there is still a slope difference between them that could be generated by the different belts used for each simulation.

Concerning injury criteria, all the results have been normalized using the baseline simulation value as a reference. Consequently, all the baseline injury risk predictions have value 1 and the passive simulation values oscillate around the value 1. Thus, the variations of the passive simulations with respect to the active one can be observed.

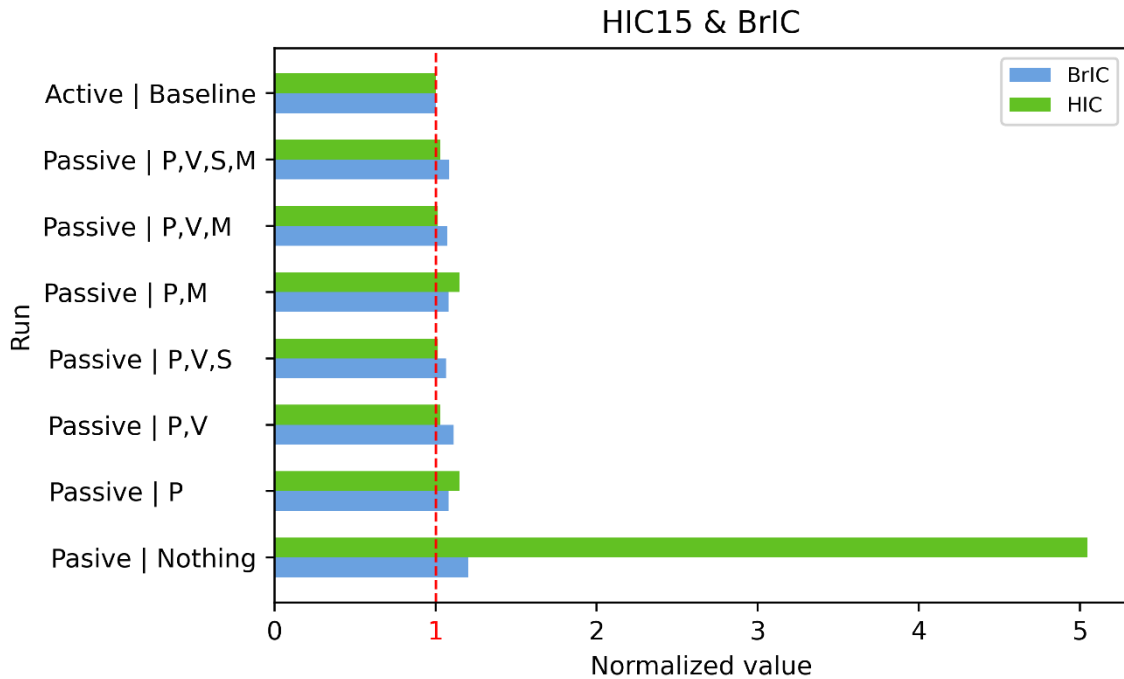


Figure 95: HIC 15ms and BrIC. Turn left and Braking + Moderate Overlap Frontal Test

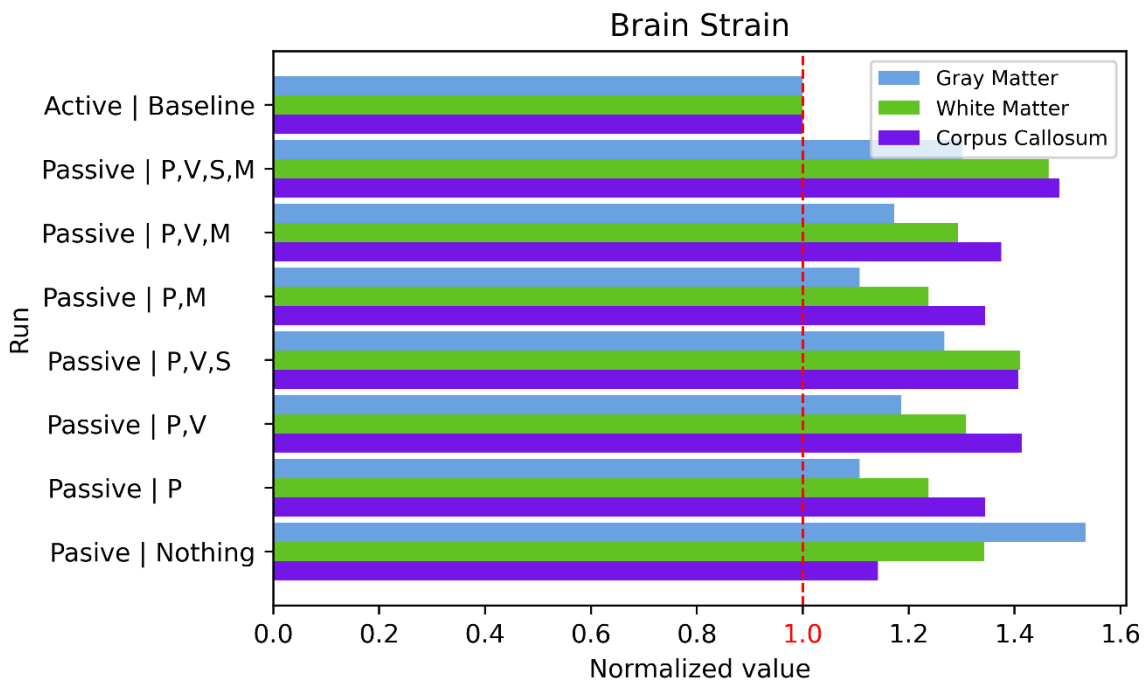


Figure 96: Brain strain. Turn left and Braking + Moderate Overlap Frontal Test

RESULTS

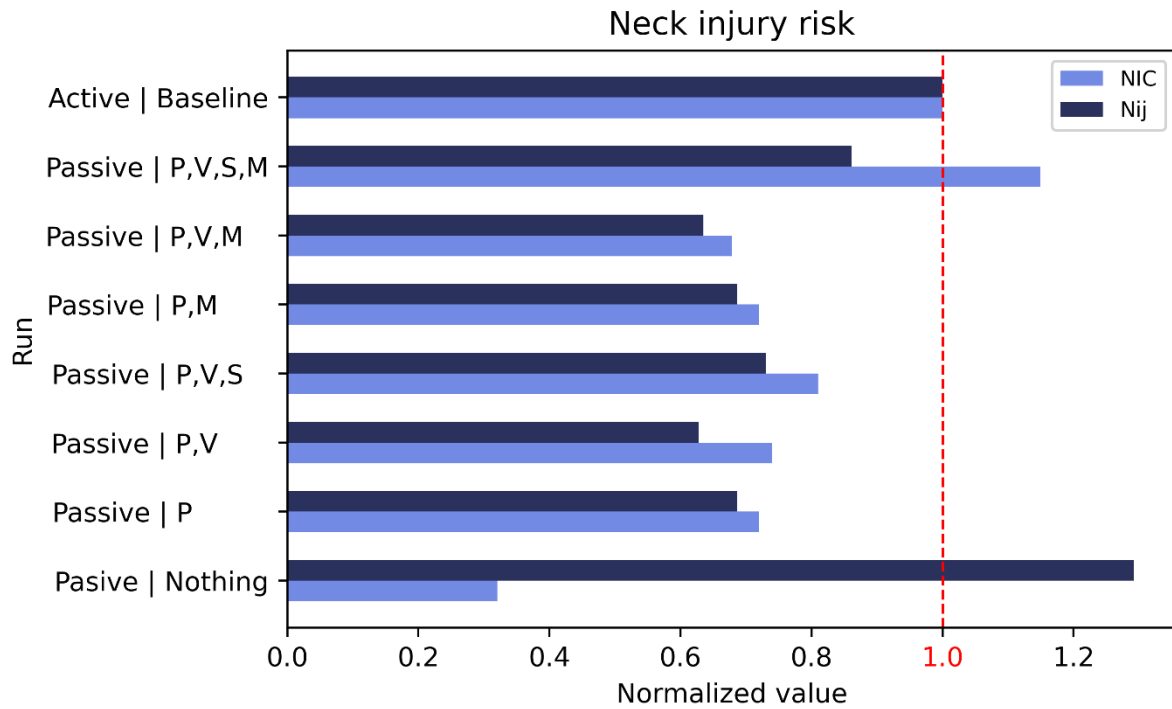


Figure 97: Neck injury risk. Turn left and Braking + Moderate Overlap Frontal Test

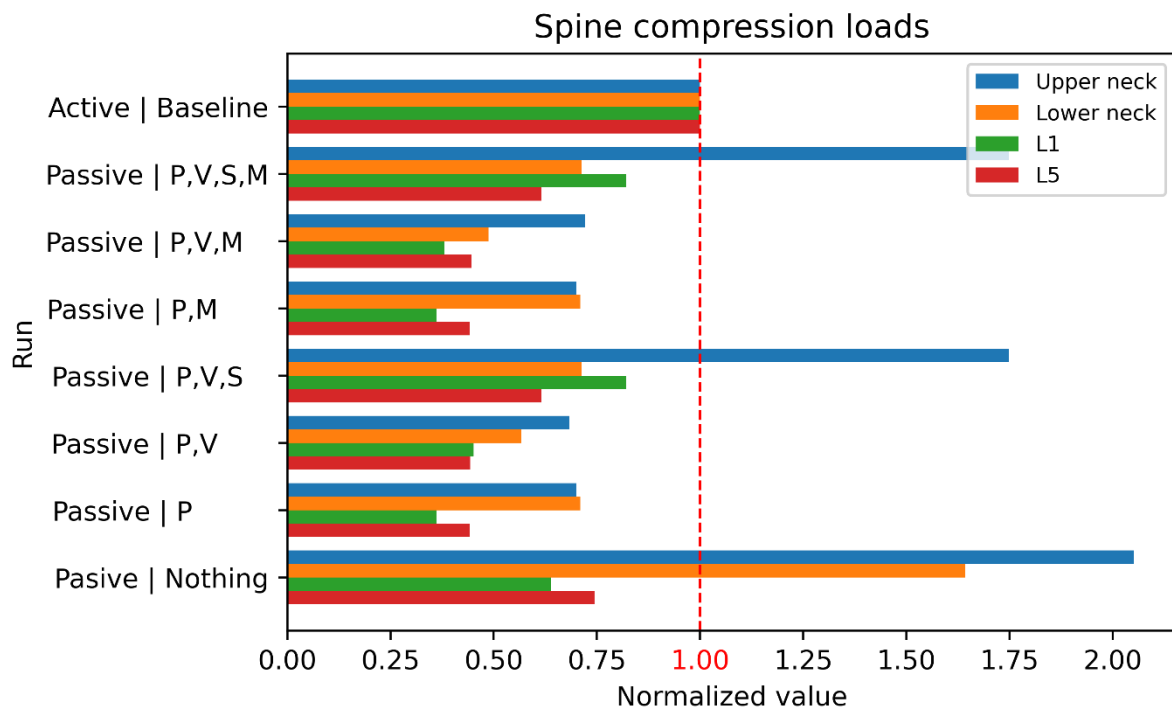


Figure 98: Spine compression loads. Turn left and Braking + Moderate Overlap Frontal Test

Regarding the head, HIC 15 ms is largely overpredicted compared to the baseline model in the passive simulation with no input. HIC and BrIC are however predicted correctly compared to the baseline model by the rest of the passive simulations. The strains in the brain are a bit overpredicted compared to the baseline model in general, the closest value is reached in the

simulation with just posture as input. Muscle activity level (MPID) seems to not affect the results.

Regarding the neck and the spine, compression loads in the upper neck are overpredicted compared to the baseline model in some cases and lumbar compression loads are underestimated compared to the baseline model. These predictions get the closest values when the posture, velocity, and stress of the HBM are included. The NIC and Nij are wrongly predicted compared to the baseline model by the passive simulations compared to the baseline. The closest values are obtained for posture, velocity, stress, and MPID input simulation.

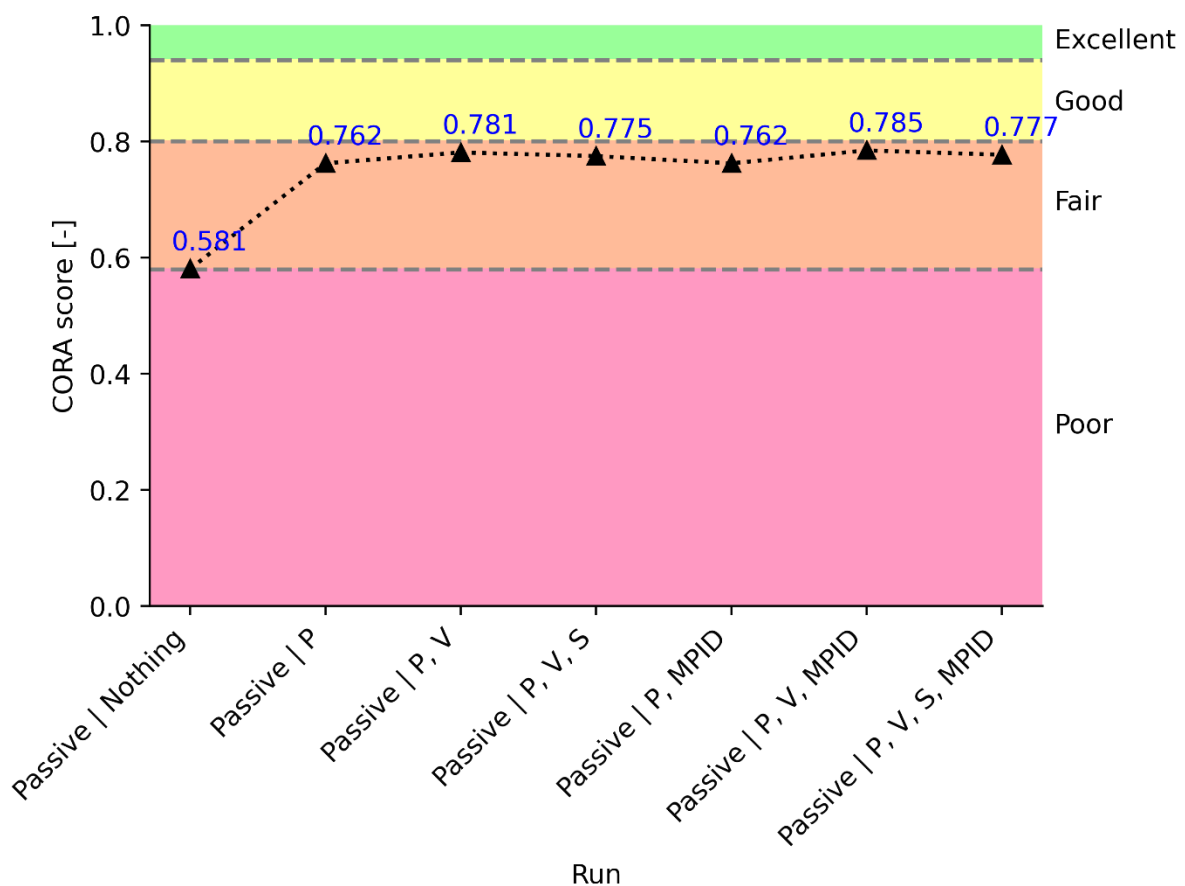


Figure 99: CORAplus acceleration ratings. Turn left and Braking + Moderate Overlap Frontal Test

Lastly, regarding the CORAplus ratings, there is an improvement if the posture of the occupant is added as an input in the passive simulation. Adding velocity and stress improves the rating, having the maximum value when posture and velocity are included as input. However, the category always stays at “Fair”. Muscle level activity does not improve results.

RESULTS

3.7.- Turn left + Mobile Progressive Deformable Barrier

Regarding excursions of the head, chest, and pelvis; there are two differentiated groups regarding passive simulations: the passive simulation with no inputs and the passive simulations that have the posture of the HBM at the end of the pre-crash as input.

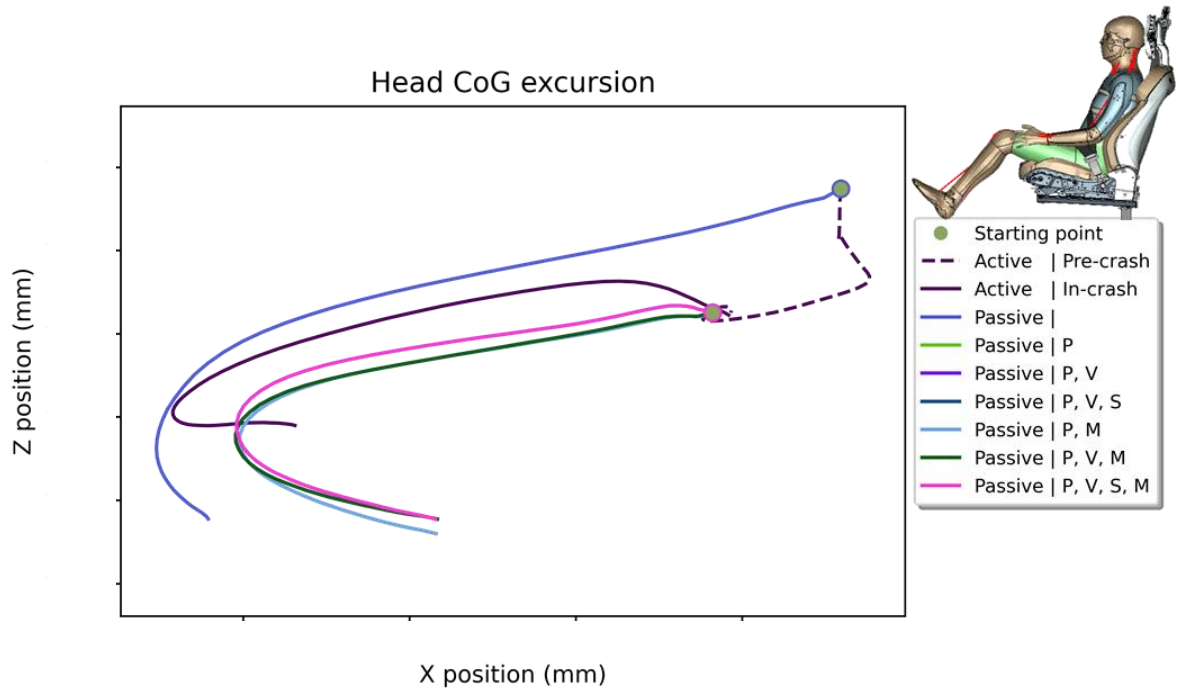


Figure 100: Head CoG excursion. XZ plane. Turn left + Mobile Progressive Deformable Barrier

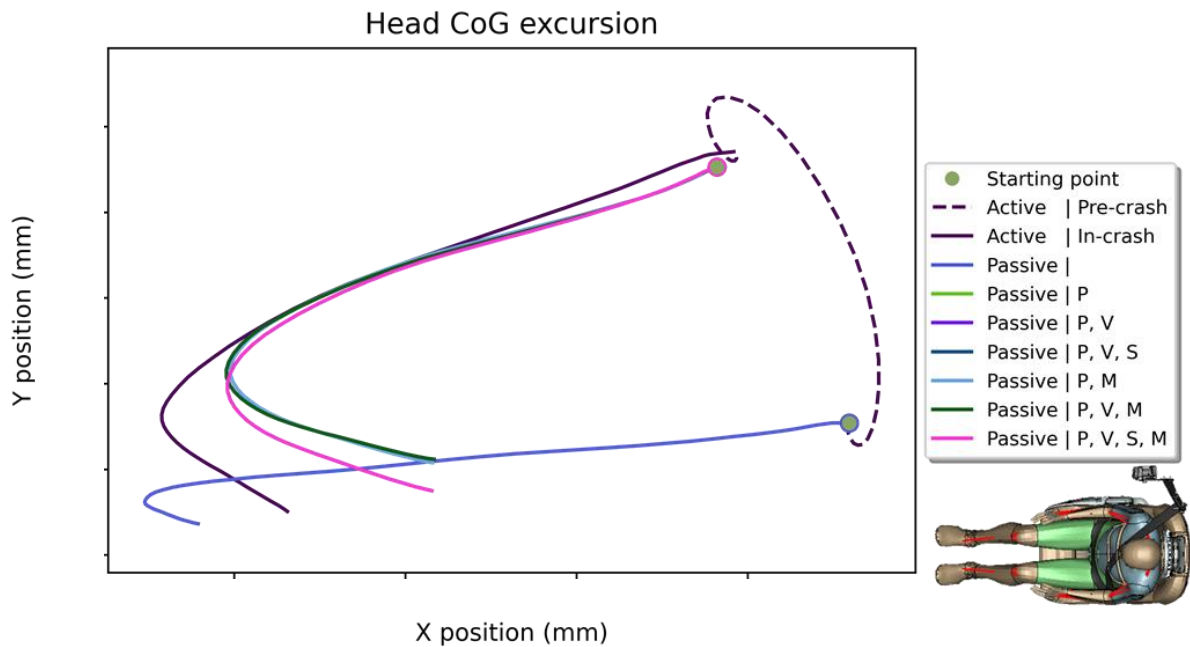


Figure 101: Head CoG excursion. XY plane. Turn left + Mobile Progressive Deformable Barrier

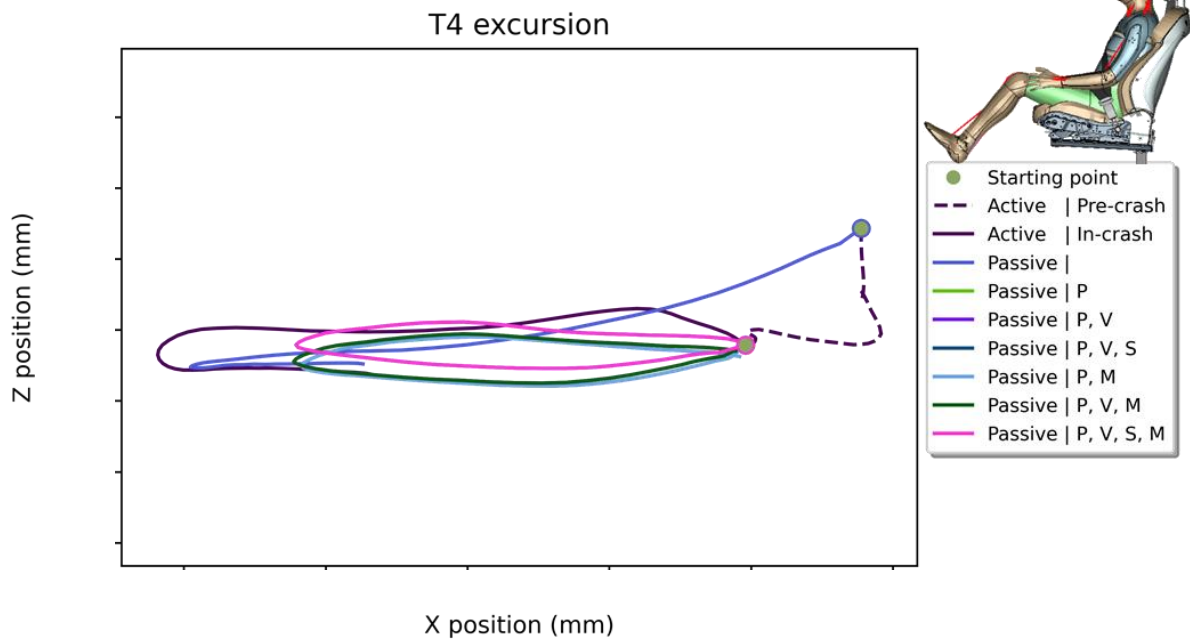


Figure 102: Chest excursion. XZ plane. Turn left + Mobile Progressive Deformable Barrier

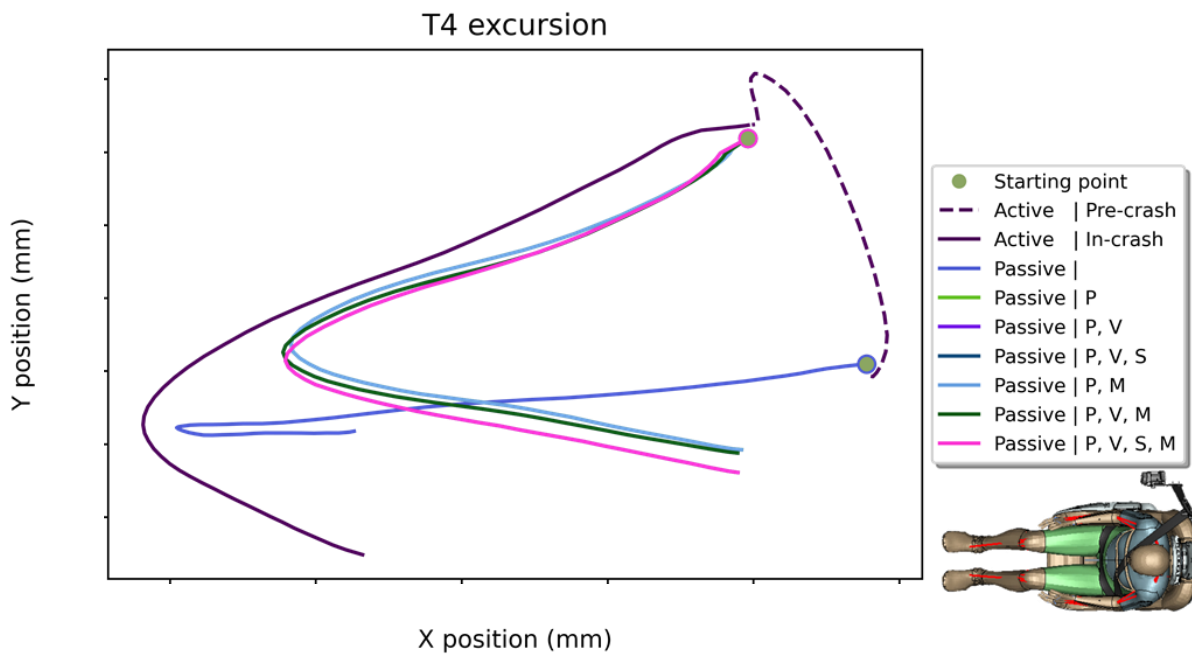


Figure 103: Chest excursion. XY plane. Turn left + Mobile Progressive Deformable Barrier

RESULTS

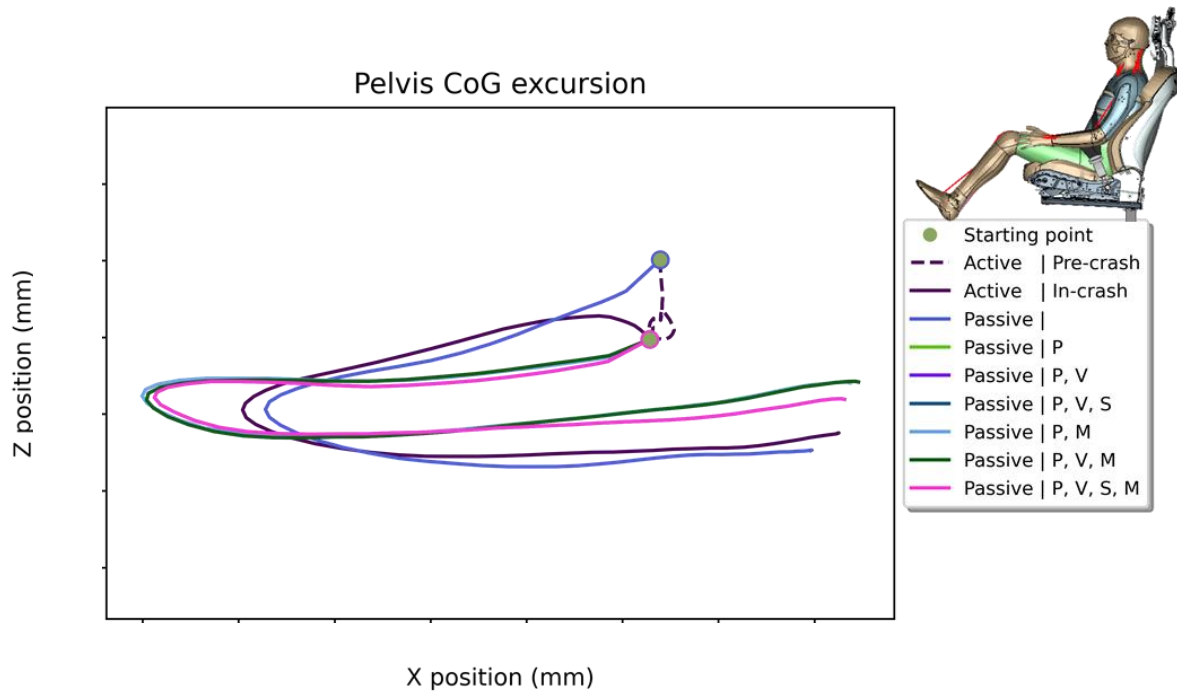


Figure 104: Pelvis CoG excursion. XZ plane. Turn left + Mobile Progressive Deformable Barrier

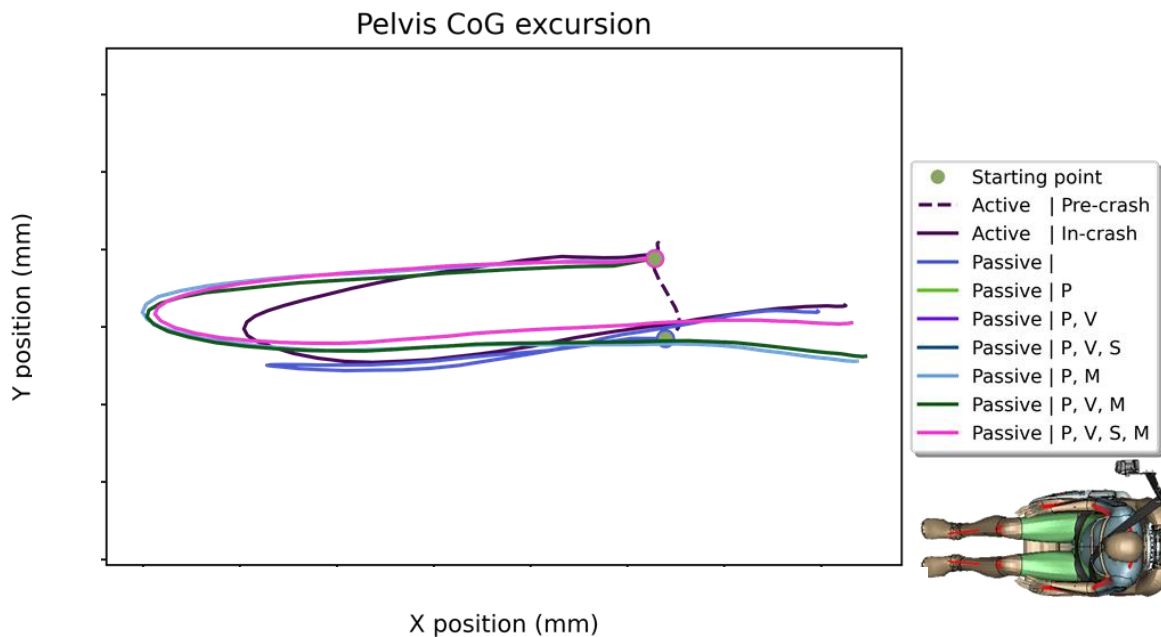


Figure 105: Pelvis CoG excursion. XY plane. Turn left + Mobile Progressive Deformable Barrier

It can be observed that the excursions of the head, chest, and pelvis in the passive simulation with no inputs are very different compared to the rest of passive simulations. Moreover, these excursions are very distant from the active simulation excursions.

Regarding the rest of the passive simulations, there are two differentiated groups of excursions: passive simulations with stresses and passive simulations with no stresses. The excursions of the simulations that have stresses seem to be closer to the excursions of the baseline simulation. However, there is still a big difference between them that could be generated by the different belts used for each simulation.

Concerning injury criteria, all the results have been normalized using the baseline simulation value as a reference. Consequently, all the baseline injury risk predictions have value 1 and the passive simulation values oscillate around the value 1. Thus, the variations of the passive simulations with respect to the active one can be observed.

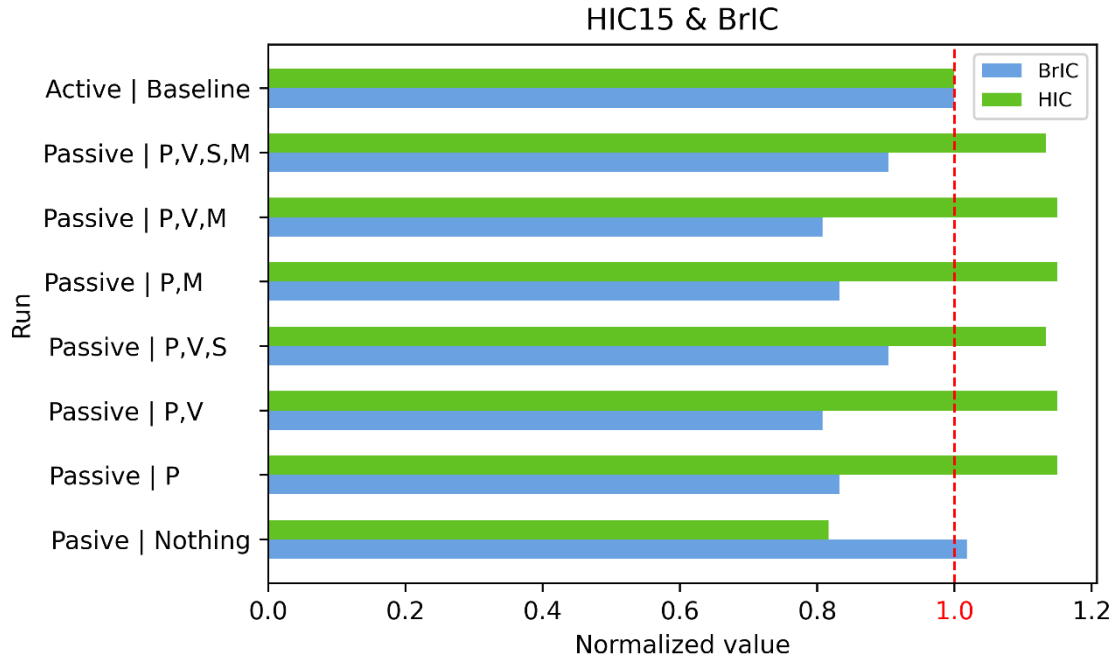


Figure 106: HIC 15ms and BrIC. Turn left + Mobile Progressive Deformable Barrier

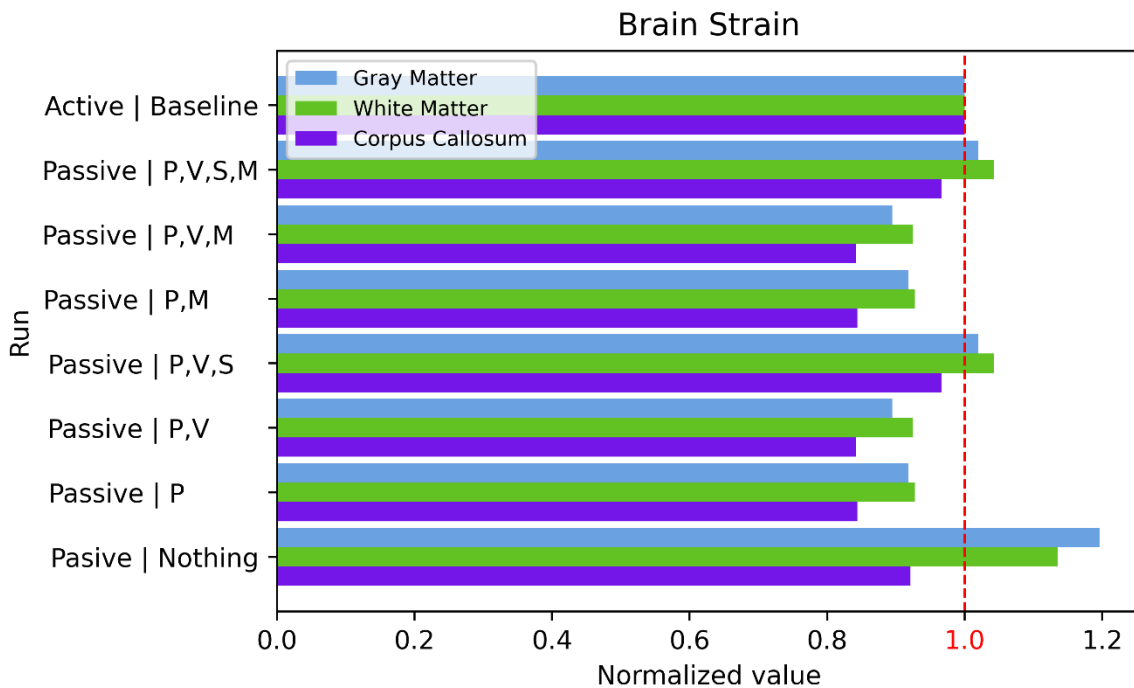


Figure 107: Brain strain. Turn left + Mobile Progressive Deformable Barrier

RESULTS

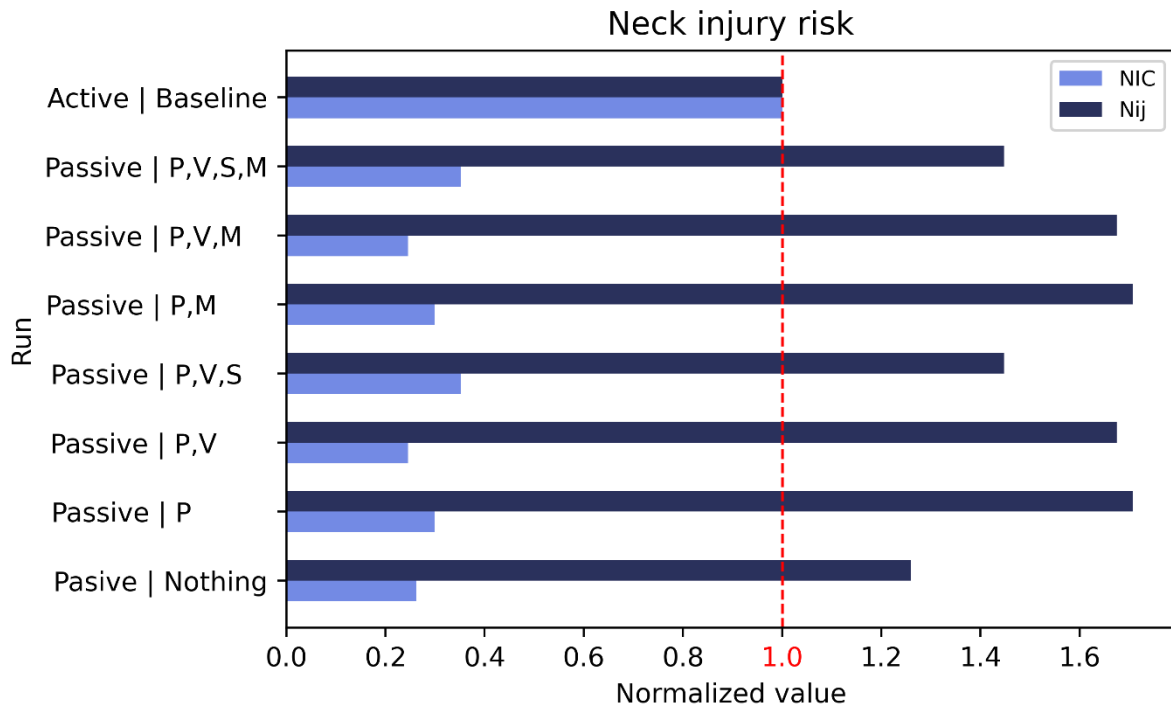


Figure 108: Neck injury risk. Turn left + Mobile Progressive Deformable Barrier

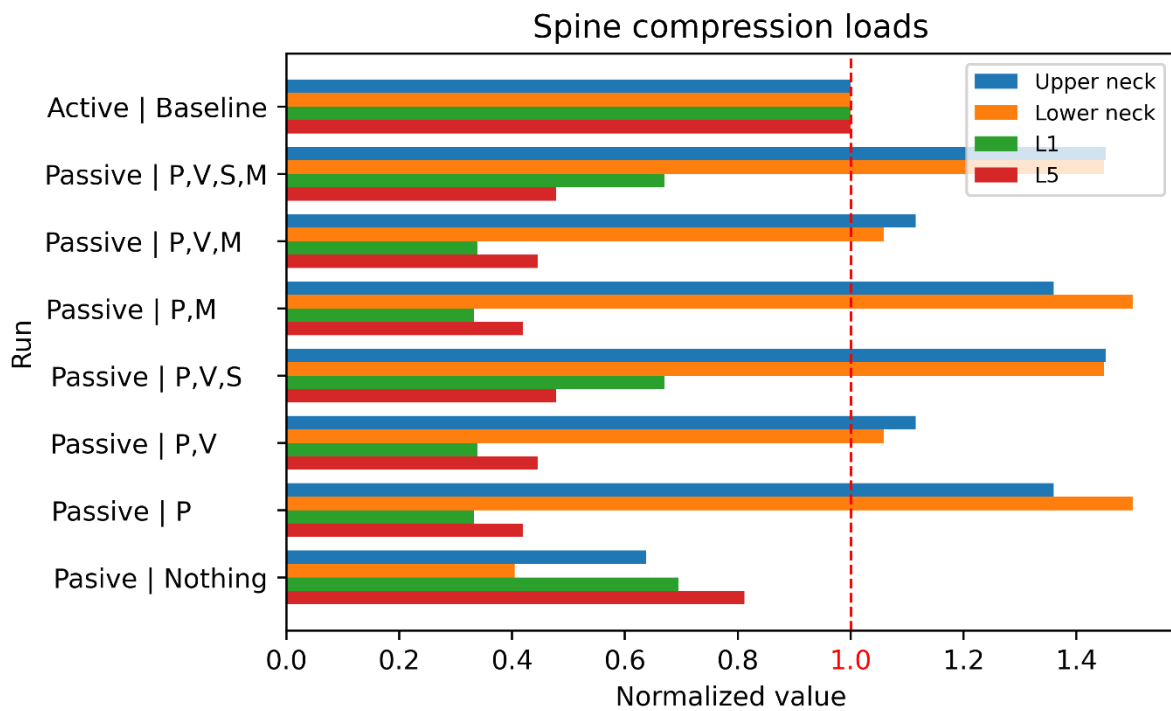


Figure 109: Spine compression loads. Turn left + Mobile Progressive Deformable Barrier

HIC and BrIC are predicted precisely compared to the baseline model in almost all the simulations, but the closest values are obtained in the passive simulation with posture, velocity, and stresses as input. The strains in the brain are a bit underpredicted compared to

the baseline model. The closest value is reached in the same simulation. Muscle activity level (MPID) seems to not affect the results significantly.

Regarding the neck and the spine, compression loads in the upper neck are overpredicted compared to the baseline model in some cases and lumbar compression loads are underestimated compared to the baseline model. These predictions get the closest values when posture, velocity, and stress of the HBM are included. The NIC and Nij are wrongly predicted by the passive simulations compared to the baseline. The closest values are obtained for posture, velocity, stress input simulation.

Regarding the rib cage strain model, risks of fracture are overpredicted in the passive simulation with no inputs for the three groups of ages. The rest of the passive simulations underpredict compared to the baseline model the risk of fracture compared to the baseline simulation.

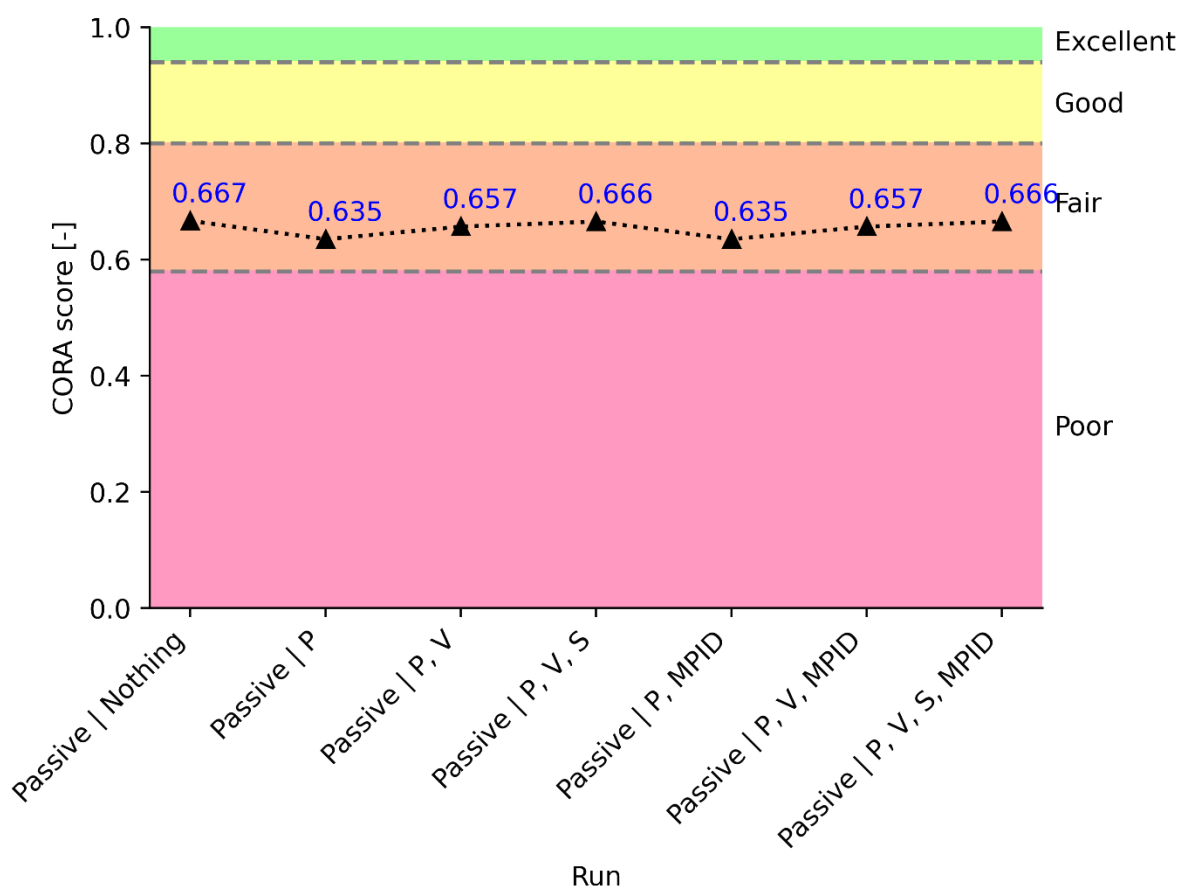


Figure 110: CORAplus acceleration ratings. Turn left + Mobile Progressive Deformable Barrier

Lastly, regarding the CORAplus ratings, there is no improvement in this case if any inputs are included. The simulation with no inputs is the one that most closely recreates the accelerations of the baseline simulation. However, all the simulations stay in the “Fair” category. Muscle level activity does not improve results.

RESULTS

3.8.- Turn left and Braking+ Mobile Progressive Deformable Barrier

Regarding excursions of the head, chest, and pelvis; there are two differentiated groups regarding passive simulations: the passive simulation with no inputs and the passive simulations that have the posture of the HBM at the end of the pre-crash as input.

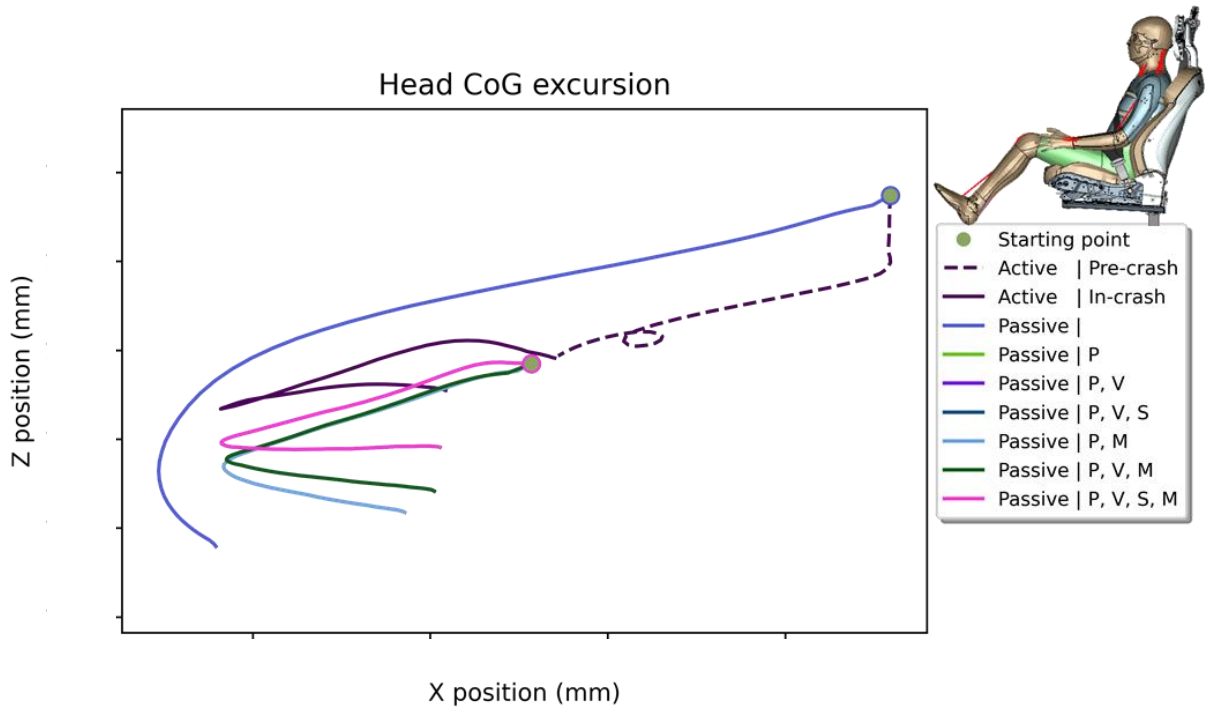


Figure 111: Head CoG excursion. XZ plane. Turn left and Braking + Mobile Progressive Deformable Barrier

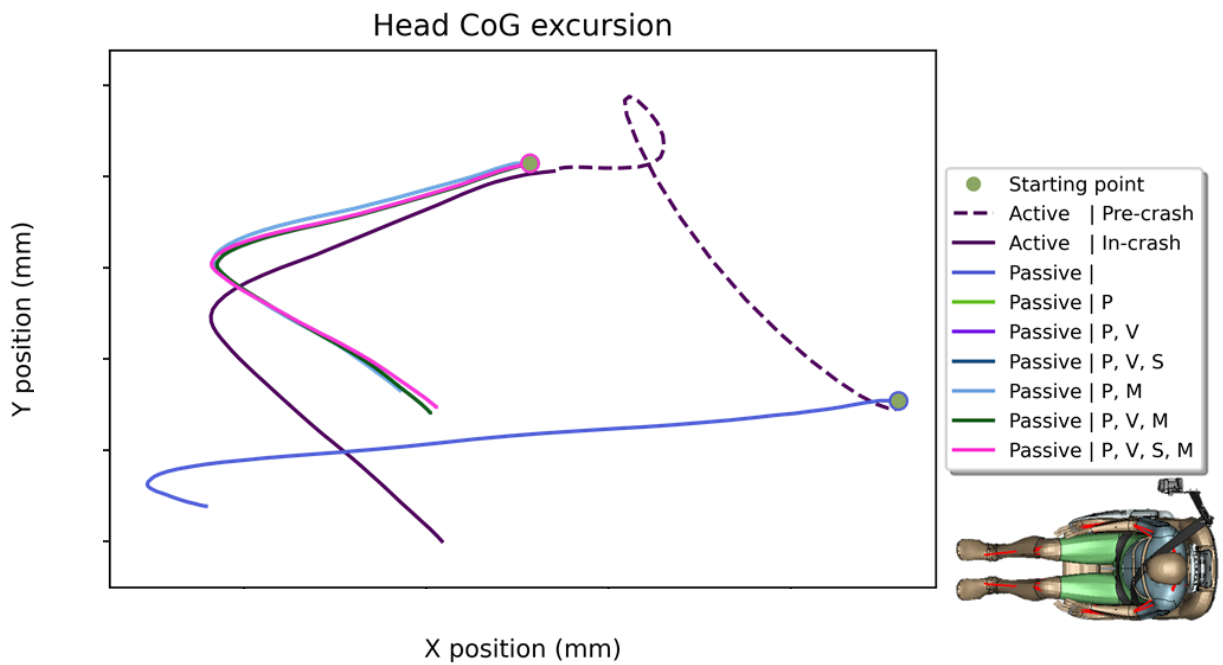


Figure 112: Head CoG excursion. XY plane. Turn left and Braking + Mobile Progressive Deformable Barrier

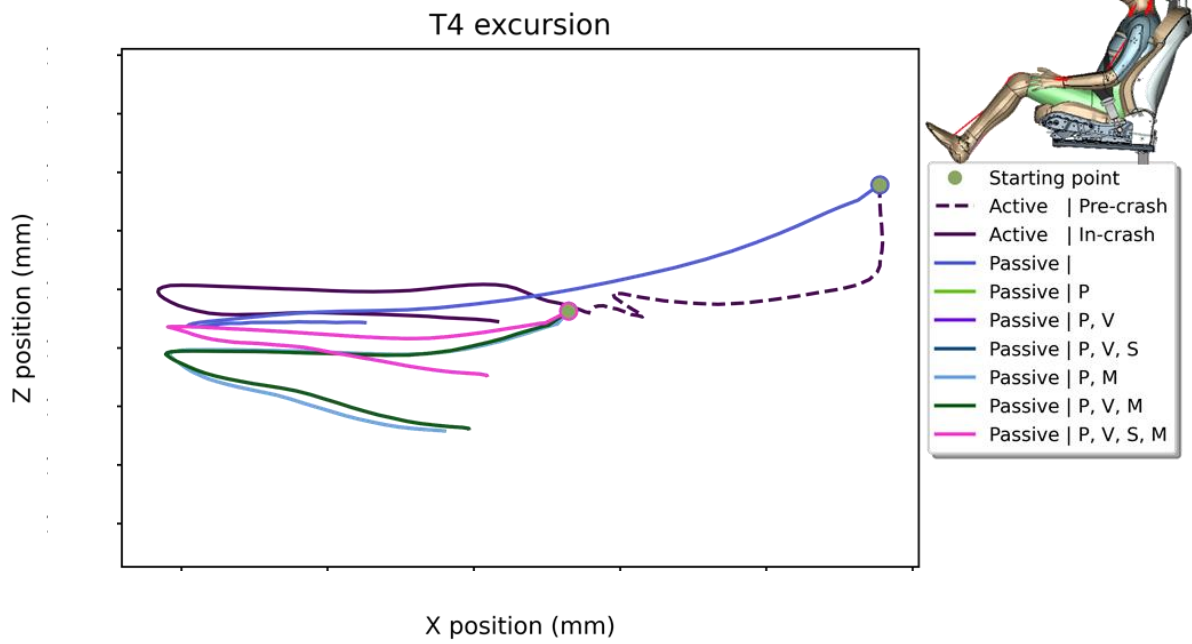


Figure 113: Chest excursion. XZ plane. Turn left and Braking + Mobile Progressive Deformable Barrier

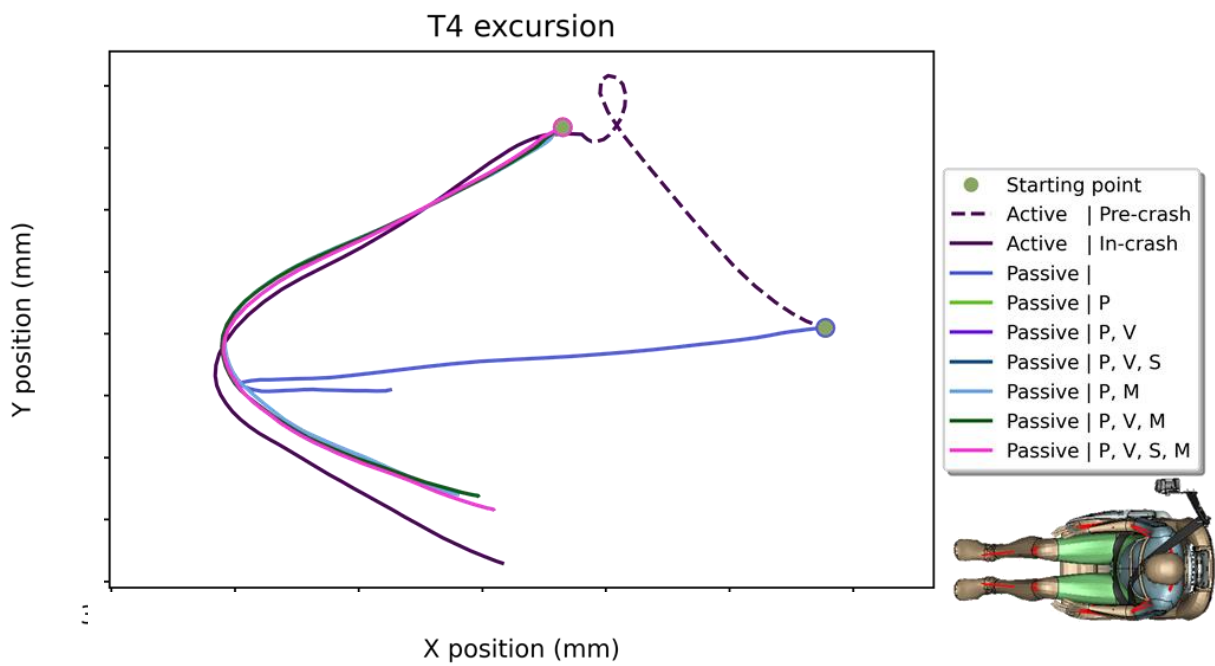


Figure 114: Chest excursion. XY plane. Turn left and Braking + Mobile Progressive Deformable Barrier

RESULTS

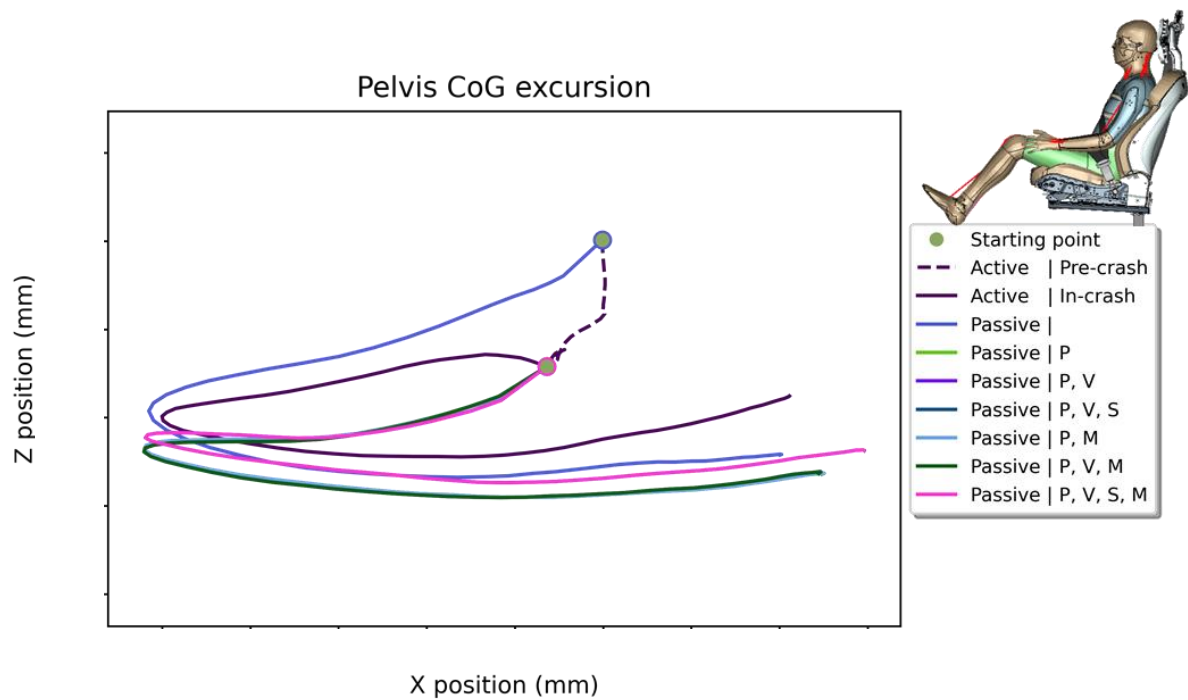


Figure 115: Pelvis CoG excursion. XZ plane. Turn left and Braking + Mobile Progressive Deformable Barrier

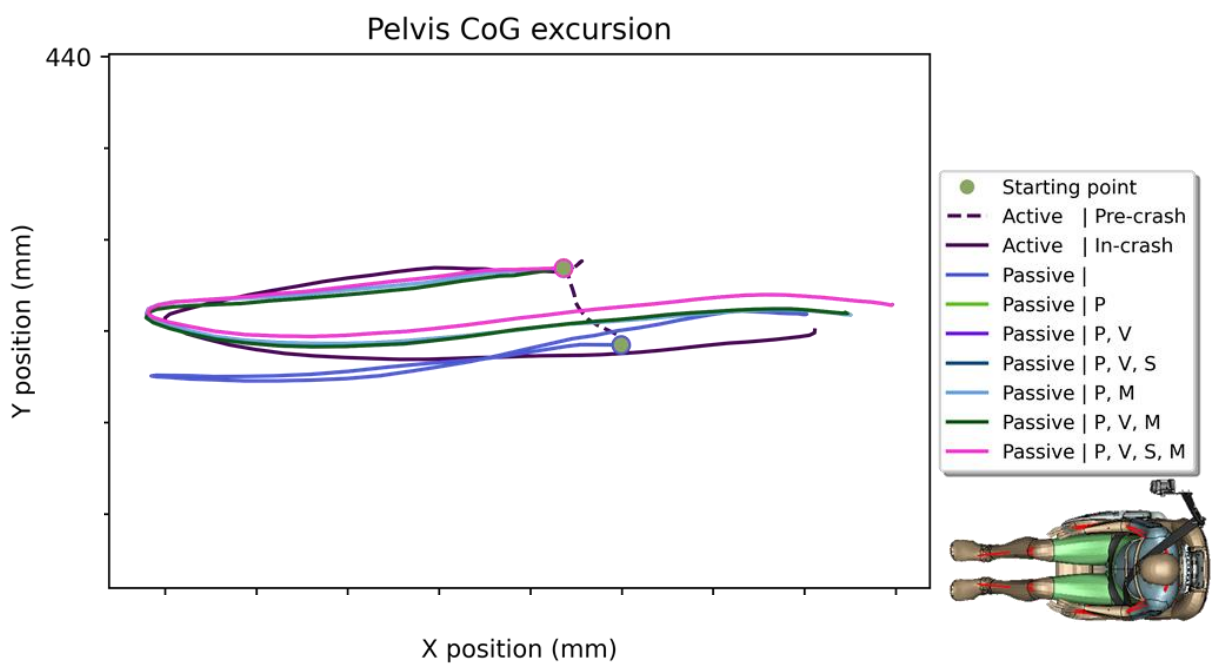


Figure 116: Pelvis CoG excursion. XY plane. Turn left and Braking + Mobile Progressive Deformable Barrier

It can be observed that the excursions of the head, chest, and pelvis in the passive simulation with no inputs are very different compared to the rest of passive simulations. Moreover, these excursions are very distant from the active simulation excursions.

Regarding the rest of the passive simulations, there are two differentiated groups of excursions: passive simulations with stresses and passive simulations with no stresses. The excursions of the simulations that have stresses seem to be closer to the excursions of the

baseline simulation. However, there is still a big difference between them that could be generated by the different belts used for each simulation.

Concerning injury criteria, all the results have been normalized using the baseline simulation value as a reference. Consequently, all the baseline injury risk predictions have value 1 and the passive simulation values oscillate around the value 1. Thus, the variations of the passive simulations with respect to the active one can be observed.

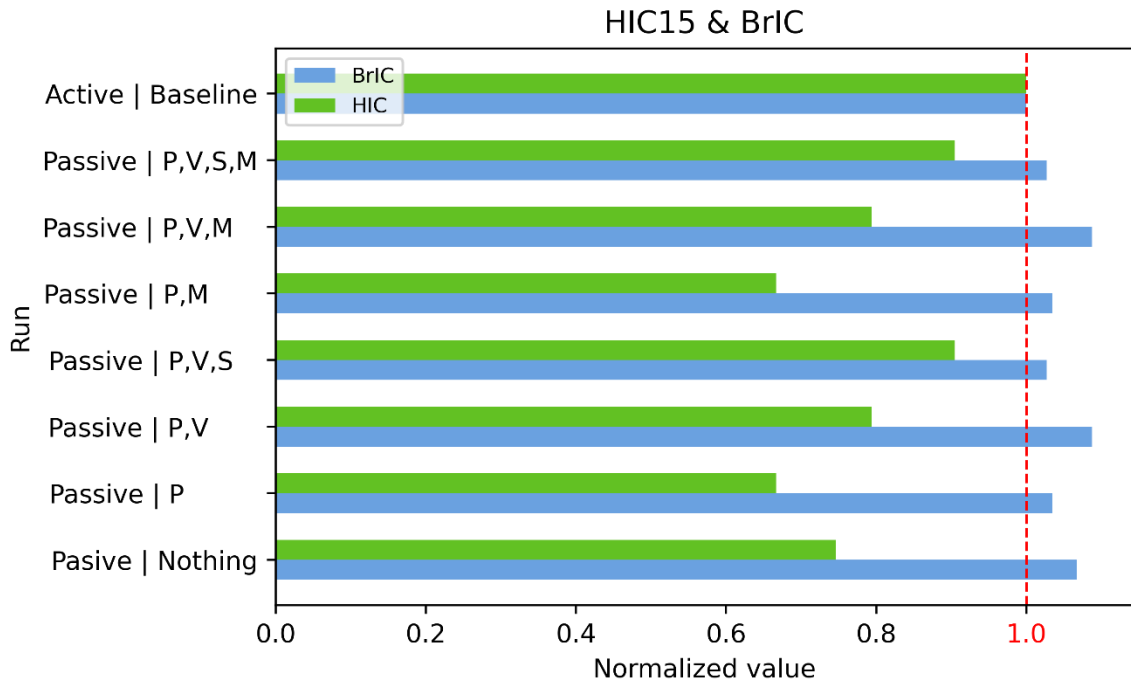


Figure 117: HIC 15ms and BrIC. Turn left and Braking + Mobile Progressive Deformable Barrier

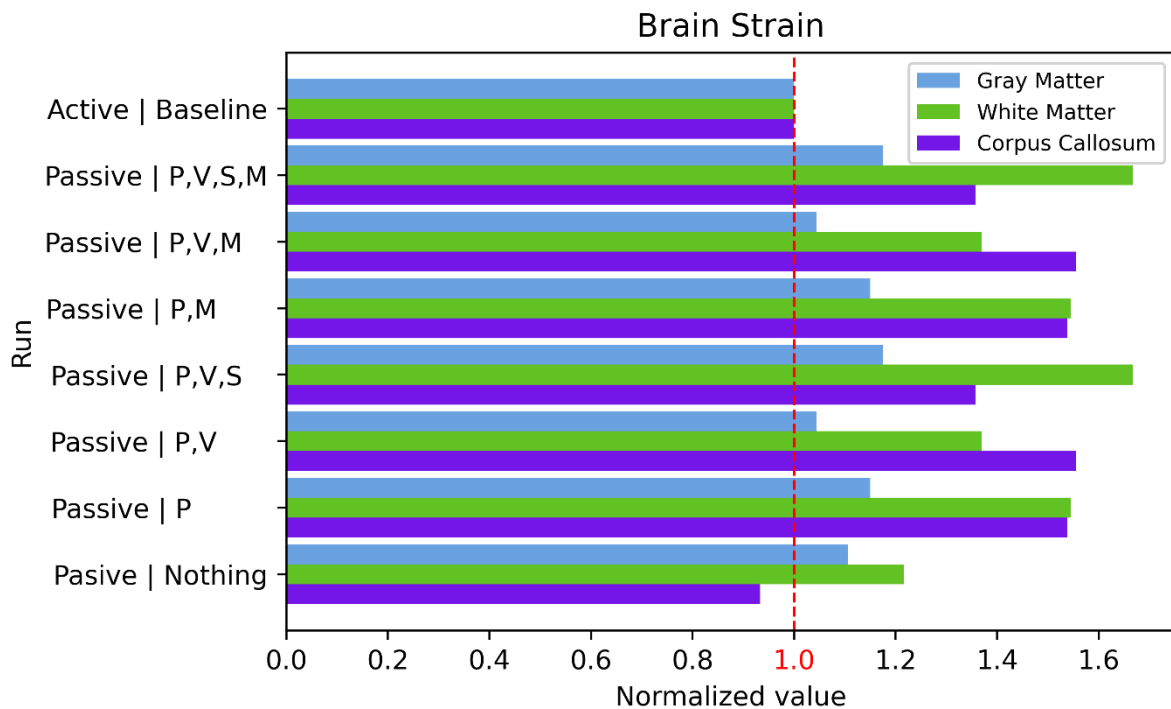


Figure 118: Brain strain. Turn left and Braking + Mobile Progressive Deformable Barrier

RESULTS

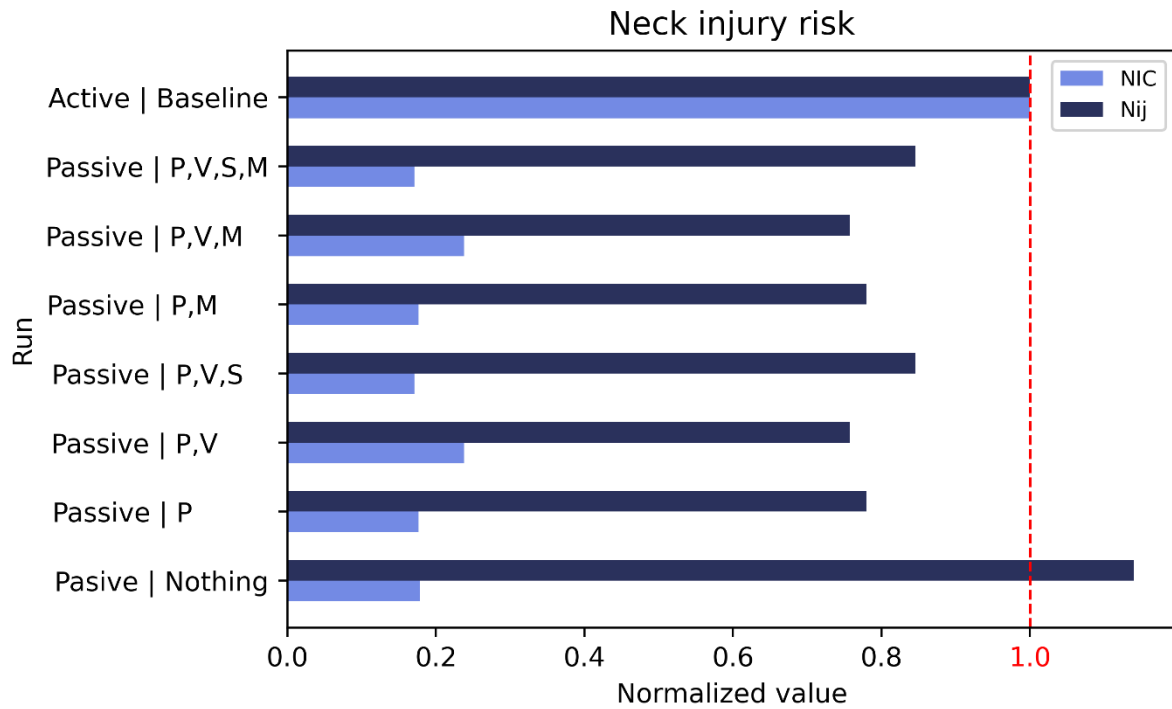


Figure 119: Neck injury risk. Turn left and Braking + Mobile Progressive Deformable Barrier

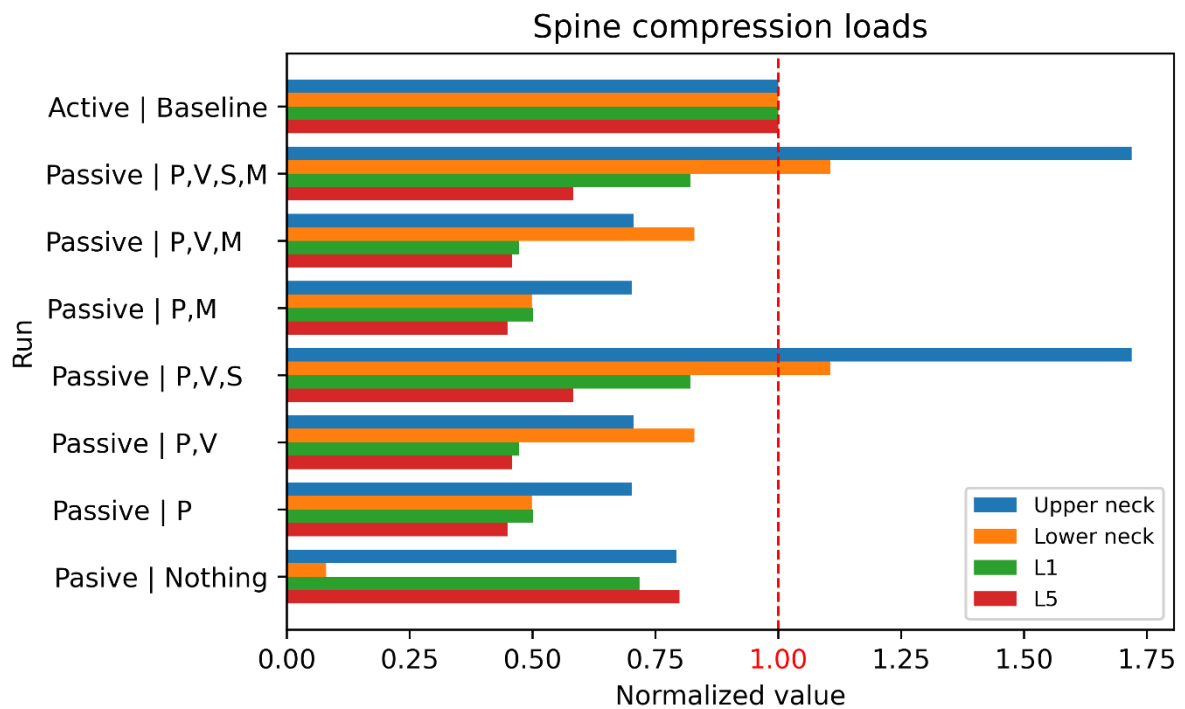


Figure 120: Spine compression loads. Turn left and Braking + Mobile Progressive Deformable Barrier

HIC and BrIC are predicted precisely compared to the baseline model in almost all the simulations, but the closest values are obtained in the passive simulation with posture, velocity, and stresses as input. The strains in the brain are a bit overpredicted. The closest

value is reached in the simulation with posture and velocity as inputs. Muscle activity level (MPID) seems to not affect the results.

Regarding the neck and the spine, compression loads in the upper neck are overpredicted compared to the baseline model in some cases and lumbar compression loads are underestimated compared to the baseline model. These predictions get the closest values when posture, velocity, and stress of the HBM are included. The NIC and Nij are wrongly predicted by the passive simulations compared to the baseline.

Regarding the rib cage strain model, risks of fracture are overpredicted compared to the baseline model in some of the passive simulations for the three groups of ages. The rest of the passive simulations predict accurately the risk of fracture of the baseline simulation.

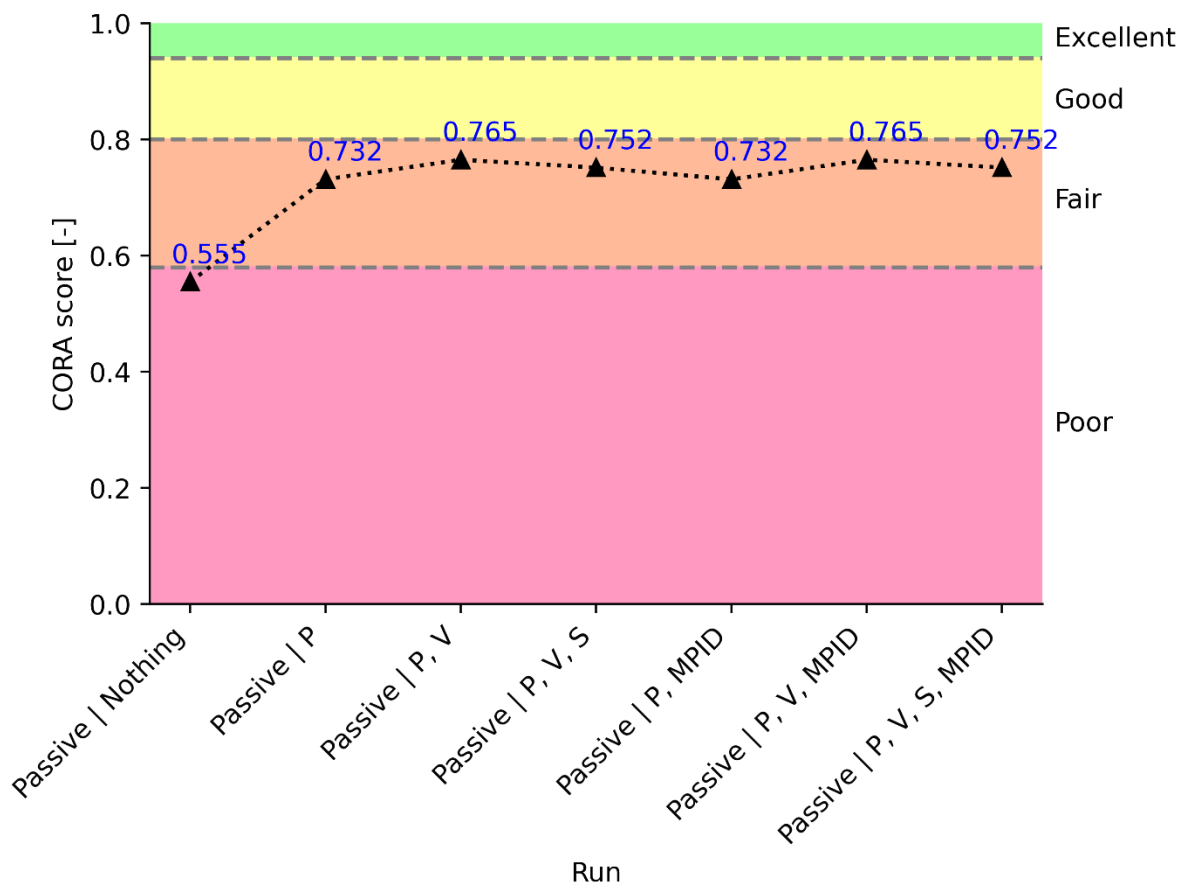


Figure 121: CORAplus acceleration ratings. Turn left and Braking + Mobile Progressive Deformable Barrier

Lastly, regarding the CORAplus ratings, there is a big improvement if the posture of the occupant is added as an input in the passive simulation, changing the overall rating from “Poor” to “Fair”. Adding velocity or velocity and stress improves the rating a bit more, but the passive model is not able to reproduce the accelerations of the active model with an “Excellent” rating. The maximum rating is reached when only posture and velocity are included in the model as inputs. Muscle level activity does not improve results.

RESULTS

4.- Discussion

The objective of the study was to evaluate the influence of the active musculature of a HBM on injury risk prediction in frontal crash scenarios and to assess which parameters of a passive model affect the injury risk more. The study showed that the passive models were not able to reproduce closely the results obtained from full sequence (pre-crash & in-crash) active simulations. However, there are differences depending on the studied scenario, as some are reproduced better by the passive models than others.

4.1.- Influence of the pre-crash maneuver

Results show that forward pre-crash motions are better reproduced by the passive models than lateral pre-crash maneuvers. This can be seen in the following figures, where several pre-crash maneuvers are compared having the same in-crash phase.

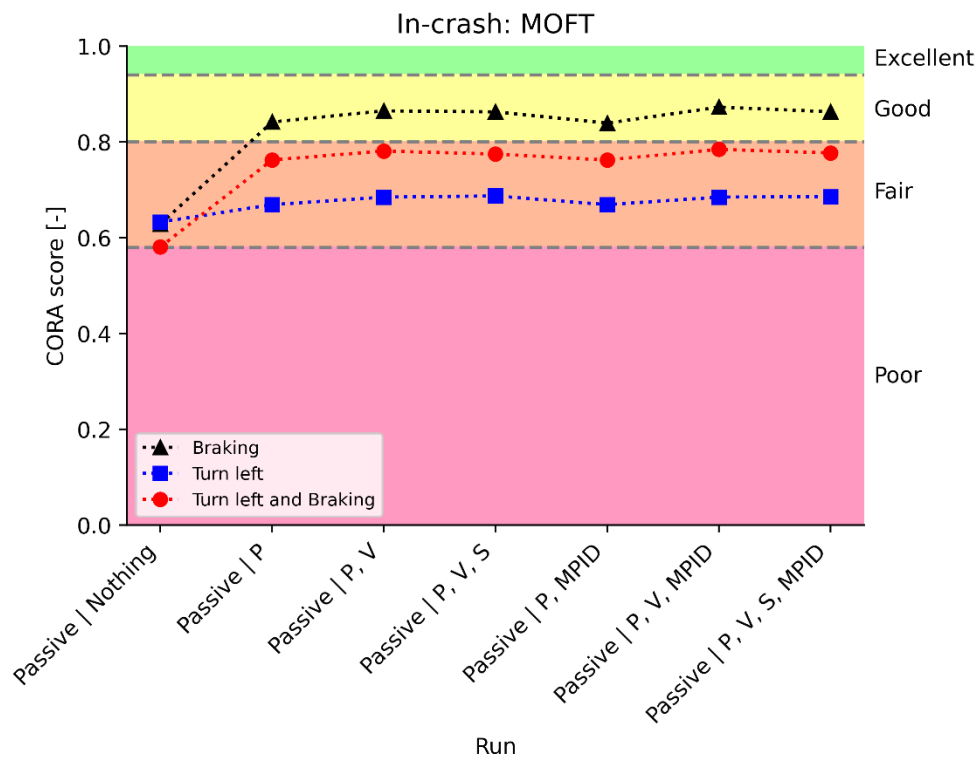


Figure 122: Influence of the pre-crash maneuver with Moderate Overlap Frontal Test in-crash

DISCUSSION

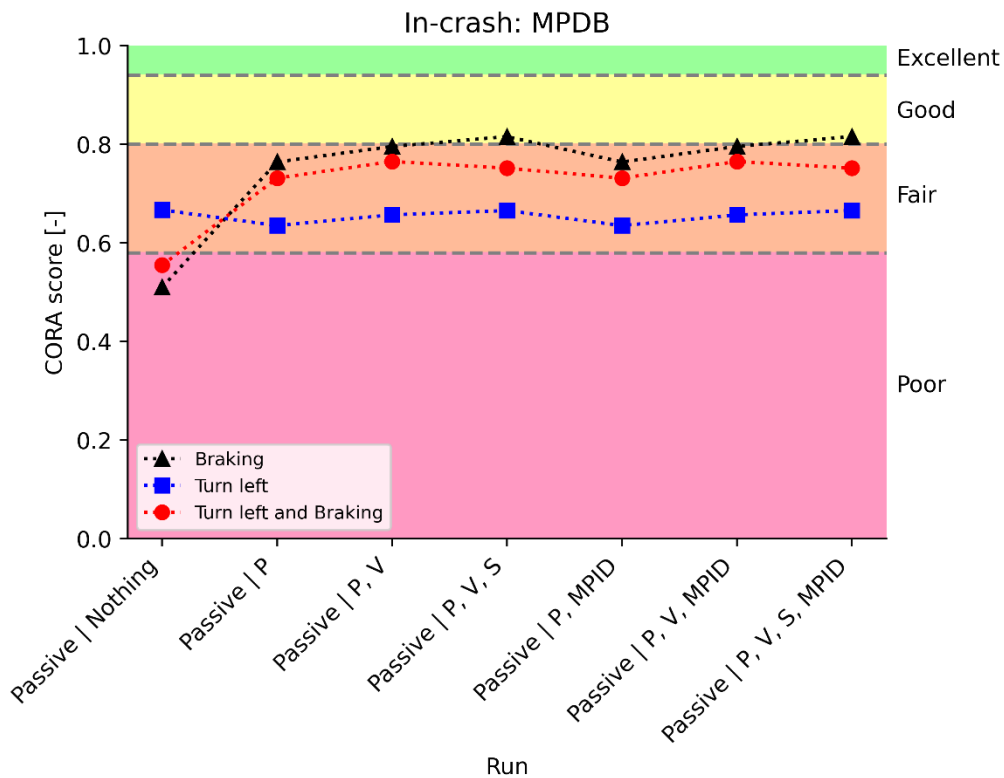


Figure 123: Influence of the pre-crash maneuver with Mobile Progressive Deformable Barrier in-crash

Pre-crash maneuvers affect clearly the CORAplus ratings obtained. Braking pre-crash obtains the best ratings and left turn obtains the worse ones. However, adding a frontal motion like braking to the lateral maneuver improves significantly the ratings.

Nevertheless, pre-crash maneuvers do not generally affect the relation between different passive simulations ratings, adding posture to the passive simulations tends to improve greatly the ratings, and adding velocity and stresses seems to improve even more the results of the passive model.

Taking this into account, passive models could be considered to reproduce a collision that had a frontal pre-crash maneuver, but active musculature could be beneficial be used in case the pre-crash is a lateral one with no frontal motion.

4.2.- Influence of the in-crash phase

The in-crash phase selected for the simulation also affects the response of the different passive models. In the following figures, a comparison between different crashes with the same pre-crash maneuver is made.

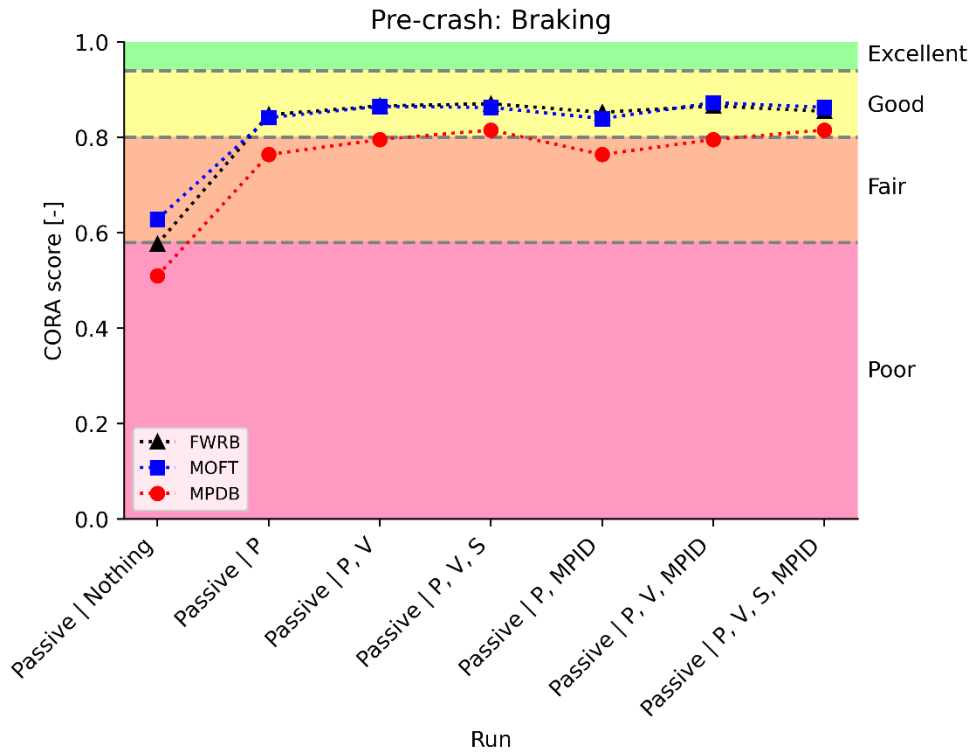


Figure 124: Influence of the crash pulse having Braking as pre-crash maneuver

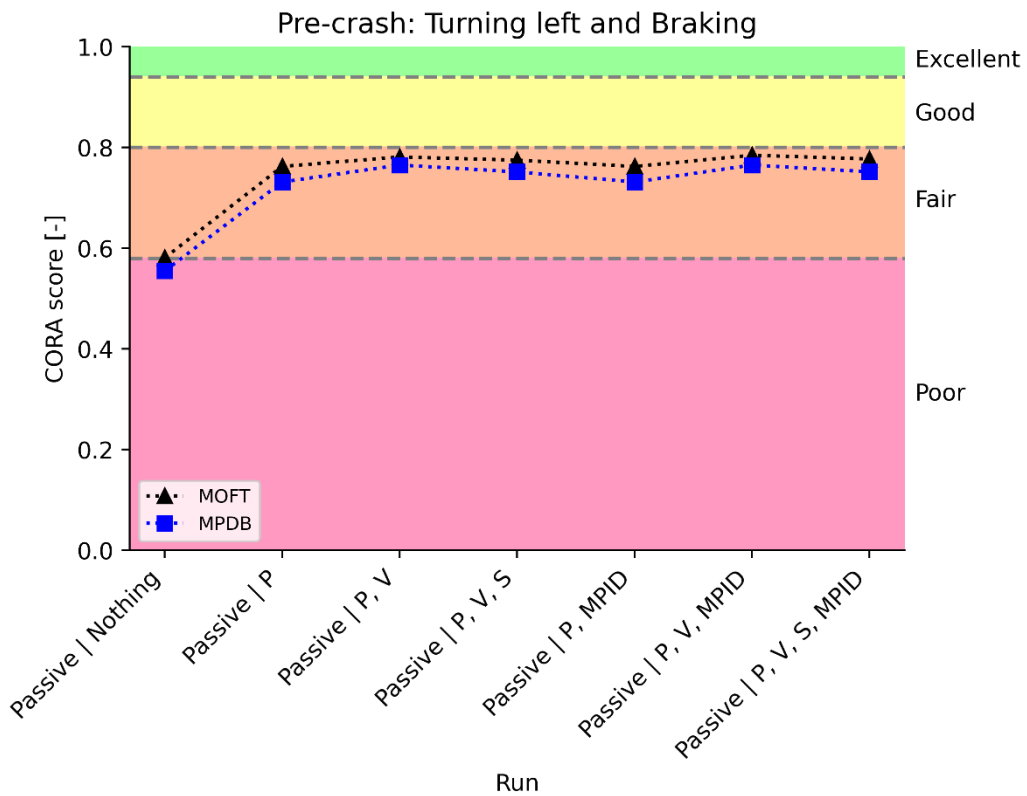


Figure 125: Influence of the crash pulse having Turning left and Braking as pre-crash maneuver

DISCUSSION

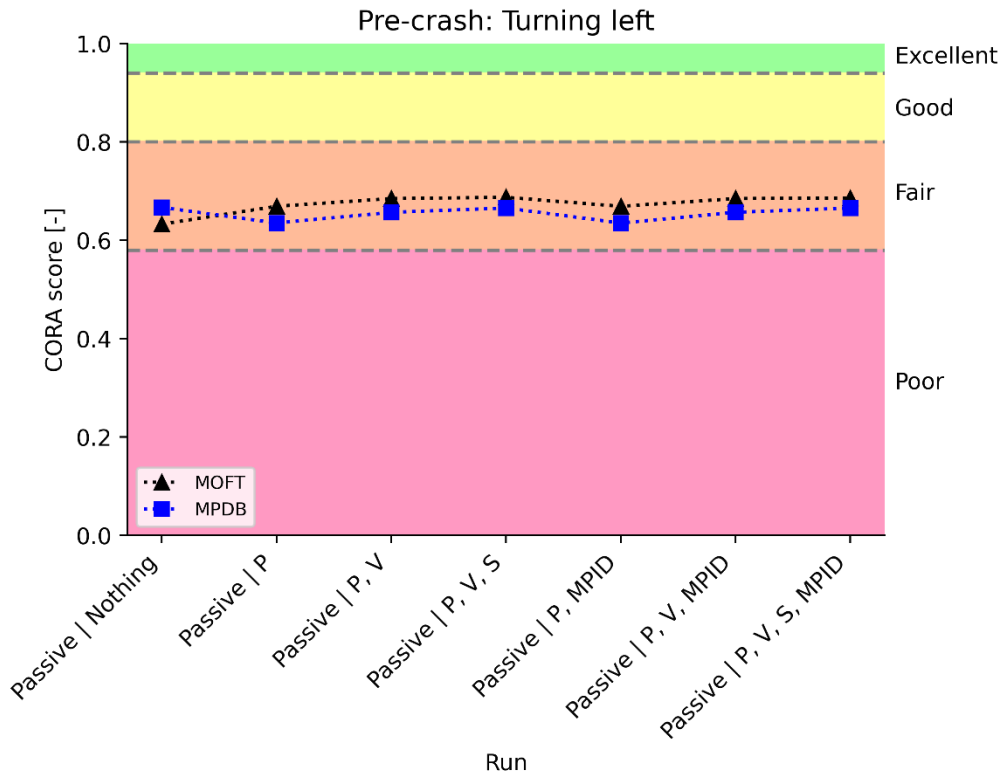


Figure 126: Influence of the crash pulse having Turning left as pre-crash maneuver

The results show that Full-Width Rigid Barrier and Moderate Overlap Frontal Test pulses might be reproduced better by the passive simulations than the Mobile Progressive Deformable Barrier when the pre-crash maneuver performed is braking. Regarding the rest of the pre-crash maneuvers, Moderate Overlap Frontal Test pulse seems to be reproduced better in general than Mobile Progressive Deformable Barrier. Therefore, MOFT and FWRB are pulses that are more likely to be reproduced by passive models but using active musculature in the HBM should be considered for the MPDB pulse.

From a generic perspective of the results, if activating the musculature of the HBM is not possible due to simulation time or other reasons, the posture of the occupant at the end of the pre-crash would improve the results compared to a simulation with no inputs. Moreover, velocities and stresses of the HBM can be added; excursions, accelerations, and injury risk predictions may be even closer to the ones obtained with the active musculature. Muscle activity level (MPID) however does not influence the results and it might even worsen the values obtained.

Regards injury risk prediction, the results show that head injury can be determined in a close way using passive models and analyzing HIC, BrIC, and the brain strain model. Nevertheless, neck and spine injuries may not be precisely predicted by a passive model, as in most of the results of this study, the obtained values from passive simulations differ substantially from the ones obtained with the active model. In relation to the rib cage strain model, a passive model with no inputs should not be used for predicting the risk of rib fracture, as the results show that the predicted risk of this model tends to be several times higher than the one from

the baseline. Also, a passive model with inputs could be used to predict the risk of fracture of 2 ribs, but the results differ considerably for 3, 4, and 5 rib fractures.

Lastly, considering that the passive model with posture, initial velocities, and stresses is generally the closest one to the active model, it can be seen that for all the cases, the best score obtained by that model does not reach the “Excellent” category and the injury risk predictions of this model are the closest one but there are most of the times a gap between them and the ones from the actual model. Moreover, excursions differ between them as well.

As it seems that muscle activity level does not influence the results and it might even worsen the values obtained, it can be concluded that active musculature may not influence the injury risk prediction during the in-crash phase.

4.2.- Limitations

There were some limitations in the development of this study. First, the initial squashing of the seat for the nominal posture used in the baseline simulations did not reach equilibrium, as during the initialization phase the HBM had a downward motion, showing that equilibrium of forces was not reached between the foam of the seat and the weight of the HBM.

Secondly, some of the shells of the HBM were made of material type *MAT_FABRIC that cannot be initialized with stresses. Most of the skin of the HBM used this type of material and could not be initialized with stresses when simulating the passive models, which may have affected the results.

Thirdly, the seatbelt had to be manually rerouted for the passive simulations, as the state of the retractor and the forces between the HBM and the belt could not be extracted to recreate the same functional seatbelt. As a result, the initial pretension of the belt at the beginning of the passive simulations and at the end of the pre-crash maneuver were not the same, affecting the results obtained.

Regarding the pre-crash lateral maneuvers, the whole motion of the pre-crash lasted around 3s. Simulating that big amount of time with the active musculature would have taken several weeks for each simulation. Due to the time duration of the project, simulating the complete motion was not possible and just around 850ms of lateral motion were simulated in order to extract the essential part of the maneuver.

Lastly, the group of simulations that had turning right as a pre-crash maneuver were not simulated due to contact problems in the simulations that could not be fixed in the limited time that this project lasted.

DISCUSSION

5.- Conclusions

The study compared excursions, accelerations, and injury risk predictions between an active HBM and passive HBMs to study the influence of active musculature over injury risk predictions. The study concluded that active musculature may not influence the injury risk predictions, excursions, and accelerations; as there is not a significant difference in results between the closest passive simulation and that same simulation with muscle activity level. Moreover, predictions of the passive models related to the spine were very different from those of the active model and it is right on the neck and the lumbar spine where the active musculature act. However, the study also showed that the methodology used to recreate the active in-crash phase is not able to reproduce closely the baseline in-crash phase, as the maximum CORA rating was 0.873 and the excursions of the passive models differed considerably from the ones of the active baseline.

Secondly, the study showed that in case using active musculature in the HBM is not possible, adding posture improves significantly the results, making the results of the simulation closer to the ones that would have been obtained. Furthermore, if velocity and stresses of the HBM are available, they might be added as well to get even closer results even though they seem to be not as essential as the posture of the occupant. Muscle activity level (MPID) however does not influence the results and it might even worsen the values obtained.

If passive simulations are used for the study, head and brain injury seem to be well predicted compared to the baseline model if some inputs are included. However, neck and spine injury risk predictions should not be used if the model is passive; instead, active musculature should be considered, as the muscles of the HBM act directly on the neck and the lower trunk of the model.

CONCLUSIONS

References

- [1] SAE International, "Taxonomy and Definitions for Terms Related to Driving Automation Systems for On Road Motor Vehicles".
- [2] SAE International, "SAE International Releases Updated Visual Chart for Its “Levels of Driving Automation” Standard for Self-Driving Vehicles," SAE International, 11 12 2018. [Online]. Available: <https://www.sae.org/news/press-room/2018/12/sae-international-releases-updated-visual-chart-for-its-%E2%80%9Clevels-of-driving-automation%E2%80%9D-standard-for-self-driving-vehicles>. [Accessed 21 06 2021].
- [3] World Health Organization, "The top 10 causes of death," 9 12 2020. [Online]. Available: <https://www.who.int/news-room/fact-sheets/detail/the-top-10-causes-of-death>.
- [4] A. McFarlane, "How the UK's first fatal car accident unfolded," BBC, 17 08 2010. [Online]. Available: <https://www.bbc.com/news/magazine-10987606>. [Accessed 19 03 2021].
- [5] World Health Organization, "Global Status Report on Road Safety," World Health Organization, Geneva, 2018.
- [6] Dirección General de Tráfico (DGT), "Las principales cifras de la siniestralidad vial. España 2019.," Observatorio Nacional de Seguridad Vial, Madrid, 2019.
- [7] H. Editors, "U.S. patent issued for three-point seatbelt," A&E Television Networks, 08 07 2020. [Online]. Available: <https://www.history.com/this-day-in-history/u-s-patent-issued-for-three-point-seatbelt>. [Accessed 10 07 2021].
- [8] D. W. B. Ashworth, "Scientist of the Day - John Paul Stapp," Linda Hall Library. Science, Engineering, Technology, 13 11 2020. [Online]. Available: <https://www.lindahall.org/john-paul-stapp/>. [Accessed 10 07 2021].
- [9] F. Zuppichini, "Effectiveness of a mechanical pretensioner on the performance of seat belts," *IRCOBI*.
- [10] Luke Gaylor, Mirko Junge, "Assesment of the efficacy of vehicle side airbags: A matched cohort of vehicle-vehicle side collisions using the GIDAS database," *IRCOBI*, vol. 15, no. 41, pp. 292-301, 2015.
- [11] B. Pipkorn, "Safer success story," SAFER, October 2015. [Online]. Available: <https://www.saferresearch.com/stories/safer-hbm-active-human-body-model>. [Accessed 19 March 2021].
- [12] Toyota, "THUMS. DESIGNED WITH YOU IN MIND," Toyota, [Online]. Available: <https://www.toyota.se/om-toyota/artiklar/2016/thums.json>. [Accessed 31 03 2021].

REFERENCES

- [13] SAFER, "Project A-HBM Step 4," SAFER, [Online]. Available: <https://www.saferresearch.com/projects/hbm-step-4>. [Accessed 31 03 2021].
- [14] E. Larsson, J. Iraeus, J. Fice, B. Pipkorn, L. Jakobsson, E. Brynskog, K. Brodin and J. Davidsson, "Active Human Body Model Predictions Compared to Volunteer Response in Experiments with Braking," 2019.
- [15] D. Robbins, *Anthropometric specifications for mid-sized male dummy*, Washington, DC: US Department of Transportation DTNH22-80-C-07502, 1983.
- [16] Euro NCAP, "Adult occupant protection," Euro NCAP, 2021. [Online]. Available: <https://www.euroncap.com/en/vehicle-safety/the-ratings-explained/adult-occupant-protection/>. [Accessed 21 06 2021].
- [17] IIHS HLDI, "About our tests," 2021. [Online]. Available: <https://www.iihs.org/ratings/about-our-tests>. [Accessed 21 06 2021].
- [18] H. C. Luke E. Riexinger, "A Preliminary Characterisation of Driver Manoeuvres in Road Departure Crashes," *IRCOBI*, vol. 79, no. 18, pp. 484-492, 2018.
- [19] R. S. H. C. G. Luke E. Riexinger, "A Preliminary Characterisation of Driver Evasive Manoeuvres in Cross-Centreline Vehicle-to-Vehicle Collisions," *IRCOBI*, vol. 15, no. 19, pp. 58-69, 2019.
- [20] J. & K. K. & G. H. Scanlon, "Analysis of Driver Evasive Maneuvering Prior to Intersection Crashes Using Event Data Recorders," *Traffic injury prevention*, pp. 182-189, 2015.
- [21] L. Wehrmeyer, "Influence of Active Musculature & Parameters of the Final Pre-Crash State on the Occupant Response," *KTH SKOLAN FÖR KEMI, BIOTEKNOLOGI OCH HÄLSA*, 2020.
- [22] Euro NCAP, "Protocols," Euro NCAP, [Online]. Available: <https://www.euroncap.com/es/para-ingenieros/protocols/>. [Accessed 26 06 2021].
- [23] C. Thunert, "CORApplus Release 4.0.4 User's Manual," 2017.
- [24] S. Kleiven, "Evaluation of head injury criteria using a finite element model validated against experiments on localized brain motion, intracerebral acceleration, and intracranial pressure," *International Journal of Crashworthiness*, vol. 1, no. 11, pp. 65-79, 2006.
- [25] L. L. S. S. A. A. Y.-S. K. A. K. D. A. S. H. & B. P. Johan Iraeus, "Detailed subject-specific FE rib modeling for fracture prediction," *Traffic Injury Prevention*, vol. 20, no. sup2, pp. S88-S95, 2019.
- [26] DEWEsoft, "PID Control," DEWEsoft, [Online]. Available: <https://training.dewesoft.com/online/course/pid-control>. [Accessed 28 06 2021].

- [27] D. Adomeit and A. Heger, "Motion Sequence Criteria and Design Proposals for Restraint Devices in Order to Avoid Unfavorable Biomechanic Conditions and Submarining," 1975.
- [28] A. M. E. a. W. G. Najm, "Problem Definition for Pre-Crash Sensing Advanced Restraints," *NHSTA, US. Department of Transportation*, 2009.
- [29] D. J. & F. S. G. Karan Devane, "Validation of a simplified human body model in relaxed and braced conditions in low-speed frontal sled tests," *Traffic Injury Prevention*, pp. 832-837, 2019.
- [30] Total Energies, "CAR SEAT BELT, INVENTION AND USE," Total Energies, 11 12 2020. [Online]. Available: <https://totalenergies.id/en/article/tips-advice/car-seat-belt-invention-and-use>. [Accessed 10 07 2021].
- [31] Akweli Parker, "What is the purpose of a seatbelt pretensioner?," HowStuffWorks, [Online]. Available: <https://auto.howstuffworks.com/car-driving-safety/safety-regulatory-devices/seatbelt-pretensioner.htm>. [Accessed 10 07 2021].
- [32] Luke E. Riexinger, Hampton C. Gabler, "A Preliminary Characterisation of Driver Manoeuvres in Road Departure Crashes," *IRCOBI*, vol. 79, no. 18, pp. 484-492, 2018.
- [33] Luke E. Riexinger, Rini Sherony, Hampton C. Gabler, "A Preliminary Characterisation of Driver Evasive Manoeuvres in Cross-Centreline Vehicle-to-Vehicle Collisions," *IRCOBI*, vol. 15, no. 19, pp. 58-69, 2019.
- [34] Scanlon, John & Kusano, Kristofer & Gabler, Hampton., "Analysis of Driver Evasive Maneuvering Prior to Intersection Crashes Using Event Data Recorders," *Traffic injury prevention*, pp. 182-189, 2015.
- [35] Johan Iraeus, Linus Lundin, Simon Storm, Amanda Agnew, Yun-Seok Kang, Andrew Kemper, Devon Albert, Sven Holcombe & Bengt Pipkorn, "Detailed subject-specific FE rib modeling for fracture prediction," *Traffic Injury Prevention*, vol. 20, no. sup2, pp. S88-S95, 2019.

REFERENCES

Appendix A: HBM controller parameters

The parameters used for the APF control strategy are shown in the following table.

Table 13: HBM controller parameters values [14]

Parameter	Value
Neck neural delay	20 [ms]
Neck link – Proportional gain	1.301 [1/rad]
Neck link – Integral gain	0 [1/rad ms]
Neck link – Derivative gain	470 [1/rad ms-1]
Lumbar neural delay	25 [ms]
Lumbar link – Proportional gain	1.210 [1/rad]
Lumbar link – Integral gain	0 [1/rad ms]
Lumbar link – Derivative gain	159 [1/rad ms-1]

The structure of a standard PID controller is shown in the following figure.

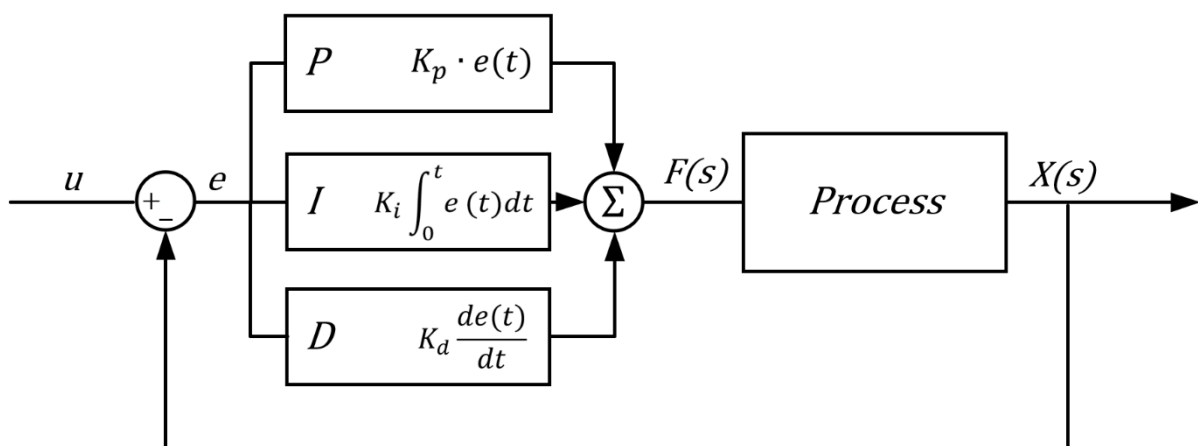


Figure 127: PID controller diagram [26]

The initial input of the controller is the reference signal (u) which indicates the desired angular position of the head. From this signal is then subtracted the actual value that is observed in the model (X) obtaining the error of the real value compared to the desired reference (e). Then, the output of the controller (F) is obtained as a sum of the Proportional, Integral, and Derivative corrections of the error. The Proportional part amplifies the output signal proportionally to the error obtained using the gain K_p (Proportional gains of the HBM controllers). The Integral part varies the signal proportionally to the amount of accumulated error in time using the gain K_i (Integral gains of the HBM controllers). The longer the output stays away from reference, the higher the integral signal would be. Lastly, the Derivative branch varies the signal proportionally to the variation of the error using the gain K_d

APPENDIX A

(Derivative gains of the HBM controllers). If the error changes rapidly, the output signal of this branch will increase substantially.

The implementation of a Proportional controller allows the system to react to the error, but it does not ensure that the final value in the model will be the reference value. The Integral controller eliminates the reference error issue integrating the error but making the controller very slow. The Derivative controller solves that issue rapidly changing its output with the derivative of the error.

Appendix B: Pre-crash and in-crash combinations

Not all the combinations of pre-crash and in-crash are equally likely to happen in a real-life scenario. The final combinations were chosen based on the different scenarios that were selected for this study. Also is important to mention that some scenarios were not chosen as the HBM model is not validated or compared with real volunteers for all the possible loads. Rear-end collisions were not chosen as the HBM is only compared for lateral and longitudinal loads.

Highway

For this scenario, it is assumed that the road is delimited with one barrier on each side and that front-to-front crashes are not likely to happen. The crash scenario is the following.

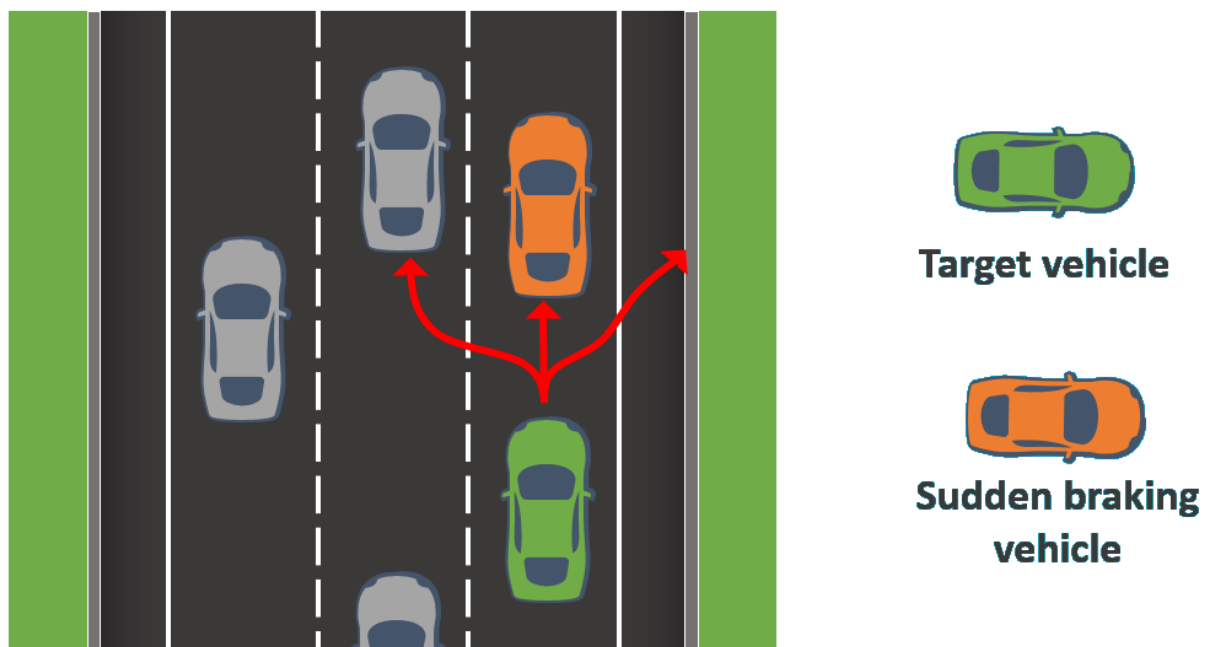


Figure 128: Highway crash scenario

The target vehicle has a sudden braking vehicle in front of it and the driver/autonomous car has only the five pre-crash maneuvers commented previously: braking, turning left, turning right, turning left, and braking or turning right and braking. For this analysis, the combination of turning and braking will be assumed to have the same crash scenario as a consequence of just turning.

If the green vehicle decides to brake, it could end up crashing with the car in front of it. This type of collision can be compared to a Full-Width Rigid Barrier test from Euro NCAP, as the full frontal of the car will be colliding with the front car, even knowing that a car does not behave as a rigid barrier.

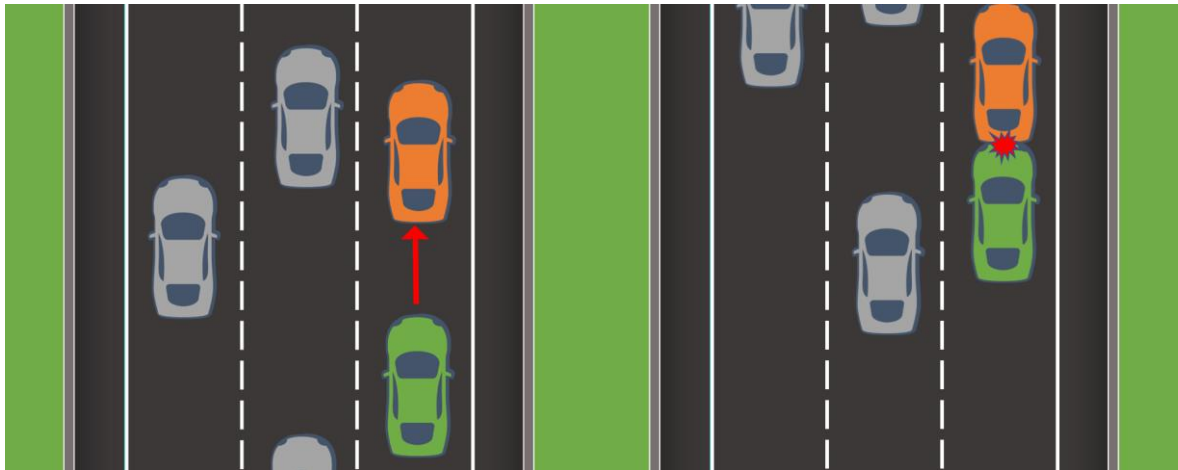


Figure 129: Option 1. Braking into Full-Width Rigid Barrier

If the vehicle decides to turn right, a crash into the right-side barrier is likely to happen. This crash against the barrier can be compared to the Passenger-side Small Overlap test from the IIHS.

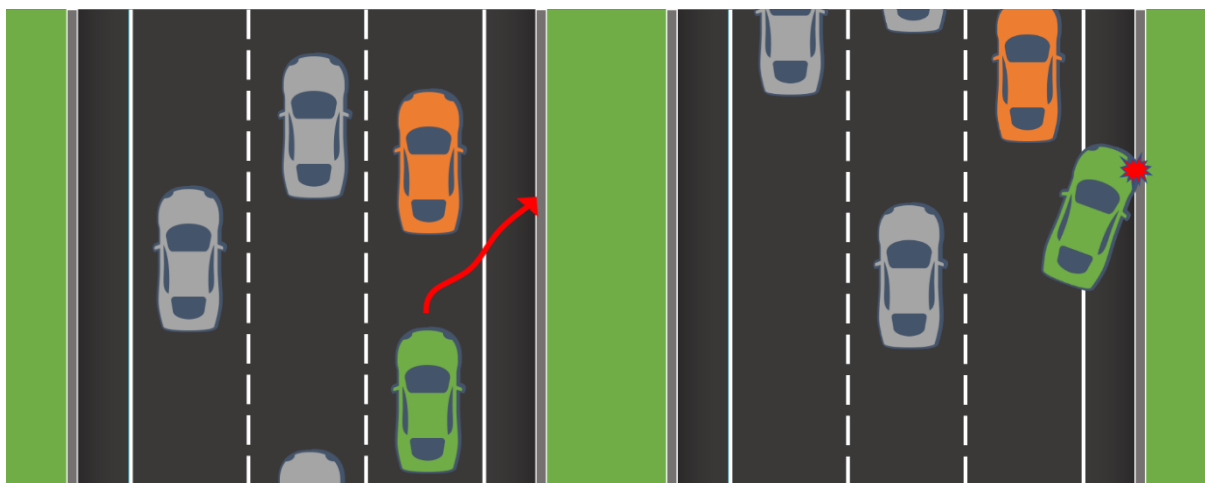


Figure 130: Option 2. Turning right into Passenger-side Small Overlap

The last option for the vehicle is to turn left, where the most probable collision (regardless of the rear-end crash for the green vehicle) is a frontal crash into a car on the left side lane. This crash can be simulated as a Moderate Overlap Frontal Test from the IIHS.

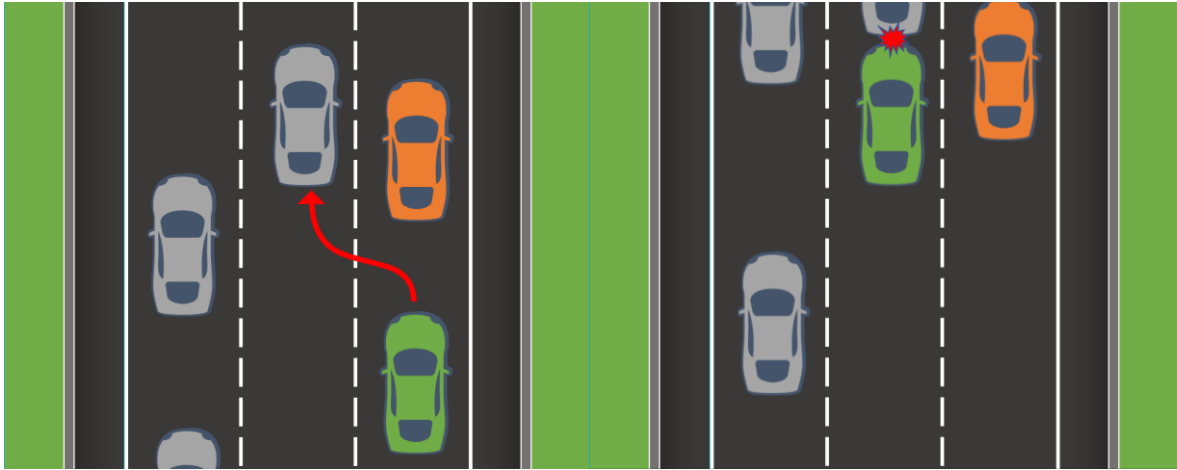


Figure 131: Option 3. Turning left and Moderate Overlap Frontal Crash

Secondary road

In this scenario, it is considered that the road has no barriers at the sides. This means that the car can get out of the road if the avoidance maneuver moves the car away from the road. It is common to see trees and electric poles at the side of these types of roads, so it will be considered that in case of a road departure, the car will be very likely to crash into one element of that type.

The studied situation is very similar to the one studied for the highway scenario. It is assumed that the car in front of the target vehicle is suddenly braking and the driver/autonomous car needs to make an avoidance maneuver to try to avoid the collision.

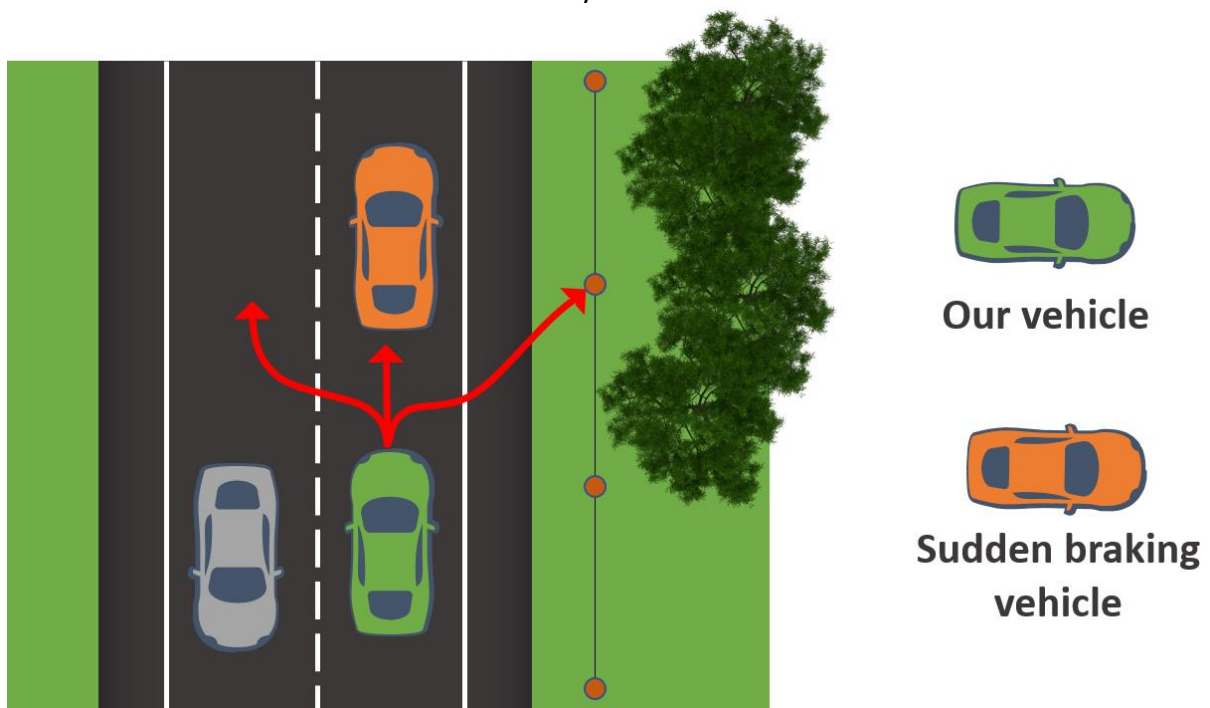


Figure 132: Secondary road crash scenario

APPENDIX A

The target car has again three possibilities to try to avoid the car. The first one would be to do an emergency braking maneuver, which would end in the same crash scenario as on the highway (Option 1). The second option would be to steer left into the opposite direction lane. In this case, the car may end up having a frontal crash against another car that comes from the other direction. This crash can be modeled with a Mobile Progressive Deformable Barrier test from Euro NCAP.

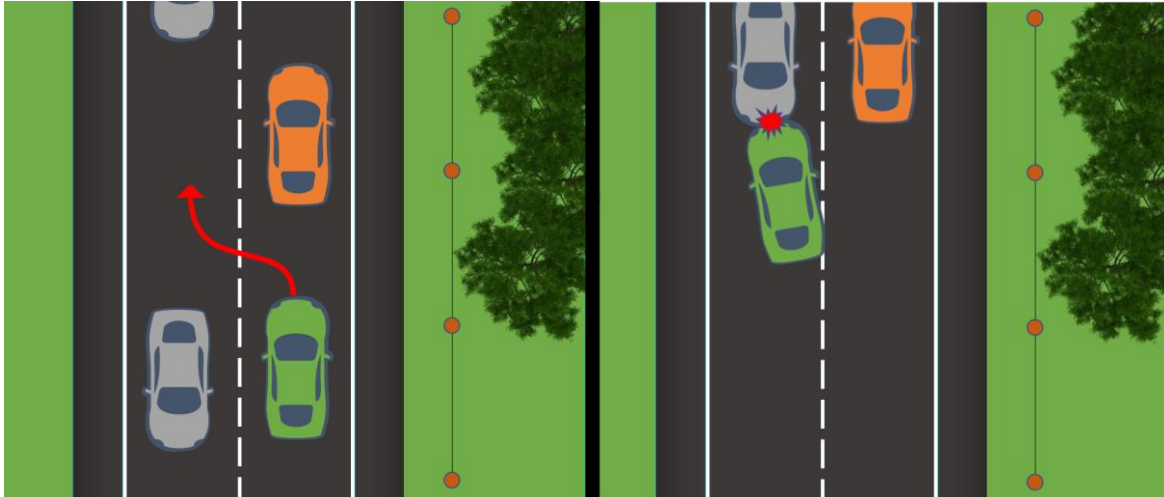


Figure 133: Option 4. Turning left into Mobile Progressive Deformable Barrier

The third option in this scenario would be to turn right, creating a road departure situation. In this case, the car may collide against a pole or a tree on the side. This crash scenario was modeled as a Passenger-Side small overlap, a similar situation as Option 2 of the highway.

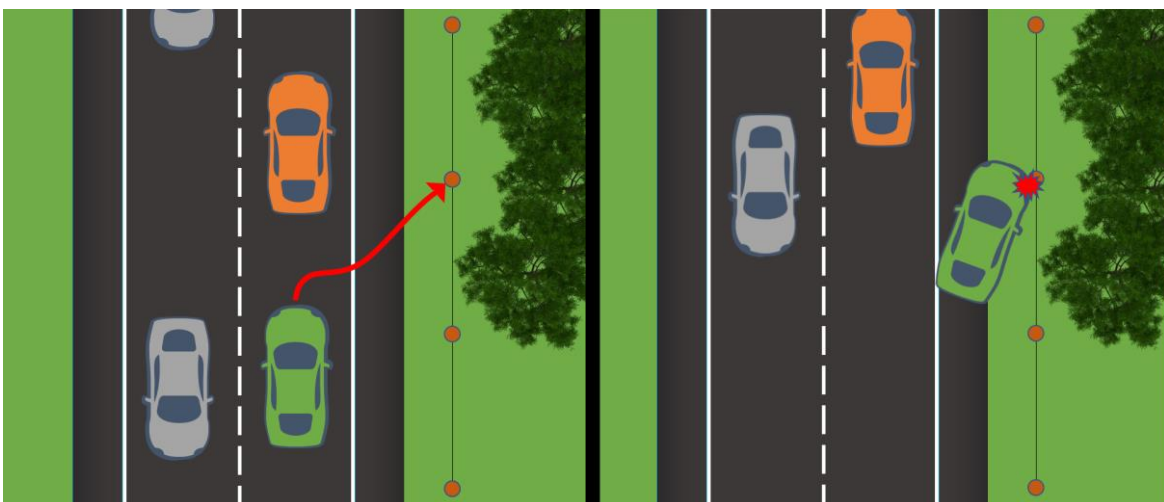


Figure 134: Option 5. Turning right and Passenger-side Small Overlap

Intersection

This last scenario is more complex than the previous ones, as it allows cars to move in several directions and following different trajectories along the intersection. Also, the crash severity depends on the behavior of the driver/autonomous vehicle. According to Kristofer D. Kusano

[20], the initial behavior of a driver when entering an intersection can be classified into one of the three following groups:

1. Complete stop: the driver stops completely before entering an intersection and then accelerates again to cross it. This behavior ends up in the lowest severity crashes of all.
2. Rolling stop: the driver slows down when entering the intersection, but the car does not stop completely. Then, the car accelerates again to cross the intersection.
3. Traveling through: the driver does not reduce its velocity when entering the intersection and just crosses it. This kind of behavior generates crashes with high severity.

His study also mentions that there are mainly three types of car-to-car crashes depending on the trajectories that both cars follow. The three types are shown in the following figures.

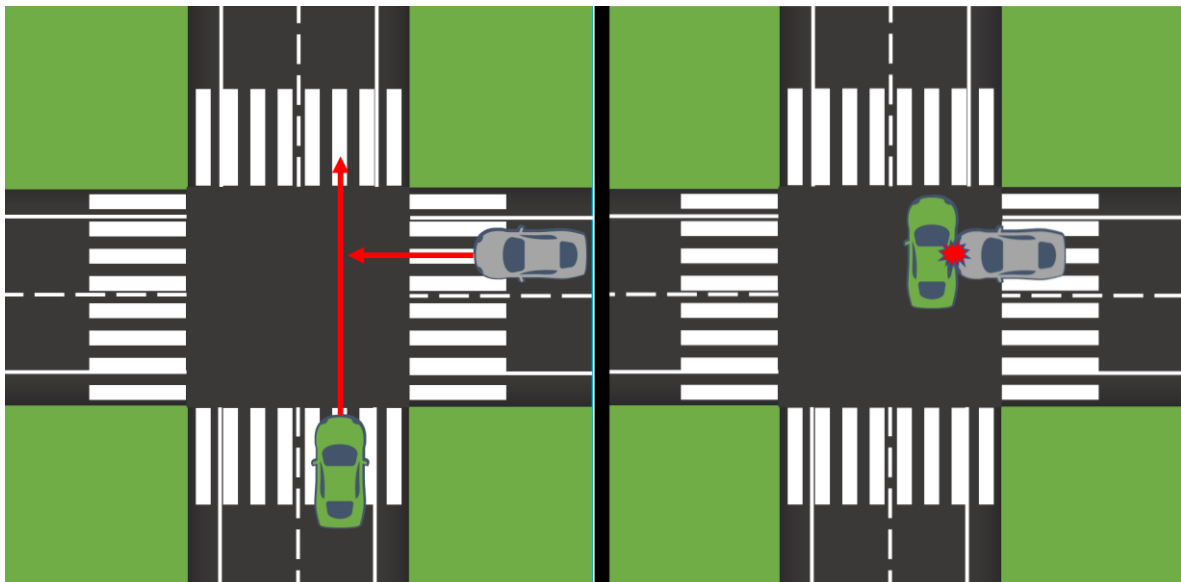


Figure 135: Straight Crossing Path (SCP) and possible crash

The first possible trajectory for two cars that are crossing an intersection is the Straight Crossing Path (SCP). This path can generate a far-side collision for the green car in the figure and a frontal collision for the grey car. In this study, just frontal collisions will be studied. The frontal collision was modeled as a braking maneuver followed by a Full-Width Rigid Barrier test from Euro NCAN, the same situation seen before in the highway or the secondary road.

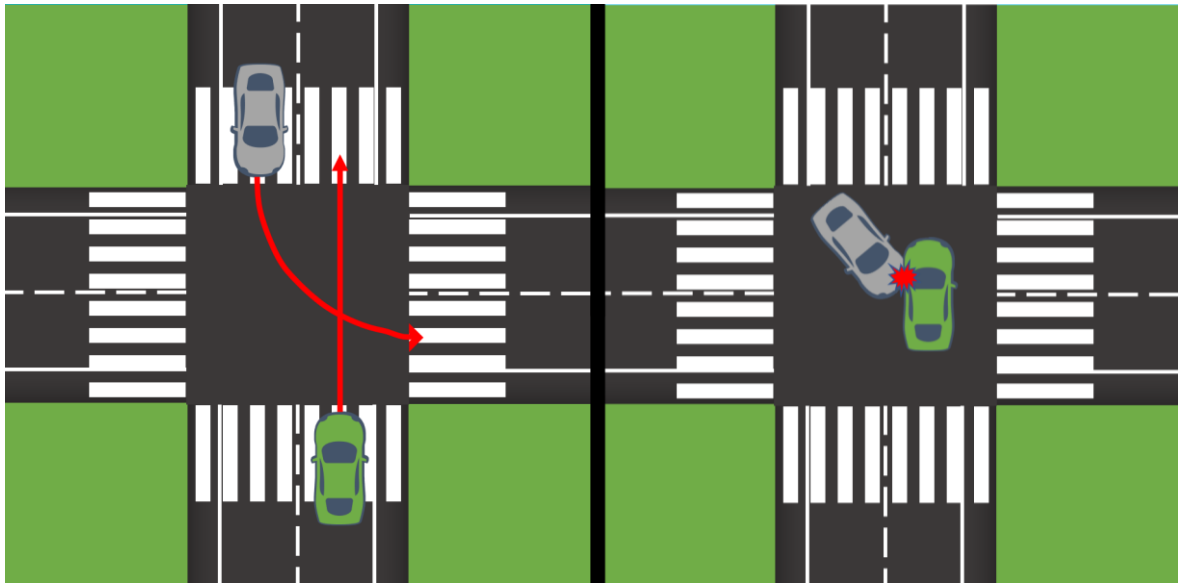


Figure 136: Left Turn Path / Opposite Direction (LTAP/OD) and possible crash

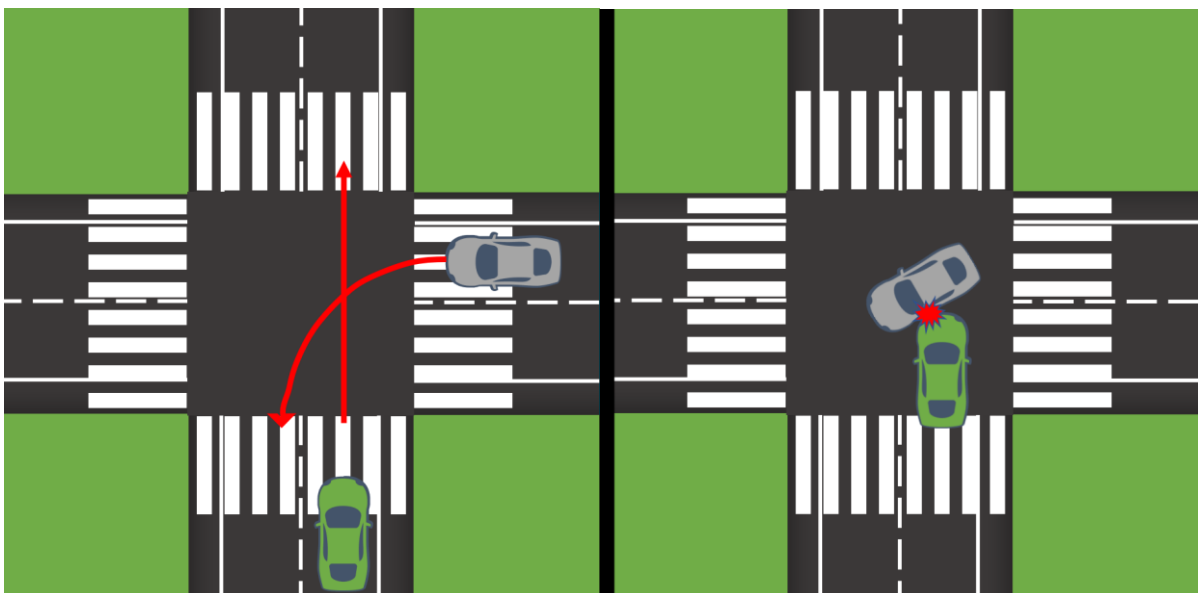


Figure 137: Left Turn Across Path / Lateral Direction (LTAP/LD) and possible crash

The other trajectories also could potentially generate frontal crashes. For the case of LTAP/OD, the frontal crash was modeled as a Mobile Progressive Deformable Barrier test, and in the case of the LTAP/LD, the crash test used to model the collision was the Moderate Overlap Frontal Test from the IIHS.

Appendix C: Sustainable Development Goals

The Sustainable Development Goals that this Project pursues are the number SDG9 and SDG10.

Sustainable Development Goal 9 (Industry, Innovation, and Infrastructure) is focused on inclusive and sustainable industrialization mixed with innovation and infrastructure. The key to this goal is to introduce and promote new technologies that enable the efficient use of resources in the industry. This project studied how active musculature influences the injury risk prediction and it showed the cases in which active musculature should be used and the cases it may not be necessary. Using active musculature in a simulation makes a simulation longer, as the number of operations to do in each time step is higher, which may end up in higher consumptions of energy, power, and data storage resources over time. Knowing how to discretize simulations that need active musculature and simulations that don't might help to save a lot of that energy and resources. Furthermore, active musculature can be considered an innovation project that may help in the development of the car safety industry, making cars safer for everyone.

Regarding Sustainable Development Goal 10 (Reduced Inequalities), this project can potentially help to reduce inequalities in car-safety terms in the world. Sadly, not all the cars that are sold in the world have the same safety systems, as including proper airbags and seatbelts have a cost expense. This study can potentially help to reduce the cost of production of safety equipment for a car, as in the future, active musculature may help to design adequate safety systems much cheaper based on simulations results rather than having to do physical tests that are much more expensive. If the cost of production is reduced, safety elements could be added in cars even in the basic models so everyone can have access to them, and all the people of the world, regardless of the country they live in, could benefit from these safety features.